

**A Gene Trap Screen Reveals the Expression of
the Transcription Factor *Gfi1.1* in Haemogenic
Endothelial Cells of the Zebrafish Embryo**

Roshana Sutharshini Thambyrajah

**Thesis submitted to the University of Nottingham
for the degree of Doctor of Philosophy**

September 2011

Not everything that can be counted counts and not everything that counts can be counted.

(Albert Einstein, 1879-1955)

In vertebrates, haematopoiesis occurs in two waves. The primitive wave gives rise to transient myeloid and erythroid cells whereas the definitive wave generates haematopoietic stem cells (HSCs), which maintain the blood system throughout life. These HSCs are able to self-renew and to give rise to progenitors that differentiate into mature cells of all blood lineages. Little is known about the cellular origin and molecular programming of HSCs. This knowledge is useful to generate HSCs *in vitro* from embryonic stem cells or induced pluripotent cells. In zebrafish, HSCs form in the intermediate cell mass (ICM), in the trunk of the embryo. Here, they develop dorsal to the primitive red blood cells and in close association with the ventral wall of the dorsal aorta (DA). Like their mammalian counterparts, they express the transcription factors *runx-1* and *c-myb*. As in other vertebrates, zebrafish HSCs are thought to arise from the haemogenic endothelium in the ventral wall of the DA. A signaling cascade that involves the Hedgehog, Vascular endothelial growth factor (Vegf) and Notch signaling pathways is needed for arterial specification of the DA and for HSC formation. Short-term lineage tracing experiments showed that cells in the ventral wall of the DA first seed the tail mesenchyme (caudal haematopoietic tissue, CHT) through blood circulation before they seed the final sites of haematopoiesis, the thymus and kidney in the adult fish.

Here, we conducted a *tol2*-transposon based gene trap vector screen with eGFP as the reporter gene with the aim to label nascent HSCs *in vivo* and to identify novel genes involved in haematopoiesis. We obtained 174 transgenic lines with tissue-specific eGFP expression in non-haematopoietic and haematopoietic tissues. We identified two lines with marker gene expression in haematopoietic cells. One of the transgenic lines, *I-551:eGFP*, showed reporter gene expression in primitive red blood cells and in endothelial cells in the ventral wall of the DA at 25 hours post fertilization (hpf). Using inverse PCR we identified the trapped gene in *I-551:eGFP* as *gfi1.1*, the homolog of the

mouse *Growth independence factor 1 (Gfi1)*, a transcriptional repressor expressed in HSCs.

Here, we present results that the transgenic line *Gfi1.1:eGFP* enables us to follow emerging haematopoietic progenitors from the ventral wall of the dorsal aorta in their subsequent migration to the CHT, before they seed the final haematopoietic sites, the kidney and thymus. We show that *Gfi1.1:eGFP* expression is restricted to the ventral wall of the dorsal aorta by combining the transgenic line with endothelial and aorta-specific transgenic lines. We further demonstrate that the endothelial expression of the eGFP in the aorta is dependent on the *vegf* and *notch* signalling pathway and co-localizes to cells which also express the transcription factors *runx1* and *c-myb*. When *Gfi1.1:eGFP* embryos are injected with the *runx1* morpholino (MO), *gfi1.1* expression in haemogenic endothelial cells initially occurs, which indicates that initial *gfi1.1* expression is independent of *runx1*. But a reduction in the number of eGFP positive cells is observed at 50 hpf in the CHT. Using time-lapse imaging, we were able to visualize *gfi1.1* positive cells detaching from the haemogenic endothelium. This observation indicates that *gfi1.1* positive cells in the CHT are derived from the haemogenic endothelium and therefore nascent HSCs. We therefore strongly suggest that this transgenic line labels haemogenic endothelial cells at 26hpf. The transgenic line *Gfi1.1:eGFP* therefore provides a tool for studying HSC development since its expression labels the emergence of nascent HSCs from haemogenic endothelial cells and continues to be expressed in larval and adult haematopoietic sites.

Acknowledgments

First of all, I would like to thank Dr Martin Gering for “adopting” me to his lab. I felt privileged to work with you. Thank you for all your supervision, time and support throughout the past four years!

I also thank the other members of the lab whom I shared a lot of fun and laughter with. Thanks for cheering me up when needed and encouraging me to keep going;-)

Thank you Jonathan, Hsu, Sunny, Penny, Chrissy, Imran and Oky.

And a big thank you to all the friends I made here in Nottingham. Especially, Cris, Felix, Jordi, Jaime, Francisco, Varvara Morrito, Muhammed, Paty and Aliya for the regular lunch and Johnson’s sessions! Life would have been very dull without you guys!

Last, but not least, I thank my dear friends Rudi and Barbara and my family for the support and encouragement.

List of contents

1. Introduction	20
1.1 Haematopoiesis	20
1.2 Characterisation of HSCs	21
1.3 The hierarchy in the haematopoietic system	24
1.4 Vertebrate hematopoiesis	27
1.5 Primitive haematopoiesis in vertebrates	28
1.6 HSCs arise in the AGM of the embryo	33
1.7 HSC emergence from the ventral aspect of the dorsal aorta	35
1.8 Models of HSC emergence in the ventral DA: haemogenic endothelium or definitive haemangioblasts	36
1.9 Primitive haematopoiesis in zebrafish	38
1.10 Haematopoietic stem cell emergence in zebrafish	42
1.11 Definitive HSCs migrate to the caudal haematopoietic tissue before they seed the thymus and the kidney	48
1.12 A subset of erythro-myeloid progenitors (EMPs) arise in the PBI independently of HSCs	51
1.13 Molecular programming of the dorsal aorta and HSCs	51
1.14 The need to identify and characterize novel genes involved in haematopoiesis	56
1.15 Current genetic tools and strategies in zebrafish Genetics	57
1.16 The <i>Tol2</i> transposable element as a tool for	63
Objectives	69
2. Materials and Methods	70
2.1 Materials	70
2.1.1 Zebrafish maintenance	70
2.1.2 Maintaining mutant and transgenic fish lines	71
2.1.2.1 Cloning of gene/enhancer trap vector <i>ptol2rst</i>	72
2.1.2.2 Creation of the <i>Flk1:tomato</i> transgenic line	73
2.1.2.3 Construction of the transgenic line <i>EfnB2a:tomato</i>	74

2.1.2.4 Construction of the transgenic line <i>12xCLS:cerulean</i>	75
2.1.2.5 The <i>pCS-TP</i> vector was used to produce <i>transposase</i>	76
2.1.3 Buffers, Solutions and Primers	78
2.2 Methods	81
2.2.1 DNA Preparation	81
2.2.1.1 Transformation and bacterial overnight cultures	81
2.2.1.2 Preparation of plasmid DNA	82
2.2.1.3 Restriction digest	82
2.2.1.4 Agarose gel electrophoresis	83
2.2.1.5 Gel- extractions	84
2.2.1.6 (Self) Ligation reactions	85
2.2.1.7 Phenol- Chloroform Extraction	85
2.2.1.8 Isolation of high molecular weight genomic DNA	85
2.2.1.9a PCR	86
2.2.1.9b Inverse PCR	86
2.2.1.9c Nested PCR	87
2.2.1.10 Southern blot	87
2.2.1.11 RNA extraction and cDNA synthesis	90
2.2.1.12 Reverse transcription	90
2.2.1.13 Whole mount <i>in situ</i> hybridisation	90
2.2.1.14 Immuno-histochemistry	96
2.2.1.15 Embedding zebrafish embryos in JB4 plastic	98
2.2.1.16 Plastic sectioning of zebrafish embryos	98
2.2.3 Manipulation of zebrafish embryos	99
2.2.3.1 Microinjections into early stage embryos	99
2.2.3.2 Treatment of zebrafish embryos with small inhibitor Molecules	101
2.2.3.3 Experiments with Tg (<i>hsp70:Gal4/ UAS: NICD/</i> <i>Gfi1.1:eGFP</i>)	102
2.2.3.4 Fluorescence-Activated Cell Sorting (FACS)	102

3. Results

3.1 Injection of the gene/enhancer trap vector <i>tol2rst</i> generates transgenic fish lines with ubiquitous and tissue-specific eGFP reporter expression during early embryogenesis	104
3.1.1 Micro-injection of the gene trap vector <i>ptol2rst</i> into one cell stage embryos	104
Summary of Chapter 3.1	107
3.2 A subset of F1 fish display reporter gene expression in a tissue-specific manner	107
Summary of chapter 3.2	111
3.3 Two transgenic fish lines displayed tissue-specific expression patterns in haematopoietic cells	112
3.3.1 The transgenic line <i>SN173-11:eGFP</i> expresses eGFP in the cells of the hatching gland and in circulating round cells	112
3.3.2 The transgenic line <i>I-551:eGFP</i> expresses the reporter gene in haematopoietic tissues throughout development	114
3.3.3 Reporter gene expression in the transgenic line <i>I-551:eGFP</i> is restricted to primitive erythrocytes and endothelial cells in the DA at 26 hpf	119
Summary of chapter 3.3	121
3.4 <i>I-551:eGFP</i> is expressed in hematopoietic cells	122
3.4.1 EGFP expression in primitive red blood cells decreases in <i>Tg(I-551:eGFP;Gata1:dsRED)</i> after 30hpf	122
3.4.1.1 Circulating round cells in the transgenic line <i>I-551:eGFP</i> co-express the erythrocyte marker gene <i>gata1</i> at 26hpf	122
3.4.1.2 Flow cytometrical analysis of <i>I-551:eGFP;Gata1:dsRed</i> allows to separate haematopoietic and endothelial cells at 26 hpf	123
3.4.1.3 In <i>Tg(I-551:eGFP/Gata1:dsRed)</i> transgenic embryos different subtypes of haematopoietic cells are labelled in the posterior blood island	127

3.4.1.4 Flow cytometrical analysis of embryos at 30hpf reveals a decrease in eGFP expression in primitive erythrocytes	129
3.4.5 The endothelial eGFP expression in the transgenic line <i>I-551:eGFP</i> is restricted to the ventral wall in the DA	132
3.4.5.1 <i>I-551:eGFP</i> and <i>Flk1:tomato</i> are co-expressed in the artery at 26hpf	132
3.4.5.2 <i>EfnB2a:tomato</i> and <i>I-551:eGFP</i> are co-expressed in the ventral wall of the artery at 27 hpf	134
3.4.5.3 <i>12xCLS:cerulean</i> and <i>I-551:eGFP</i> are co-expressed in the ventral wall of the artery at 28hpf	136
Summary of chapter 3.4	138
3.5 The trapped gene in the transgenic line <i>I-551:eGFP</i> is identified as <i>gfi1.1</i>	139
3.5.1 Southern blot analysis of <i>Tg(I-551:eGFP)</i> reveals 7 genomic integrations of the gene trap vector <i>ptol2rst</i>	139
3.5.2 The <i>ptol2rst</i> insertion is mapped to the first intron of <i>gfi1.1</i>	141
3.5.3 Two sets of PCRs confirm the insertion in <i>I-551:eGFP</i> as <i>gfi1.1</i>	143
Summary of chapter 3.5	145
3.6 <i>Gfi1.1</i> is expressed in the haemogenic endothelium	146
3.6.1 Endothelial eGFP expression in <i>gfi1.1:eGFP</i> is downstream of VEGF signalling	146
3.6.2 Notch signalling is required for the formation of eGFP positive endothelial cells in <i>Gfi1.1:eGFP</i> transgenic embryos	148
3.6.2.1 Endothelial expression of eGFP in the <i>Gfi1.1:eGFP</i> transgenics can be blocked by DAPM treatment	148
3.6.2.2 Blocking the <i>notch</i> pathway by injecting the <i>rpja/b</i> morpholino abrogates endothelial expression of <i>Gfi1.1:eGFP</i>	151
3.6.2.3 <i>Gfi1.1:eGFP/mib^{-/-}</i> mutant embryos lack reporter gene expression in endothelial cells	153
3.6.3 <i>Gfi1.1</i> positive cells in the wall of the dorsal aorta also express the haematopoietic marker genes <i>runx1</i> and <i>c-myb</i>	156
Summary of chapter 3.6	159

3.7 The dose and timing of <i>notch</i> signalling impacts the expression of <i>gfi1.1</i> in endothelial cells	160
3.7.1 Over-expression of <i>NICD</i> in <i>Gfi1.1:eGFP</i> transgenics leads to an expansion of <i>gfi1.1</i> positive endothelial cell population	160
3.7.2 Notch signalling is needed before 18 somite cell stage for endothelial <i>gfi1.1</i> expression in the ventral artery	163
Summary of chapter 3.7	166
3.8 <i>Runx1</i> and blood circulation are essential for the seeding of the CHT by <i>gfi1.1</i> positive cells	166
3.8.1 In <i>silent heart</i> morphant embryos <i>Gfi1.1:eGFP</i> positive red blood cells do not switch off the eGFP expression after 30 hpf and the endothelial cells remain flat	166
3.8.2 <i>Runx1</i> morphants have no <i>Gfi1.1 eGFP</i> positive cells in the caudal haematopoietic tissue at 50 hpf	170
Summary of chapter 3.8	174
3.9 <i>Phosphoinositide 3-kinase</i> pathway is essential for <i>gfi1.1</i> positive cell development in the ventral DA	175
Summary of chapter 3.9	177
3.10 <i>Gfi1.1</i> positive cells detach from the haemogenic endothelium and join the blood circulation	178
Summary of chapter 3.10	180
3.11 <i>Gfi1.1</i> positive cells are found in the kidney of adult fish	180
Summary of chapter 3.11	183
3.12 Zebrafish <i>gfi1.1</i> is a homolog of the mouse <i>Gfi1</i>	184
3.12.1 Identification of the novel gene <i>gfi1b-like</i> in zebrafish	185

3.12.2 The novel transcript <i>gfi1b-like</i> is an ortholog of the murine <i>Gfi1b</i> gene	188
Summary of chapter 3.12	189
3.13 The expression patterns of GFIs during zebrafish development	190
3.13.1 The mRNA expression pattern of <i>gfi1.1</i> is similar to the expression of eGFP in <i>gfi1.1:eGFP</i> transgenics	190
3.13.2 The mRNA expression profile of <i>gfi1.2</i> throughout development reveals expression in the ventral wall of the dorsal aorta at 2 dpf	193
3.13.3 The novel transcript <i>gfi1b-like</i> is exclusively expressed in erythroid cells	194
Summary of chapter 3.13	197
Discussion	198
4.1 <i>ToI2</i> mediated transgenesis in zebrafish is an effective tool to generate transgenic animals	200
4.2 The trapped gene in <i>I-551:eGFP</i> is identified as <i>gfi1.1</i>	201
4.3 The transgenic line <i>Gfi1.1:eGFP</i> expresses eGFP in multiple haematopoietic tissues	202
4.4 The endothelial expression in <i>Gfi1.1:eGFP</i> is downstream of <i>vegf</i> and <i>notch</i> signalling	208
4.5 <i>Gfi1.1</i> positive cells need blood flow to seed the CHT	211
4.6 <i>Gfi1.1</i> positive cells are putative HSCs in zebrafish	213
4.7 The <i>Gfi1.1:eGFP</i> transgenic line is a powerful tool to study zebrafish HSC formation	214

4.8 The <i>Gfi1.1:eGFP</i> transgenic line is a powerful tool to study zebrafish HSC formation	218
Summary	221

Supplemental material

Supplemental Figure 1: An overview of the tomato expression in the transgenics <i>Flk1:tomato</i> and <i>EfnB2a:tomato</i> at 25 hpf and 27 hpf respectively	224
Supplemental Figure2, Gfi sequences used for the building of the phylogenetic tree	225
Figure 3, supplemental data: <i>runx1</i> and <i>I-551</i> expression in the ventral artery are lost in DAPM treated embryos	230
Figure 4, supplemental data: c-myb positive cells are decreased in <i>runx1</i> morphants	231
Supplemental Figure 5: Primitive red blood cells in Ly 294002- treated embryos are stuck between the blood vessels	232
References	222

The movies are attached on the CD-disk.

Supplemental movie 1, I-551andgata1-26hpf co animation

Supplemental movie 2-I-551 gata1 pbi 30 hpf

Supplemental movie 3 I-551gata1sih50hpf

I-551 gata1 37hpf timelapse1

Flk1tomato/Gfi1.1eGFP 33 hpf time lapse

List of Figures

Figure 1.1: Classical model of the haematopoietic developmental hierarchy	26
Figure 1.2: Classical model of blood island Development	30
Figure 1.3: Hematopoietic stem cells are generated intra-embryonically	32
Figure 1.4: Haematopoiesis in the mouse embryo	34
Figure 1.5 Models of hematopoietic stem cell emergence within the embryo	38
Figure 1.6: Endothelial and haematopoietic cell formation during somitogenesis	40
Figure 1.7: Haematopoietic and endothelial genes are expressed in the midline at 24 hpf	41
Figure 1.8: Definitive haematopoiesis is initiated in the ventral wall of the dorsal aorta	47
Figure 1.9: <i>C-myb</i> positive cells are found in the CHT before they colonize the adult haematopoietic sites, the thymus and the kidney	50
Figure 1.10: Signalling molecules involved in DA specification and HSC emergence	55
Figure 1.11: Transposon-based gene- trapping vectors	66
Figure 2.1: Construct map of the gene/enhancer trap <i>pTol2rst</i>	72
Figure 2.2: The <i>Flk1:tomato</i> construct	73
Figure 2.3: The <i>EfnB2a:tomato</i> construct	74
Figure 2.4: The <i>12xCLS:cerulean</i> construct	75

Figure 2.5: the vector map of <i>pCS-TP</i>	76
Figure 2.6: <i>Gfi1.1</i> and <i>gfi1b-like</i> fragments in <i>pGEMT</i> Vector	91
Figure 3.1: Germ line transmission frequency in zebrafish embryos injected with <i>tol2rst</i>	106
Figure 3.2 Examples of embryos with tissue-specific eGFP expression	110
Figure 3.3: Primitive erythroid cells are labelled in <i>SN 173-11</i> transgenics	113
Figure 3.4a: <i>I-551:eGFP</i> is expressed in putative haemogenic endothelium and primitive red blood cells	115
Figure 3.4b: <i>I-551:eGFP</i> transgenics retain eGFP expression in haematopoietic sites into larval	116
Figure 3.5: Transverse sections through the trunk of a 5 dpf embryo reveals eGFP expression in the kidney, spleen and pancreas	118
Figure 3.6: EGFP is expressed in the ventral wall of the dorsal aorta in the transgenic line <i>I-551:eGFP</i> at 26hpf	120
Figure 3.7: <i>I-551:eGFP</i> and <i>Gata1:dsRED</i> are co-expressed in the primitive erythrocytes at 26 hpf	123
Figure 3.8a: Control FACS plots which were used to analyse Tg (<i>I-551:eGFP</i>; <i>Gata1:dsRED</i>) embryos at 26 hpf and 30 hpf	125
Figure 3.8b: <i>I-551</i> positive primitive red blood cells and endothelial cells can be efficiently separated by using FACS	126
Figure 3.9: The PBI of <i>I-551:eGFP</i> and <i>Gata1:dsRED</i> double transgenic embryos show a decreased expression of eGFP in primitive red blood cells at 30hpf	128
Figure 3.10: <i>I-551:eGFP</i> primitive erythrocytes decrease in their fluorescence after 30 hpf	130
Figure 3.11: <i>I-551:eGFP</i> and <i>Flk1:tomato</i> are co-expressed in the ventral wall of the dorsal aorta	133

Figure 3.12: EGFP and Tomato are co-expressed in the ventral wall of the DA in Tg(<i>I-551:eGFP</i> ; <i>EfnB2a:tomato</i>) embryos	135
Figure 3.13: <i>notch</i> signalling is active in <i>I-551</i> positive cells of Tg (<i>I-551:eGFP</i> ; <i>12xCLS:cerulean</i>)	137
Figure 3.14: Southern blot analysis of Tg(<i>I-551:eGFP</i>) and Tg(<i>173-11:eGFP</i>)	140
Figure 3.15: The insertion responsible for the reporter gene expression in the line <i>I-551:eGFP</i> can be localized to the gene <i>gfi1.1</i>	141
Figure 3.16: nested Inverse PCR with gDNA from <i>I-551:eGFP</i> and <i>SN:413:eGFP</i>	143
Figure 3.17: PCR on genomic DNA confirms the trapped gene in the transgenic line <i>I-551:eGFP</i> as <i>gfi1.1</i>	144
Figure 3.18: Endothelial <i>Gfi1.1:eGFP</i> expression is lost in embryos treated with 5 μ M VegfR inhibitor	145
Figure 3.19: Endothelial expression of <i>Gfi1.1:eGFP</i> is lost in DAPM treated embryos	150
Figure 3.20: <i>Rpbja/b</i> MO-injected <i>Gfi1.1:eGFP</i> embryos lose eGFP expression in the ventral wall of the DA	152
Figure 3.21: Endothelial expression of <i>Gfi1.1:eGFP</i> is lost in <i>mib</i> ^{-/-} embryos	154
Figure 3.22: <i>Gfi1.1</i> and <i>runx1</i> are co-expressed in the ventral wall of the dorsal aorta at 26 hpf	157
Figure 3.23: <i>Gfi1.1</i> and <i>c-myb</i> are co-expressed in the ventral wall of the DA	158
Figure 3.24: Over expression of NICD leads to an expansion of endothelial <i>Gfi1.1</i> positive cells into the vein	162
Figure 3.25: DAPM treatment reveals the need for <i>notch</i> signalling in HSC formation up until 18 somite stage	165
Figure 3.26: The endothelial cells in <i>Gfi1.1:eGFP</i> embryos injected with <i>sih</i> antisense morpholino remain flat	167

Figure 3.27: Z-stack images reveal the absence of <i>gfi1.1:eGFP</i> positive cells in the posterior blood island of <i>sih</i> depleted embryo	169
Figure 3.28: <i>Runx1 MO</i> injection does not abrogate <i>gfi1.1</i> expression at 27 hpf	171
Figure 3.29: The number of <i>gfi1.1</i> eGFP positive cells are reduced in the CHT of <i>runx1</i> morphants at 50 hpf	172
Figure 3.30: <i>Gfi1.1</i> positive endothelial cells are lost in LY294002 treated embryos	176
Figure 3.31: A <i>Gfi1.1:eGFP</i> positive cell leaves the haemogenic endothelium	179
Figure 3.32a: Light scatter view of <i>Tg(Gfi1.1:eGFP; Gata1:dsRED)</i> WKM and fluorescent view of wild-type WKM	181
Figure 3.32b: <i>Gfi1.1:eGFP</i> positive cells are present in the WKM of adult <i>Tg(Gfi1.1:eGFP;Gata1:dsRED)</i> fish	182
Figure 3.33a: A zebrafish locus on Chromosome 21 has a high similarity with the mouse GFI1B	186
Figure 3.33 b: LOC100151531 encodes an uncharacterised protein in zebrafish	187
Figure 3.34: Evolutionary relationships of the zebrafish GFI1.1, GFI1.2 and GFI1B-like (LOC100151531)	188
Figure 3.35: Early expression pattern of <i>gfi1.1</i> in the zebrafish embryo	191
Figure 3.36: <i>Gfi1.1</i> is expressed in the artery at 30 hpf	192
Figure 3.37: <i>Gfi1.2</i> is expressed in the ventral wall of the DA at 2 dpf	194
Figure 3.38: <i>Gfi1b</i> expression marks the development of primitive red blood cells	195
Figure 3.39: <i>Gfi1b</i> expression is restricted to the erythroid lineage	196
Figure 4.1: <i>Tg (Gfi1.1:eGFP)</i> is more restricted in its expression pattern than <i>Tg (Runx1:eGFP)</i>	219

List of Graphs and Tables

Buffers and Solutions	78
Primers	80
List of probes	92
List of morpholinos	100
Table 3.1: Survival rate of embryos injected with <i>tol2rst</i>	105
Table 3.2: Cell count of embryonic cell extracts	131
Table 3.3: Cell count of whole kidney marrow extracts	183
Graph1: The number of eGFP positive cells in the CHT of <i>gfi1.1</i> embryos is significantly lower in <i>runx1</i> morphants than in wild type embryos	218

Abbreviations:

Ac-LDL	acetyl low density lipoprotein
AGM	aorta-gonad-mesonephros
ALM	anterior lateral mesoderm
amp	ampicillin
bea	beamter
BL-CFC	blast colony-forming cells
BMP	bone morphogenetic protein
BM	Bone marrow
BMSU	Biomedical science unit
bp	base pair
BSA	Bovine serum albumin
CD	Cluster of differentiation
CFU-C	Colony forming units-colony
CFU-S	colony forming units-spleen
CHT	caudal haematopoietic tissue
CLP	common lymphoid progenitor
CMP	common myeloid progenitor
CMV	cytomegalovirus
CVP	caudal vascular plexus
Dil-AcLDL	1,1'-dioctadecyl-3,3',3'- Tetramethylindocarbocyania- labeled Ac-LDL
DLP	dorsal lateral plate
DMNB	2,3-dimethyl-2,3- dinitrobutane
DMSO	Dimethylsulfoxide
dpf	day post-fertilised
E	Embryonic day
EGFP	enhanced green fluorescent protein
EMP	Erythro-myeloid progenitor
ENU	N-ethyl N-nitrosourea
ES	embryonic stem cells
EST	Expressed sequence tags
FACS	Fluorescent activated cell sorting
flu	flurescein
FP	Frog prince
FS	forward scatter
FSC	Foetal calf serum
g	gram
GMP	granulocyte-monocyte progenitor
hpf	Hour post-fertilised
HSC	Haematopoietic stem cell
Hsp70	Heat shock promoter 70
Hrp	Horse radish peroxidase
ICM	intermediate cell mass
ISV	Intersomitic vessel
ITR	Internal terminal repeats
kb	kilo base pair

L	liter
LB-medium	Luria-Bertani medium
LSK	Lineage- Sca1+ c-kit+
LT-HSC	Long term haematopoietic stem cell
MEP	Megakaryocyte/erythroid progenitor
ml	millilitre
MLV	Maloney lenti virus
mib	Mind bomb
MPP	Multi potential progenitor
MO	morpholino
mRNA	messenger Ribonucleotide
NC	notochord
NCID	Notch intercellular domain
NK	Natural killer cells
ng	nanogram
nM	nanomol
NO	Nitric oxide
NT	neural tube
PAC	P1-derived artificial chromosome
PBI	Posterior blood island
PCR	polymerase chain reaction
PCV	posterior cardinal vein
PGE2	prostaglandin E2
PLM	posterior lateral mesoderm
Poly(A)	Poly adenylation site
PTU	phenylthiourea
RT	room temperature
SB	Sleeping beauty
Sih	silent heart
smo	slow muscle-omitted
SP	Side population
SS	side scatter
ST-HSC	Short-term haematopoietic stem cell
Su(H)	suppressor of hairless
SNP	Single nucleotide polymorphism
syu	sonic you
Tg	Transgenic line
TILLING	Targeting Induced Local Lesions in Genomes
UTR	untranslated region
UAS	Upstream activator sequence
UV	Ultra violet
VEGF	vascular endothelial growth factor
VEGFR	vascular endothelial growth factor receptor
VSV	Vesicular stomatitis virus
yot	You too
WKM	Whole kidney marrow
WT	Wild type

Introduction

1.1 Haematopoiesis

The blood system of an adult human replaces a trillion of blood cells each day (Emerson et al, 1991). This lifelong process involves gradual differentiation of a multipotential haematopoietic stem cells into more lineage restricted progenitor cells and finally to the unipotent, functionally distinct and differentiated blood cell types, including red blood cells, monocytes/macrophages, platelets, lymphocytes, neutrophils, eosinophils and basophils. The haematopoietic stem cell is further characterised by its ability to self-renew. Self-renewal involves asymmetrical or symmetrical divisions of HSCs that result in one or two daughter cells with the same developmental potential as the mother cell (reviewed in He et al, 2009). This ability ensures to keep the pool of HSC constant, even after injuries, when elevated numbers of blood cells need to be produced.

In developing mouse embryos, blood formation first occurs as cell clusters in the yolk sac, which are called blood islands. Subsequently, haematopoietic cells are generated in different tissues of the embryo including the allantois, placenta and the aorta-gonad-mesonephros (AGM) region and the cells colonize the haematopoietic sites such as the liver, thymus, spleen and the bone marrow after the onset of blood circulation at around embryonic day E8 in the embryo (Figure 1.4, for a review see Dzierzak et al, 2008). Once the bone marrow has developed, the bone marrow eventually starts to form the blood cells for the entire organism. However, maturation, activation, and some proliferation of lymphoid cells occur in secondary lymphoid organs (spleen, thymus and lymph nodes).

1.2 Characterisation of HSCs

HSCs are defined as cells, which have the potential to fully replenish the adult blood system, give rise to all blood lineages and have the ability to self-renew. In the 1950s and 1960s bone marrow (BM) cells were transplanted into lethally irradiated mice. These donor BM cells were found to generate microscopic erythro-myeloid colonies in the spleen of the host after 12 days (McCulloch et al, 1960; Till et al, 1961; Becker et al, 1963). The number of colonies grew in proportion to the amount of BM cells injected and each colony was shown to be of clonal origin (Till et al, 1961; Becker et al, 1963). The self-renewal property of these cells was shown by transplanting cells from a single colony into a new recipient and the donor cells were able to give rise to new colonies in the recipient (Siminovitch et al, 1963). The cells were termed colony forming units spleen (CFU-S). These experiments provided first evidence for the existence for a group of cells in the BM, which have the potential for extensive proliferation, differentiation and self-renewal. In the following years haematopoietic progenitor cells were further enriched by physical e.g. equilibrium density centrifugation and cell surface characteristics (Visser et al, 1981; Visser et al, 1984) by up to 80 fold. The development of fluorescence-activated cell sorting (FACS) helped the researchers in the field enormously to separate cells based on their surface phenotype. The purified cells were then tested *in vivo* by transplanting them into irradiated mice (reconstitution assay) in order to assess if they could reconstitute the blood system and/or *in vitro* by their ability to form colonies of differentiated cells in culture (for a review see Purton et al, 2007). Using this strategy, a number of cell surface marker were identified to be expressed on hematopoietic progenitors and used to define haematopoietic progenitors (Muller-Siegburg et al, 1986; Smith et al, 1991; Okada et al, 1992). At the same time, assays to test the potential of the haematopoietic cells were developed. In the reconstitution assay, the BM cells need to have the ability to differentiate into all blood lineages, be

able to proliferate and to self-renew in order to fully reconstitute the recipients' blood system. In the serial transplantation assay, the cells are transplanted serially into irradiated recipients, mainly to test the extent of their self-renewal capacity (Lemischka et al, 1986). The idea is that the most immature haematopoietic progenitor should be able to reconstitute the blood system in each of the recipients. The competitive repopulation assay (Harrison et al, 1980) is able to test the re-populative and proliferative capacity of the cells in comparison to wild-type cells. In this assay, a set number of cells from two types of donors are transplanted into irradiated recipients and allowed to compete with each other. Since both cell groups are distinguishable from each other based on their congenic traits, this experiment can determine if one cell group has an advantage over the second group of cells by analyzing the contribution of each cell population to the engraftment of the host. The limiting dilution assay allows to enumerate HSCs. Here, a descending number of potential progenitors are transplanted into irradiated mice in order to define the minimal number of cells needed for multi-lineage, long-term reconstitution (Szilvassy et al, 1990). These approaches have helped to subdivide the haematopoietic progenitors into different sub-classes. Long-term repopulating stem cells (LT-HSCs) have the ability to reconstitute the blood system for life, whereas the short-term subset retains this ability only up to 8 weeks (Osawa et al, 1996).

Today, LT-HSCs can be isolated and characterised with different methods. One of these methods to purify HSCs is based on the Hoechst 33342 dye. This fluorescent dye is actively and specifically effluxed out of HSCs and therefore these cells are located in the side population on the FACS plot and are hence termed side population (SP) cells (Goodell et al, 1996). The most widely used method to isolate HSCs is to sort the cells for the presence or absence of surface markers. Most of the markers used to enrich HSCs are developmental stage, context and species dependent and are often

expressed by many different cell types. Therefore, multiple surface markers and cell properties like the side population property are used in combination (for a review see Rossi et al, 2011). Classically, the presence or absence of a variety of cell surface molecules on white blood cells, called clusters of differentiation (CD), are used to enrich HSCs. Recently, a new group of cell surface markers termed SLAM factors, CD 150, CD 244 and CD 48 have been introduced to enrich LT-HSCs (Kiel et al, 2005). Almost all of the HSC purification methods in mouse are based on the positive selection for the markers *C-kit* and *Sca-1* and negative selection for markers of mature haematopoietic cell lineages (*Lin*⁻) (LSK) (see Figure 1.1). In order to further enrich HSCs, a variety of strategies can be applied. Based on the two additional markers CD34 and CD135 for example, the HSCs can be separated into long-term HSCs (LT-HSCs) (LSK CD34⁻ CD135⁻), short-term HSCs (ST-HSCs) (LSK CD34⁻ CD135⁺) and multipotential progenitors (MPP) (LSK CD34⁺ CD135⁺) (Figure 1.1; Yang et al, 2005; Challen et al, 2009). These subclasses represent approximately 0.007%, 0.04% and 0.05% of the total BM respectively. These numbers indicate the low abundance of HSCs in the BM, but with the use of multiple markers, HSCs can be purified to a high degree. Recent publications show multi-lineage engraftment of the host with 1 out of 2 cells (Yilmaz et al, 2006) when LSK CD150⁺CD48⁻ HSCs are used, compared to 1 out of 5 if the SLAM factors, CD150⁺CD48⁻ are used for the HSC purification process (Kiel et al, 2005) and 1 out of 10 cells if the LSK compartment alone is employed for the transplantation (Morrison et al, 1994).

Clinical approaches such as bone marrow transplants into patients with leukemia or lymphoma benefit from HSC research. However, a large numbers of purified HSCs are needed to successfully reconstitute the patient's blood system. At the moment, bone marrow transplants require HLA- matched siblings and still there is a 5-10% mortality

rate due to graft versus host disease (Persons et al, 2009). The main aim of the research is to either find ways to expand the number of HSCs *in vitro* or to further optimize the purification process for clinical HSC transplantations. Therefore it is important to study the underlying mechanisms, which lead to HSC formation. This knowledge can help to reprogramme various cell types into LT-HSCs. Moreover, the identification of more surface markers of HSCs can help to purify these cells even further.

1.3 The hierarchy in the haematopoietic system

Based on the self-renewal capacity, HSCs can be subdivided into 2 classes: long-term HSCs and short-term HSCs (Figure 1.1; Yang et al, 2005). The ST-HSCs in turn give rise to multi-potential progenitors (MPPs) which can generate all mature blood cell types, but have no self-renewal capacity. Therefore, MPPs can only maintain the blood system transiently (Morrison et al, 1994). In the classical model, the MPPs subsequently give rise to the common lymphoid progenitors (CLP) and to the common myeloid progenitors (CMPs) that are able to generate the haematopoietic lineages through committed lineage specific progenitors. The continued loss of self-renewal capacity from the HSC to a lineage restricted progenitor is linked to a rising proliferative index. HSCs at the top of the hierarchy proliferate rarely, whereas committed oligo-progenitors have the highest proliferative rate (Figure 1.1). The rate of proliferation in the committed progenitors enables the blood system to respond to infections and blood loss efficiently. The CLP generates B- and T-cells and natural killer cells. The CMP give rise to Megakaryocyte and erythroid progenitors (MEP) and the granulocyte-macrophages progenitors (GMP) (Figure 1.1). MEPs generate erythrocytes and Megakaryocyte, while the GMP gives rise to macrophages and neutrophils, eosinophils and basophils. The

cellular origin of the dendritic cells remains unclear (Figure 1.1). They can be generated by CLP or CMPs. Studies in foetal liver haematopoiesis suggest that the commitment to the CLP or CMP is fluid. So far, no CLPs have been identified in the foetal liver. The cells with the phenotype of CLPs in the foetal liver found so far can also give rise to macrophages. It remains to be clarified if this fluidity in the progenitors is due to the difference in the micro-environment in the foetal liver and the bone marrow. But even in the bone marrow micro-environment, fluidity can occur. Next to the classical MPPs, which can diverge into either CLPs or CMPs, there are also haematopoietic progenitors, which only gradually lose their CMP potential and become restricted to the lymphoid lineage, once in the thymus (Kondo et al, 2010). Based on these findings, a myeloid-biased haematopoietic differentiation model is proposed. These findings support the notion at the haematopoietic hierarchy is fluid and flexible and further research need to be done to investigate relationships between the lineages in detail.

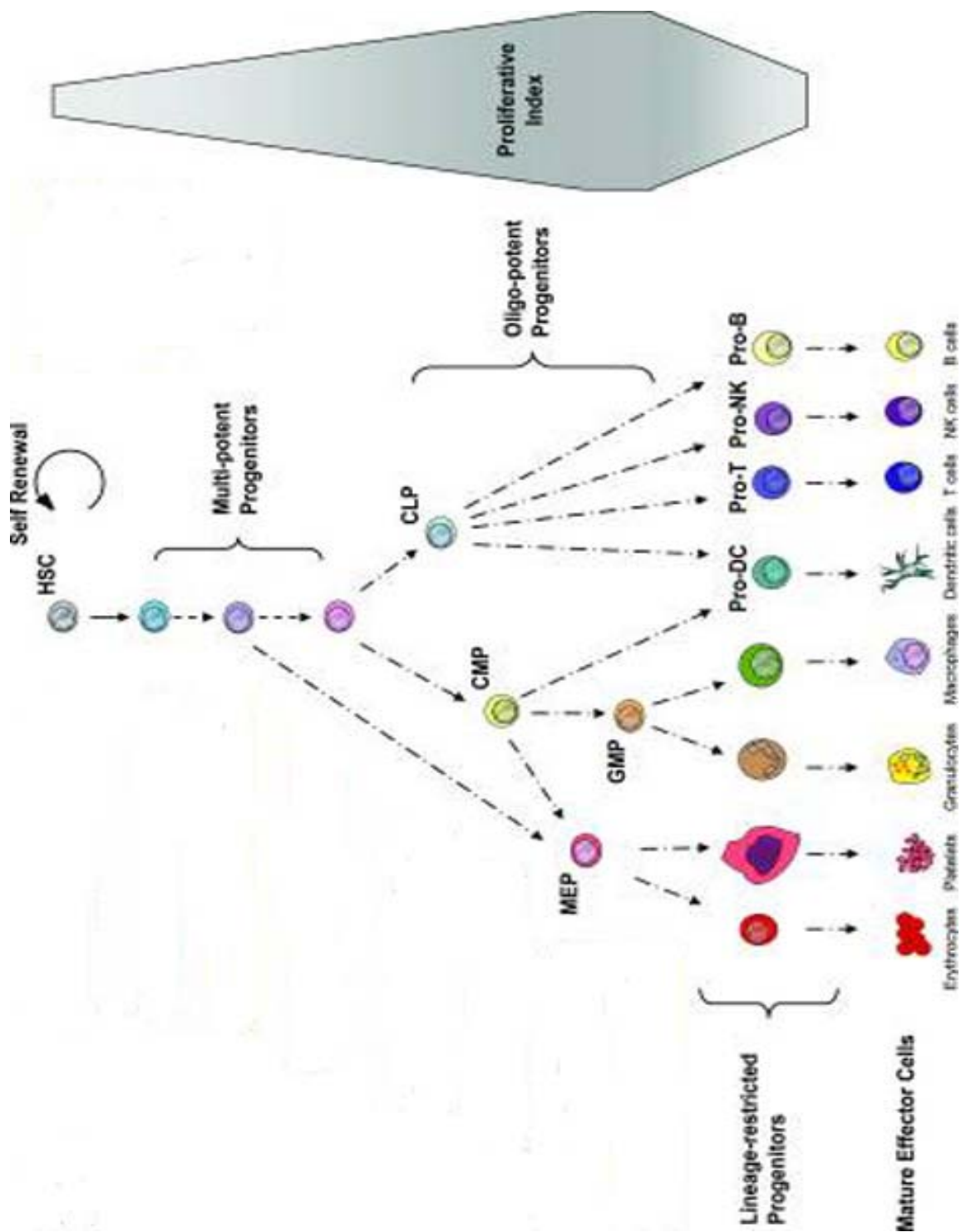


Figure 1.1: Classical model of the hematopoietic developmental hierarchy.

HSCs which reside at the top of the hierarchy give rise to multi-potent progenitors (MPPs). These MPPs generate oligo-potent progenitors, the common myeloid progenitor (CMP) and the common lymphoid progenitor (CLP). The CLP gives rise to mature B-lymphocytes, T-lymphocytes and natural killer (NK) cells. The CMP can generate granulocyte-macrophage

progenitors, which give rise to monocytes/macrophages and granulocytes. The megakaryocyte/erythrocyte progenitors differentiate into megakaryocytes/platelets and erythrocytes. Dendritic cells are believed to be derived from both CMPs and CLPs. The oligo-potent progenitors go through a number of intermediate stages before becoming lineage-restricted (not shown). The differentiation process from the HSC to a lineage-specific progenitor is generally associated with an increase in the proliferative index. The developmental relationships of some of the subsets are not fully resolved. There is evidence e.g. that the megakaryocyte and erythrocyte lineage might not pass through a CMP intermediate. Adapted from Bryder et al, 2006.

1.4 Vertebrate haematopoiesis

Vertebrate haematopoiesis can be separated into two major waves. The first primitive wave is only transient and gives rise to primitive erythrocytes and macrophages, which provide the embryo with oxygen and an innate immune defense mechanism, respectively. The second wave occurs intra-embryonically in a region where the aorta, gonad and mesonephros (AGM) form and gives rise to HSC, which then produce all blood cell lineages for life. Between these two major waves there are further haematopoietic waves in the mouse which give rise to haematopoietic cells with increasing haematopoietic potential, but which lack long-term reconstitution potential, until definitive HSCs are generated in the AGM region at embryonic day (E) 10.5 (for a review see Dzierzak et al, 2008). The pro-definitive cells have the ability to form erythro-myeloid cells and have been described in the allantois between E7.5 and E9.0 (Corbel et al, 2007; Zeigler et al, 2006), in the yolk sac between E8.25 and E9.25 (Palis et al, 1999; Rampton et al, 2003; Lux et al, 2007) and the placenta (Alvarado-Silva et al, 2003). Multi-potential haematopoietic cells with erythroid, myeloid and lymphoid potential are found in the para-aortic splanchnopleura, the prospective AGM region, before the onset of blood circulation at E8.5 (Cumano et al, 1996) (Figure 1.4, meso-definitive wave). In contrast to yolk sac derived cells, cells isolated from the prospective

AGM region have the ability to reconstitute recipients with multi-lineage haematopoiesis at a low level after being in organ culture for 4 days (Cumano et al, 2001). A further class of haematopoietic progenitors are found at E9.0,, just after blood circulation started at E8.5, in the yolk sac and the AGM region (Figure 1.4, meta-definitive progenitors) (Yoder et al, 1997; Medvinsky et al, 1993). These haematopoietic progenitors have the ability to reconstitute only new born mice, but not adult recipients (Yoder et al, 1997). *In vitro* culture assays have shown that these meta-definitive cells can also form CFU-S (Medvinsky et al, 1993). HSCs, which have the potential to engraft adult recipients with long-term, multi-lineage haematopoiesis, are only generated at E10.5 in the AGM. This thesis will focus on the first primitive wave and the adult definitive wave, which generates LT-HSCs (Figure 1.4).

1.5 Primitive haematopoiesis in vertebrates

The first haematopoietic cells to arise in the embryo are primitive erythrocytes that form in close association with the developing blood vessels (Sabin et al, 1920). Based on their close proximity, it was postulated that they are derived from a common progenitor for blood and endothelial cells, the haemangioblast. The first evidence for the existence of haemangioblasts came from *in vitro* models of yolk sac haematopoiesis. The strategy used the ability of embryonic stem (ES) cells to generate various differentiated cell types, including blood progenitors. Using this system, a precursor cell type, called blast colony forming cell (BL-CFC) was identified, which could give rise to haematopoietic and endothelial cells (Kennedy et al, 1997; Choi et al, 1998). *In vitro*, these cells express the genes *fetal liver kinase 1 (kdrl/flk1)* which encodes a receptor for the vascular endothelial growth factor (vegf) and the mesodermal transcription factor *brachyury* (Fehling et al, 2003). Embryonic cells co-expressing both of these genes were identified *in vivo*, in the posterior region of the primitive streak stage (E7- E7.25) of

the mouse embryo, prior to the yolk sac development (Huber et al, 2004). But these cells are very rare in the embryo with numbers ranging between 1 and 5 per embryo at E7 (Huber et al, 2004). The existence of the haemangioblast is further supported by the fact that *flk1* knock-out mice do not form blood islands (Shalaby et al, 1995; 1997) arguing for a common precursor for haematopoietic and endothelial lineage. Cell labeling experiments with caged fluorescein in gastrulating zebrafish embryos has also been able to identify bi-potential progenitors for endothelial and haematopoietic cells (Vogeli et al, 2006). In the classical view, these mesodermal cells migrate from the primitive streak of the mouse conceptus to the extra-embryonic yolk sac and there form blood islands. In the blood islands, the peripheral cells differentiate into endothelial cells while the inner cells turn into primitive red blood cells (Jaffredo et al, 2005; Palis et al, 2001). The concept that blood and endothelium of one blood island are derived from resident haemangioblasts was challenged recently. Using lineage tracing experiments, Ueno et al showed that endothelial and haematopoietic cells in blood islands are derived from different progenitors (Ueno et al, 2006). This data is consistent with the fact that haemangioblasts *in vivo* are very rare and of transient nature (Huber et al, 2004; Vogeli et al, 2006). Therefore the majority of the endothelial cells might be of non-haemangioblastic origin. The first primitive red blood cells from the blood island enter circulation at E8.5 and are distinct from adult red blood cells (Palis et al, 2001). They are larger in size and retain their nuclei while entering circulation (Palis et al, 2001). The primitive red blood cells can be found in circulation for several days after birth (Kingsley, 2004).

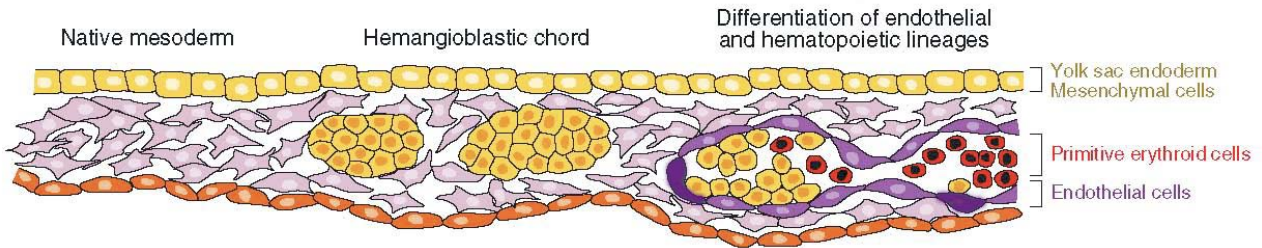


Figure 1.2: Classical model of blood island development in the mouse yolk sac the schematic shows the differentiation of endothelial and haematopoietic cells from the haemangioblastic chord. The inner cells of this chord develop into primitive red blood cells while the outer cells take on endothelial fate. Adapted from Cumano and Godin, 2007.

In the following phase, the yolk sac generates definitive myelo-erythroid progenitors (Cumano et al, 1996, Palis et al, 1999), which are believed to seed the fetal liver and differentiate into adult blood cells (Mikkola et al, 2006). The adult erythrocytes are smaller, express only adult globin genes and enucleate before entering circulation.

The yolk sac was also regarded as the source for HSC formation since it is the first embryonic site of blood production. In addition, experiments with avian embryos supported this view. Male and female sex chromosomes are easily distinguishable in chicks. This cell tracking method was used to study the engraftment of haematopoietic tissues by joining the yolk sac vasculature of the embryos and by analyzing the contribution of the donor cells to different haematopoietic compartments in the recipient (Moore et al, 1965; 1967). The engrafting HSCs in the recipients were thought to be located in the yolk sac of the donor (Moore et al, 1965). Dieterlen-Lièvre challenged the concept that HSCs are generated in the yolk sac by creating chick and quail chimeras consisting of chick yolk sac and quail embryonic tissue. Here, early embryos (E2) without a developed vasculature were used to avoid cross-contamination by circulating precursors (Figure 1.3). In the initial phase of the development, the majority of the blood cells were derived from the chick, but haematopoietic cells derived from the quail

embryonic tissue were over-represented in the chimeras just before hatching (Dieterlen-Lièvre, 1975). Thus, the definitive haematopoietic cells must have formed intra-embryonically. But there is also evidence that yolk sac cells contribute towards multi-lineage haematopoiesis. Embryonic cells from the yolk sac were isolated at E 9.0 and injected into yolk sac of age-matched mouse siblings. Histological staining of the recipient 43 days after birth revealed contribution of the donor cells to the recipient's bone marrow and thymus (Weissman et al, 1978) and transplantation of large numbers (1000) of day E9 yolk sac cells into new-born mice were able to reconstitute irradiated mice for up to 11 months (Yoder et al, 1997). In a recent publication *runx-1* positive cells were followed *in vivo* to determine their contribution to definitive haematopoiesis (Samokhvalov et al, 2007). Runx1 is not only essential for definitive haematopoiesis, but is also expressed in primitive red blood cells (Okuda et al, 1996; North et al, 1999). Transgenic *loxP-STOP-loxP-LacZ* mice are crossed to mice, which have the tamoxifen inducible *cre-recombinase* knocked into the *runx1* locus. Once these mice are mated to each other the *loxP* sites are deleted by the *cre-recombinase* in the progeny and *lacZ* expression can occur in a *runx1* specific expression pattern. The application of tamoxifen can induce time- specific labeling of *runx1* positive cells in the progeny. Samokhvalov et al could show the contribution of *runx1* positive cells from the yolk sac to adult haematopoiesis for 15 months. Furthermore, *in vitro* culture assays confirmed the presence of multipotential (erythro-myeloid) progenitors amongst the yolk sac cells (Moore et al, 1970; Nishikawa et al, 1998). The recent data suggests a contribution of yolk sac cells towards definitive hematopoietic, but it needs to be determined, how big the contribution is.

The avian yolk sac chimera experiment.

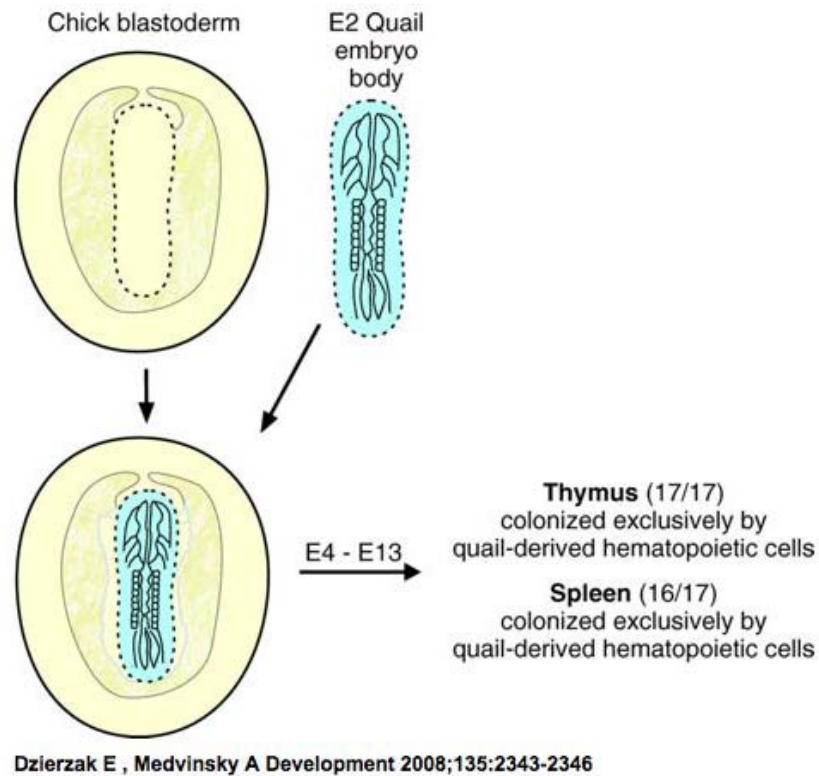


Figure 1.3: Hematopoietic stem cells are generated intra-embryonically The strategy generated to analyze the origin of HSCs in yolk sac chimeras consisted of placing a day2 (E2) quail embryo body onto a chick presumptive yolk sac before the onset of circulation in either of the tissues. The spleen and the thymus were analyzed for the natural marker that can distinguish quail cells from chick cells after several days of *in vivo* development (E4- E13). Chick cells have finely dispersed heterochromatin whereas quail embryos contain large, irregular nucleus, with a large heterochromatin mass. The analysis of the chimeras revealed that the progeny of cells derived from the quail embryo body (and not the chick yolk sac) contributed to the haematopoietic tissues in the adult. Adapted from Dzierzak and Medvinsky, 2008.

1.6 HSCs arise in the AGM of the embryo

Two groups showed that precursors with B lymphoid potential were present in the embryo, before those cells could be isolated from the yolk sac (Ogawa et al, 1988; Cumano et al, 1993). The embryonic compartment containing these precursors was finally confined to the splanchnopleura, the presumptive AGM in the embryo (Godin et al, 1993; Godin et al, 1995). The early yolk sac and the splanchnopleura were dissected out of the embryo and the cells derived from each tissue were cultured *in vitro* and analysed for its haematopoietic potential (Godin et al, 1995). Using this strategy it was shown that only the cells from the presumptive AGM could generate lymphoid cells. The cells from the AGM were shown to be multi-potential and reconstitute the blood system of adult irradiated mice with all blood lineages when harvested after E 10.5 (Muller et al, 1994; Medvinsky et al, 1996).

Other reported sources of HSCs include the vitelline and umbilical arteries and the placenta (see Figure 1.4) (Alvarez-Silva et al, 2003; Gekas et al, 2005; Ottersbach et al, 2005). Especially the placenta is thought to be a niche for HSC expansion (Cumano et al, 2007) before they seed the fetal liver. Prior to birth the HSCs colonize the bone marrow, the site of adult haematopoiesis (Figure 1.4).

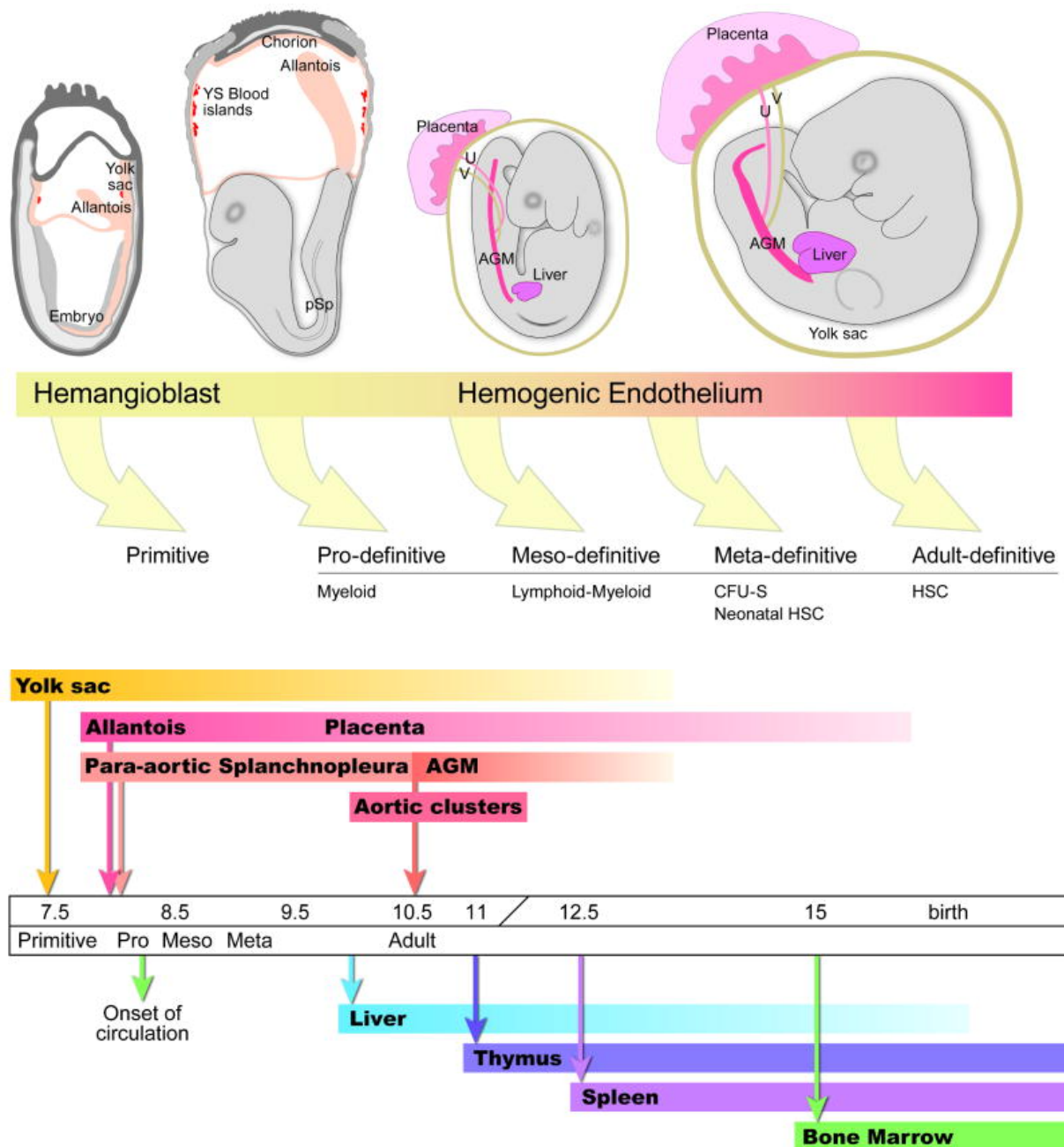


Figure 1.4: Haematopoiesis in the mouse embryo At least five classes of haematopoietic cells can be defined in the mouse embryo (indicated by the arrows) at E7.5, E8.25, E9 and E10.5 respectively. The E7.5 and E8.25 embryos show outgrowing allantois that will fuse with the chorion and form the placenta. The onset of circulation takes place between E8.25 and E8.5. The E9 embryo has turned and is enveloped in the yolk sac and the liver is seeded by haematopoietic progenitors at late E9.0. At E10.5 the embryo contains haematopoietic clusters in the AGM region, and in the vitelline (v) and umbilical (u) arteries. The arrows above time indicate the appearance of specific haematopoietic cells and the arrows below show the earliest time of colonization of the secondary haematopoietic tissue. Adapted from Dzierzak et al, 2008.

1.7 HSC emergence from the ventral aspect of the dorsal aorta

In the embryo HSCs first occur in the AGM region. In order to define the precise site of the origin of the HSCs the mouse AGM was dissected into its various components and assayed for haematopoietic activity *in vitro*. The majority of the precursors were found in the aorta and the surrounding mesenchyme (Godin et al, 1999; de Bruijn et al, 2000). By using a *sca-1* transgenic mouse line, researchers were able to show that all E11 AGM HSCs come from the dorsal aorta (deBruijn et al, 2002). Long-term repopulating HSC activity was found in the GFP positive fraction and these cells were shown to be localized in the endothelial lining of the aorta (deBruijn et al, 2002). The transcription factor *runx1* is a key regulator of HSC formation in various species (Kalev-Zylinska et al, 2002; Burns et al, 2005; for a review see Swiers et al, 2010). Although primitive erythropoiesis is almost normal (Yokomizo et al, 2008) *runx1* knock-out mice die by E 12.5 since the embryos lack fetal liver haematopoiesis due to missing HSCs (Okuda et al, 1996). *Runx1* is expressed in the ventral aorta starting from E9.5 and clusters of *runx1* positive cells were detected in the lumen of the blood vessel (North et al, 1999; 2002). These clusters of cells express the hematopoietic marker CD45 and are absent in *runx1*^{-/-} embryos (North et al, 2002). The missing cluster formation in *runx1* mutants is closely associated with lack of HSC activity (North et al, 2002; Cai et al, 2000). Histological staining for the HSC marker *CD34* in mice and humans revealed clusters of HSCs in the ventral wall of the dorsal aorta (DA) (Tavian et al, 1996; Wood et al, 1997). Such clusters were also identified in the chick, fish and amphibian embryos (Jaffredo et al, 1998; Dieterlen-Lièvre, 1981; Kalev-Zylinska, 2002; Gering and Patient, 2005; Cia-Uitz et al, 2000). Recently, Tauodi et al were able to show that only the ventral wall of the aorta gives rise to the HSCs (Tauodi et al, 2007). Here, the E11.5 aorta was

dissected into the ventral and dorsal part. 11/13 mice receiving cells from the ventral aorta were reconstituted long-term compared to 1/12 mice transplanted with the dorsal aortic cells (Taoudi et al, 2007). These observations support the view that HSC arise from the ventral wall of the dorsal aorta.

1.8 Models of HSC emergence in the ventral DA: haemogenic endothelium or definitive haemangioblasts

There are several possible modes for HSC emergence. An endothelial precursor can give rise to endothelial cells which becomes resident in the ventral aorta and later on in development gains the potential to become haemogenic endothelial cells which generate HSCs. This theory is likely since the endothelial cells and HSCs are intimately associated with each other. HSCs are most commonly observed in the ventral aspect of the endothelium, which is also referred to as the haemogenic endothelium, since it can generate definitive haematopoietic cells (Figure 1.5A). Consistent with these observations, lineage tracing experiments whereby chick and mouse endothelial cells were labeled using acetylated low-density protein with the fluorescent red dye DiI were performed (Jaffredo et al, 1998, Suriyama et al, 2003). The labeled dye is endocytosed specifically by endothelial cells and macrophages. After an incubation period, the labeled dye was also detected in *CD45* positive clusters attached to the ventral aorta, providing evidence that these cells in the clusters are derived from endothelial cells (Jaffredo et al, 1998). Retro-viral labeling of the vasculature with *lac-Z* expressing vector came to the same conclusion. The intra- and sub-aortic cell foci had an endothelial origin (Jaffredo et al, 2000). When mice endothelial cells were labeled using DiI, circulating erythrocytes were shown to be derived from endothelial cells (Suriyama et al, 2003). In fact, most of the genes, which define HSCs, are also expressed in the

endothelium of the DA at E10-E11 (Dzierzak et al, 2008). Although marker genes are not only restricted to HSCs, they are applied to characterise these cells. Several of such marker genes including *runx1*, *sca1*, *CD45* or *VE-Cadherin* are also expressed in the mesenchyme below the DA (Jaffredo et al, 1998; deBruijn et al, 2002; North et al, 2002). *VE-Cadherin*, an endothelial marker expressed in tight junctions, is also expressed by most of the AGM HSCs (Taoudi et al, 2005; North et al, 2002). Therefore, a further model proposes the mesenchyme beneath the DA as the birthplace for HSCs (North et al, 2002, Bertrand et al, 2005). The migration model (Figure 1.5 B) proposes a mesenchymal precursor cell (definitive haemangioblast), which migrates into the ventral aspect of the DA and there gives rise to endothelial and hematopoietic cells. But the contribution of these sub-aortic cells towards long-term multi-lineage haematopoiesis in adults remains unclear (North et al, 2002, Bertrand et al, 2005, Zovein et al, 2008). The conclusion remains that developing HSCs need to go through an endothelial stage. A combination of both the haemangioblast and a haemogenic endothelium model can be used to explain the existing data. In this combined model, mesenchymal haemangioblasts are able to generate a cell, which in turn gains the ability to either give rise to or turn into HSCs once in the endothelium. In support of this idea, ES-cell derived blast-colony-forming cells, which give rise to both endothelial and yolk-sac like haematopoietic components, were observed to generate a transient haemogenic endothelium (Lancrin et al, 2009). The haemogenic endothelial cells were characterized by their high expression of *tie2*, and endothelial marker and *c-kit*, a haematopoietic marker. This *tie2^{hi} c-kit⁺* population also contained *CD41⁺* and *CD41⁻* cells. *CD41* is one of the earliest HSC markers (Emambokus et al, 2003; Mikkola et al, 2003). The *CD41⁻* cells showed expression of further endothelial markers such as *flk1* and *VE-Cadherin*. Subsequently, these cells start to express *CD41* and down regulate *tie2* (Lancrin et al, 2009). *Tie2^{hi} c-kit⁺ CD41⁻* cells were also found in vivo at E10.5 in the AGM region of

mice (Lancrin et al, 2009), but further experiments are needed to see whether these cells have the same characteristics as the ES-cell derived haemangioblasts.

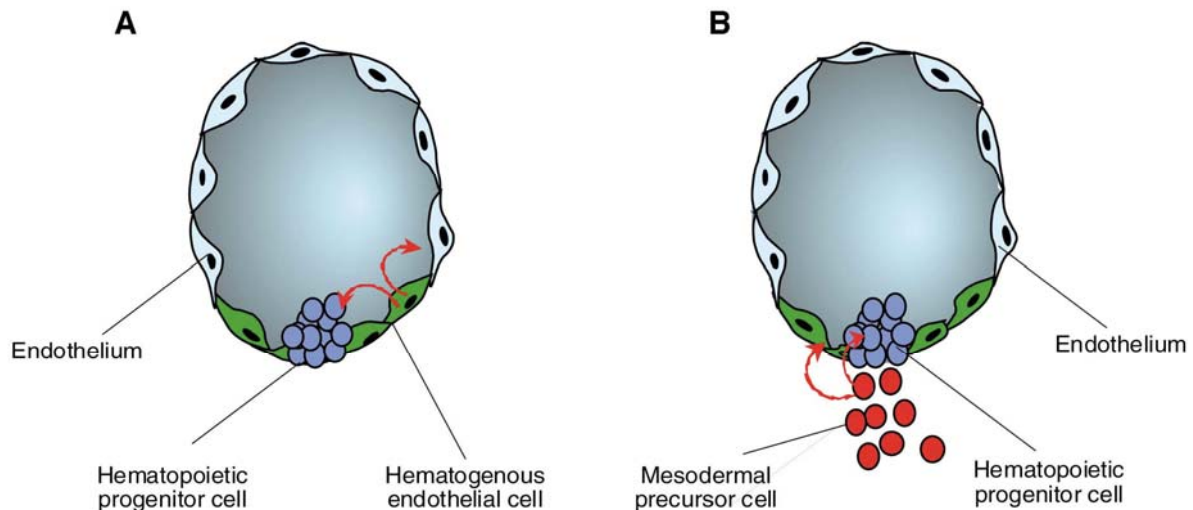


Figure 1.5 Models of hematopoietic stem cell emergence within the embryo. (A) Redifferentiation model: pre-existing endothelial cells (green) in the ventral wall of intra-embryonic arteries differentiate locally into blood cell progenitors (blue). **(B)** Migration model: haematopoietic cell precursors (haemangioblasts) (red) colonize the ventral vascular wall and give rise to endothelial cells (green) and hematopoietic cell clusters (blue). Adopted from Tavian et al, 2005.

1.9 Primitive haematopoiesis in zebrafish

Zebrafish also experience waves of haematopoiesis, but unlike in other vertebrate models, both primitive and definitive wave occur intra-embryonically in the intermediate cell mass (ICM), which is derived from the ventral mesoderm (Dietrich et al, 1995). The ICM lies wedged between the somites to either side and ventral to the notochord and gives rise to primitive red blood cells and to the two major axial blood vessels, the dorsal aorta (DA) and the posterior cardinal vein (PCV) (Figure 1.7, 1.8). The specification of the endothelial cells to either arterial or venous cell fate is established through the expression of the ligand *efnb2a* in the DA angioblasts and the receptor

efnB4 in venous cells (for a review see De Val, 2011). Lineage-tracing experiments have been able to trace endothelial and haematopoietic progenitors back to the prospective ventral mesoderm of the early embryo (Warga et al, 2009; Vogeli et al, 2006; Warga et a, 1999).

The anterior lateral mesoderm (ALM) (Figure 1.7) develops into the site of primitive myelopoiesis (macrophages and neutrophils), while the posterior lateral mesoderm (PLM) (Figure 1.7) gives rise to primitive erythrocytes (for a review see Paik et al, 2010; Palis, 2008).

From the two somites stage on, cells in the ALM and PLM begin to co-express endothelial and haematopoietic marker genes, including the transcription factors *scl*, *lmo2*, *fli1* and *etsrp* (Thompson et al, 1998; Liao et al, 1998; Gering et al, 1998; Sumanas et al, 2005; Pham et al, 2007). In the *cloche* mutants some of the essential endothelial and haematopoietic genes are absent in the ALM and PLM, including the haemangioblast genes *scl*, *lmo2*, erythro-myeloid genes *gata1*, *i-plastin*, *mpo* and the endothelial gene *kdr/flk1*, but pronephric duct cells are unaffected, arguing for a close relationship of blood and endothelial cells (Stainier et al, 1995; Liao et al, 1998; Thompson et al, 1998). *Scl* morphants also have defects in haemangioblasts specific genes. They do not initiate primitive or definitive haematopoiesis and have no *gata1*, *pu.1* or *runx1* positive cells (Patterson et al, 2005). On the contrary, over-expression of *scl* and *lmo2* is sufficient to specify haemangioblasts from the mesoderm into primitive red blood cells and endothelial cells (Gering et al, 1998; Gering et al, 2003). Both genes have overlapping expression patterns (Figure 1.8) and act together in a complex (Patterson et al, 2007). Forced expression of *scl* or *etsrp* can rescue the blood and endothelial defects in *cloche*, placing *scl* and *etsrp* downstream of *cloche* (Liao et al, 1998; Liao et al, 2000; Sumanas et al, 2005).

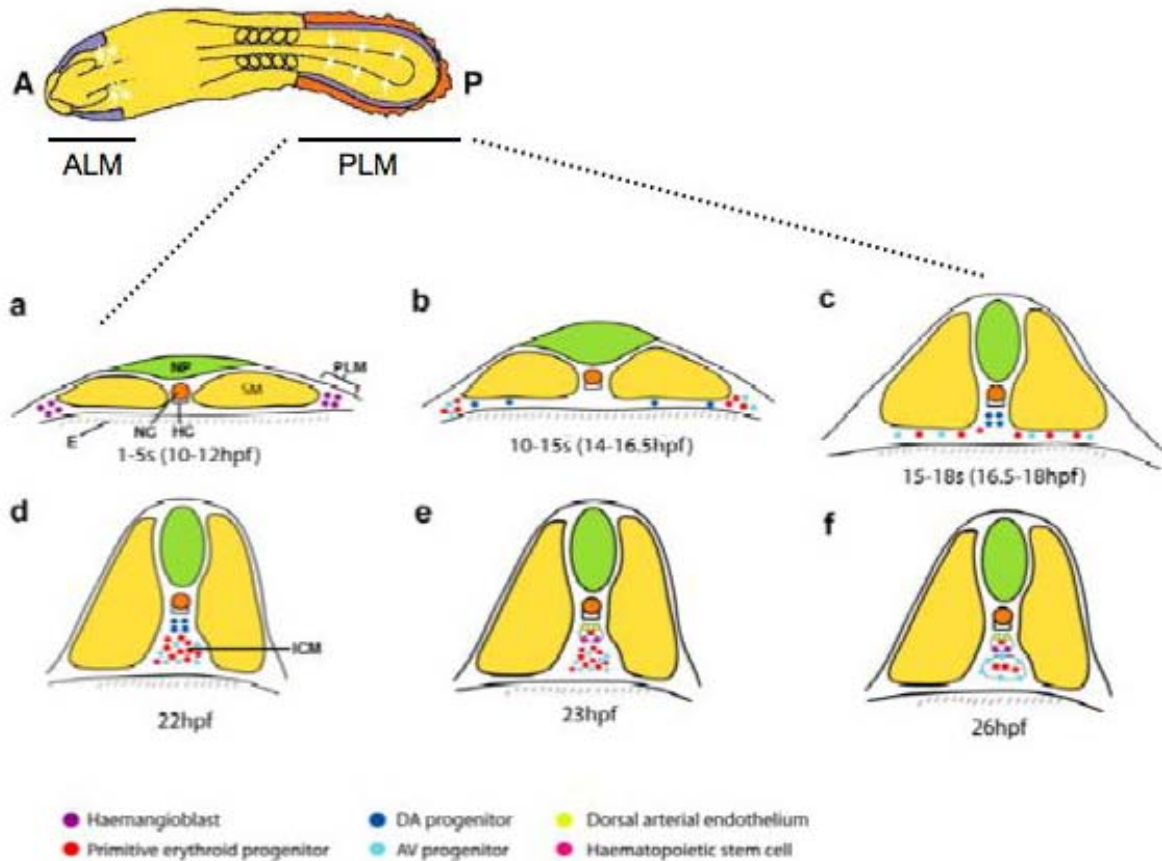


Figure 1.7: Endothelial and haematopoietic cell formation during somitogenesis The ALM and the PLM in the embryo give rise to haematopoietic and endothelial cells. **a**: In the PLM, haemangioblasts are found present within the bilateral stripes. **b**: DA progenitors migrate first, closely followed by primitive erythroid progenitors and venous angioblasts. **c, d** and **e**: The dorsal aorta forms between 22 and 23hpf. **d**: The cells in the midline form the ICM. **f**: the axial vein is developed and with the onset of circulation at (26hpf) and primitive erythrocytes enter circulation. Abbreviations: **E**, endoderm; **HC**, hypochord; **NC**, notochord; **NP**, neural plate; **SM**, somite; **ICM**, intermediate cell mass, Adapted from Gering et al, 2005 (bottom two lines of graphics) and Davidson et al, 2004 (top graphic).

The haemangioblasts soon give rise to either blood or endothelial cells. In the ALM, the haemangioblasts turn into either *pu.1* positive myeloid progenitors (Figure 1.8) or *kdr/flk1* positive endothelial cells of the head vasculature (Figure 1.8) (Lieschke et al, 2002).

The cells in the PLM either take on an erythroid cell fate, evident by the expression of the erythroid marker gene *gata1* (Dietrich et al, 1995; Long et al, 1997), or an

endothelial cell fate by expressing *kdr/flk1* (Figure 1.8). These genes are expressed in a bilateral manner and the cells in the PLM ingress towards the midline from 12 somite stage and form the ICM at 18 hpf (Dietrich et al, 1995; Liao et al, 1997; Forquet et al, 1997; Sumoy et al, 1997) (Figure 1.7, Figure 1.8).

Primitive erythropoiesis in the ICM and myelopoiesis in the lateral head mesoderm are governed by the antagonistic function of *gata1* and *pu.1*. Loss of *gata1* in the ICM transforms the erythroid precursors into myeloid precursors, suggesting that *GATA1* normally functions in part to limit *PU.1* and *PU.1* blocks erythroid differentiation by directly antagonizing *GATA1* activity (Galloway et al, 2005; Rhodes et al, 2005).

With the onset of circulation at 24 hpf the erythroid cells are actively detached by ADAM8 (a member of a disintegrin and metalloprotease family) from the lining of the blood vessels and enter the blood flow simultaneously (Iida et al, 2010).

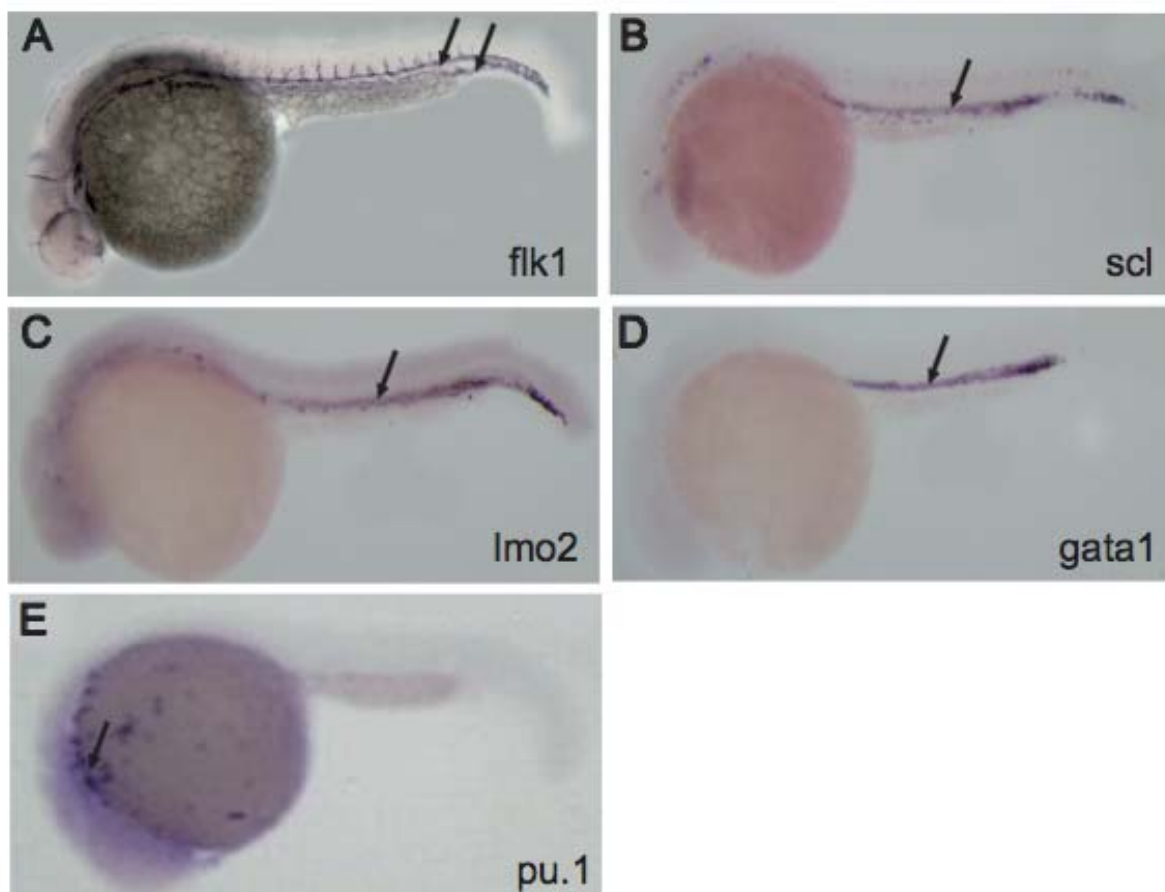


Figure 1.8: Haematopoietic and endothelial genes are expressed in the midline at 24 hpf

A: *Kdr/flk1* expression marks the developing vasculature in the embryo. In the trunk, the DA and PCV are prominent (black arrows). **B:** *scl* is expressed in red blood cells **C:** *lom2* is expressed in the endothelium. **D:** *gata1* is restricted to the trunk (black arrow). **E:** *pu.1* is exclusively expressed in the lateral head mesoderm. Images adapted from the following publications: A from Sumanas et al, 2006; B and C from Yue et al, 2009; D from Hart et al, 2009 and E from Kitaguchi et al, 2009.

1.10 Haematopoietic stem cell emergence in zebrafish

As in other vertebrates, HSCs are believed to develop in the ventral wall of the dorsal aorta. Analysis of the HSC marker genes *in vivo*, antisense-morpholino mediated knock-down of genes associated with HSCs and the creation of transgenic lines in which putative HSCs are labeled, have helped to study the formation of HSCs.

In zebrafish development, *runx1* is the first known gene to mark the emergence of HSCs. The mRNA for *runx1* is detectable as early as 24hpf in the ventral wall of the DA (Figure 1.9 A-D) (Thompson et al, 1998; Burns et al, 2002; Kalev-Zylinska et al, 2002; Gering et al, 2005). In *runx1* morphants, where the transcript level was knocked-down by injecting an anti-sense morpholino, the embryos lose the expression of *c-myb* at 50 hpf (Kalev-Zylinska et al, 2002). In addition, *runx1* morphants also do not express the *recombination activated gene 1 (rag1)* or *ikaros* genes in the thymus at 6 days post fertilization (dpf) (Gering et al, 2005). Both these genes are commonly used to assess the lymphoid development in the thymus (Willett et al, 1997; Georgopoulos et al, 1997). The loss of these genes in the thymus is consistent with the loss of HSCs in *runx1* morphants (Burns et al, 2005; Gering et al, 2005; Kalev-Zylinska et al, 2002). A recent report suggest that the *runx1* morphant cells are able to transit from a endothelial to a hematopoietic fate initially, but the putative HSCs are suggested to burst shortly after (Kissa et al, 2010). Consistent with the morpholino data, definitive haematopoiesis is lost in a recently described *runx1* mutant which only makes a truncated version of the

protein (Sood et al, 2010). Mutant embryos are bloodless between 8 and 12 days and most of them die between 15 and 20 days. Surprisingly, 20% of these embryos escape embryonic lethality and manage to establish haematopoiesis in the absence of *runx1* at a reduced level and with lineage-specific abnormalities. The molecular mechanism is unclear.

A further gene associated with HSCs and expressed in the ventral DA at 26hpf is the transcription factor *c-myb* (for a review see Greig et al, 2008). Mice homozygous for an inactivated allele of *c-myb* die at E15 due to a failure of the fetal liver to develop haematopoiesis (Mucenski et al, 1991). Since primitive erythropoiesis, megakaryocytes and macrophages are present in the mutant foetal liver it is suggested that the defect lies in the specification of HSCs in the AGM region (Mukonyama et al, 1999). In chimeras generated by injecting *c-myb* homo- or heterozygous mutant ES-cells into WT-blastocysts, *c-myb*^{-/-} ES cells could not contribute towards hematopoietic cells (Sumner et al, 2000). In the foetal liver, *c-myb*^{-/-} cells expressing *c-Kit* and *CD41* can be found at E10-E11, but decrease by E14 (Sumner et al, 2000). These findings argue that *c-myb*^{-/-} cells arrive in the foetal liver and express genes associated with haematopoiesis, but the cells are unable to retain the expression. Consistent with the data obtained from the *c-myb* knock-out mice and chimeras, *c-myb*^{-/-} ES cells lack the potential to form haematopoietic colonies *in vitro*, although mRNA derived from *c-myb* deficient cells showed expression of haematopoietic genes such as *scl*, *gata1* and *lmo2* (Clarke et al, 2000). This is indicative for a role for *c-myb* in proliferation and differentiation.

In zebrafish, a recent *N-ethyl-N-nitrosourea* (ENU)-induced mutant screen has identified a *c-myb* mutant. The loss of *c-myb* does not affect primitive erythropoiesis (as assessed by *gata1* expression), confirming the phenotype in mice, but leads to a defect in definitive haematopoiesis. Embryos become severely anemic from 20 dpf, but survive

for 2-3 months, possibly because oxygen diffusion through the skin is sufficient for survival. The mutants are devoid of *rag-1* and *ikaros* expression at 5dpf. In an experiment where the *c-myb* mutants were crossed into the *ikaros:GFP* transgenic background, there were no GFP positive cells in the thymus, indicating that *c-myb*-deficient cells cannot contribute towards the lymphoid lineage (Soza-Ried et al, 2010). Collectively, these data show that *c-myb*'s role in definitive haematopoiesis is conserved from fish to mammals.

The *ikaros* gene is a transcription factor not only essential for B and T lymphoid lineage specification (Wang et al, 1996), but is also required for the self-renewal of HSCs (Papathanasiou et al, 2009). *Ikaros* null mutant mice have severely reduced numbers of LT-HSCs in the bone marrow and a decrease in the ability to form CFU-S after 14 days (Nichogiannopoulou et al, 1999). Analysis of another *ikaros* mutant mice, which carry a point mutation in the *ikaros* gene, revealed that the foetal liver of these mice contains a normal pool of LT-HSCs (LSK Thy1.1^{lo} CD150⁺), but these cells disappear by E14.4 and E15.5, and the embryo is left with large numbers of non-LT, self-renewing haematopoietic progenitors (Papathanasiou et al, 2009). This data is indicative for a role of *ikaros* in the maintenance and self-renewal of LT-HSCs. During zebrafish development, *ikaros* is expressed as two stripes in the ALM and PLM, similar to *gata1* (Willett et al, 2001) and by 3 dpf the *ikaros* positive cells appear in the thymic lobe (Willett et al, 2001). *C-myb* positive cells can be detected at 5 dpf in the thymus (Figure 1.10 B, red arrows) (Jin et al, 2007). In contrast, *CD41* positive cells reach the thymus between 54-56 hpf (Murayama, 2006). Subsequently, after 96 hpf, the developing thymocytes lose *CD41* expression (Bertrand et al, 2008) and start to generate mature lymphocytes. The differentiation of the lymphocytes is initiated by 4 dpf is marked by the expression of *rag1/2* (Willett et al, 1997). In *runx1* MO injected embryos *rag1* expression in the thymus is lost, consistent with the loss of HSCs in *runx1* morphants (Gering et al,

2005). Zebrafish *Ikaros* mutants have an absent lymphogenesis in the first 14 days, but recover some abnormal and inefficient lymphoid development later (Schorpp et al, 2006).

The information gained by studying the expression of these transcription factors in zebrafish delivered the first indication of HSC emergence in the ventral wall of the DA, starting just prior to the onset of blood circulation at 24hpf. The expression patterns of these transcription factors also reveal a seeding of HSCs in different haematopoietic tissues during development. *C-myb* expression for example can be detected in the caudal haematopoietic tissue (CHT) in the tail of the embryo, and subsequently in the thymus and kidney (Murayama et al, 2006; Jin et al, 2007). These observations suggest a migratory behaviour of HSCs. In order to study the behaviour of these emerging HSCs *in vivo* and to trace the HSCs to their subsequent haematopoietic sites, a number of transgenic lines have been created. Most commonly, the transgenic lines were made using the promoter and/or upstream sequence of haematopoietic genes fused to a fluorescent marker gene in order to drive marker gene expression in HSCs. But since not all of the essential regulatory elements of the gene might be included in the transgenic constructs, and since the expression of none of the HSCs marker genes are restricted to HSCs alone, most of the transgenic lines show either non specific marker gene activity. But these transgenic lines are useful for imaging the formation of HSCs *in vivo*. The *CD41:GFP* transgenic line was made in an attempt to study thrombocyte development (Lin et al, 2005). Two *gfp* positive populations can be distinguished. Next to the cells expressing GFP at a high level, a gfp^{low} population was observed. The first GFP^{low} cells could be detected by 33hpf as scattered cells along the trunk in the thin mesenchyme between the DA and PCV. (Kissa et al, 2008). Transplantation of the *CD:41^{low}* fraction from the kidney marrow showed long-term reconstitution of the blood system in adult irradiated zebrafish (Ma et al, 2011). Collectively, the experiments

performed on the *CD41:GFP* line argues for an origin of HSCs from the mesenchyme between the vessels. The site of HSC emergence was further narrowed down to the ventral wall of the DA using further transgenic lines. The *c-myb* transgenic line was created by recombining the eGFP reporter gene into the first intron of the *c-myb* gene in an P1-derived artificial chromosome (PAC) and by injecting the resulting construct into one cell stage embryos (North et al, 2007). A double transgenic line where (*c-myb:eGFP*) was combined with a red fluorescent line labelling all endothelial cells in red (*Kdr/flk1:mCherry*) was established to show the emergence of *c-myb* positive cells from the endothelium in the ventral DA beginning from 30 hpf *in vivo* (Figure 1.9 E-H) (Bertrand et al, 2010). Endothelial cells in the ventral wall of the DA were observed to take on a round shape and lose contact with the neighbouring cells in order to enter circulation through the vein (Kissa et al, 2010). In order to further confirm that HSCs arise from the haemogenic endothelium, *c-myb*⁺ cells were purified at different stages using FACS. Bertrand et al were able to show that the *c-myb*^{low} positive cells express endothelial genes whilst in the endothelium, but as the *c-myb* expression intensifies, endothelial genes are switched off and expression of *CD45*, a pan-haematopoietic gene occurs (Bertrand et al, 2010). Further confirmation for this data comes from a *runx1:eGFP* transgenic line. Here, the first *runx1:eGFP* positive cells were observed at 36hpf between the DA and the PCV (Lam et al, 2010; 2009). By crossing the *runx1:eGFP* line with a *kdr/flk1:mCherry* line, they were able to image the emergence of *runx1* positive cells from the *kdr/flk1* positive endothelium in the ventral wall of the dorsal aorta at 40hpf (Lam et al, 2010). In addition, they were able to trace cells from between the vessels which were positive for *runx1* and *flk1* at 48 hpf to the thymus and kidney at 5 dpf (Lam et al, 2010). These findings demonstrate that haematopoietic progenitors originate in the dorsal wall of the DA and subsequently move to various haematopoietic tissues.

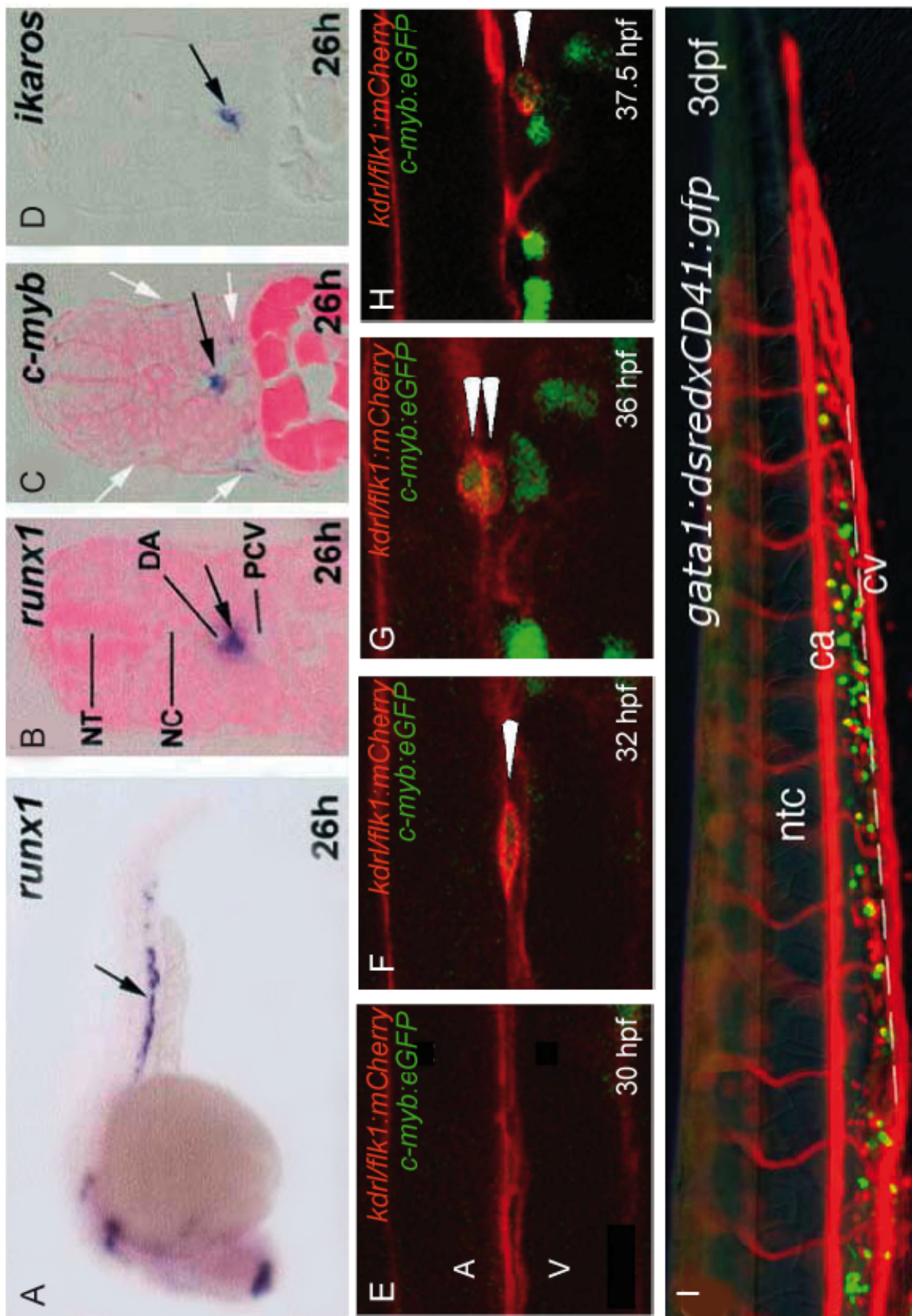


Figure 1.9: Definitive haematopoiesis is initiated in the ventral wall of the dorsal aorta
Marker genes of HSCs are expressed in the ventral wall of the DA at 26 hpf. **A:** lateral view of a whole mount embryo shows *runx1* expression in the DA. **B:** In the sagittal section through the trunk *runx1* expression is restricted to the ventral wall of the DA. **C, D:** The expression of *c-myb* and *ikaros* is also confined to the ventral aspect of the DA at 26 hpf. **E -H:** *Kdrl/flk1:mcherry; c-myb:eGFP* double transgenic embryos were observed over a period of time starting from 30 hpf. The time-lapse images show the emergence of *c-myb* positive cells from the *kdrl/flk1*-positive endothelium. At 30 hpf, the endothelium in the ventral DA appears flat. Two hours later, a cell (white arrowhead in F) takes on a spherical shape and seems to undergo cell division and both cells are positive for *c-myb* (white arrowheads in G). The *c-myb*-positive cell has detached from the ventral endothelium and can now be found in the mesenchyme between the vessels (white arrowhead in H). **I:** The putative HSC move from the ventral endothelium to the tissue in the caudal tail, the CHT, which is located between the caudal artery (ca) and caudal vein (cv). The *CD41:GFP* positive cells can be found amongst *Gata1:dsRed* positive cells in the CHT. The images were adapted from A-D from Gering et al, 2005, E-G from Bertrand et al, 2010 and I from Murayama et al, 2006.

1.11 Definitive HSCs migrate to the caudal haematopoietic tissue before they seed the thymus and the kidney

The newly formed HSCs undergo several consecutive migratory waves. In the first instance, the HSCs appear in the CHT as assessed by the expression of *c-myb* (Figure 1.10 A) (Jin et al, 2007). In order to trace the cells *in vivo* from the site of emergence to their niches, 1-4 cell stage embryos were injected with a photo activatable cell tracer, 4,5-di-methoxy-2-nitrobenzyl (DMNB) caged fluorescein (flu). Once this tracer is activated with a laser in the cells of interest, its persistence in the progeny of the labelled cell can be used to follow the fate of the cell. Murayama et al activated a four somite wide area in the trunk of the embryo at 50 hpf and subsequently observed labelled cells in the thymus at 5 dpf (Murayama et al, 2006). If cells were activated in the caudal part of the CHT, the progeny was also detected in the thymus at 5dpf (Murayama et al, 2006). These results indicated that the HSCs from the trunk and

caudal tail region migrate to the thymus. However, Kissa et al and Jin et al used a similar laser-activated uncaging approach in *CD41:GFP* and *Fli1:eGFP* transgenics. The *fli1:gfp* transgenic line (Lawson et al, 2002), in which early cells of the endothelial and haematopoietic lineage are labelled (Brown et al, 2000), was utilised. Jin et al used this strategy to label the cells at 30 hpf in the ventral DA. The activated cells or their progeny was then also analysed for the expression of *c-myb*. By looking for the double positive cells they suggest that the putative HSCs derived from the DA move to the CHT by day 2 and are more abundant by day 3, consistent with the *in situ* data obtained for *c-myb* in the CHT (Jin et al, 2007). Kissa et al activated the fluorescent dye at 48 hpf since the *CD41:eGFP* is at its brightest in the HSCs at this time-point (Kissa et al, 2008) and observed labelled cells in the CHT at 3 dpf (Kissa et al, 2008). Both groups reveal that the labelled cells appear more frequently at 3 dpf then on 2 dpf in the CHT. In an attempt to establish the earliest time-point for CHT seeding, cells in the ventral endothelium were uncaged at 26 hpf. Here they were able to observe that the first cells seed the CHT between 32-34 hpf (Kissa et al, 2008). Since the number of putative HSCs in the CHT increases from 2dpf to 3dpf, it is thought that this micro-environment provides a niche for HSC proliferation, the zebrafish equivalent to the mouse foetal liver (Murayama et al, 2006). Recently, a gene, *cpsf1*, has been found to be responsible for HSC survival in the CHT. TUNEL staining and determination of the *caspase-3* activity in *grechetto* mutants, which carry mutation in the *cpsf1* gene, suggests that the *c-myb* positive cells in the CHT undergo apoptosis if *cpsf1* is absent (Bolli et al, 2011).

The HSCs are believed to reach the CHT through the blood circulation. In silent heart embryos (*sih*^{-/-}), where the heart beat and blood circulation are blocked by injecting an antisense morpholino against cardiac tropomyosin (Sehnert et al, 2002), *CD41* positive cells initially emerged from the ventral DA at 50 hpf with a reduced frequency, but they were not observed in the CHT (Murayama et al, 2006). Consistent with the seeding of

the HSCs in the CHT, a number of blood genes are expressed by cells in the CHT. These include genes that play important roles in HSC biology and genes that are usually expressed in mature blood types like *runx1*, *c-myb*, *CD41*, *CD45*, *ikaros*, *rag1*, *scl*, *β E1-globin*, *gata1*, *lmo2*, *l-plastin*, *mpx* and *pu1* (Bertrand et al, 2010b; Bertrand et al, 2008; Bertrand et al, 2007; Jin et al, 2009; Jin et al, 2007; Kissa et al, 2008; Lam et al, 2009, Liao et al, 1998; Murayama et al, 2006; Zhang et al, 2007). This suggests that the CHT contains a heterogeneous population of blood cells, including haematopoietic stem and progenitor cells.

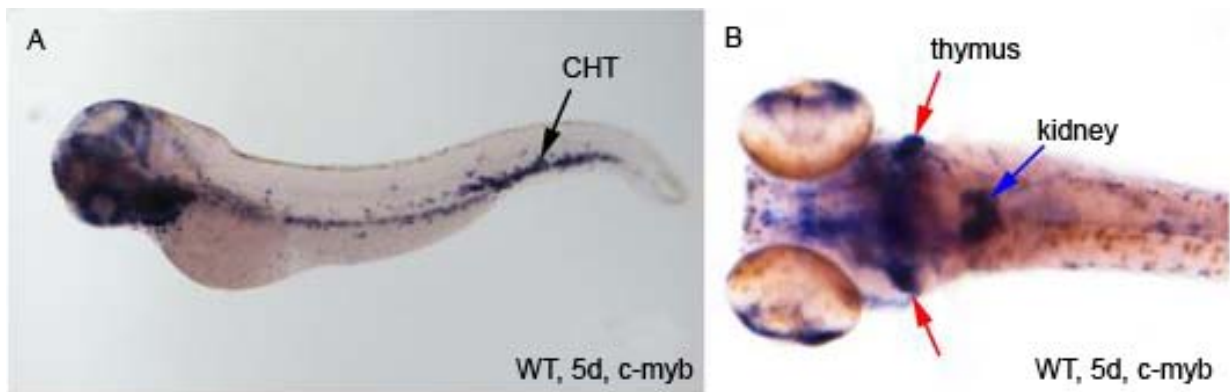


Figure 1.9: *C-myb*-positive cells are found in the CHT before they colonise the adult haematopoietic sites, the thymus and the kidney. *C-myb* positive cells populate the caudal haematopoietic tissue, CHT (A, black arrowhead) and the thymus and kidney (red and blue arrow, respectively). Source of images: Martin Gering.

The kidney is a destination for the HSCs as shown by the presence of *c-myb* positive cells (Figure 1.10 B). In the *CD41:eGFP* transgenic line *CD41* positive putative HSCs have been demonstrated to colonise the kidney, the main sites of adult haematopoiesis in fish (Murayama et al, 2006; Kissa et al, 2008; Bertrand et al, 2008) and in *runx1:eGFP* transgenic line, progeny of the *runx1* positive cells were also traced to the kidney (Lam et al, 2010). By day 5, the kidney was seeded by the cells from the ventral

wall of the DA from day 2 (Murayama et al, 2006) and similarly, cells labelled at day 3 in the CHT were traced to the kidney at day 5 (Murayama et al, 2006).

1.12 A subset of erythro-myeloid progenitors (EMPs) arise in the posterior blood island (PBI) independently of HSCs

A transient population of erythro-myeloid cells have been described in the posterior blood island as early as 30 hpf (Bertrand et al, 2007). The posterior blood island is located behind the anus, in the tail mesenchyme of the embryo. Here, *in situ* hybridisation expression revealed cells that expressed the erythroid markers *gata1* and the myeloid lineage specific markers *pu.1* and *mpx* (Bertrand et al, 2007). These haematopoietic cells were characterized to be independent of notch signalling (Bertrand et al, 2010b). Notch signalling is essential for the emergence of HSCs from the ventral DA (discussed later in this thesis). The analysis of these cells for erythroid and myeloid marker genes in *notch*-deficient embryos showed no difference to wild type embryos (Bertrand et al, 2010). Therefore, it was concluded that these erythro-myeloid progenitors arise independently from HSCs, and that they are equivalent to the mouse yolk sac blood cells (Bertrand et al, 2007).

1.13 Molecular programming of the dorsal aorta and HSCs

The common signalling pathways required to specify the DA and definitive haematopoietic cells are *hedgehog*, *vascular growth factor (vegf)* and the interactions between *notch* receptors and its ligands (Figure 1.11). *Hedgehog (hh)* is a member of the hedgehog family and is active in numerous developmental processes (Ingham et al, 2011). Hedgehog signals acts as a secreted molecule through the transmembrane

receptor *patched* (*ptc*) and the signal transducing protein Smoothed (*smo*). Hedgehog is secreted from the floor plate and the notochord in the midline of the embryo and is needed for the migration of the *kdr1/flk1* expressing angioblasts towards the midline, for the arterial specification of these angioblasts and for the generation of *runx1* positive cells at 26 hpf (Gering et al, 2005; Lawson et al, 2002). *Hh* acts by inducing the expression of the *vegf* in the adjacent somites (Lawson et al, 2002) and by promoting arterial specification by repressing venous fate (Williams et al, 2010). Zebrafish embryos, which have a homozygous mutation in *sonic you* (*syu*) or *you-too* (*yot*) encode for the zebrafish homologs of *shh* and *gli2*, a downstream target of *hh*, respectively. These embryos lack *vegf* expression and arterial expression of *efnB2a*, a transmembrane protein of the ephrin family, but the lack of *efnB2a* expression can be rescued by *vegf* mRNA injections (Lawson et al, 2002), suggesting a role for *shh* upstream of *vegf*. *Vegf* is also needed for the generation of *runx-1* positive cells at 26 hpf (Gering et al, 2005). Injections of *vegf* mRNA into *hh*-deficient embryos can rescue the lack of *runx1* positive cells in morphant embryos (Rowlinson et al, 2010). The family of *vegfs* and their receptors are regulators of vasculogenesis and angiogenesis. The receptors VEGFR1, VEGFR2 (KDRL/FKL1) and VEGFR3 (FLT4) are transmembrane tyrosine kinases that are expressed by endothelial cells during development (for a review see Jakobsson et al, 2009). *Vegfa* acts as a mitogen on the VegfR2 (*Kdr1/flk1*) expressing angioblasts (Liang et al, 2001). Loss of *vegf* in morpholino-injected embryos leads to a loss of the arterio-venous identity in the trunk vessels. The morphants lack the expression of *ephrinB2a*, a gene specifically expressed in the DA of the vasculature. Furthermore, *flt4*, a gene which is first present throughout the vasculature, but then becomes restricted to the vein, is ectopically expressed in the DA of *Vegf* morphants (Lawson et al, 2002). Since the defects in the *vegf* morphants are similar to embryos with defective notch activity, it was proposed that both *vegf* and *notch* act in the same

cascade to induce arterial specification. Consistent with this hypothesis, embryos injected with the *vegf* MO showed a specific loss of Notch5 from the DA (Lawson et al, 2002). The arterial specific *efbB2a* expression in *notch* deficient embryos could not be rescued with *vegf* mRNA injections (Lawson et al, 2002). But induction of *notch* using the two-component transgenic line *Tg(hsp70:gal4)(uas:notch1a)* was able to rescue arterial gene expression in *vegf*-deficient embryos, arguing for a downstream role for *notch* and *vegf*. Although these findings suggest a link between *vegf* and *notch* signalling in establishing arterial and venous identity, it remains unclear how these pathways interact to drive endothelial fate development. A putative link is the *Ras-Merk-Erk* signalling downstream of *vegf* in DA angioblasts, which is responsible for an arterial differentiation and is antagonized by PI3K-Akt pathway (for a review see Siekmann et al, 2008; Hong et al, 2006). In the DA angioblasts, however, Notch receptors and the membrane bound ligands of the Delta and Jagged families communicate between neighbouring cells (for a review see Phng et al, 2009). Upon ligand binding to the Notch receptor, the intracellular domain of the ligand gets ubiquitinated by the E3 ubiquitin ligase. The Notch intracellular domain (NICD) is cleaved by γ -secretase and is free to enter the nucleus to form a complex with the transcription factor Lag1/Su(H)/CSL (also known as RBPjk) in order to regulate downstream *notch* targets (reviewed in Borggreffe et al, 2009). Zebrafish *mind bomb (mib)* mutants, which have a mutation in the *E3 ubiquitin ligase* gene show no expression of *runx-1*, consistent with a loss of HSCs (Gering et al, 2005). Similarly, embryos treated with the inhibitor DAPT, which blocks γ -secretase show a loss of *runx-1* (Gering et al, 2005, Burns et al, 2005). Over expression of *notch* induces, as expected, ectopic expression of *runx-1* into the venous cells (Burns et al, 2005). These experiments demonstrate the requirement of a common signalling pathway for the specification of DA cells and HSCs. However, the Notch

target gene *hey2* has been shown to act upstream of *notch* signalling in HSC specification (Rowlinson et al, 2010).

Molecular pathways, which only affect HSCs include the *bone morphogenetic protein 4* (BMP4), blood flow, *prostaglandin E2* (PGE2) and *Wnt* signalling. Nitric Oxide (NO) can influence angiogenesis and endothelial migration and the expression of NO is dependent on blood flow (Lucitti et al, 2007). Since the NO synthase *enos1* is expressed in the endothelium and HSCs of zebrafish embryos, morpholino-mediated knock-down of Enos1 was performed to assess its effect on *runx1* and *c-myb* positive cells (North et al, 2009). In these experiments, a knock-down of Enos1 had a negative impact on HSC development. The decreased expression of Enos1 in *sih*^{-/-} embryos further confirmed these observations. Furthermore, a chemical screen with blood flow decreasing or enhancing compounds was able to provide more evidence that blood flow positively regulates HSC emergence. Consistent with these findings, embryos treated with the compound L-NAME which blocks the Enos1, the number of *runx1* and *c-myb* positive cells are reduced whereas the blood flow stimulating compound SNAP enhanced the number of HSCs (North et al, 2009). Another pathway which influences HSC development is *wnt*. Wnt signalling involves a network of proteins and can be categorised into the *canonical* and *non-canonical* Wnt pathway (for a review see Staal et al, 2010). In the canonical Wnt pathway, Wnt proteins bind to the cell-surface receptors of the *Frizzled* family and activate Dishevelled family proteins, which leads to a modulating the amount of β -catenin that is translocated into the nucleus. B-catenin interacts with TCF/LEF family of transcription factors to control downstream gene targets. The non-canonical Wnt pathway is independent of β -catenin and includes many pathways (eisenmann et al, 2005). Recent investigations suggest that Wnt16, member of the non-canonical pathway, induces the expression of the Notch ligands DeltaC and DeltaD from the somites of 15- 17 hpf (12 – 16 somite stage).

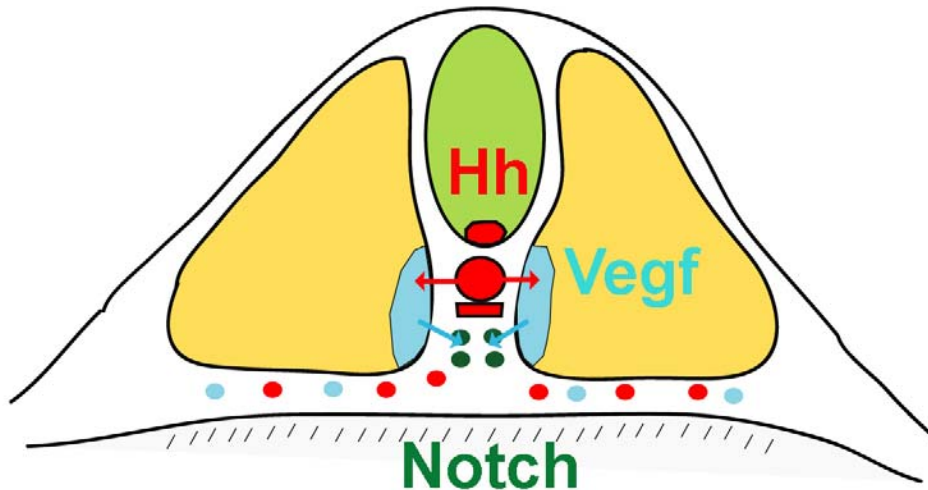


Figure 1.10: Signalling molecules involved in DA specification and HSC emergence. The schematic shows a transverse section through the trunk at around 22 hpf. Hedgehog (Hh, red) is secreted from the notochord (green) and induces Vegf (light blue) expression from the adjacent somites (yellow). This in turn activates notch (green) signalling in the DA. The primitive red blood cells (red round cells ventral to the somites) and the venous progenitors (light blue round cells ventral to the somites) are still migrating toward the midline at this time point. Adapted from Gering et al, 2005.

DeltaC and DeltaD have been shown to be essential for the formation of *runx-1* positive cells at 24 hpf, *c-myb* positive cells at 36 hpf and *rag-1* positive cells at 4.5 dpf. *DeltaD* morpholino injections into *beamter* (*bea*) mutants, which carry a mutation in the *deltaC* gene create double morphants and lead to a loss of haematopoietic marker gene expression (Clements et al, 2011). The researchers claim that this newly discovered pathway is independent of the above described *Shh*, *vegf* and *notch* interaction since vascular and arterial specification are unaffected in *Wnt16* morphants (Clements et al, 2011). This newly un-revealed pathway also demonstrates that *notch* is required twice during HSC development. Here, *notch* signalling acts extrinsically through the somites, whereas in the *shh-vegf-notch* pathway, *notch* is required in the cells. The canonical Wnt signalling has also been implicated in HSC emergence. Using *top:GFP* transgenic line, in which the embryonic cells respond to B-catenin with elevated GFP fluorescence,

it was shown that (a) β -catenin was expressed in the trunk of the fish at 36 hpf and (b) that addition of the compound PGE2 enhanced the B-catenin complex leading to increased number of top:GFP cells between the axial vessels (North et al, 2007; North et al, 2009; Goessling et al, 2009). From these observations it was concluded that Wnt signalling positively regulates HSC formation. Another pathway implicated in HSC specification is BMP4. Morpholino knock-down experiments revealed its importance in the generation of *runx-1* and *c-myb* positive cells from the ventral endothelium and *rag1* positive cells in the thymus (Wilkinson et al, 2009). These recent publications are beginning to reveal the different inputs arterial cells in the DA need in order to generate HSCs. It still remains unclear how these different pathways interact to specify HSCs from the haemogenic endothelium.

1.14 The need to identify and characterize novel genes involved in haematopoiesis

The pathways leading to the specification of the DA and the emergence of HSCs are only poorly understood. Some of the major pathways and transcription factors involved in this process have been identified such as *hedgehog*, *vegf*, *notch*, *wnt* and *bmp4*, but how these pathways interact and which downstream targets they use to regulate each other still remains largely unclear. A major remaining question is how the haemogenic endothelium gains the ability to generate HSCs and how these HSC are programmed to leave the endothelium. It is also unknown which intrinsic and extrinsic signals they follow to migrate to the CHT. The mechanism underlying their migration to the CHT and the signals in the niche for proliferation are also undetermined. Lastly, the factors that are responsible for the homing of the HSCs to their definitive sites also remain unidentified. We are only now in the process of unravelling genes and pathways

involved in this chain of events. It is therefore important to establish strategies, which allow the identification of novel genes involved in this process.

1.15 Current genetic tools and strategies in zebrafish genetics

The ultimate quest is to characterise each gene involved in haematopoiesis and elucidate transcription factors and signalling molecules underlying the biological processes like cell division, differentiation and specification. Traditionally there are two approaches for these tasks. One approach is to randomly mutate the chosen organism, screen the progeny for interesting mutant phenotypes and at last to track back the mutation to a gene. This approach is termed forward genetics; reverse genetics is the opposite procedure. The gene of interest is mutated in order to determine its function. Both approaches are equally important and have been applied in the zebrafish. The most widely used forward genetics approach is to block the translation of the mRNA into a protein by injecting antisense morpholino into early zebrafish embryos. Morpholinos are synthetic DNA analogs with altered backbones. They can bind to complementary sequences and can sterically block the translation or splicing event. The altered backbone consists of morpholine rings instead of deoxyribose rings and linked through phosphorodiamidate groups instead of phosphates which make them resistant to nucleases and less likely to interact with cellular proteins (Corey et al, 2001). Morpholinos are easy to use and inexpensive. But the major disadvantage of this method is that the gene expression is only knocked-down. Furthermore, the knock-down can only reduce the mRNA level up to 90% (Corey et al, 2001) and there will be a minimum amount of wild type protein left. Therefore, they are a temporary solution to circumvent the difficulties in generating mutant lines with high efficiency in zebrafish.

The recently established zinc finger nuclease based technology allows sequence directed mutagenesis. Here, the non-specific type II restriction endonuclease *FokII* is combined with a sequence specific DNA binding domain. The zinc finger nucleases are engineered to recognize between 9 and 18 bp. In zebrafish, the zinc finger nuclease is injected as mRNA into one-cell stage embryos. A high percentage of animals carried the desired mutation or phenotype, which was passed to the next generation through the germ line (Foley et al, 2009; Meng et al, 2008; Doyon et al, 2008). This method is a powerful tool to mutate a gene of interest, but is not suitable for a genome wide mutagenesis approach since its time- and money consuming.

A lot of scientific effort has been put into developing fast and easy transgenesis methods in zebrafish. The forward genetics approaches range from irradiation and chemical mutagenesis to injections of plasmid constructs and retroviral infections. The main aim of these efforts is to saturate the zebrafish genome with mutations in order to characterize every gene. Gamma-radiation or the chemical ENU can be used to induce mutations in the male zebrafish germ-line (Streisinger et al, 1981; Grunwald et al, 1992). ENU creates point mutations via DNA alkylation, whereas gamma-irradiation causes DNA double strand breakage (Rothkamm et al, 2003). The ENU-mediated mutagenesis was favoured for the large-scale saturation screen published in 1996 (Haftner et al, 1996). A newer approach to *ENU*-mediated mutagenesis is TILLING (Targeting induced local lesion in genomes) (for a review see Moens et al, 2008). This method helps to identify mutations in genes of interest in a large ENU-mutagenised population. In order to find a point mutation in the gene of interest, either genomic DNA from individual fish are re-sequenced or genomic DNA from a number of fish are pooled and screened simultaneously using *Cel1*. *Cel1* is an endonuclease that cleaves heteroduplex DNA at all possible single mismatches. In order to screen the mutated fish population with *Cel1*, a primer-pair with fluorescent tags are used to amplify the gene of

interest. Cel1 is able to digest sites of single base pair mismatches induced by the ENU and sites of single nucleotide polymorphism (SNPs). SNP occur every 600-3000 bp. The digested gDNA is separated on an acryl-amid gel and analyzed for the presence of a restriction in the labelled fragment. This method is sensitive enough to detect mutation in one of 16 alleles. But this approach requires a large number of mutated fish and is therefore performed by large international collaborations. Another way to mutate an organism was pioneered in the early 1980s. It was reported that the injection of plasmid DNA containing sequences from the transposable P-element into early embryos could result in genomic integration in *Drosophila* with high efficiency (Rubin et al, 1982). The integrated plasmid could both act as an insertional mutagen and, furthermore, the sequence could be used as a tag to localise the integration in the host genome. Since there were no transposable elements known to integrate into the zebrafish genome upon introduction back then, the microinjections in zebrafish were done with plasmid DNA containing just a constitutive promoter followed by a marker gene, e.g. lacZ or GFP, but the transgenesis frequency proved to be poor, ranging from only 5%-17% (Stuart et al, 1988; Culp et al, 1991; Amsterdam et al, 1995). Furthermore, the plasmid DNA was integrating as concatemers leading to chromosomal rearrangements and deletions (Stuart et al, 1988). In an attempt to increase the transmission frequency, pseudo typed retroviral vector, which has a genome based on the Maloney murine leukaemia virus (MLV) and the envelope glycoprotein of the vesicular stomatitis virus (VSV), was used as an insertional mutagen (Gaiano et al, 1996). Retroviruses infect their host cells by interacting with their surface receptors. It was shown that zebrafish cell lines could be effectively infected with MLV, if the MLV envelope protein was replaced by the glycoprotein of VSV (Burns et al, 1993). Once in the host cell, the RNA genome, is reverse transcribed and integrated into the host genome as a provirus with the help of enzymes, which are encoded in the viral genome. The retroviruses, which

are used for mutagenesis, lack the coding sequence for replication and packaging and are termed proviruses. The viruses are produced in cell lines, where the necessary proteins are supplied in *trans*. This method ensures a stable infection without additional virus replication in the host. The proviruses are harvested and used for infecting mid-blastula stage zebrafish embryos (Gainano et al, 1996). Each founder fish can harbour 6-22 pro-viral insertions (Gaiano et al, 1996) and every 1 in 85 insertion produces a mutation (Amsterdam et al, 1999; Gaiano et al, 1996b). Another group, which conducted a similar retroviral based screen in zebrafish claims to have reached frequency rate of 76% (Wang et al, 2007), while Ellingsen et al report 30% transmission frequency with an enhancer construct (Ellingsen et al, 2005). But the average germ line transmission frequency is only about 30% (Gaiano et al, 1996). Although the transgenesis rate is higher than with plasmid injections, there are other problems using viral infections for mutagenesis in zebrafish. The frequency of obtaining morphologically visible embryonic mutations is very low, with only one per 80-85 integrations and is therefore 7 to 10 fold lower than with *ENU* mutagenesis (Amsterdam et al, 2003). The use of high titer virus can increase the number of viral integration in each founder, resulting in a lower number of founder fish to screen for mutant phenotype (Amsterdam et al, 2003). But the high number of insertions in each founder genome will make the segregation of each insert into a single transgenic line time-consuming and almost impossible, especially if insertions are closely located to each other. Furthermore, in 50% of the active pro-viral integration the mRNA level of the affected gene is only knocked-down to 30% of the wild type protein level if they are bred to homozygosity (Wang et al, 2007). Therefore retroviral insertions are not reliable for creating knock-out genotypes. Studies with avian and murine retroviruses have also suggested that factors such as chromatin and accessibility might bias the viral integration towards transcriptionally active or 5' ends of genes (Wang et al, 2007; Amsterdam et al, 2006).

This might explain the reason for obtaining a large proportion of down regulation of gene expression instead of gene knock-out. Furthermore, the production and harvesting of high titer virus is difficult and time-consuming and not every laboratory has the safety measurements to produce and stock proviral vectors.

An alternative “tag” for insertional mutagenesis is a transposable element. Transposable elements are naturally occurring mobile elements in the genome of plants and animals. They have the ability to integrate into the genome at a new site within the cell of origin (Kazazian, 2004). The mobility of the transposable element is dependent on the enzymes, which are encoded in the sequence between the flanking inverted terminal repeats (ITR). Autonomous transposons are self-sufficient, whereas non-autonomous either lack or have mutations in either their enzyme-coding region or in their repeat region. Transposable elements can accumulate mutations in a time-dependent manner and become inactive in their host genome (Miskey et al, 2005). Such non-autonomous elements can be mobilised by repairing the mutated sequences *in vitro* and are then called “reconstructed”. Transposable elements can be classified into two major classes: DNA transposons and Retrotransposons. Retrotransposons and retroviruses are very similar in their structure. They both encode the enzymes reverse transcriptase and integrase to transcribe their RNA genome into cDNA and to integrate into the host genome (Kazazian, 2004) and use long terminal repeats to flank their coding region. DNA transposons, on the other hand, shift from their original genomic locus to a close by position by a “cut and paste” mechanism (Kazazian, 2004). This class of elements code for the enzyme transposase, which is sufficient to excise and relocate the element. They are extensively used in prokaryotic and lower eukaryotic systems for insertional mutagenesis and gene delivery (Wadman et al, 2005). In a typical vector, which is based on a transposon, the enzyme-coding region of the element is replaced with a sequence of interest, e.g. marker gene, flanked by the repeat elements. The

transposase enzyme is delivered in a limited amount in order to prevent unwanted transposon activity. The transposon based vector and the transposase are co injected into one-cell stage embryos. The enzyme recognizes the ITRs of the transposon, which is then cut out of the plasmid and integrated into the genome of the embryo (Mates et al, 2007). The early developmental stage of the embryo increases the possibility of the vector integrating into the precursors of the embryonic germ line cells. Transgenic animals are identified by screening the progeny for the marker gene. It is also important to ensure that the transposable element, which is used for transgenesis purposes, is not already active or present in the host. Different transposable elements have been tested for activity in zebrafish. The P-element from *Drosophila* was soon shown not to be active in non-drosophilid insects, zebrafish and mammalian cells due to host factor dependency (Gibbs et al, 1994; Miskey et al, 2005). The reconstructed vertebrate transposable elements *Sleeping beauty* (SB), *Minos*, the human reconstructed *Hmar1* and *Frog prince* (FP) have been shown to be active in vertebrates (Ivics et al, 2009; Miskey et al, 2005). However, the transgenesis rate for *Sleeping beauty* was low with only 30% (Davidson et al, 2003). The vertebrate specific transposable element *frog prince* has been reported to be active in a wide range of vertebrate cell lines (Miskey et al, 2003). The transmission frequency of the transposon was as high as 70% in zebrafish cell lines (Miskey et al, 2003). It was proposed that the high efficiency was due to fact that *sleeping beauty* transposon was reconstructed from another teleost fish genome, which is closely related to the zebrafish and therefore might have SB suppressing factors like the frog, unlike in the case of FP which derives from a more distantly related species (frog) and where suppressing factors are not phylogenetically conserved between zebrafish and the frog (Miskey, 2005). But *Frog prince* has not been used for *in vivo* transgenesis screens in zebrafish, yet (Miskey et al, 2005). The only

transposon, which has been used by different research groups for transgenesis techniques in zebrafish is the *tol2*.

1.16 The *Tol2* transposable element as a tool for transgenesis in zebrafish

The *tol2* transposable element was isolated from the fish medaka as the first autonomous vertebrate transposable element (Koga et al, 1996). It was found in the tyrosinase gene locus where its insertion caused an albino phenotype of the fish (Koga et al, 1996). The DNA sequence of the element was similar to the members of the *hAT* family transposable elements: *Ac* element of maize, *hobo* of *Drosophila* and *Tam3* of the snapdragon (Koga et al, 1996). There are about 10-30 copies of endogenous *tol2* in medaka, but no copy of a transposon belonging to the *hAT* family has been found in zebrafish (Kawakami et al, 1998). An excision assay confirmed that this element is autonomous and leaves 8 base pair (bp) long duplications flanking the integration site (Kawakami et al, 2000). It has also been reported to be active in the frog (Kawakami et al, 2004), in human and mouse cell lines (Koga et al, 2007) and mice (Ivics et al, 2009). The germ line transmission frequency of *tol2* in zebrafish is reported to be as high as 50% with 5.6 insertions per founder fish (Kawakami et al, 2004). The pilot-project used the ubiquitous EF1 θ promoter to drive the expression of GFP. Half of the injected embryos carried the *tol2* based construct in their germ line and were able to transmit it to their progeny (Kawakami et al, 2004). The exact insertion site of the vector in the genome was located with Inverse-PCR (Kawakami et al, 2004; Kotani et al, 2006). This initial publication demonstrated that *tol2* could be used for easy and efficient transgenesis in zebrafish. A *tol2* transposon based insertional mutagenesis screen has the potential to generate more mutant phenotypes, since the system showed a higher

transmission frequency than the screens based on microinjection of plasmid DNA or retroviral infections. A *tol2* based vector transgenesis approach can be conducted by every laboratory since there is no need for cell cultures and high safety standards, such as in the case of handling retroviral vectors. Furthermore, a vector based on *tol2* can take up to 10,2kb of foreign sequence without showing any reductions in its activity (Balciunas et al, 2006) whereas a retroviral vector is very restricted in the size of insert it can carry (Korzhanov et al, 2007). All these advantages make the *tol2* transposon a good candidate for insertional mutagenesis screens. *Tol2* based gene trap studies were attempted in zebrafish shortly afterwards (Kawakami et al, 2004; Kotani et al, 2006; Parinov et al, 2004).

A gene trapping assay uses different gene trapping vectors to elucidate distinct aspects of the gene organisation and gene expression. There are four major gene trap approaches: Enhancer-, Promoter-, and Poly (A)- trap and a gene trap.

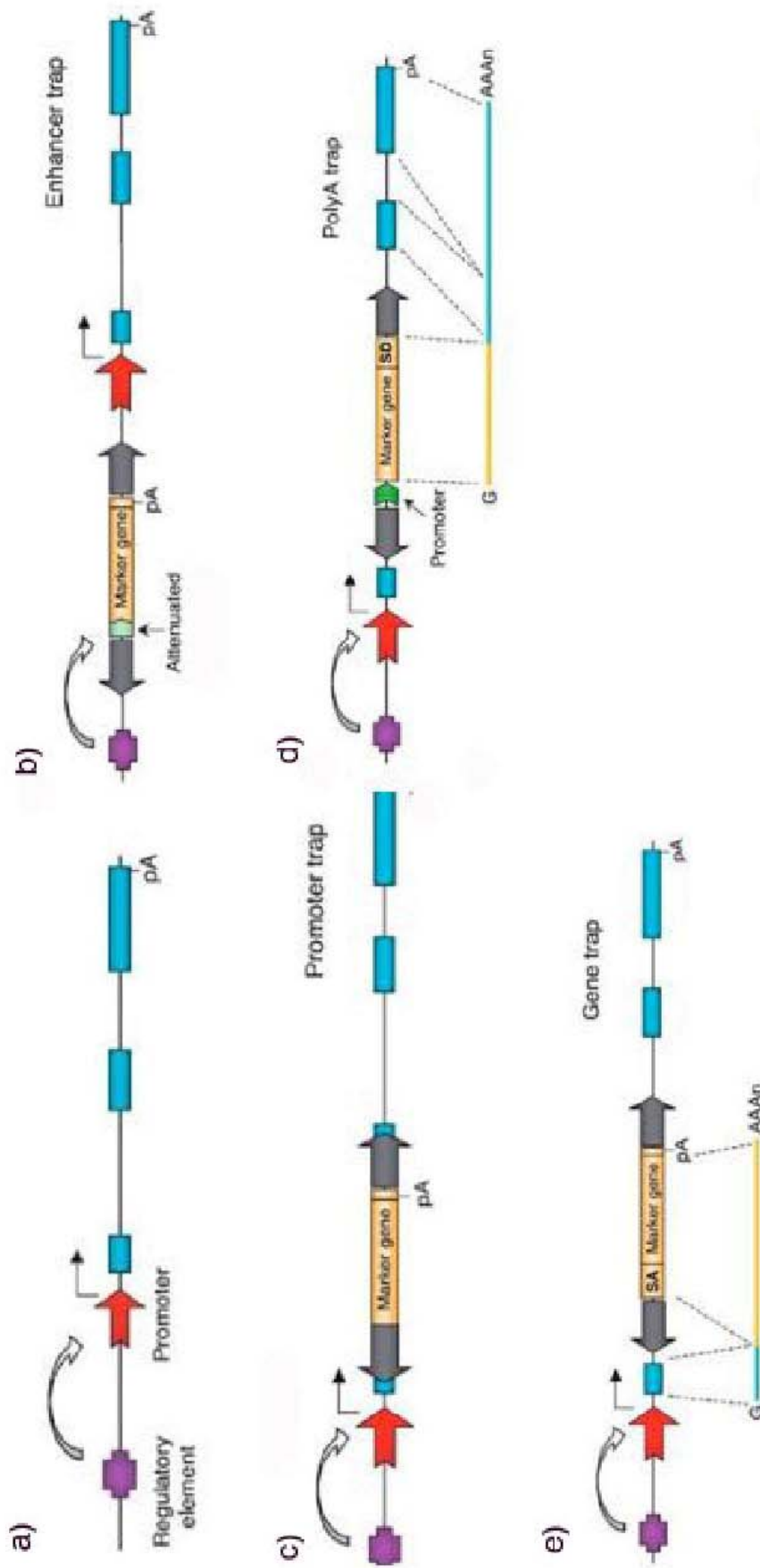


Figure 1.1o: Transposon-based gene-trapping vectors. The schematic depicts a transcription unit (a) with a regulatory element (purple box), a promoter (red arrow) and the exons (blue boxes). A hypothetical transposon-based trap vector insertion in different sites of the transcription unit is shown in b – e. The enhancer trap vector has a minimal promoter followed by a marker gene and a (poly)A site (b). In this scenario, the trap vector is able to capture the spatio-temporal activity of the enhancer. The promoter trap vector lacks a minimal promoter and only consists of a marker gene followed by a poly (A) (c). Here, the reporter is only active, if the insertion happens close to an active promoter. The poly (A) trap construct is a combination of a promoter, reporter gene followed by a splice donor site (d). This construct has the ability to activate even silent genes upon inserting into a transcription unit since it has its own constitutive promoter. The gene-trap vector has a splice acceptor site followed by a marker gene and poly (A) site (e). Thus, the construct needs to insert into an intron of the transcription unit in order to activate the marker gene. Adapted from Miskey et al, 2005.

The enhancer-trap vector consists of a minimal promoter sequence upstream of a marker gene and a Poly (A) site. The reporter gene expression is dependent on active enhancer sequences within the reach of the minimal promoter. The reporter gene is able to phenocopy the spatio-temporal activity of the regulatory element. An enhancer-trap in zebrafish was applied to detect 24 unique expression patterns (Parinov et al, 2004). In the screen a *tol2* based construct with the keratin-8 minimal promoter sequence was co-injected with transposase mRNA into 230 zebrafish embryos. Only 37 (16%) could be identified as transmitters (Parinov et al, 2004). Nearly a third of these lines only showed the weak expression of the keratin-8 promoter, whereas the rest of the insertions (24) were able to capture the specific activity pattern of nearby enhancer elements (Parinov et al, 2004). The identification of the captured regulatory sequence is difficult since these can reside at a distance from their actual operating sphere. Furthermore, it will be difficult to identify all the genes which might be affected by this regulatory element, since nearby genes can shield themselves with insulators. The Promoter trap has no promoter element at all, but has a reporter upstream of a Poly (A) site. In this case the reporter can only be expressed if the construct inserts either in the

5' untranslated region (UTR) or in the right reading frame and orientation of the protein-coding exon of an active gene. This trap vector restricts the trap events to active promoter sequences and the vector has to integrate in a particular way to allow a promoter to drive tissue-specific expression of the reporter gene that is encoded by the promoter trap. The Poly (A) trap vector consists of a constitutive promoter upstream of the marker and a splice Donor. In contrast to the promoter trap and gene trap constructs, the Poly (A) trap can capture all exons downstream of a promoter, once it inserts into an intron. Since the vector has a constitutive promoter the marker gene expression does not depend on the activity of the trapped gene. Every insertion will be reported by the marker gene expression. Furthermore, the Poly (A) trap vector is able to pick up splice variants downstream of the insertion site, since the splice donor can take part in the normal splicing process. This vector can therefore potentially trap all protein-coding transcripts independent from their transcriptional activity. It is a great vector for annotating the zebrafish genome. The activity of the gene trap vector is strictly bound to its insertion site. The gene trap vector has no promoter sequence, but consists of a splice acceptor upstream of a marker gene and a Poly (A) site. The marker gene expression can only be detected if the construct inserts within an active gene. Furthermore, the vector has to insert into an intronic sequence of the gene and also be in the correct reading frame in order to express the marker. These requirements make sure that the marker gene expression reproduces the spatio-temporal expression of the trapped gene. The gene sequence upstream of the insertion is fused into a fusion-protein together with the marker gene sequence. Insertions in introns near the promoter sequence might not affect function of the protein as much as an insertion in introns further downstream. Depending on the insertion site, the gene trap event can lead to non-functional protein synthesis. The gene trap assay in zebrafish resulted in 36 lines with unique marker gene expression patterns (Kawakami et al, 2004; Kotani et al,

2006). 80 founder fish were identified from 156 injected fish embryos (51% germ line transmission rate). The percentage of founders with unique marker gene expression is only 23% (Kawakami et al, 2004; Kotani et al, 2006). Only a fraction of the progeny expresses the marker due to strict requirements laid upon the gene trap vector. In cases where the vector has integrated into a non-coding genomic regions, wrong orientation to the transcriptional direction of the gene, exon or out of frame, the vector will not be activated. However, the captured genes have the potential to be knocked-out when the mutation is bred to homozyosity. All the insertion vectors have the potential to knock-out. But the gene trap is the best approach since the marker gene only responds to active genes, unlike Poly (A) trap, which picks up every transcript, including silenced genes. The Enhancer-trap has the disadvantage that it is very difficult to identify which genes it influences. An Enhancer trap insertion could even influence or abrogate the expression of more than just one gene. The activity of the promoter trap vector depends on its insertion into an exon or in the 5'UTR of a gene. But in higher metazoa only a small fraction of the genome encodes for exon (mammals: 1,5%) (Korzh et al, 2007), whereas as introns are known to span several kilobases between protein-coding exons. Therefore it might be more effective construct vectors, which aim at introns like the gene trap vector, but have the capacity to detect active genes.

Objectives

The main aim of this PhD project was to create a transgenic zebrafish line in which haematopoietic progenitors are labelled with a fluorescent marker gene. The creation of such a line would not only allow to study the emergence of these cells in the ventral wall of the dorsal aorta in vivo, but would also allow to follow their migratory behaviour before they reach the final haematopoietic organs in the fish. Furthermore, such a transgenic line would also facilitate to isolate haematopoietic progenitors by using flow cytometry based on their fluorescence. Microarrays or RNA sequencing on purified isolated cells in turn will enable to determine the transcription factors and genes which are either under or over represented in this cell population. The obtained data from such techniques can help to unravel novel signalling molecules which are active in haematopoietic progenitors and help to establish a gene regulatory network.

In order to reach this goal, there are two different possibilities. In the first instance, the promoter or regulatory elements of a transcription factor or gene which is known to be expressed in these cells can be used to drive the expression of a fluorescent marker. This approach requires testing different combinations of regulatory elements in order to define the most efficient combination of regulatory elements to drive the expression in the cells of interest. This approach is undertaken by a fellow PhD student with the aim to dissect the regulatory elements responsible for *c-myb* expression in HSCs (J Hsu, unpublished data).

The second approach involves a random insertion mutagenesis with a gene trap vector. Gene trap vectors can be successfully applied in zebrafish to capture the spatio-temporal expression pattern of novel genes (Kawakami et al, 2004; Kotani et al, 2004). This approach is uncertain since the chance of trapping a gene expressed in haematopoietic progenitors is small. But this approach has the added advantage of

trapping novel genes. In order to increase the chances of trapping haematopoietic transcription factors or genes, a large number of embryos need to be included in the initial screen. Once such a transgenic line is isolated, the expression pattern of the fluorescent marker gene will be studied in detail by co-staining for endothelial/ arterial markers such as *flk1* or *efnb2a* and haematopoietic markers such as *gata1*, *runx1* and *c-myb* in order to define the nature of the labelled cells. If the expression can be located to the ventral wall of the dorsal aorta or to haematopoietic cells, we will identify the trapped gene by using inverse PCR. Knock-down and over-expression studies of *vegf*, *notch* and *runx1* signalling pathway will enable to localise the function of the trapped gene within the known gene regulatory network governing haematopoietic development.

2. Materials and Methods

2.1 Materials

2.1.1 Zebrafish maintenance

Zebrafish were maintained at 28.5°C on a 12 hours light / 12 hours dark cycle. Fish were fed brine shrimp and flake food. Embryos were collected following natural spawning and raised in system water containing methylene blue as a fungicide and staged according to Kimmel (Kimmel et al., 1995)¹. In accordance with the home office rules, larvae beyond 4 days were either humanly killed by anaesthetizing in MS222 (4g/L) and then frozen at -20°C or bred in the fish facility to adulthood.

2.1.2 Maintaining mutant and transgenic fish lines

All transgenic fish lines were maintained as described above (2.1.1). Potential transgenic fish of the gene trap screen were out-crossed to wild type (WT) fish in order to identify carriers (F0). Embryos with GFP expression were raised as described

above (2.1.1). The subsequent generations of these GFP positive fish were repeatedly out-crossed to WT in order to reduce the number of insertions.

Transgenic lines *Fk1:tomato*, *EfnB2a:tomato* and *12x CLS:cerulean* were in-bred in order to increase the number of the transgene.

I-551/mindbomb fish were kept as heterozygous carriers and were crossed with each other to obtain homozygous mutants in the Mendelian ratio of 0.25.

2.1.2.1 Cloning of gene/enhancer trap vector *pTol2rst*

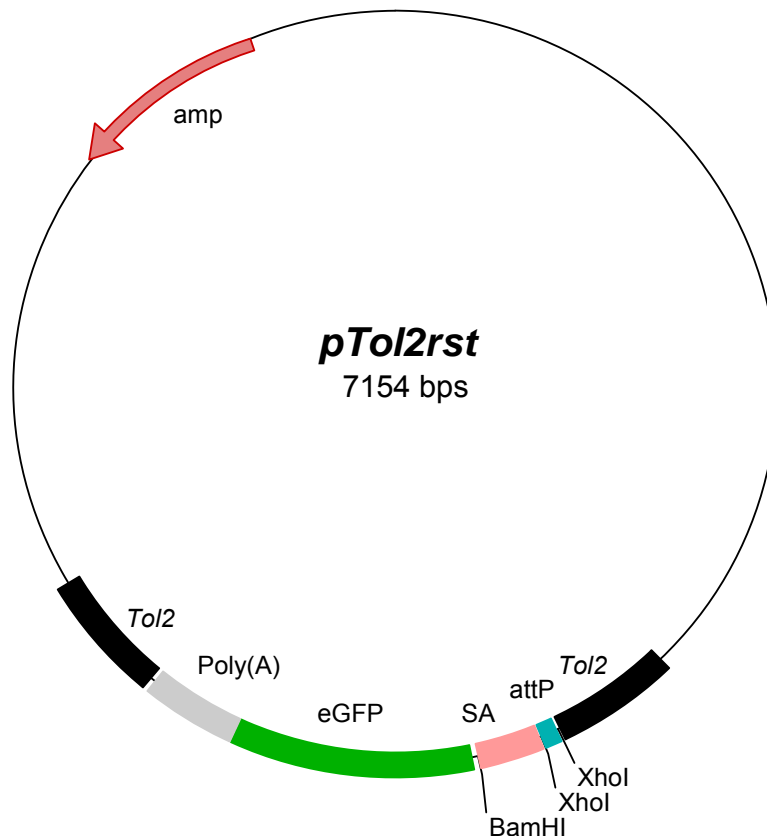


Figure 2.1: Construct map of the gene trap *pTol2rst* The gene trap vector consists of an attP site, splice acceptor (SA) site, the coding region for eGFP and a Poly-adenylation (Poly(A)) signal. These components are flanked by *tol2* repeats elements (*Tol2*) on either side. The backbone of the construct is the pBluescript vector.

The construct *pTol2rst* was generated by modifying the *tol2* vector *pT2KIXG* (Kawakami et al, 2004). The splice acceptor (SA) site was amplified from the pCI neo vector (kindly provided by F.Dahnfis-Calas) with the primer pair *rt splice acceptor for* and *rt splice acceptor rev* (see 2.1.3 primer list) and inserted into the vector after deleting the *Ef1alpha* promoter. An additional *attP* site was also cloned into the construct to allow ϕ C31 *Integrase* mediated homologous recombination if the technology becomes available in zebrafish. The construct was injected together with *transposase* mRNA into one-cell staged embryos (2.2.3.1ii).

2.1.2.2 Creation of the *Flk1:tomato* transgenic line

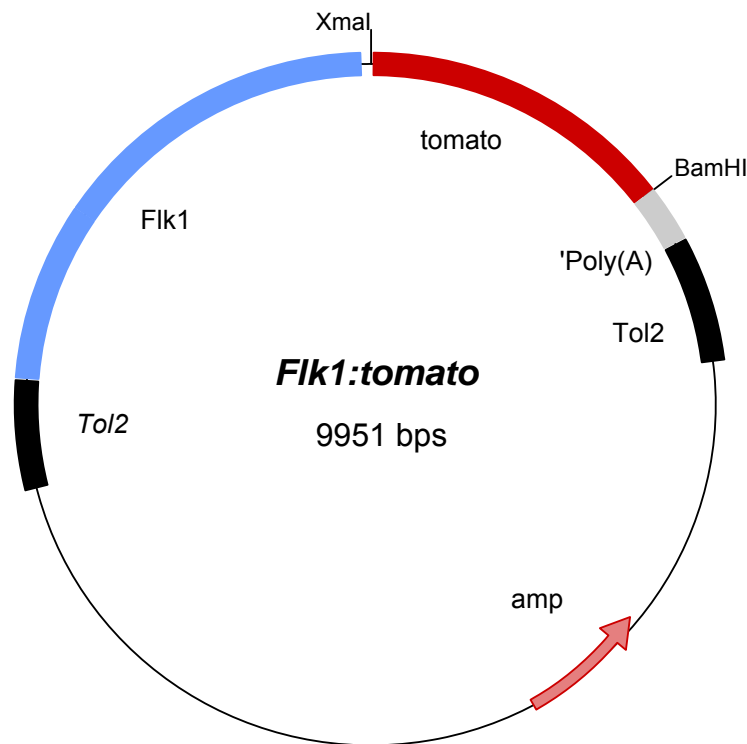


Figure 2.2: The *Flk1:tomato* construct The *Flk1:tomato* construct was made by cloning a 2.8 kb fragment of the *flk1* gene (kindly provided by K. McMahon) upstream of the *tomato* gene and the Poly-adenylation signal (Poly(A)). The construct is flanked by the *tol2* repeats (*Tol2*) on either side.

The vector *Flk1:tomato* was made by exchanging the eGFP sequence in the *Flk1:eGFP* construct for the *tomato* coding sequence. The *tomato* sequence was amplified from a *pBluescript* vector containing the sequence (kindly provided by F. Dafhnis-Calas) by using the primers *tomato/flk1* for *Xma1* and *tomato/flk1 rev BamHI* (see 2.1.3, primer list). 2 nl of a mix consisting of 50 ng/ μ l construct and 50 ng/ μ l of *transposase* (2.1.2.5) were injected into one- cell stage embryos (2.2.3.1 ii). Potential founder fish were raised to adulthood (2.1.2) and their progeny was screened for reporter gene expression.

2.1.2.3 Construction of the transgenic line *EfnB2a:tomato*

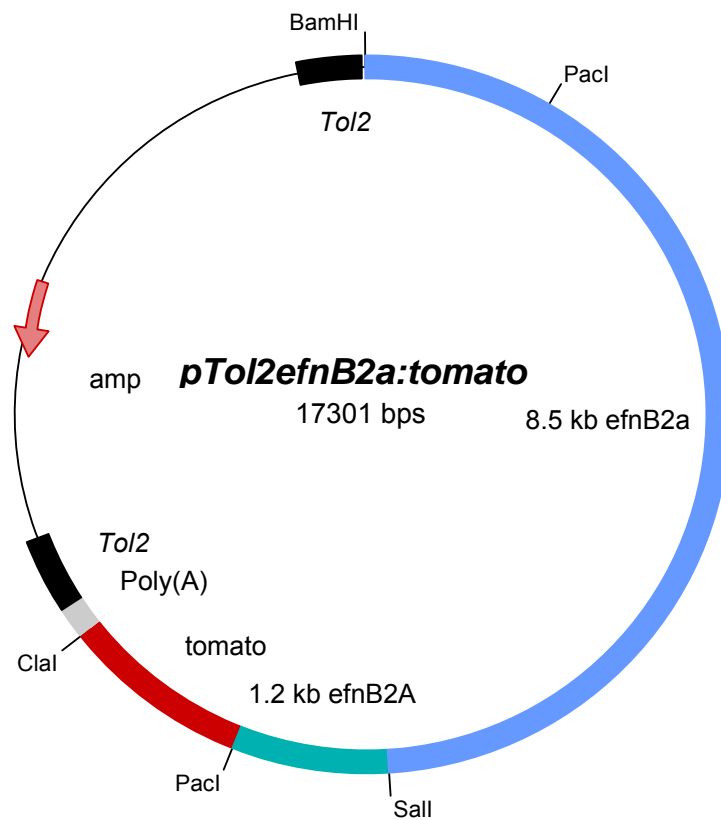


Figure 2.3: The *EfnB2a:tomato* construct The *EfnB2a:tomato* construct consists of a 9.7 kb promoter and upstream sequence of the *efnB2a* gene followed by the *tomato* coding sequence (*tomato*) and a Poly-adenylation (Poly(A)) site. The construct is flanked by *tol2* repeat elements (*Tol2*).

The *EfnB2a:tomato* construct was made in several steps. We used the original vector containing the 9.7kb upstream and promoter sequence construct to amplify the 1.2kb promoter sequence of the *efnB2a* locus using the primer pair *Efb2a Sall-kozak/BamHI-Sall* for and *EfnB2a Sall-kozak/PacI+ClaI* rev (see 2.1.3, primer list). The fragment was cloned into a *tol2* vector (*pTol2mcs*). Next, the *tomato* coding region was PCR-amplified with the primer pair *tomato/efnB2a PacI* for and *tomato/efnB2a ClaI* rev (see 2.1.3, primer list). The *PacI* and *ClaI* sites which were introduced into the vector with reverse primer of the 1.2kb fragment was used to clone

the *tomato* fragment into the vector. The 8.5 kb big *BamHI-Sall* fragment of the upstream sequence was cut out of the original vector and ligated into the *EfnB2a:tomato* construct. 2nl of 50ng/μl of the final vector was co-micro-injected with *transposase* mRNA 2.1.2.5) into one cell staged embryos. The resulting potential founder fish were raised to adulthood and their progeny was scored for *EfnB2a:tomato* transgenics.

2.1.2.4 Construction of the transgenic line *12xCLS:cerulean*

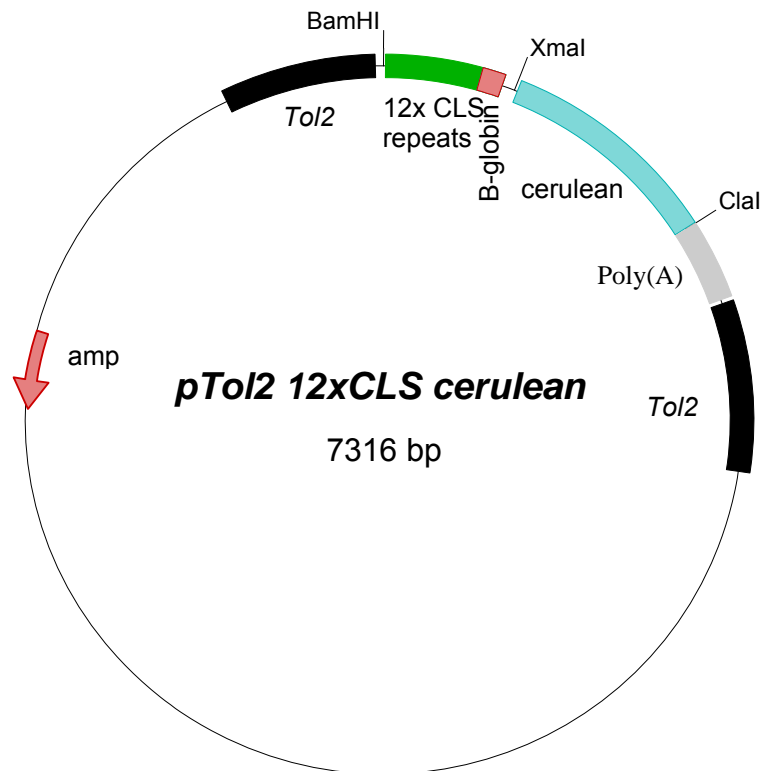


Figure 2.4: The *12xCLS:cerulean* construct The construct consists of 12 repeats for *CLS* binding (12x*CLS*) and a β -*globin* minimal promoter. Further downstream are the coding sequences for the *cerulean* gene and a site for Poly-adenylation (Poly(A)). These elements are flanked by the *tol2* repeats (*Tol2*). The construct is embedded in a *pBlueScript* backbone.

The *12xCLS:cerulean* construct was created in two successive steps. In the first step, the 12x*CLS* repeats including the β -*globin* minimal promoter were amplified using the primer pair 12x *CLS*- notch *Bam*HI for and 12x *CLS*-notch/*Xma*I, *Cla*I rev from the original vector 12x*CLS:venus* (A Haase, K McMahon, unpublished data).

The *Xma*I and *Cla*I sites in the reverse primer were used to introduce the *cerulean* coding sequence into the vector. The *cerulean* gene was PCR-amplified from the vector *hot-Cre* (A Haase, unpublished data) with the primer pair *cerulean* for 12x *CLS*/*Xma*I for and *cerulean* for 12x *CLS*/*Cla*I rev. The resulting 12x*CLS:cerulean* construct was co-injected into one cell staged embryos with *transposase* mRNA

(2.1.2.5). The embryos with transient expression of *cerulean* were raised to adulthood and their progeny were screened for marker gene expression.

2.1.2.5 The *pCS-TP* vector was used to produce *transposase* mRNA

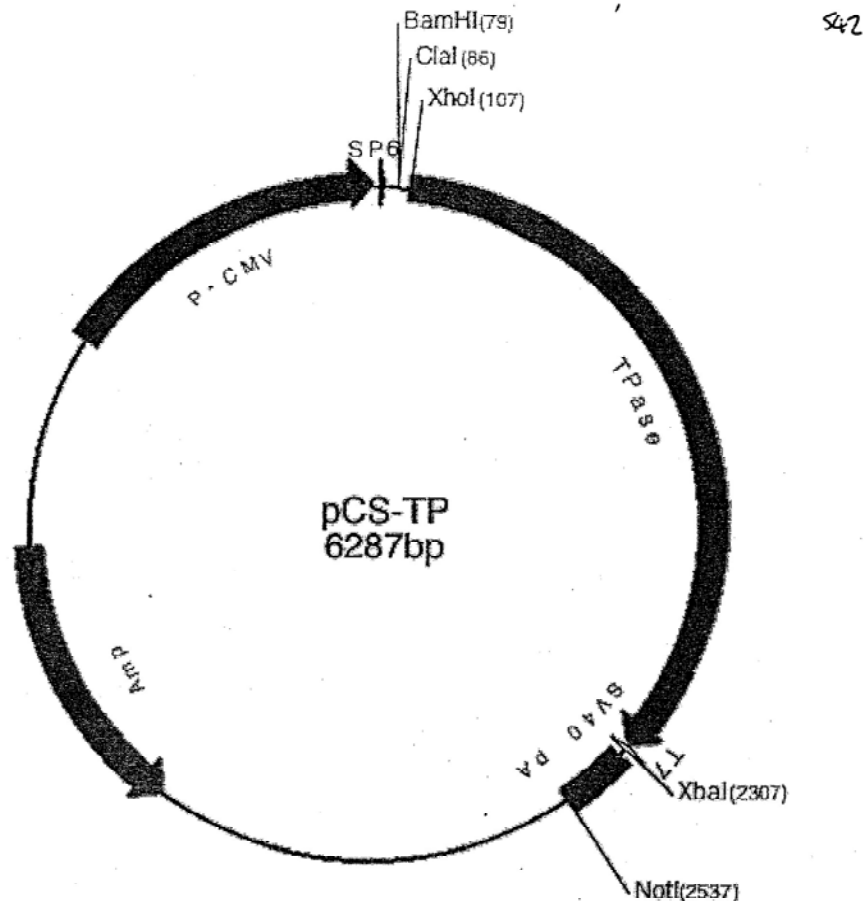


Figure 2.5: the vector map of *pCS-TP* The vector contains the promoter of the cytomegalovirus (CMV) to drive the transcription of *transposase* (TPase) and terminates with a Poly(A)-adenylation signal (SV40 pA). The *transposase* coding region is flanked by a *Sp6* promoter region at the 5' end and by a *T7* promoter region at the 3' end.

This vector was used to transcribe *transposase* mRNA. The vector was linearized using *Not1* and the *Sp6* promoter was used to produce mRNA of the *transposase*.

The mRNA was generated using the mMessage mMASCHINE kit (Ambion, catalogue numberAM1340).

2.1.3 Buffers and Solutions

Buffers/solutions	Ingredients	Store
20x SSC	3 M NaCl; 0.3 M Sodium citrate	RT*
4% PFA	2 g paraformaldehyde; 1 M NaOH; 1xPBS	4 °C
50x TAE	2 M Tris-acetate; 50 mM EDTA	RT*
BCL3	0.1 M Tris-HCL pH9.5; 0.1 M NaCl; 50 mM MgCl ₂ ; 0.1% Tween20	RT* (fresh)
Hybe-/- pH6.0	50% Formamide; 5xSSC; 9.2 mM Citric acid; 0.1% Tween20	-20 °C
Hybe+/- pH6.0	50% Formamide; 5xSSC; 9.2 mM Citric acid; 0.1% Tween20; 0.5 mg/ml tRNA; 50 mg/ml Heparin	-20 °C
MAB pH7.5	0.1 M Maleic acid; 0.15 M NaCl; 0.1% Tween20, added when needed	4 °C
MAB block	2% Boehringer Blocking Regent™ in MAB	-20 °C
MS222 pH7-7.5	4 g MS222 (Tricaine methanesulfonate) in 1 L distilled water	4 °C
PBS	150 mM Phosphore buffer (pH7.2); 0.85% NaCl	RT*
PBS _{tw}	1xPBS; 0.1% Tween20	RT*
TBS	Tris/HCl pH7.5	RT*
TBS Triton X-100	TBS; 0.025% Triton X-100	RT*
TBS-Block	TBS; 10% goat serum; 1% bovin serum albumin (BSA)	RT*
gDNA extraction buffer	10 mM Tris pH 8; 100mM EDTA pH8; 0.5% SDS; 200 µg/ml ProteinaseK	-20
Denaturing solution	1.5 M NaCl; 0.5 M NaOH	RT*
Neutralizing buffer	0.5 M Tris; 1.5 M NaCl, pH 7.5	RT*
5x HPB buffer	2.5 M NaCl ; 0.5 M Na ₂ HPO ₄ /7H ₂ O; 0.025 M EDTA	RT*
LB- Medium	10g Bacto-Tryptone; 5g Bacto-yeast extract; 10g NaCl; ddH ₂ O to 1 liter	RT*
0.3% PTU	0.3g of PTU in 100ml of ddH ₂ O	4 °C
Goat serum	10g in 10ml goat serum powder	-20 °C
10% BSA	0.1g BSA powder in 10ml of ddH ₂ O	

Room temperature

Restriction enzyme	recognition/cut site	storage
Apal	5'... GGGCC [▼] C... 3' 3'... C [▲] CCGGG... 5'	-20 °C
BamHI	5'... GGATC [▼] C... 3' 3'... CCTAG [▲] G... 5'	-20 °C
Cla I	5'... ATCGAT... 3' 3'... TAGC [▲] TA... 5'	
EcoRI	5'... GAATTC... 3' 3'... CTTAAG [▲] ... 5'	-20 °C
MboI	5'... GATC... 3' 3'... CTAG [▲] ... 5'	-20 °C
NcoI	5'... CCATGG... 3' 3'... GGTAC [▲] C... 5'	-20 °C
NotI	5'... GCGGCCGC... 3' 3'... CGCCGG [▲] CG... 5'	-20 °C
PacI	5'... TTAAT [▼] TAA... 3' 3'... AAT [▲] TAATT... 5'	-20 °C
PstI	5'... CTGCAG... 3' 3'... G [▲] ACGTC... 5'	-20 °C
Sall	5'... GTCGAC... 3' 3'... CAGCT [▲] G... 5'	-20 °C
SpeI	5'... ACTAGT... 3' 3'... TGATC [▲] A... 5'	-20 °C
SphI	5'... GCATGC... 3' 3'... C [▲] GTACG... 5'	-20 °C
XbaI	5'... TCTAGA... 3' 3'... AGATC [▲] T... 5'	-20 °C
XmaI	5'... C [▼] CCGGG... 3' 3'... GGGCC [▲] C... 5'	-20 °C

Primer	sequence
rt splice acceptor for	5'-agctagggccAGTATCAAGGTTACAAGACAG-3'
rt splice acceptor rev	5'-agctaggatccATAGTGAGTCGTATTAAGTACTC-3'
tomato/flkl for Xmal	5'-agctacccggggccaccATGGTGAGCAAGGGCGAGG
tomato/flkl rev BamHI	5'-agctaggatccAGCTACTTACTTGTACAGCTCGTCC
tomato/efnB2a PacI for	5'-agctattaattaagccaccATGGTGAGCAAGGGCGAGG-3'
Tomato/efnB2a ClaI rev	5'- agctatcgatCTTACTTGTACAGCTCGTCC-3'
Efb2a Sall-kozak/BamHI-Sall for	5'-agctaggatccagctagtcgacCTCAACCTAAATAAATG-3'
EfnB2a Sall-kozak/PacI+ClaI rev	5'agctatcgatagctattaattaCACGACCGTTACGGTCAAATC
12x CLS- notch BamHI for	5'-CTCTAGAGGATCCCGACTCG-3'
12x CLS-notch/Xmal, ClaI rev	5'agctatcgatagctacccgggCATGTGCGAGGGATTGCAAGTA AAC-3'
cerulean for 12x CLS/Xmal	5'-agctacccgggCAACATGGTGAGCAAGGGC-3'
cerulean for 12x CLS/ClaI rev	5'-agctatcgatCGATCTTTACTTGTACAGCTCGTC-3'
rt inpcr tol2 5' f1	5'-AGTACTTTTTTACTCCTTACAATT-3'
rt inpcr tol2 5' rev1	5'-GATTTTTTAATTGTAAGTAA-3'
rt inpcr tol2 5' f2	5'-GGAGATCACTTCATTCTATTTCC-3'
rt inpcr tol2 5' rev2	5'-CAAGTAAAGTAAAAATCCCCAA-3'
rt inpcr tol2 3' f1	5'-CAAGTACAATTTTAATGGAGTAC-3'
rt inpcr tol2 3' rev1	5'-GGAAGTAAAAGTAAAAGCAAG-3'
rt inpcr tol2 3' f2	5'-CTCAAGTAAGTATCTAGCCAG-3'

rt inpcr tol2 3' rev2	5'-GAAAGAAAACCTAGAGATTCTTG-3'
zfGfi1.1 intron1 for	5'-CGGAGGAACTGTTACCTACAG-3'
zf Gfi1.1 intron1 rev	5'-CTACCTGGGTCTCCACTTTTGC-3'
EGFP for	5'-GGACGGCGACGTAAACGGC-3'
EGFP rev	5'-CCATGCCGAGAGTGATCCCG-3'
Gfi1.1 cDNA probe for	5'-CTTCTCCAGACGACTCTCAGC-3'
Gfi1.1 cDNA probe rev	5'-CCTGAGATCTACTTTGCGCTG-3'
Gfi1b-like for	5'-ATGCCACGGTCGTTTCTGGTG-3'
Gfi1b-like rev	5'-GGCTCTCGTGGTGTCTGCG-3'

2.2 Methods

2.2.1 DNA Preparation

2.2.1.1 Transformation and bacterial overnight cultures

The bacterial strain DH5 alpha *E. coli* (Invitrogen) was used to amplify plasmids. Plasmids were co-incubated with the bacteria on ice for 20min followed by a heat-shocked to 42°C for 90s. The sample was chilled on ice for 2 minutes and the volume of the suspension was topped up to 1 ml by adding LB-medium. The growth of the bacteria was facilitated by an 1 hour incubation at 37°C. Subsequently, the culture was spread out onto LB agar containing 50µg ml⁻¹ampicillin and was incubated overnight at 37°C. The following day, colonies were picked from the LB-plates and incubated overnight in LB containing 50mg/ml⁻¹ ampicillin at 37°C as required, with moderate shaking.

2.2.1 .2 Preparation of plasmid DNA

Plasmid DNA was isolated in either a small scale (1-5 ml of overnight culture) or in a medium scale (50-100 ml). Mini- and Midi plasmid kits from Qiagen (catalogue number 51304 and 12143 respectively) were used for this procedure.

The overnight cultures were filled in either Eppendorf- tubes (Mini-preparation) or 50 ml Falcon tubes (Midi- prep) and centrifuged at 4500rpm (rounds per minute) for 5 min at 4°C. The resulting bacteria pellet was resuspended in P1. By adding P2 and inverting the tubes, the bacteria are lysed under the alkaline condition. The reaction is left on ice for 5 minutes. In the following step, P3 is added to the reaction. The NaOH in the P3 neutralizes the reaction, but the proteins and the gDNA are unable to re-nature to their original conformation, while the plasmid DNA which never really denatured because of its small size and its super coiled conformation is left in the supernatant. The supernatant was further cleaned from the cell debris by centrifugation at 13000 rpm. The supernatant was loaded into a new tube and the plasmid DNA was precipitated using 0.7 Volume of Isopropanol and centrifuging at 13000 rpm for 20 minutes. The plasmid DNA pellet was then washed with 70% EtOH before being air dried and resuspended in an appropriate amount of dH₂O.

2.2.1 .3 Restriction digest

Restriction digests were set up in a final volume of 20 µl with 1µg of template DNA.

Digest:

1 µg	template DNA
2 µl	Buffer (10x)
[2 µl	BSA (10x)]
10 U	enzyme (each)
<u>x µl</u>	<u>dH₂O</u>
20 µl	

The restriction reactions were incubated for 2h to overnight at the suitable temperatures for the enzymes.

2.2.1 .4 Agarose gel electrophoresis

Agarose gel electrophoresis is an easy way to separate DNA fragments by their sizes and visualize them. The technique of electrophoresis is based on the fact that DNA is negatively charged at neutral pH due to its phosphate backbone. For this reason, when an electrical potential is placed on the DNA it will move toward the positive pole. The rate at which the DNA will move toward the positive pole is slowed by making the DNA move through an agarose gel. The agarose forms a porous net in the buffer solution and the DNA must slip through the holes in the mesh in order to move toward the positive pole. This slows the molecule down. Larger molecules will be slowed down more than smaller molecules, since the smaller molecules can fit through the holes easier. As a result, a mixture of large and small fragments of DNA that has been run through an agarose gel will be separated by size. The separation of the fragments can be further enhanced by varying the concentration of the agarose. High concentration of agarose produces smaller pores and was used to separate small fragments whereas low concentration of agarose is sufficient to segregate large fragments. In general a 0.8- 1% agarose gel was used for electrophoresis and was run at 110 Volt. These gels were visualized on a U.V. trans-illuminator by staining the DNA with a fluorescent dye (ethidium bromide) which was added to the running buffer. A DNA molecular weight marker (1 Kb Ladder from NEB) was used to determine the sizes of the unknown fragments.

2.2.1.5 Gel- extractions

DNA fragments were purified from the agarose gel by using QIAquick Gel Extraction Kit (catalogue number 28704). The fragments of interest were cut out of the gel under

a low UV- light to prevent mutations and the manual in the kit was followed to purify the DNA fragments.

2.2.1.6 (Self) Ligation reactions

DNA ligation is the process of joining together two DNA molecule ends (either from the same or different molecules). Specifically, it involves creating a phosphodiester bond between the 3' hydroxyl of one nucleotide and the 5' phosphate of another. This reaction is usually catalyzed by a DNA ligase enzyme. This enzyme will ligate DNA fragments having blunt or overhanging, complementary, 'sticky' ends. The *T4* DNA ligase is a widely used enzyme for this process. In the case of ligation between a vector and an insert, the molar ratio plays a significant role. Molar ratios can vary from a 1:1 insert to vector molar ratio to 10:1. The *T4* DNA ligase was purchased from Invitrogen (catalog number 15224-041).

The amount of insert needed for a 6:1 insert to vector ratio can be determined using the formula:

$$\text{Insert Mass in ng} = 6 \times \left[\frac{\text{Insert Length in bp}}{\text{Vector Length in bp}} \right] \times \text{Vector Mass in ng}$$

The ligation reactions between a vector and an Insert were set up in a final volume of 20 μ l, self-ligations of DNA- fragments were set up in 100 μ l reactions. The reactions were incubated at 16°C overnight and transformed into DH5 alpha *E. coli* the following day (see 2.2.1.1).

2.2.1.7 Phenol- Chloroform Extraction

The Phenol- Chloroform extraction allows purifying DNA from solutions. The DNA will dissolve in the upper aqueous layer, while the proteins and other components will go with the bottom, non-aqueous layer.

One equal volume of phenol:chloroform:isoamyl alcohol (25:24:1) (Sigma, Cat. No. 77617) was added to the DNA solution. After vigorous shaking, the sample was centrifuged at maximum speed in a table-top centrifuge. The upper, aqueous layer was transferred into a fresh tube and extracted with an equal volume of Chloroform. The upper phase was transferred into a fresh tube and precipitated with 1/10 volume of sodium acetate (3M, pH 5.2) and 0.7 volume of Isopropanol. The resulting DNA pellet was washed in 70% ethanol and re-suspended in an appropriate amount of ddH₂O.

2.2.1.8 Isolation of high molecular weight genomic DNA

Genomic DNA prepared by this method was used for all purposes, including southern blots. Care was taken to carry out all mixing and re-suspension steps gently. Embryos, tissues or adult fish were shock-frozen in liquid nitrogen. The tissue was ground using a grinder before adding 10 ml of genomic extraction buffer per 1g of material. The sample was incubated at 50°C overnight. Subsequently, the reactions were cooled down to room temperature and extracted 2x with one volume of phenol-chloroform (2.2.1.7). All centrifugation were carried out at 3000-5000rpm. Following an extraction with chloroform, the aqueous phase was removed into a fresh tube and NaCl was added to a final volume of 200mM. This was overlaid with two volumes of Ethanol by slowly inverting the tube. The DNA will precipitate immediately and will be easily visible. The precipitated DNA was removed into a fresh tube containing 70%

Ethanol. The pellet was washed for minutes and then air-dried before being resuspended in dH₂O.

2.2.1.9a PCR

The Polymerase chain reaction (PCR) enables the amplification of a specific DNA fragment. The method is based on cyclic cooling and heating of the template DNA which allows repeated de-naturation and enzymatic re-amplification of the DNA fragment. The DNA of interest is flanked by two primers. Primers are short DNA fragments which are complimentary to the 3' of each target DNA strand. In a conventional PCR the 3' ends of the primers are pointing towards each other.

During the heating period, the double stranded DNA is denatured into single strands. The Primers bind to their target sites in the single strands and generate the starting points for the amplification. The enzyme *taq- Polymerase* recognizes these starting points and amplifies the missing sequence by incorporating the complementary nucleotides. With each cycle of cooling and heating, the number of specific DNA fragments increases exponentially. Taq-Polymerase was purchased from NEB (M0273) and dNTPs were ordered from bioline (Bio-39025).

2.2.1.9b Inverse PCR

The Inverse PCR is a variation of the standard PCR which is used to amplify unknown sequence adjacent to a known sequence. It is usually used to determine the genomic location of insertions.

The DNA first undergoes a restriction with an enzyme (see 2.2.1.3) which is known to cut once in the known insert sequence, the second restriction will occur randomly in the adjacent genomic DNA. Following a Phenol-Chloroform extraction (see 2.2.1.7)

the fragments were self ligated (see 2.2.1.6) overnight. The reaction was extracted with Phenol- Chloroform and the DNA was resuspended in 20-30 μ l of dH₂O.

Since the self-ligation of the DNA results in a looped DNA fragment, both primers can be positioned in the known sequence with the 3' ends pointing away from each other. The primer pair *rt inpcr tol2 5' f1* and *rt inpcr tol2 5' rev1* were used for the left side of the insertion, the primer pair *rt inpcr tol2 3' f1* and *rt inpcr tol2 3' rev1* were used to amplify the right hand side of the insertion. 1 μ l of the primary PCR-products was used for a nested PCR with appropriate primers (see 2.1.3 for primer list). The PCR will enrich the DNA fragment with the unknown sequence for subsequent sequencing.

2.2.1.9c Nested PCR

For the nested PCR, 1 μ l of the primary PCR product was diluted 1:10 and used as a template. The nested PCR of the inverse PCR products were performed using the primer pair *rt inpcr tol2 3' f2* and *rt inpcr tol2 3' rev2* (see primer list).

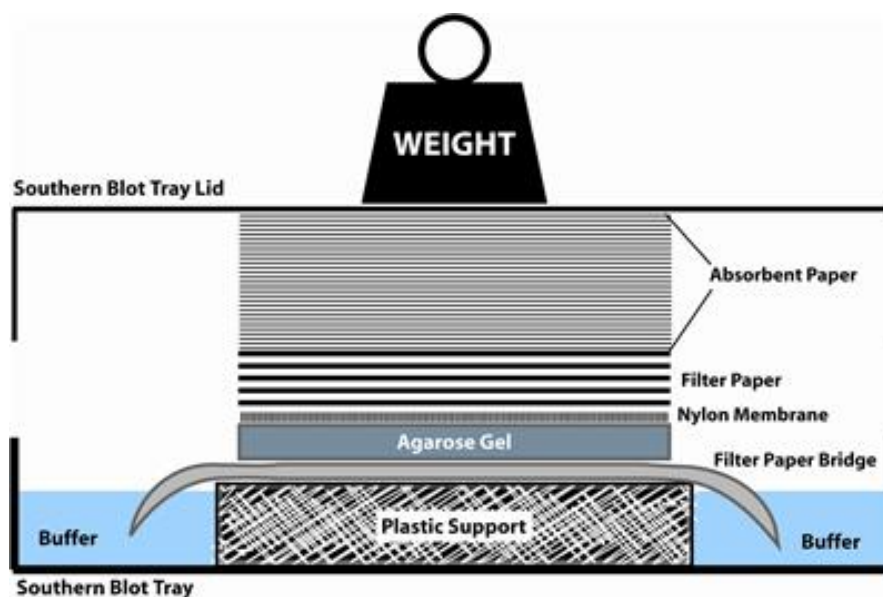
2.2.1.10 Southern blot

The southern blot detects the occurrence of specific DNA fragments in a sample. Here, it was performed to determine the number of insertion in a given transgenic line.

High molecular weight DNA was isolated from carriers of interest (see 2.2.1.8). Each genomic DNA sample was subject to two restriction digests. The four base pair cutters *BglII* and *PstI* were both known to cut in the insert DNA and were therefore used in these experiments. The restriction digests were done overnight and precipitated with Ethanol. The DNA fragments were run on a 0.8% agarose gel for 16

hours at 25 V or 60 mAmps. The gel was soaked for 5 minutes in 0.2N HCl in order to improve the transfer efficiency of larger fragments. The gel was quickly rinsed in deionised water and soaked in denaturing buffer for 45 minutes. A quick rise in deionised water followed before the gel was neutralized in neutralization buffer for 45 minutes. DNA fragments were transferred onto the nylon membrane overnight. Just prior to the transfer, the nylon membrane was wet thoroughly in 20x SSC buffer, pH7 for at least 5 minutes. The left hand corner of the membrane was cut off for orientation.

The set up for the transfer was done in a large electrophoresis tray. The schematic diagram depicts the set up in the tray.



In the middle of the blot tray, a plastic support is placed and the tray is filled with 20x SSC buffer, pH7. A large piece of filter paper is placed on top of the bridge, reaching into the buffer on both sides. The gel is placed on the filter bridge upside down and is covered with the nylon membrane. All air bubbles are smoothed out with a glass pipette carefully. A weight is placed on top of the set up to gently apply pressure. This has the consequence that the buffer is sucked from a region of high water potential,

the tray, to a region of low water potential, the paper tissues, thereby moving the DNA from the gel into the nylon membrane. Since the nylon membrane is positively charged, the negatively charged DNA will bind to it. The transfer is carried out overnight. After that, the membrane is washed in 6x SSC, pH 7 and air dried for one hour. The DNA on the damp membrane is immobilized to the nylon by UV- cross linkage (120mJ/cm²). The dried membrane is then placed in the pre-hybridisation buffer. The pre-hybridisation consists of 1% Sakosyl (Sigma, order number L-5125) in HPB buffer with 0.5 µg/µl salmon sperm DNA (Sigma, order number D-9156) at 65°C for 3 hours.

In order to determine the number of insertions, a 788bp *Bam*HI- *Cl*al fragment of the *To*l2 *rst* plasmid was used as a probe for the southern blot analysis. This fragment consists largely of the EGFP coding sequence and is therefore unique for the insertions.

25 ng of this fragment along with 2ng of 1 kb DNA ladder were used as a template for the random P32 radioactive labelling (ready mix labelling reaction). The labelling reaction was cleaned up by running the sample over a G50 column (GE-Healthcare, order number 27-5330-01). The radioactive probe was boiled and quenched on ice for 5 minutes before being added to the pre-hybridisation solution. The hybridisation was done overnight. The following day the membrane was soaked twice in 2xSSC/0.1% SDS at 37°C. The subsequent washing steps consisted of washes at 55°C and 50°C with 1x SSC/ 0.1% SDS for 20-30 minutes each, respectively. The membrane was blotted with filter paper to remove excess moisture, wrapped in cling film and imaged using a phosphor-imager.

2.2.1.11 RNA extraction and cDNA synthesis

RNA was extracted using TRIzol® Reagent. Embryos and tissues were stored in 500µl of the reagent and kept at -80°C until use. The samples were carefully homogenized using a pestle and incubated for 5 minutes at room temperature. 150 µl of chloroform was added to the suspension and inverted a few times before an incubation for 5 minutes at room temperature. After centrifugation at 13000 rpm for 20 minutes, the colourless upper phase containing the RNA was transferred into a new tube and 0.7 volume of Isopropanol was added to the samples. The samples were incubated for 10 minutes at room temperature and subsequently, the RNA was pelleted by a centrifugation step at 13000 rpm for 15 minutes, washed with 75% ethanol, air dried and resuspended in 50 µl of dH₂O. The RNA was stored at -80°C.

2.2.1.12 Reverse transcription

The process of reverse transcription utilizes the RNA-dependent DNA polymerase of the Moloney murine leukemia virus (M-MLV) to transcribe RNA into single strand DNA. The RNA template was produced from TRIzol® extractions and the commercially available kit from Promega (catalogue number M1701) was used for this process.

2.2.1.13 Whole mount *in situ* hybridisation

In situ hybridisation is a method which allows the detection of a particular mRNA in whole embryos. The probe used in this technique is a labelled mRNA sequence which is complementary to the mRNA of interest. MRNA sequences are openly available from the zebra fish genome sequence platform ensembl.org or zfin.org.

2.2.1.13 i probe synthesis for whole-mount in situ Hybridisation

The sequence of interest is amplified using PCR with sequence specific primers on cDNA. The appropriate DNA fragment was cloned into either pGEMT easy or pBlueScript KS vector and linearized with a restriction enzyme for *in vitro* transcription (see 2.2.1.13 ii). The vectors have promoter binding sites for the commonly used reverse transcriptases T3, Sp6 or T7. These enzymes are able to convert the DNA sequence into a complementary RNA sequence. The probe is labelled with Digoxigenin (DIG) or Flouresein (FI) (both from Roche, order number 11745832910 and 11685619910, respectively) in this process. The reaction is allowed to proceed for 2 hours at 37°C or overnight at room temperature. The DNA template is removed from the reaction through a digest with DNaseI for 15 minutes at 37°C. The reaction is stopped by adding EDTA at a final concentration of 10mM and the RNA probe is precipitated with ethanol, washed in 70% ethanol, air dried and resuspended in 50µl of dH₂O.

2.2.1.13 ii Vector maps of the probes used in *insitu hybridisation*

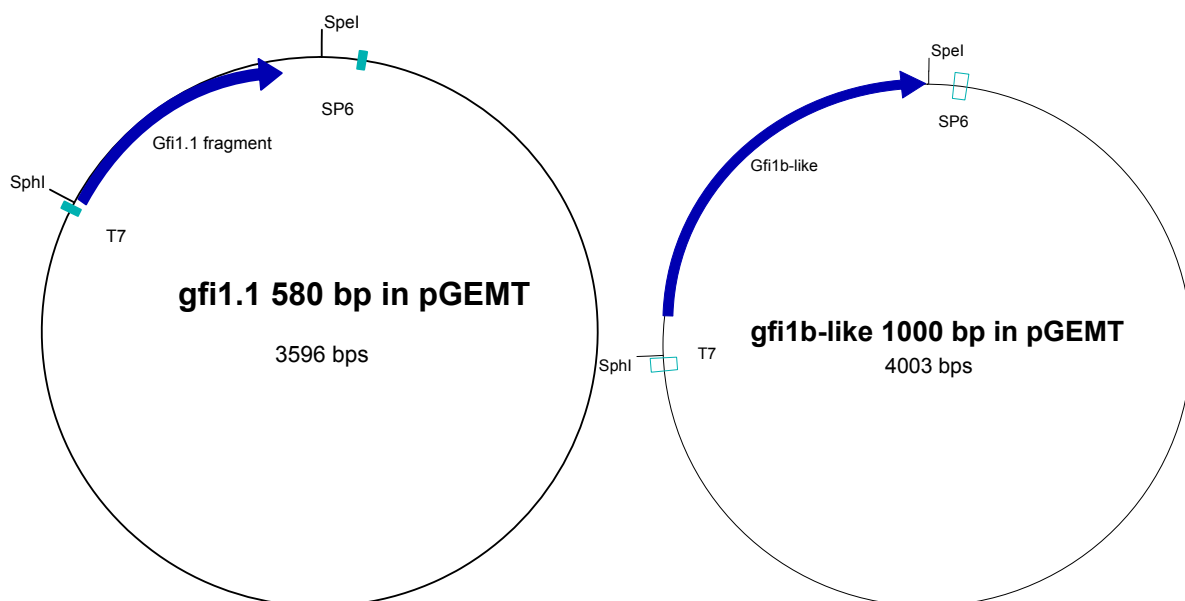


Figure 2.5: *Gfi1.1* and *gfi1b-like* fragments in *pGEMT* vector A 580 bp fragment of the *gfi1.1* gene and a 1000bp fragment of the *gfi1b-like* gene were cloned into the *pGEMT* vector in order to synthesize probes for *in situ hybridisation* experiments.

Both fragments illustrated in Figure 2.5 were amplified from a embryonic cDNA library using the primer pairs *Gfi1.1 cDNA probe for* and *Gfi1.1 cDNA probe rev* for *gfi1.1* and *Gfi1b-like for* and *Gfi1b-like rev* for *gfi1b-like*. Both fragments were successfully cloned into *pGEMT* for probe synthesis. Other probes used in this thesis are listed in the table below.

Gene	Probe length	Source
<i>c-myb</i>	300 bp	Thompson et al, 1998
<i>runx-1</i>	1280 bp	Kalev-Zylinska et al, 2002
<i>β-E1 globin</i>	590 bp	Quinkertz et al, 1999

2.2.1.13.iii Fixing and preparation of embryos for *in situ hybridisation* and immunohistochemistry

Embryos older than 26 hpf at the time of the staining experiments were subject to 0.003 % phenylthiourea (Sigma, order number P-7629) (PTU)-treatment in order to decrease pigmentation of the embryo. In this case, 0.5 ml of 0.3% PTU were added to the petri-dishes containing the embryos in fish water at the beginning of the somitogenesis stage. Embryos were then fixed in 4% PFA in PBS, overnight at 4°C. Fixed embryos were subsequently washed three times in PBStw for 5mins. The

embryos were then taken through 5min washes in 25%, 50%, and 75% methanol in PBStw, and then washed into 100% methanol for storage at -20°C.

2.2.1.13 iv PFA treatment of the embryos

Fixed embryos in 100% methanol were gradually rehydrated through 5 minute washes in 75%, 50% and 25% methanol. Subsequently, they underwent three consecutive washes in PBStw for 5 minutes before being treated with proteinase K (Sigma, order number P2308) at a final concentration of 10 µg/ml. Embryos younger than 24 hpf were excluded from this process, embryos at the age between 24 hpf - 32 hpf were treated for 15 minutes at room temperature, 2 and 5 days old embryos were subject to 30 minutes and 45 minutes treatment, respectively. The proteinase K treatment enables the penetrance of the probes into the embryonic tissue. The reaction was terminated by two 5 minute washes in glycine at a final concentration of 2 mg/ml. The embryos were re-fixed in 4% PFA in PBStw for 20 minutes.

Alternatively, embryos were treated with 100% acetone (Sigma, order number 179124) to ensure penetrance of the probe into the tissue. Here, fixed embryos in 100% methanol were gradually rehydrated through 5 minute washes in 75%, 50% and 25% methanol. Subsequently, they underwent three consecutive washes in PBStw for 5 minutes before being rinsed once for 5 minutes at room temperature in sterile distilled water. The water was removed and the pre-cooled acetone (-20°C) was added to the embryos. The embryos were incubated at -20°C for 7 minutes. The acetone was removed by washing the embryos for five minutes at room temperature in deionised water. After this step, the embryos were transferred into PBST at room temperature. A re-fixing in PFA is not necessary if embryos are treated with acetone instead of proteinase K.

2.2.1.13 v Pre-hybridisation and hybridisation

The fixative is washed off by rinsing the embryos five times for 5 minutes in PBStw and they are gently equilibrated to the pre-hybridisation solution by washing them in 50% pre-hybridisation solution and 50% PBStw. In the following step, the embryos are hybridised in 100% pre-hybridisation solution for at least one hour at 65°C. The probes are added at a dilution of 1:150 to the samples and the hybridisation is left on overnight. All probes (2.2.1.13ii) were hybridised at 65°C, except the *runx1* hybridisation for fluorescent *in situ* which was done at 55°C.

2.2.1.13 vi probe removal and incubation with antibody

The following day, the probes are removed and the samples undergo a series of washes from 100%, 75%, 50% and 25% hybridisation solution in 2x SSC every 30 minutes 65°C. Subsequently there are a two stringency washes of 2x SSC and 0.2x SSC at 65°C for 30 minutes each. The samples are cooled down to room temperature and equilibrated gradually to MABtw in 25%, 50%, 75% and 100% MABtw in 5 minute washes. The embryos are then blocked in 2% blocking reagent (Roche #11096176001) for at least one hour at room temperature. This was replaced with either anti-DIG coupled to alkaline phosphatase (AP)(1:5000) or anti-Fluorescein AP (1:2000) antibody diluted in MAB containing 2% Blocking Reagent and incubated overnight at 4°C.

For fluorescent colour reactions the embryos were incubated with anti-DIG and/or anti-Fluorescein coupled to horse-radish peroxidase (POD) (Roche, order number 11207733910) instead of AP.

The next morning, the samples are washed eight times for 5 minutes at room temperature in MABtw solution.

2.2.1.13 vii staining reaction for BMPurple

If the embryos are to be stained with BMPurple (Roche, order number 11442074001), they are equilibrated in developing buffer for 15 minutes and then placed in the staining solution which consists of 50% developing buffer and 50% BMPurple solution. The reaction is monitored regularly under a stereo microscope for staining and is stopped by adding PBStw with 20mM EDTA. Subsequently the embryos are fixed in 4%PFA in PBS overnight and are washed in a series of 5 minutes washes into 80% Glycerol for long term storage at 4 °C.

2.2.1.13 viii staining reaction for fluorescent tyramide

In the case of fluorescent labelling, the embryos are equilibrated into PBStw after the MABtw washes. The embryos are incubated in 100 µl of 1:25 dilution of Cy3 tyramide or Fluorescein tyramide in amplification reagent (Perkin-Elmer, order number NEL753001KT) for 30 minutes in the dark at room temperature. After the staining reaction excessive tyramide substrate and the high background signal in the samples are eliminated by extensive washes in PBStw for several hours.

2.2.1.13 ix post-staining treatment

For subsequent immune-histochemistry, the embryos were not re-fixed in 4% PFA, but were carried forward to the blocking step in 2.2.1.14. Otherwise the stained embryos were then fixed in 4%PFA in PBS overnight and gradually washed into 80% glycerol for long term storage at 4°C.

2.2.1.14 Immuno-histochemistry

Immuno-histochemistry is a method which allows the detection of a protein on a cellular level. The primary antibody is raised against the antigen of interest. The secondary antibody is coupled to a fluorophore e.g. Alexa Fluor 488 and Alexa Fluor 568 and is raised to detect the primary antibody.

Alternatively, a biotin label on the primary antibody can be detected by streptavidin coupled to horseradish peroxidase (HRP). Here, the substrate 3, 3' Diaminobenzidine (DAB) is used by the HRP to produce a brown staining.

The embryos used in this protocol are either embryos carried forward from an *insitu* staining step (2.2.1.14) or are transgenic fish embryos which express eGFP and/or dsRED proteins under different promoters. Since both primary antibodies were raised in different host animals, both can be used simultaneously without cross-reactions.

2.2.1.14i Streptavidin- Alexa 488 and Streptavidin Alexa 568

Embryos were collected at the time points of interest, fixed, stored in methanol overnight and treated with PFA as described in 2.2.1.13ii and 2.2.1.13iii.

The samples were first equilibrated into PBS with 0.025% Triton X (TBS) and then blocked in blocking solution (10% goat serum and 1% bovine serum albumin (BSA) in TBS) for two hours at room temperature.

Both the anti GFP and the anti-dsRED antibodies (abgene, catalogue number 6658 and clontech, order number 632496, respectively) were diluted 1:250 in TBS with 1% BSA and incubated at 4 °C overnight.

The primary antibodies were washed off with TBS washes for at least 3 hours and Streptavidin-Alexa488 (Invitrogen, catalogue number S3235) or Streptavidin Alexa 568 (Invitrogen, order number A10037) were diluted 1:400 in TBS with 1% BSA and

incubated at 4 °C over night .The next day the samples were washed in TBS for several hours and the staining was assessed under a fluorescent microscope. The embryos were prepared for long term storage as described in 2.2.13.viii.

2.2.1.14 ii Vectastain ABC kit-DAB

The commercially available Vectastain ABC kit-DAB (Vector laboratories, order number PK6100) was used for this protocol. Embryos were collected at the desired developmental stage, fixed, stored in methanol overnight and treated with PFA as described in 2.2.1.13ii and 2.2.1.13iii.

The samples were first equilibrated into PBS with 0.025% Triton X (TBS) and then blocked in blocking solution (10% goat serum and 1% bovine serum albumin (BSA) in TBS) for two hours at room temperature. The anti GFP was diluted 1:250 in TBS with 1% BSA and incubated at 4 °C overnight. The primary antibody was washed off with TBS washes for at least 3 hours. The avidin/HRP-biotin mix was prepared by diluting 5 µl of both reagents in 0.5 ml of PBStw. The mix was incubated at room temperature for 30 minutes before being transferred onto the embryos. The embryos were left in the mix for one hour and then washed in PBStw for 15 minutes in 5 minutes steps.

The DAB solution was made up by adding 30 µl of HRP-Biotin to 1 ml of Avidin solution. The embryos were then transferred into this staining solution. The staining reaction itself is very fast. The brown staining was assessed under a dissecting microscope and the excessive staining solution was rinsed off with PBStw for 15 minutes. The embryos were fixed in 4%PFA overnight and prepared for long-term storage as described before (2.2.1.13 viii).

2.2.1.15 Embedding zebrafish embryos in JB4 plastic

The JB4 embedding kit is available from biosciences (order number GH06d).

DAB stained embryos were gradually dehydrated in alcohol containing 30%, 50%, 70% and 95% of ethanol in dH₂O. In the mean time the infiltration solution is made up by dissolving 1.25 g of benzoyl peroxide in 50 ml of JB-4 solution a monomer. The embryos are transferred into this solution and incubated in it over night for optimal infiltration of the tissue. The following day the polymerization solution is made up by mixing 1ml of JB-4 solution B (accelerator) with 24 ml of the infiltration solution. The embryos are orientated in the moulds and overlaid with the polymerization solution. The mould is placed in an air- tight box and the oxygen level inside is reduced by overlaying the plastic box with nitrogen gas since the polymerization needs anaerobic conditions. The box is kept overnight at room temperature in the dark for the polymerisation to occur.

2.2.1.16 plastic sectioning of zebrafish embryos

The embryos are removed from the moulds and the plastic blocks were trimmed to a pyramid shape using a razor blade. The mounting medium (technovit 3040 combi, order number T224) is made up by mixing two parts of the powder with one part of the liquid. The embryo blocks are placed on the plastic chucks and mounted onto with the mounting solution. The chucks are left for a few hours to harden properly.

10 µm sections were taken on a microtome (Leica Jung, RM2055). The sections were carefully placed on glass slides and embedded using coverslips and DPX solution (Leica, order number 3808600E).

2.2.3 Manipulation of zebrafish embryos

2.2.3.1 Microinjections into early stage embryos

Microinjections are used in the zebra fish embryos in order to introduce DNA, RNA, morpholinos or proteins into fertilized embryos. The setup uses a microinjection needle which is filled with the molecule of interest and is attached to a microinjection machine that forces the solution out of the needle and into the embryo.

2.2.3.1 i Preparation of microinjection needles

Microinjection needles were prepared by pulling glass capillaries into micropipettes using the micropipette puller (Sutter instruments Co) with the setting heat: 316, time: 115 and velocity: 115.

2.2.3.1 ii DNA injections into one cell stage embryos

DNA injections were done on one cell stage embryos in order to introduce transgenic construct into wild type embryos. All transgenic lines were generated by cloning the sequence of interest into *tol2* vectors. These vectors possess the *tol2* ends which are essential for a stable integration of the transgenes into the genomic DNA. The transposase enzyme which catalyzes the integration reaction was supplied in a limited quantity in form of mRNA.

The microinjections were performed using a picospritzer® III (Intracell). The embryos were collected at one cell stage and were injected with a mix of 50 ng/μl vector DNA and 50ng/μl transposase mRNA in dH₂O. The amount of the injection volume was calibrated to one nanoliter (nl) by using the graticule on the dissecting microscope. Each one cell stage embryos was therefore injected with 50 picogram of vector DNA and mRNA.

Injected embryos were raised at 28.5 °C and were scored for transient reporter gene expression the following day. Fish embryos with mosaic transgene expression were grown up to adulthood.

2.2.3.1. iv Morpholino injections into early stage zebra fish embryos

Morpholinos can be injected into one to eight cell stage embryos since the small size of the molecules allow efficient diffusion in the embryo.

The morpholinos were dissolved to a stock solution of 25 µg/µl and diluted further to a working solution of 10 µg/µl. The amount of the injected amount was estimated using the graticule. Each morpholino was titrated to give a phenotype without or with only minimal off-target effects.

List of used morpholinos:

Gene	Type	Exon/Intro n	sequence	source	concentratio n
runx1	splice	Ex1b/ln1b	5'AGCGCTCTTACCGTATT TGCCT 3'	Gering et al, 2005	8 ng
Su(H)	splice	Ex1/Ex2	5'CAAACCTCCCTGTCACA ACAGGCGC 3'	Sieger et al, 2004; Echeverri et al, 2007	5 ng
Sih (Tnnt2)	ATG		5'CATGTTTGCTCTGATCT GACACGCA-3'	Sehnert et al., 2002	4 ng

Embryos were collected at one cell stage and injected as described in 2.2.3.1 iii.

The development of the injected embryos was closely monitored using a dissecting microscope.

2.2.3.2 Treatment of zebrafish embryos with small inhibitor molecules

2.2.3.2.i Treatment with γ -secretase Inhibitor XVI

The inhibitor was resuspended to a stock concentration of 12.5 mM in DMSO. Embryos were collected at shield, tailbud, 10 somites, 14 somites or 18 somites stage and treated with 100 μ M of γ -secretase Inhibitor XVI (Calbiochem, order number 565777-5MG) in 5 ml of fish water. As a negative control equal amount of embryos were treated with DMSO (Sigma, order number 472301) in fish water. All embryos were grown at 28.5 °C until they reached the developmental stage of 32hpf. They were then fixed in 4% PFA in PBStw overnight and washed into 100% methanol (see 2.2.1.13 ii) for subsequent *insitu* hybridisation and/or Immuno-histochemistry.

2.2.3.2.ii Treatment with the *Vegf receptor tyrosine kinase* inhibitor

The inhibitor was made up in DMSO at a stock concentration of 12.5 mM. Embryos were collected at tailbud stage and treated with 5 μ M *Vegf receptor tyrosine kinase* inhibitor (Calbiochem, order number 341607-5MG) in 5 ml of fish water. The embryos grown in the presence of the inhibitor until 28 hpf and were subsequently fixed in 4% PFA for subsequent experiments (see 2.2.1.13 ii).

2.2.3.2.iii Treatment with the inhibitor LY294002

The LY 294002 inhibitor (Calbiochem, catalogue number 440202) was made up to a stock concentration of 10mM in DMSO. Embryos were collected at 10 somites stage and treated with 25 μ M of the inhibitor in fish water. The morphants were fixed in 4% PFA in PBStw at 33hpf for subsequent Immunohistochemistry (see 2.2.1.13 ii).

2.2.3.3 Experiments with Tg (*hsp70:Gal4/ UAS:NICD/ Gfi1.1:eGFP*)

2.2.3.3.i Genotyping of Tg (*hsp70:Gal4/UAS:NICD/ Gfi1.1:eGFP*) fish

The Tg (*hsp70:Gal4/UAS: NICD/ Gfi1.1: eGFP*) fish were in-bred and the progeny was assessed for eGFP expression. Crosses which gave rise to eGFP positive progeny were further examined for the presence of the two transgenes *hsp70:Gal4* and *UAS: NICD* by PCR. The genomic DNA from each batch was extracted (see 2.2.1.8) and a PCR (see 2.2.1.9) with specific primers for each transgene was performed (see 2.1.3 for a primer list). Clutches of embryos which were positive for both transgenes were helpful to link the batch of embryos to the parental cross. These were then identified as carriers of the three transgenes and were used for heat-shock experiments.

2.2.3.3.ii Heat-shock experiments with Tg (*hsp70:Gal4/UAS: NICD/ Gfi1.1: eGFP*)

The induction of Gal 4 expression is dependent on heat activation. The promoter can be induced by raising the temperature up to 38 °C. Tg (*hsp70:Gal4/UAS: NICD/ Gfi1.1: eGFP*) embryos were collected at one cell stage and raised to 16 -18 somite stage at 28.5 °C. They were transferred into 5 ml of fish water into 50 ml Falcon tubes and heat- shocked at 38 °C for 20 minutes in a water bath. After this period the embryos were transferred into petri dishes with unheated fish water and grown up to 33hpf at 28.5. °C. The embryos were then collected and fixed in 4%PFA in PBStw for subsequent *insitu* hybridisation and Immunohistchemistry.

2.2.3.4 Fluorescence-Activated Cell Sorting (FACS)

Flow cytometry is a technique for examining and counting microscopic particles, such as cells. The cells are passed through a stream of fluids into an electronic detection

apparatus. In the detection apparatus, beam laser light of a single wavelength is directed onto a focused stream of fluid and a number of detectors are aimed at the point where the stream passes through the light beam: one in line with the light beam (Forward Scatter or FS) and several orthogonal to it (Side Scatter (SS) and one or more fluorescent detectors. The cell which passes the stream is electronically charged and consequently, this process allows sorting a mixture of biological cells into two or more containers, one cell at a time, based upon the specific light scattering and fluorescent characteristics of each cell.

Initially, embryos were collected and left to develop up to the developmental stage of interest. The embryos were decorinated if necessary and placed in E3 buffer. The embryos are then transferred into 33mm petri-dishes containing 10mM of DTT (Sigma, D9779-5G) in 2 ml of E3 buffer and incubated for 30 min at room temperature on a rocker. The embryos are then rinsed in E3 buffer to remove the DTT and are then placed in Hank's balanced salt solution (HBSS) (with Calcium and Magnesium, Invitrogen, order number 14175-046)). 80 μ l of Liberase Blendzyme (Roche, order number 11988468001) is added to per ml of HBSS and incubated for one hour at 28- 32 °C. The cell dissociation is improved by macerating with a pipette every 15 minutes. When the embryos are completely dissociated, 5 ml of 0.9x PBS with 10% foetal calf serum (FCS) is added and the suspension is passed through a cell strainer into a 15 ml Falcon tube. The Falcon tube is filled with PBS/FCS and centrifuged at 1500 rpm for 5 minutes. The washing step is repeated twice more before the cells are taken up in 1ml of 0.9x PBS with 1% FCS. The cell density is determined by counting them using a haemocytometer and trypan blue to exclude dead cells.

The 15 ml falcon tubes used for collecting the FACS sorted cells are pre-coated with FSC containing 5 ml of Lawson collection media with 10 % FCS. The sorting buffer consists of 0.9x PBS. The cells are sorted twice to ensure a purity of 95-100%.

3. Results

3.1 Injection of the gene trap vector *tol2rst* generates transgenic fish lines with ubiquitous and tissue-specific eGFP reporter expression during early embryogenesis

3.1.1 Micro-injection of the gene trap vector *ptol2rst* into one cell stage embryos

In order to generate transgenic zebrafish lines with tissue specific expression patterns, we used a gene trap approach. We hoped to obtain a line, which expresses the reporter gene in haematopoietic tissue. We therefore injected 2853 zebrafish embryos at the one cell stage with the *Tol2* transposon-based gene trap vector *tol2rst* and transposase mRNA. Successful injections of the transposon into the genome will result in mosaic reporter gene expression in the embryo, which was scored for the following day. In 2104 injected embryos (73%; Table 1), mosaic eGFP expression could be detected. This observation confirmed the efficient delivery of the construct and the mRNA into the embryo through microinjection. Embryos with transient eGFP expression were raised to adulthood. Of these, 639 reached adulthood (Table 1). The survival rate of 30% (Table 1) was comparable to that of wild type fish grown up during the same period (wild type survival rate of 30- 40 % (stock book, BMSU), which demonstrated that the injected embryos displayed normal viability.

	Injected embryos	Embryos with transient GFP expression	Potential founder fish that survived to adulthood
Number of embryos	2853	2104	639
Percentage of embryos	-	73%	30%

Table 3.1: Survival rate of embryos injected with *tol2rst* 2853 zebrafish embryos were injected with the *tol2rst* plasmid together with transposase mRNA. Of these, 2104 (73%) showed transient expression in the following days and were raised to adulthood. Only 639 embryos reached adulthood (30%) and were subject to crosses to wild type fish of the opposite sex.

3.1.2 A screen of the progeny of F0 founder fish identifies stable transgenic lines

639 potential founder fish were mated to wild-type fish of the opposite sex in order to screen their germ line for the presence of the transgene. 536 of these mating were successful. The progeny of the crosses were screened for eGFP expression every 10-15 hours from 10 hpf until 4 dpf. Special care was taken to screen the progeny between 24-29 hpf for eGFP expression, since this is the crucial time-point for the emergence of HSCs in the ICM in zebrafish (Kalev-Zylinska et al, 2002; Gering et al, 2005, Lam et al, 2009, 2010; Murayama et al, 2010, Jin et al, 2007, Bertrand et al, 2010).

In total, we were able to visually identify 174 gene trap events in the 536 fertile founders (Figure 3.1). This means that we were able to visually identify a germ line transmission frequency of 30% in the founder fish population. 105 (60%) of these insertions captured ubiquitously expressed genes, whereas 69 (40%) of the insertions trapped genes with tissue-specific expression patterns (Figure 3.1). From these results, we could conclude that our construct *tol2rst* can efficiently integrate into the germ line of the founder fish. In addition, gene trap events in the germ line

are visible in the progeny. We noted that the progeny of one founder fish can display more than one gene trap event. 9 fish gave rise to a mosaic progeny population. In these cases, we were able to obtain two or three distinct subgroups of embryos, which express eGFP in different spatio-temporal expression pattern. Here, the transposition events must have happened independently in individual germ line cells of the founder fish.

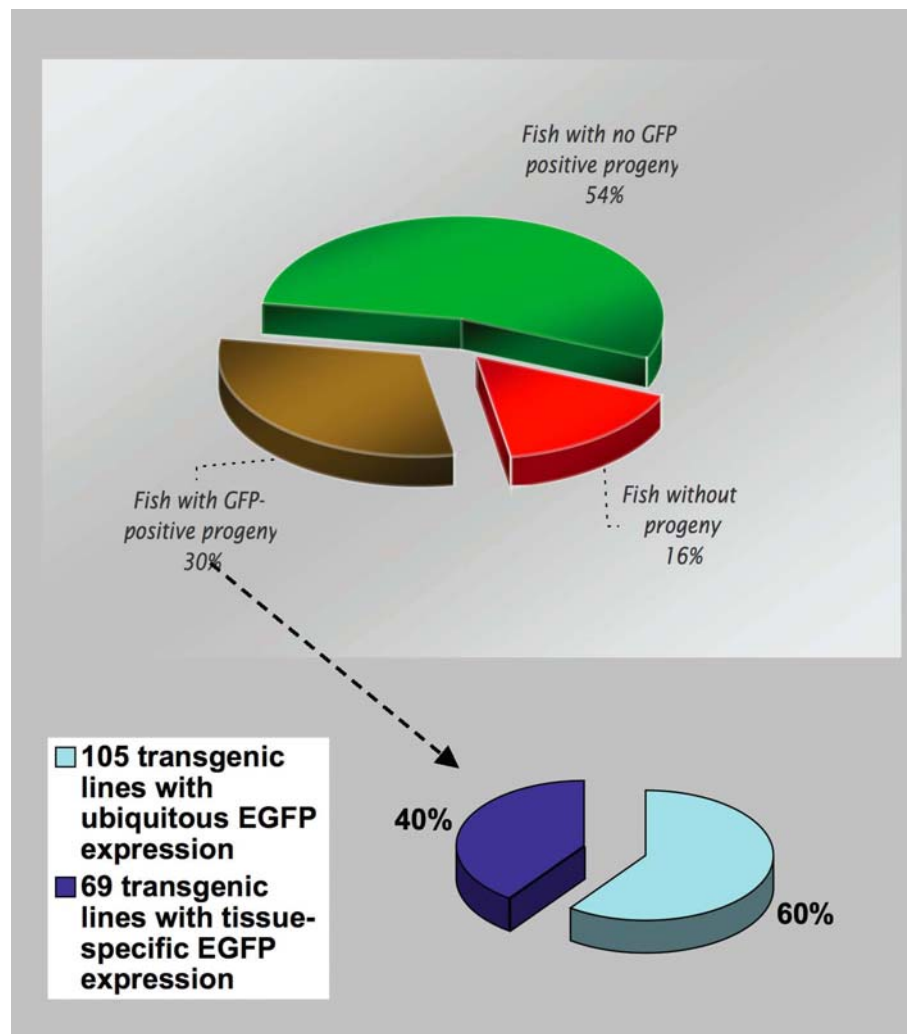


Figure 3.1: Germ line transmission frequency in zebrafish embryos injected with *tol2rst* From the total of 639 potential founder fish, 536 (84%) were fertile and 30% gave rise to transgenic progeny with either ubiquitous or with tissue-specific reporter gene expression. 105 of these transgenic fish (60%) showed ubiquitous expression whereas in 69 (40%) transgenics the eGFP expression was restricted to specific tissues or organ.

Summary of Chapter 3.1:

- the gene trap vector *ptol2rst* is functional in zebrafish
- the vitality of the founder fish was not compromised by the genetic manipulation
- the majority of the founders were able to reproduce
- 160 founder fish gave rise to progeny with eGFP expression and 69 of these transgenic lines displayed tissue-specific expression pattern

3.2 A subset of F1 fish display reporter gene expression in a tissue-specific manner

The *tol2rst* based gene trap screen resulted in 69 transgenic fish with tissue-specific reporter gene expression patterns, including haematopoietic sites. The Figure 3.2 shows examples of transgenics. The chosen examples verify that the reporter gene expression is not restricted to a subset of tissues, but can be detected in almost any cell type. The first transgenic line (*I-115*) in the panel (Figure 3.2 A) shows spotted expression of eGFP along the yolk cell extension beginning from 24 hpf to 2d. The nature of these cells is undetermined. The eGFP positive cells are round and large at the beginning of the reporter gene expression, but become smaller thereafter and on day 3 the expression is lost or not detectable. *SN 172-38-1* (Figure 3.2 B) shows eGFP expression in the lens of the embryo at day 3. The expression is still present at day 4, but it is unknown if the reporter gene expression persists into adulthood. The transgenic embryos of *SN 172-53* express eGFP in the hypochord and in the floor plate. The hypochord is a row of cells wedged between the DA and the notochord

and is derived from the mesoderm. It is known to secrete Hedgehog molecules (Mueller et al, 1999). The floor plate is of ectodermal origin and forms the ventral aspect of the spinal nerve cord. It gives rise to glial structures and is conserved across vertebrates. The expression in both of these tissues was observed at 24 hpf and persisted until 4 dpf. The next transgenic *SN 172-30* expresses eGFP in the developing cartilage, in the head of the embryo (Figure 3.2 D). The chondroblasts which form the cartilage are of mesodermal origin and give rise to connective tissue between joints. The expression starts at 4 dpf and its not known if it stays on during adulthood. The midbrain-hindbrain boundary originates from the ectoderm and is positive for eGFP in *SN 172-38-2* (Figure 3.2 E).

In line *SN 172-68* the CNS (red arrowhead) and retina (white arrowhead) are positive for eGFP expression. The reporter gene expression was observed at 3 dpf. *SN 177-9* expresses the fluorescent protein in the heart tissue (Figure 3.2 F) of the developing embryo. The heart develops from the lateral plate mesoderm (cardiogenic mesoderm) and gives rise to the myocardium and the endocardium (Glickman et al, 2002). The cells from the endocardium line the heart and the myocardium, the skeletal element of the heart. In the case of *SN 177-9* we are not sure which of these cells types are labelled by the eGFP expression. Embryos of *I-1* express the reporter gene in the cells of the lateral line organ, an ectodermal structure consisting of polarised hair cells (neuromasts) and in region of the thymus at day 3 (Figure 3.2 F). The thymic epithelium forms the endodermal third pharyngeal pouch and the haematopoietic cells seed the thymus from the CHT in the fish (Murayama et al, 2006). The transgenic line *I-14* expresses eGFP in several tissues. Marker gene expression can be seen in the olfactory placode and the retina, which are both ectodermal, and in cells around the mouth of the embryo at 24 hpf (*I-14*, Figure 3.2

G). The last example, *SN 172-68* is shown in Figure 3.2 H. These embryos show reporter gene expression in the ectodermal nerve chord and the retina of the embryo.

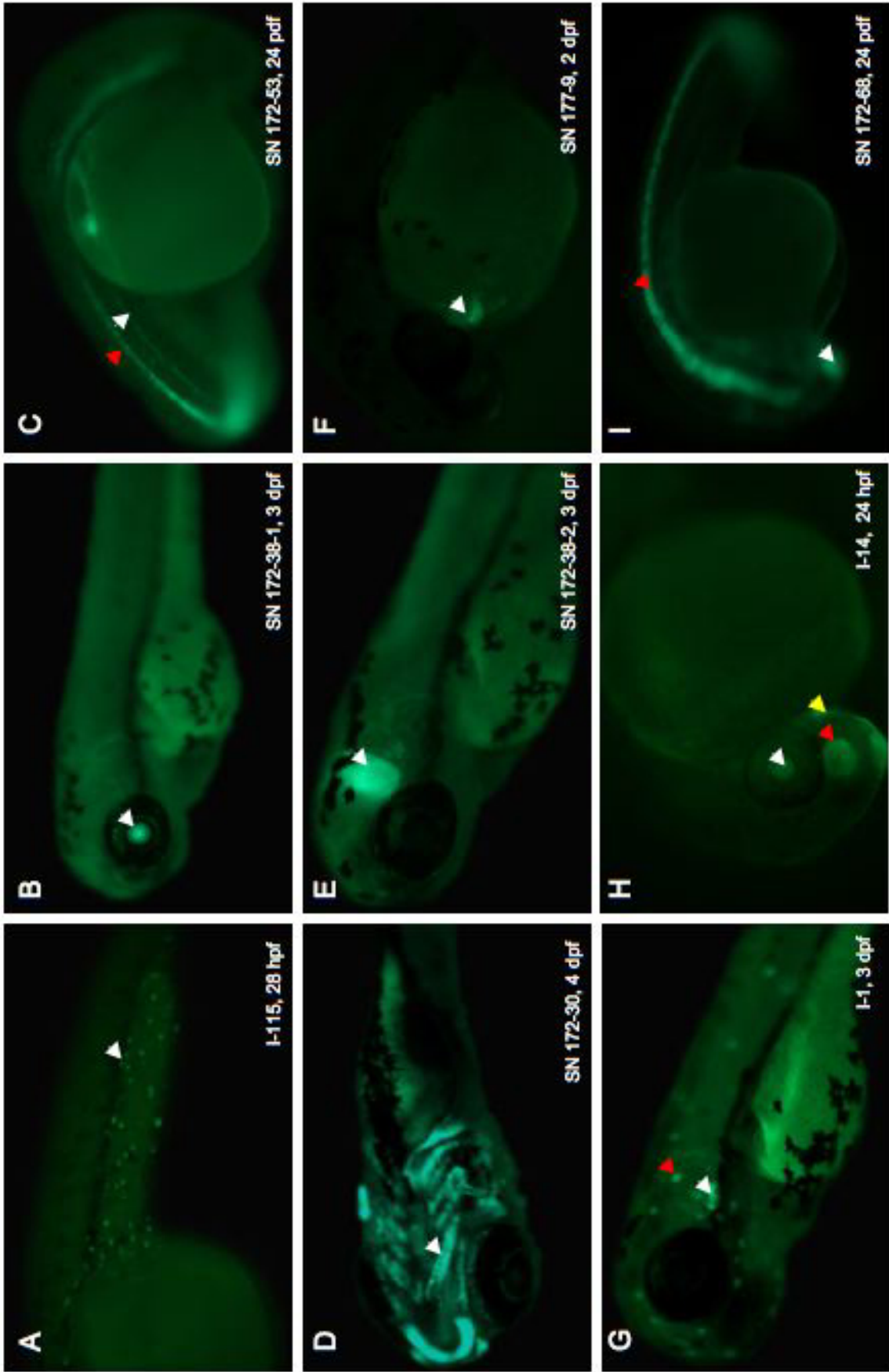


Figure 3.2: Examples of embryos with tissue-specific eGFP expression A: Embryos of line *I-115* display spotted expression of eGFP along the yolk cell extension of the embryo (white arrowhead). B: In line *SN 177-38-1* eGFP expression can be detected in the lens (white arrowhead). C: Reporter gene expression can be seen in the floor plate (red arrowhead) and in the hypocord (white arrowhead) in line *SN 172-53*. , D: The cartilage in the head of the embryo is positive for eGFP in line *SN 172-30* (white arrowhead). E: Cells in the midbrain- hindbrain boundary in line *SN 172-38-3* are expressing eGFP (white arrowhead), F: EGFP expression is restricted to cells to the heart in line *SN 177-9* (white arrowhead). G: In line *I-1*, cells of the lateral line organ (red arrowhead) and the thymus (white arrowhead) are showing reporter gene expression. H: *I-14* expresses the eGFP in different cell types including the lens (white arrowhead), the olfactory placode (red arrowhead) and cells in the cells around the mouth (yellow arrowhead).

Summary of chapter 3.2:

- the gene trap vector *tol2rst* is able to capture the expression of the reporter gene in a variety of tissues and in tissues derived from all three germ layers

3.3 Two transgenic fish lines displayed tissue-specific expression patterns in haematopoietic cells

Two lines were identified in which eGFP was expressed in haematopoietic cells. Since our construct was able to trap genes expressed in different cell types and from all three germ layers, there was a chance that we also had trapped a gene that was expressed in haematopoietic cells. We were able to isolate two transgenic lines with eGFP expression in haematopoietic cells.

3.3.1 The transgenic line *SN173-11:eGFP* expresses eGFP in the cells of the hatching gland and in circulating round cells

Figure 3.3 shows the transgenic line *SN 173-11* at 24 hpf. In this line the eGFP expression is located in the hatching gland and in round cells in the ICM beginning from around 22 hpf. The round cells go into circulation at 24 hpf (Figure 3.3, A and B). The reporter gene expression in these round cells is lost at 27 hpf, whereas the cells in the hatching gland keep the expression beyond 4 dpf. Thus, the round circulating cells are most likely primitive erythroblasts. The line was discontinued due to the low expression level of the eGFP.

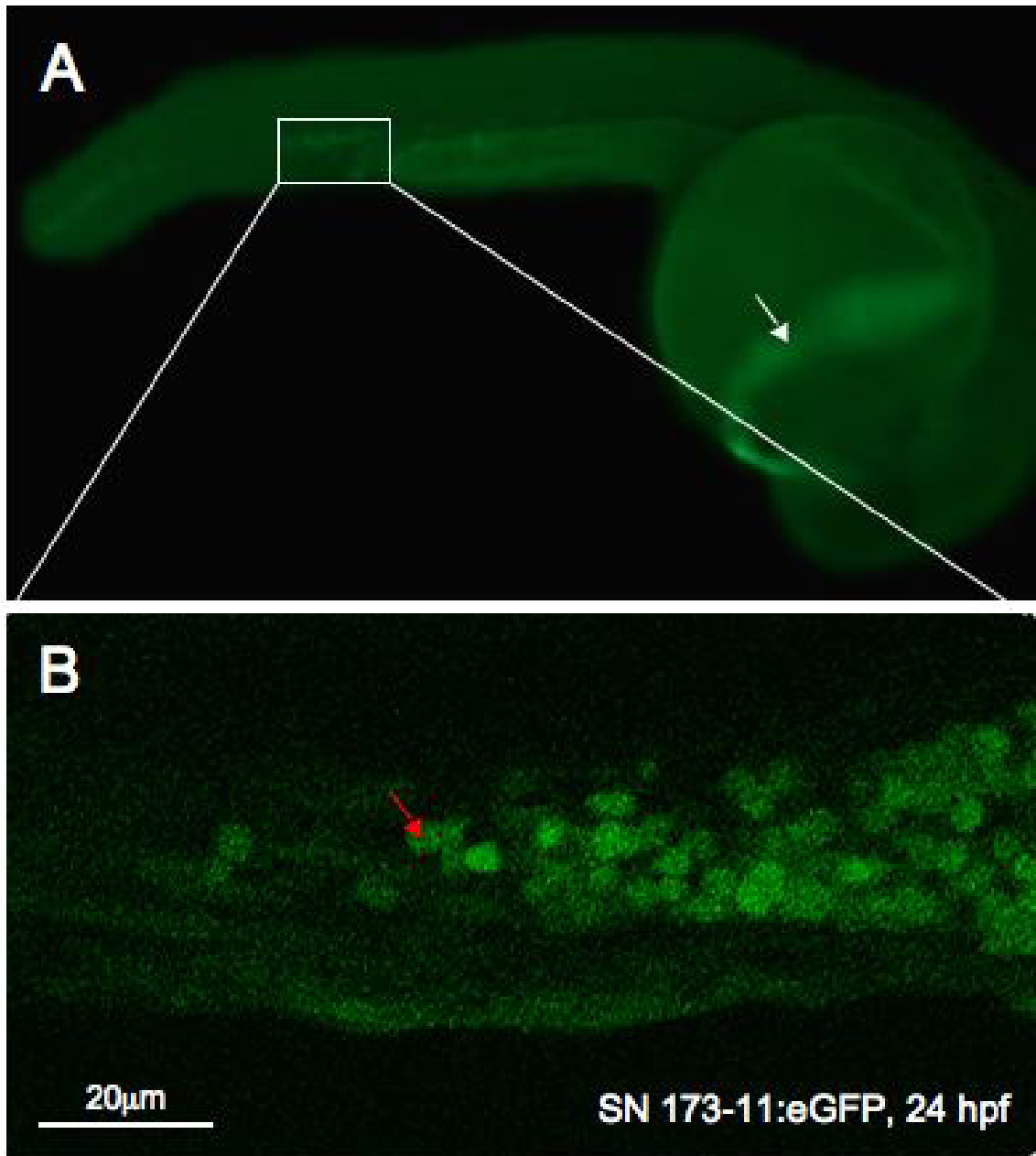


Figure 3.3: Primitive erythroid cells are labelled in *SN 173-11* transgenics The transgenic line *SN 173-11* expresses eGFP in the cells of the hatching gland (white arrow, A) and in primitive red blood cells (red arrow, B). Picture B represents the magnified view of the white box in A. The top picture was taken under a dissecting microscope, picture B was imaged using a confocal laser microscope. A 2µm section through the posterior blood island of the embryo is depicted, the head of the embryo is to the right.

3.3.2 The transgenic line *I-551:eGFP* expresses the reporter gene in haematopoietic tissues throughout development

The second transgenic line, *I-551:eGFP*, starts to weakly express the transgene from about 12hpf (data not shown) in the lateral plate mesoderm. By 16 hpf, the eGFP positive cells are seen migrating medially into the forming ICM of the embryo (Figure 3.4a). These cells are most likely precursors of endothelial cells and primitive erythrocytes. At 25 hpf, just after the onset of blood circulation (Figure 3.4a), two distinct cell populations are labelled by the eGFP expression. Firstly, there are round cells in circulation (red arrow) that are found in the DA and in the posterior cardinal vein. Secondly, there are elongated cells, which look like endothelial cells in the position of the ventral wall of the DA (white arrow). A magnified view of the AGM region in the embryo shows that the eGFP expression in the endothelial-like cells is restricted to the ventral part of the top blood vessel (Figure 3.4a, white arrow). By day two the reporter gene expression in the round circulating cells is lost and the majority of the eGFP positive cells are found in the caudal haematopoietic tissue in the tail of the embryo (Figure 3.4a and b, white arrow). Two days later, at 4 dpf, EGFP expression is more widespread in the embryo. The lateral line organ, the sensory organ of the fish, is labelled by eGFP expression (Figure 3.4b, yellow arrow). Furthermore, there appears to be also reporter gene expression in the thymus (Figure 3.4D, green arrow) and the kidney (Figure 3.4b, purple arrow), both are haematopoietic organs in the fish.

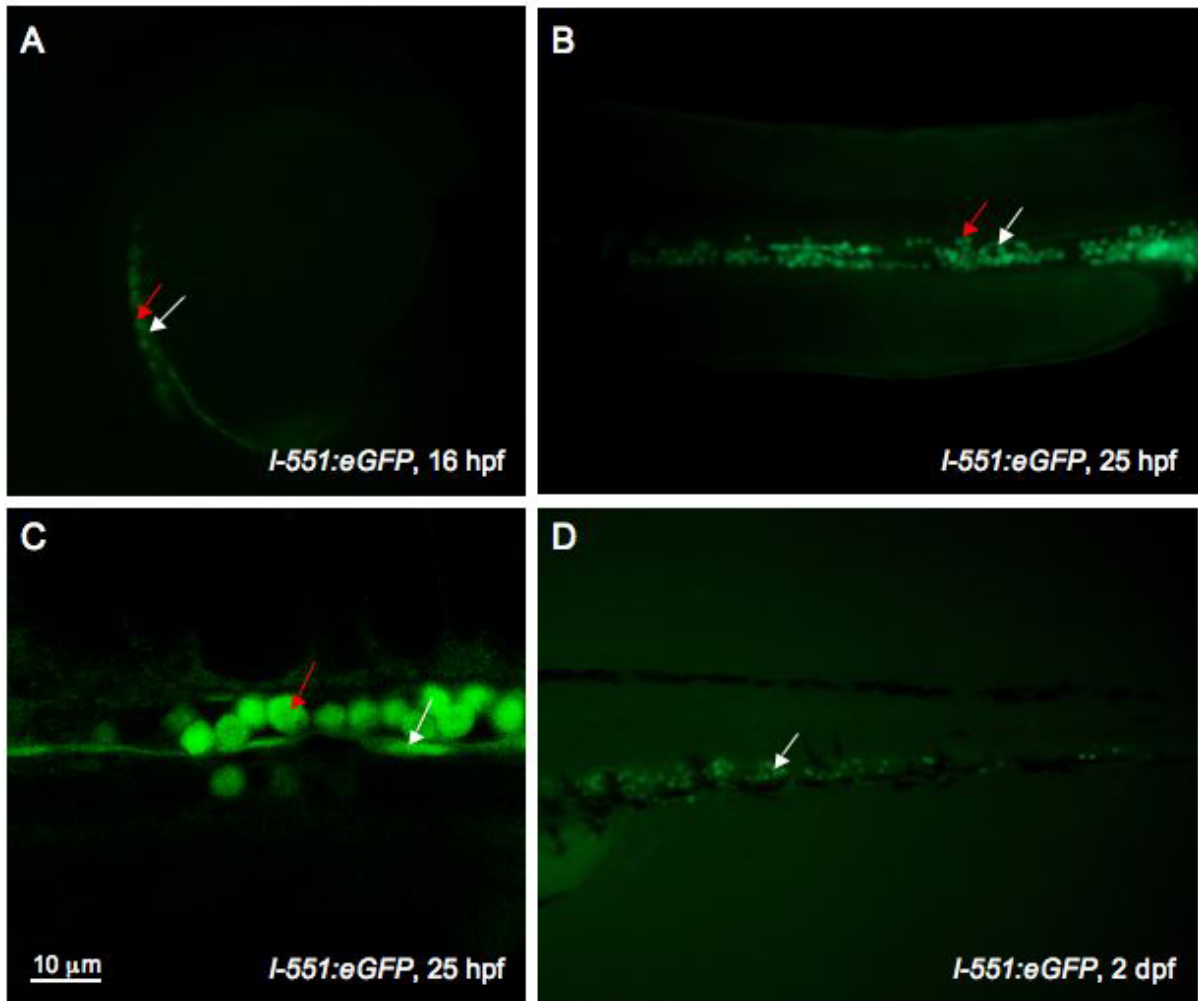


Figure 3.4a: *I-551:eGFP* is expressed in putative haemogenic endothelium and primitive red blood cells The reporter gene expression in *I-551 eGFP* begins at 16 hpf in precursors of primitive erythroblasts and endothelial cells and is expressed in the CHT on day 2. A: *I-551:eGFP* is first detected at 16 hpf. The expression marks the primitive erythrocytes (red arrow) and endothelial cells (white arrow). B,C: At 25 hpf, the expression is restricted to circulating round cells (red arrow) and to elongated cells in the ventral wall of the DA (white arrow). Image C was taken using a confocal microscope, a 5µm section through the trunk of the embryo. D: eGFP positive cells can be detected in the CHT on day 2 (white arrow). Lateral view of the embryos, with the anterior to the left in B, C and D, in A the head is pointing towards the top of the picture. *I-551:eGFP* embryos depicted in image C were subject to immuno-histochemistry for eGFP, all other images were taken from live embryos.

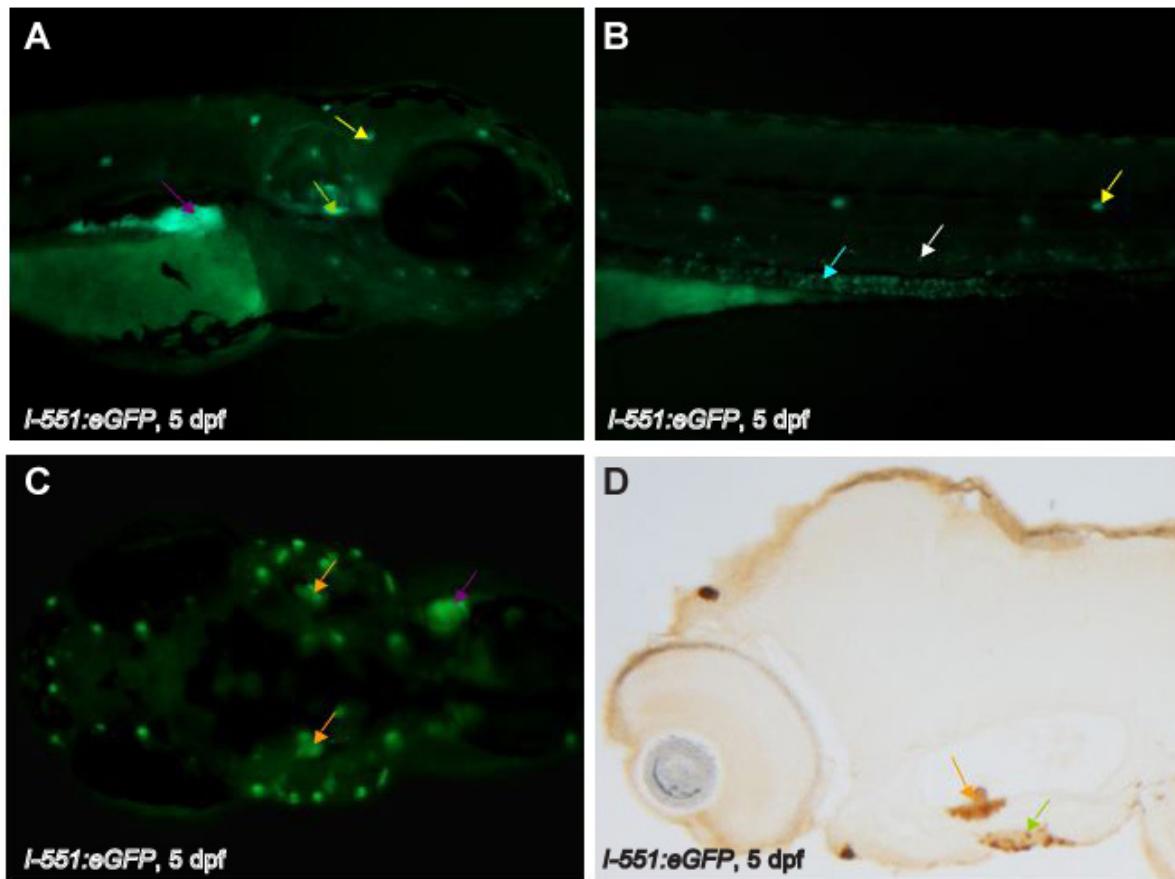


Figure 3.4b: *I-551:eGFP* transgenics retain eGFP expression in haematopoietic sites into larval stage. A and B: At 4 dpf, the *I-551:eGFP* line shows expression in the lateral line organ along the body (yellow arrows), the thymus (green arrow), in the kidney and pancreas (purple arrow), in the cells of the intestine (blue arrow), inner ear hair cells (orange arrow) and in the mesenchyme between the DA and the PVC. C and D: A 10µm sagittal section through the head shows eGFP expression in the inner hair cells in the otic vesicle (orange arrow) and in the thymus (green arrow). All pictures, apart from C, show the embryo in a lateral view. Picture C shows the embryo in a dorsal view. In picture A the anterior side of the embryo is to the right, in all other pictures to the left. The images A-C were taken from live embryos, the embryo depicted in image D was subject to immuno-histochemistry for eGFP. The antibody was detected with DAB staining and 10µm sagittal sections were taken through the 5 dpf embryo. The embryo in image D was sectioned by J Field (project student).

In addition, there are eGFP positive cells in the pancreas (Figure 3.4b purple arrow), inner ear hair cells (Figure 3.4b, 3.4b D orange arrows) and in the intestine of the *I-551:eGFP* line (Figure 3.4b, blue arrow). EGFP expression is retained in the

mesenchyme between the dorsal aorta and the posterior cardinal vein and the CHT. The number of eGFP positive cells in these regions seems to decrease by day 5 (Figure 3.4b, D white arrow). We further analyzed the eGFP expression pattern in 5 dpf old, *I-551:eGFP* larvae by sectioning. Here we detected eGFP positive cells in the kidney (Figure 3.5, B), pancreas and spleen (Figure 3.5 C). In conclusion, the *I-551:eGFP* transgenic line shows reporter gene expression in haematopoietic tissues in the embryo, but in addition, there is also expression in non- haematopoietic tissues.

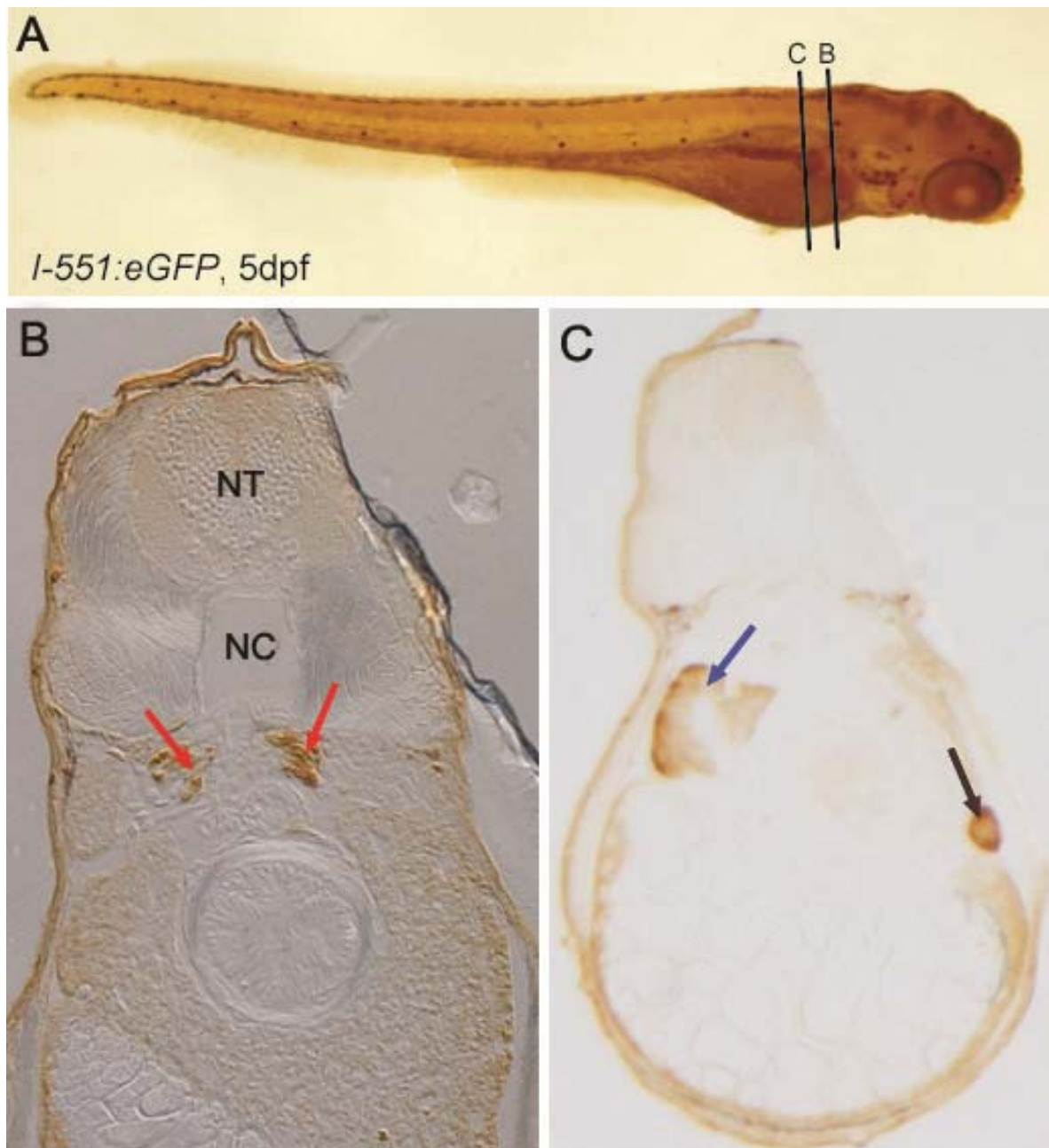


Figure 3.5: Transverse sections through the trunk of a 5 dpf embryo reveals eGFP expression in the kidney, spleen and pancreas A: lateral view of a 5 dpf whole mount immuno-stained *I-551:eGFP* embryo. B: A 10µm transverse section through the trunk of the embryo depicts the kidneys ventral to the notochord (red arrows). C: A 10µm transverse section through the trunk of the embryo. The black arrow highlights the spleen, the blue arrow is pointing at the pancreas. The embryo was immuno-stained for eGFP using DAB as the chromogenic substrate for the color reaction. Notochord (NC), neural tube (NT). The embryos were sectioned by J Field (project student).

3.3.3 Reporter gene expression in the transgenic line *I-551:eGFP* is restricted to primitive erythrocytes and endothelial cells in the DA at 26 hpf

To ensure that the fluorescence seen in the transgenic line *I-551:eGFP* at 26 hpf was not auto fluorescence, but due to the presence of eGFP, we performed immunohistochemistry on 26 hpf embryos. We applied a biotinylated GFP antibody conjugated to streptavidin and horseradish peroxidase and DAB as a chromogenic substrate to detect the eGFP. We compared the DAB staining with the eGFP expression observed in the live *I-551:eGFP* embryos (Figure 3.4a A and B). Both expression profiles were identical. To better localise the spindle-shaped endothelial cells, we cut 10µm transverse section of the DAB stained embryos (Figure 3.6, C). The sections revealed eGFP expression in primitive red blood cells and spindle shaped endothelial cells. The bilateral bending of the endothelial cell suggests that the cell is indeed positioned in the ventral wall of the DA (Figure 3.6 C, green arrow).

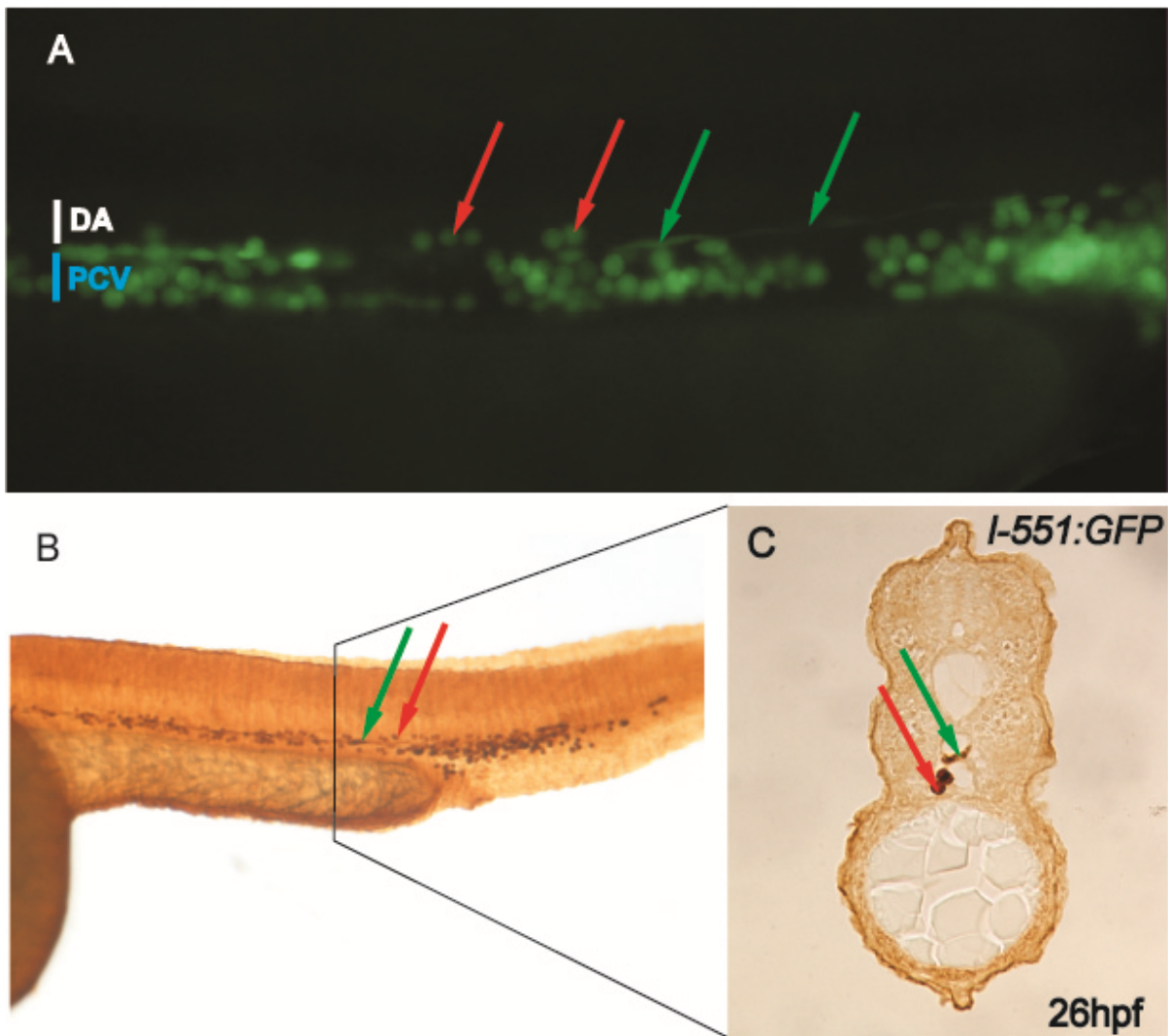


Figure 3.6: EGFP is expressed in the ventral wall of the dorsal aorta in the transgenic line *I-551:eGFP* at 26 hpf A: *I-551:eGFP* expression is confined to round circulating cells (red arrows) and to endothelial cells in the DA (green arrows). B: DAB staining for eGFP at 26 hpf confirms the expression pattern observed with the fluorescent microscope. C: a 10 µm transverse section through the trunk of the embryo in B (black line) locates the endothelial expression to the ventral wall of the DA (green arrow). The heads of the embryos in A and B are localized to the left. Image A was taken from a live embryo. DA: dorsal aorta, PCV: posterior cardinal vein.

The gene-trap screen resulted in two transgenic lines with eGFP expression in hematopoietic cells (3.3.1 and 3.3.2). The eGFP expression in SN173-11 is only transient in primitive red blood cells. The transgenic line *I-551:eGFP* on the other

hand, seems to recapitulate the development of hematopoietic progenitors although the expression is not confined to hematopoietic cells. The first eGFP expression was observed in the ICM (Figure 3.4a), moved to the CHT (Figure 3.4a) and could be detected in the kidney and thymus at 5 dpf (Figure 3.4b). By analysing transverse sections through the embryo at 26 hpf, we could localize eGFP expression in two different cell populations. Firstly, round cells within the vessels were labelled which most probably represent red blood cells. Secondly, we detected staining in the ventral wall of the dorsal aorta. Especially the latter finding suggests that the transgene might be expressed in emerging blood stem cells.

Summary of chapter 3.3:

- two transgenic line from the gene-trap screen show eGFP expression in haematopoietic cells
- *SN173-11* expresses the transgene in primitive red blood cells transiently
- *I-551:eGFP* seems to recapitulate the development of haematopoietic progenitors
- Transverse section through the trunk of the *I-551:eGFP* embryos at 26 hpf strongly suggest expression in primitive red blood cells and in endothelial cells in the ventral wall of the dorsal aorta
- *I-551:eGFP* is also expressed in non-haematopoietic tissues

3.4 *I-551:eGFP* is expressed in hematopoietic cells

3.4.1 EGFP expression in primitive red blood cells decreases in *Tg (I-551:eGFP;Gata1:dsRED)* after 30hpf

3.4.1.1 Circulating round cells in the transgenic line *I-551:eGFP* co-express the erythrocyte marker gene *gata1* at 26hpf

We further wanted to confirm that the round circulating cells in the *I-551:eGFP* transgenics were primitive erythrocytes. We crossed the line with *Gata1:dsRED* transgenics and analyzed the progeny for co-expressing cells using fluorescent microscopy. *Gata1* is a characterised marker for erythrocytes and previous work has established transgenics under the control of this promoter (Long et al, 1997). An overlap in the reporter gene expression between the *Gata1:dsRED* and the round circulating cells would indicate that we are looking at primitive erythrocytes. We were able to confirm that the circulating round cells in the embryo of *I-551:eGFP* transgenics are primitive erythrocytes since the expression of both transgenes coincide (Figure 3.7 B, red arrow and supplemental movie 1). The endothelial eGFP expression is unaffected by the *Gata1:dsRED* expression (Figure 3.7 B and supplemental movie 1).

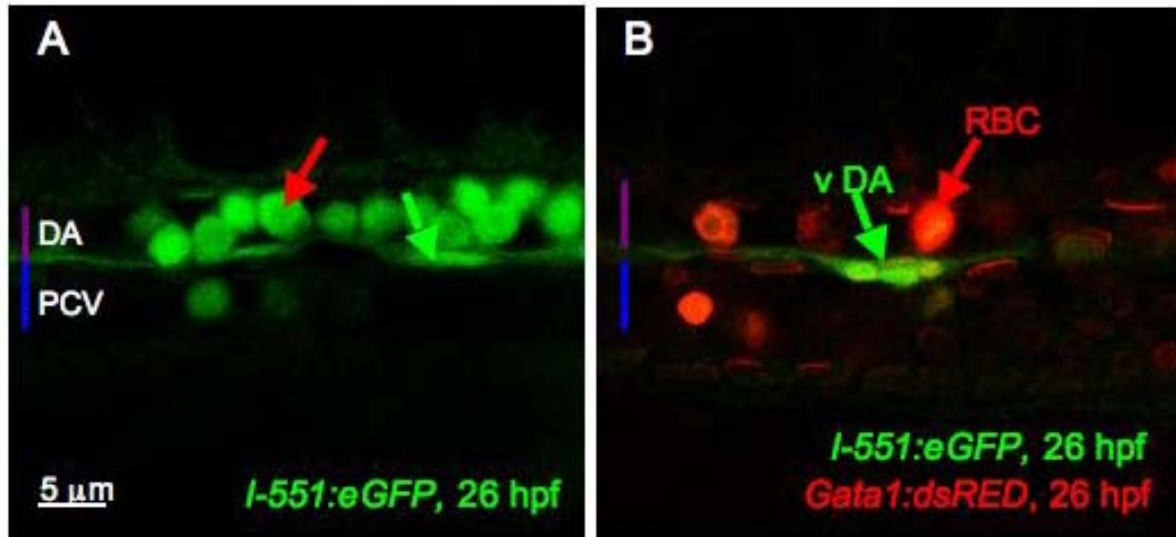


Figure 3.7: *I-551:eGFP* and *Gata1:dsRED* are co-expressed in the primitive erythrocytes at 26 hpf The eGFP positive round circulating cells in the *I-551:eGFP* line overlap with the expression pattern of *Gata1:dsRED* (red arrow). The endothelial cells are not positive for the red fluorescent protein (green arrow). These images were taken using a confocal microscope and a 4 μ m section is depicted. *I-551:eGFP* and *Gata1:dsRED* double transgenic embryos were immuno-stained for both fluorescent reporters at 26 hpf. DA: dorsal aorta, PCV: posterior cardinal vein, vDA: ventral wall of the dorsal aorta, RBC: red blood cell.

3.4.1.2 Flow cytometrical analysis of *I-551:eGFP*; *Gata1:dsRed* allows to separate haematopoietic and endothelial cells at 26 hpf

To further validate our data, we employed flow cytometry on cells derived from double transgenic embryos. FACS analysis has been successfully performed by other investigators to characterise haematopoietic cells from zebrafish (Bertrand et al, 2007; Traver et al, 2003). This method can be used to separate between the endothelial and haematopoietic cell population.

The flow cytometry plot for the sorting experiment performed on 26 hpf old *I-551:eGFP* and *Gata1:dsRED* double transgenics show four different cell population based on the fluorescence, size and granularity. We used wild type non-fluorescent embryos to exclude cell debris and dead cells (Figure 3.8a A). We then analysed

single transgenic embryos for either *I-551:eGFP* or *Gata1:dsRED* in order to define the gates for the different cell populations (Figure 3.8a B-D). We were able to distinguish four different cell population in cells harvested from double transgenic embryos at 26 hpf (Figure 3.8b). Three populations of cells express *I-551:eGFP*. Two of these populations express *I-551* at a high level (*I-551:eGFP*^{high}) and can be subdivided into cells which only express *I-551* alone (top plot to the left) and cells which co-express *I-551:eGFP* and *Gata1:dsRED* (top plot to the right). They represent 1.1% (471 cells) and 1.1% (476 cells) of the total embryo extract, respectively. Both these cell populations show a similar distribution in the FS/SS view. They appear as a compact accumulation of cells with similar size and granularity. We assume that they represent primitive red blood cells. The remaining two cell populations are either positive for *I-551:eGFP* or *Gata1:dsRED*. The *Gata1:dsRED* positive cells represent 0.23% (101 cells) of the embryo extract and are likely to include primitive red blood cells which do not express *I-551*. In support of this hypothesis, their FS/SS profile is similar to that of *I-551:eGFP* and *Gata1:dsRED* double positive red blood cells (Figure 3.8b). It seems likely that the cells of these three subpopulations represent red blood cells at various differentiation stages, with *I-551*^{high} cells being the least mature cells, double positive cells representing an intermediate stage and *Gata1:dsRED* single positive cells being the most mature erythroblasts.

In contrast to the 3 cell populations, the population of *I-551*^{low} cells has a very different FS/SS profile. While it contains a number of cells with a cell size and granularity similar to red blood cells, most of the cells are much larger and are much more granular (Figure 3.8b). These cells account for 0.85% (348 cells) of the embryo extract. We assume that these cells are endothelial cells.

This experiment reveals the possibility to separate the endothelial cells from the primitive red blood cells by the means of flow cytometry.

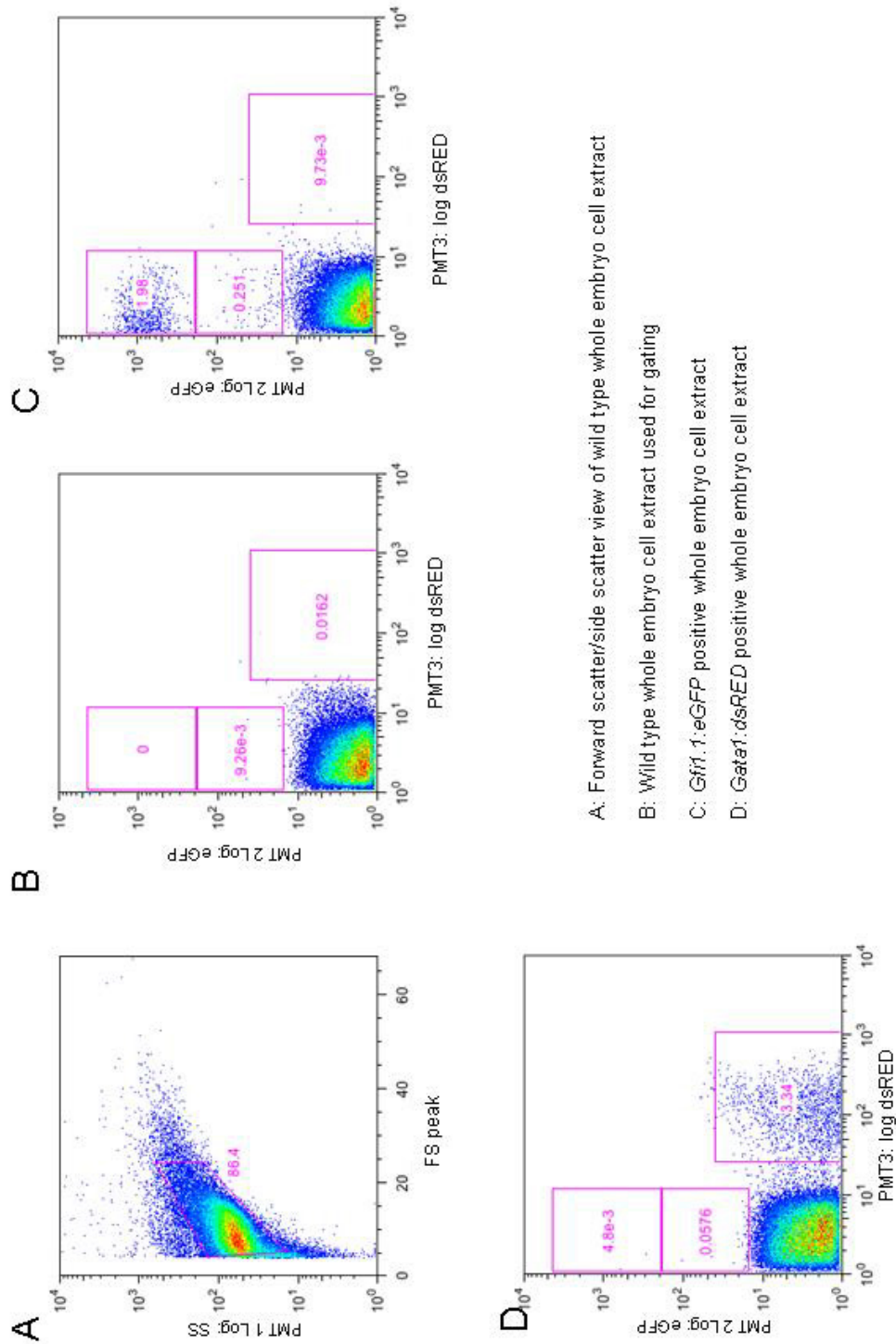


Figure 3.8a: Control flow cytometry plots which were used to analyse Tg (*I-551:eGFP*,*Gata1:dsRED*) embryos at 26 hpf A: FS/SS scatter plot of non-fluorescent cell suspension derived from wild type embryos. **B:** Non-fluorescent wild type cells used for setting the gates. **C:** *I-551:eGFP* single transgenic embryo extracts show a eGFP^{high} and eGFP^{low} population. **D:** Cells derived from *Gata1:dsRED* single transgenic embryos label a homogenous cell population.

I-551:eGFP/Gata1:dsRED, 26hpf

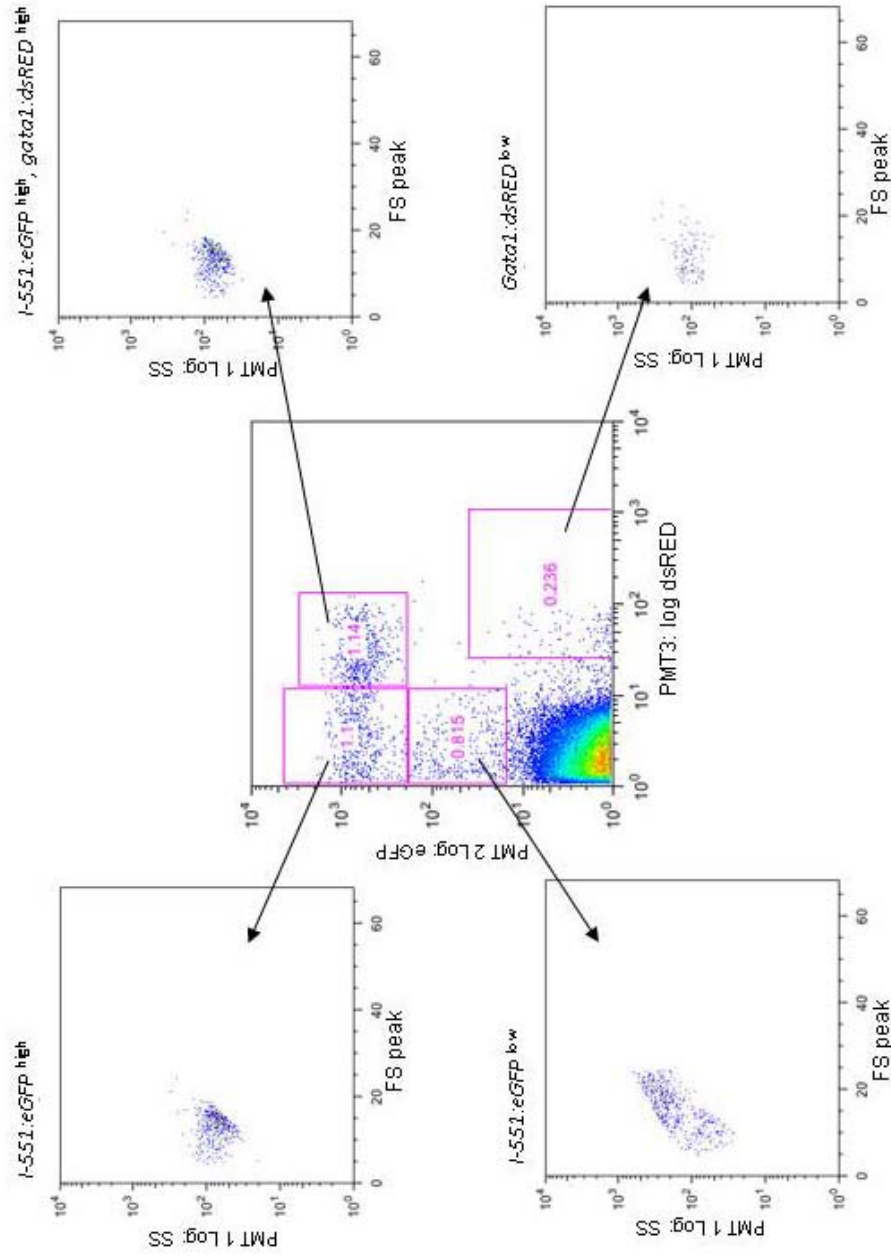


Figure 3.8b: I-551 positive primitive red blood cells and endothelial cells can be efficiently distinguished by using FACS. Cell-suspension isolated from 26 hpf *I-551:eGFP* and *Gata1:dsRED* double transgenic embryos were analyzed by FACS. Each gated cell population was then analysed for their forward scatter (x-axis) and side scatter (y-axis) characteristics. Four different cell populations were distinguished on the basis of their level of red and green fluorescence and gated as shown in Figure 3.8a.

3.4.1.3 In *Tg(I-551:eGFP/Gata1:dsRed)* transgenic embryos different subtypes of haematopoietic cells are labelled in the posterior blood island

Tg(I-551:eGFP;Gata1:dsRED) embryos were also analyzed at 30 hpf. Here, we found a decrease of eGFP expression in the primitive red blood cells as seen in the PBI region of the embryo (Figure 3.9). This region is known to accommodate different haematopoietic progenitors. A z-stack through the PBI of the embryo revealed different subtypes of fluorescently labelled cells (Figure 3.9, Supplemental movie 2).

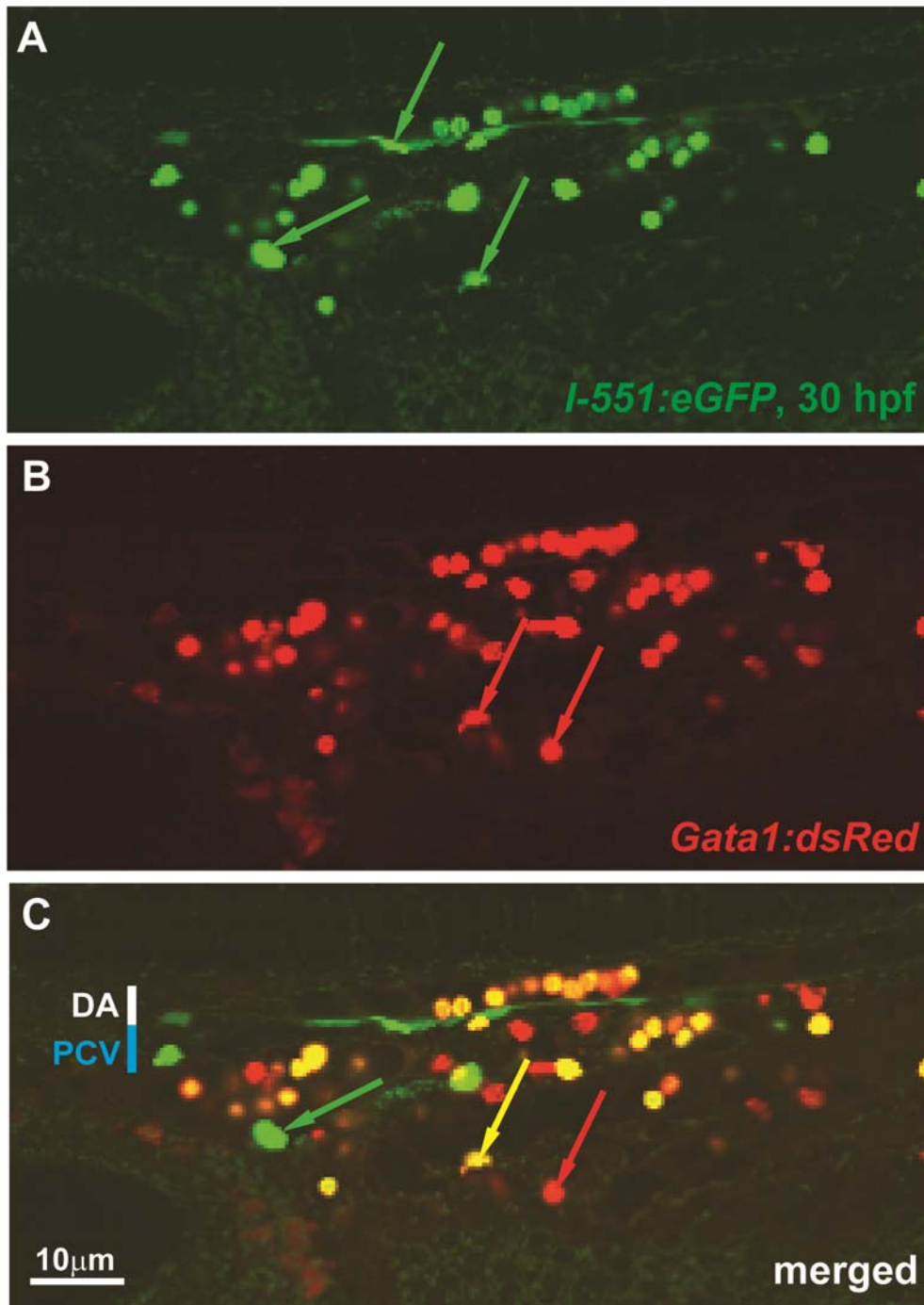


Figure 3.9: The PBI of *I-551:eGFP* and *Gata1:dsRED* double transgenic embryos show a decreased expression of eGFP in primitive red blood cells at 30 hpf *I-551:eGFP* positive cells can be detected in the primitive red blood cells and in endothelial cells at 30 hpf (A, green arrows), whereas the *gata1* positive cells are restricted to the erythroid lineage (B, red arrows). In the merged view, a variety of cell types can be distinguished based on their fluorescent identity. Some cells are expressing either eGFP (C, green arrow) or dsRED only (C, red arrow), while others are expressing both transgenes (C, yellow arrow). DA: dorsal aorta, PCV: posterior cardinal vein.

There are rare eGFP only positive cells, next to a mixture of double positive, yellow cells and a few red only cells (Figure 3.9, C green, yellow and red arrows, respectively). This indicates that different haematopoietic progenitors populate the posterior blood island.

3.4.1.4 Flow cytometrical analysis of embryos at 30hpf reveals a decrease in eGFP expression in primitive erythrocytes

We employed flow cytometrical analysis on 30 hpf *I-551:eGFP* and *Gata1:dsRED* embryos since we knew from *in vivo* observations that primitive red blood cells had less *I-551:eGFP* expression. We expected this to be reflected in the flow cytometry analysis. We therefore expected to find less *I-551:eGFP⁺/gata1:dsRED⁺* cells. Indeed, the FACS plot shows that hardly any *eGFP^{high}/dsRED⁺* double positive cells are present (Figure 3.10). We also saw less *I-551:eGFP^{high}* cells, which are only represented by 0.12% (49 cells) of the embryo extract. Instead, higher percentage of *eGFP^{low}/dsRED⁺* and *eGFP/gata1:dsRED⁺* cells (2.86% and 1.5%, respectively) were observed, consistent with the idea that the less mature *I-551^{high}* red blood cells had matured in circulation and eventually developed into *Gata1:dsRED* single positive cells. These findings are reflected in the number of red blood cells. At 26 hpf only 1.1% (476 cells) express both transgenes and therefore represent primitive red blood cells, whereas at 30 hpf, the population of the double positive has increased to reach 2.86% (1186 cells) (table 3.2). The *eGFP^{low}/gata1:dsRED⁻* cells are still present and displayed a FS/SS profile similar to that observed at 26 hpf, but their population has reached a higher percentage (Figure 3.10 and table 3.2). Consistent with ongoing *I-551:eGFP* expression in the ventral DA in the live embryo we assume that these cells are endothelial in nature. Using flow cytometry, we were able to confirm

the *in vivo* observations we initially made in *Tg(I-551:eGFP;Gata1:dsRED)* embryos. The eGFP expression in the primitive red blood cells decreases after 30 hpf whereas the endothelial expression remains constant.

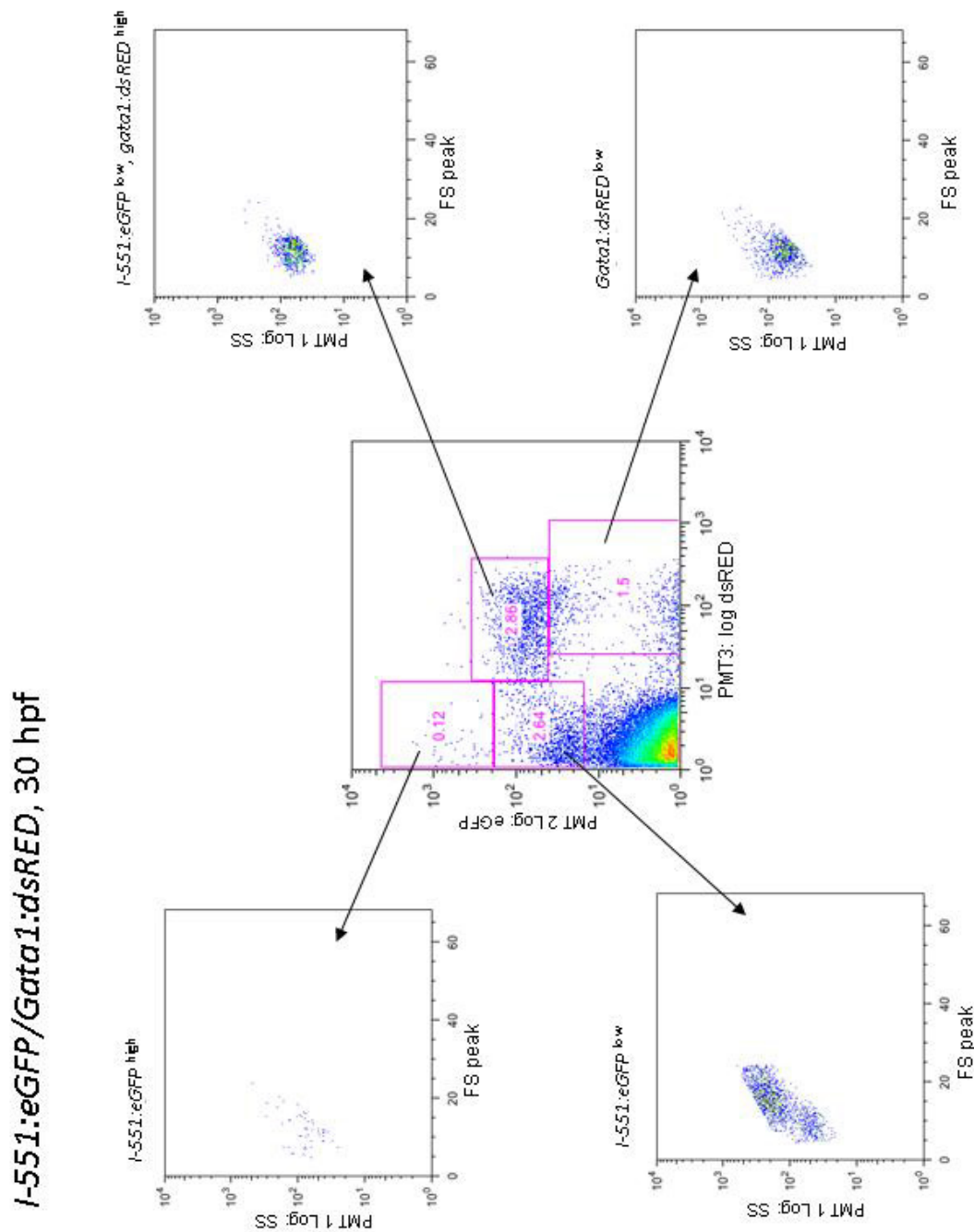


Figure 3.10: *I-551:eGFP* primitive erythrocytes show a lower eGFP fluorescence after 30 hpf Cells were isolated from 30 hpf embryos and analyzed by flow cytometry. Cells were analysed for green and red fluorescence and gated according to their forward scatter and

side scatter properties (Figure 3.8a). *I-551^{high}* cells represent only 0.13% of the embryo extract. *I-551^{low}/gata1⁻* cells scatter along the x-axis (bottom left plot) as seen at 26 hpf. *I-551^{low}/gata1⁺* cells have shifted lower on the plot compared to 26 hpf (Figure 3.8b) and appear as a compact cell population in the SS/FS plot (top right plot). The single *gata1⁺* positive cells represent of the total embryo extract.

Genotype of embryonic cell extract	Percentage of cells	Cell count
Wilde type <ul style="list-style-type: none"> ▪ live cells ▪ <i>gata1</i> positive ▪ <i>Gfi1.1^{high}</i> ▪ <i>Gfi1.1^{low}</i> 	-	50000
<ul style="list-style-type: none"> ▪ live cells ▪ <i>gata1</i> positive ▪ <i>Gfi1.1^{high}</i> ▪ <i>Gfi1.1^{low}</i> 	86.4 0.0162 0 9.26e-3	43188 7 0 4
<i>I-551:eGFP</i> <ul style="list-style-type: none"> ▪ live cells ▪ <i>gata1</i> positive ▪ <i>Gfi1.1^{high}</i> ▪ <i>Gfi1.1^{low}</i> 	-	50000
<ul style="list-style-type: none"> ▪ live cells ▪ <i>gata1</i> positive ▪ <i>Gfi1.1^{high}</i> ▪ <i>Gfi1.1^{low}</i> 	82.2 9.73e-3 1.98 0.25	41115 4 815 103
<i>Gata1:dsRED</i> <ul style="list-style-type: none"> ▪ live cells ▪ <i>gata1</i> positive ▪ <i>Gfi1.1^{high}</i> ▪ <i>Gfi1.1^{low}</i> 	-	50000
<ul style="list-style-type: none"> ▪ live cells ▪ <i>gata1</i> positive ▪ <i>Gfi1.1^{high}</i> ▪ <i>Gfi1.1^{low}</i> ▪ <i>Gfi1.1^{high}/Gata1</i> 	83.3 3.34 48e-3 0.0576 1.14	41674 1390 2 24 476
<i>I-551:eGFP/Gata1:dsRED, 26 hpf</i> <ul style="list-style-type: none"> ▪ live cells ▪ <i>gata1</i> positive ▪ <i>Gfi1.1^{high}</i> ▪ <i>Gfi1.1^{low}</i> ▪ <i>Gfi1.1^{high}/Gata1</i> 	-	50000
<ul style="list-style-type: none"> ▪ live cells ▪ <i>gata1</i> positive ▪ <i>Gfi1.1^{high}</i> ▪ <i>Gfi1.1^{low}</i> ▪ <i>Gfi1.1^{high}/Gata1</i> 	85.4 0.23 1.1 0.815 1.14	42711 101 471 348 476
<i>I-551:eGFP/Gata1:dsRED, 30 hpf</i> <ul style="list-style-type: none"> ▪ live cells ▪ <i>gata1</i> positive ▪ <i>Gfi1.1^{high}</i> ▪ <i>Gfi1.1^{low}</i> ▪ <i>Gfi1.1^{low}/Gata1^{high}</i> 	-	50000
<ul style="list-style-type: none"> ▪ live cells ▪ <i>gata1</i> positive ▪ <i>Gfi1.1^{high}</i> ▪ <i>Gfi1.1^{low}</i> ▪ <i>Gfi1.1^{low}/Gata1^{high}</i> 	81.6 1.5 2.86 0.12 2.64	40804 614 1168 49 1076

Table 3.2: Cell count of embryonic cell extracts The table summarizes the percentage and number of cells found in each gate of the flow cytometrical analysis performed with whole embryo cell extract of *I-551:eGFP* and *Gata1:dsRED* single transgenic and Tg(*I-551:eGFP;Gata1:dsRED*) double transgenic embryos at 26 hpf and 30 hpf.

3.4.5 The endothelial eGFP expression in the transgenic line *I-551:eGFP* is restricted to the ventral wall in the DA

3.4.5.1 *I-551:eGFP* and *Flk1:tomato* are co-expressed in the artery at 26hpf

In order to confirm the endothelial nature of the spindle-shaped cells, we crossed *I-551:eGFP* to a *Flk1:tomato* transgenic line that we created for this purpose. In these *Flk1:tomato* transgenic embryos, the red fluorescent reporter gene is under the control of the promoter of the pan-endothelial gene *flk1* (see 2.1.2.2). The *flk1* gene is expressed at higher levels in the DA than in the vein. When double transgenic embryos were analyzed we found co-expression of the transgenes in the ventral wall of the dorsal aorta (Figure 3.11, yellow arrow).

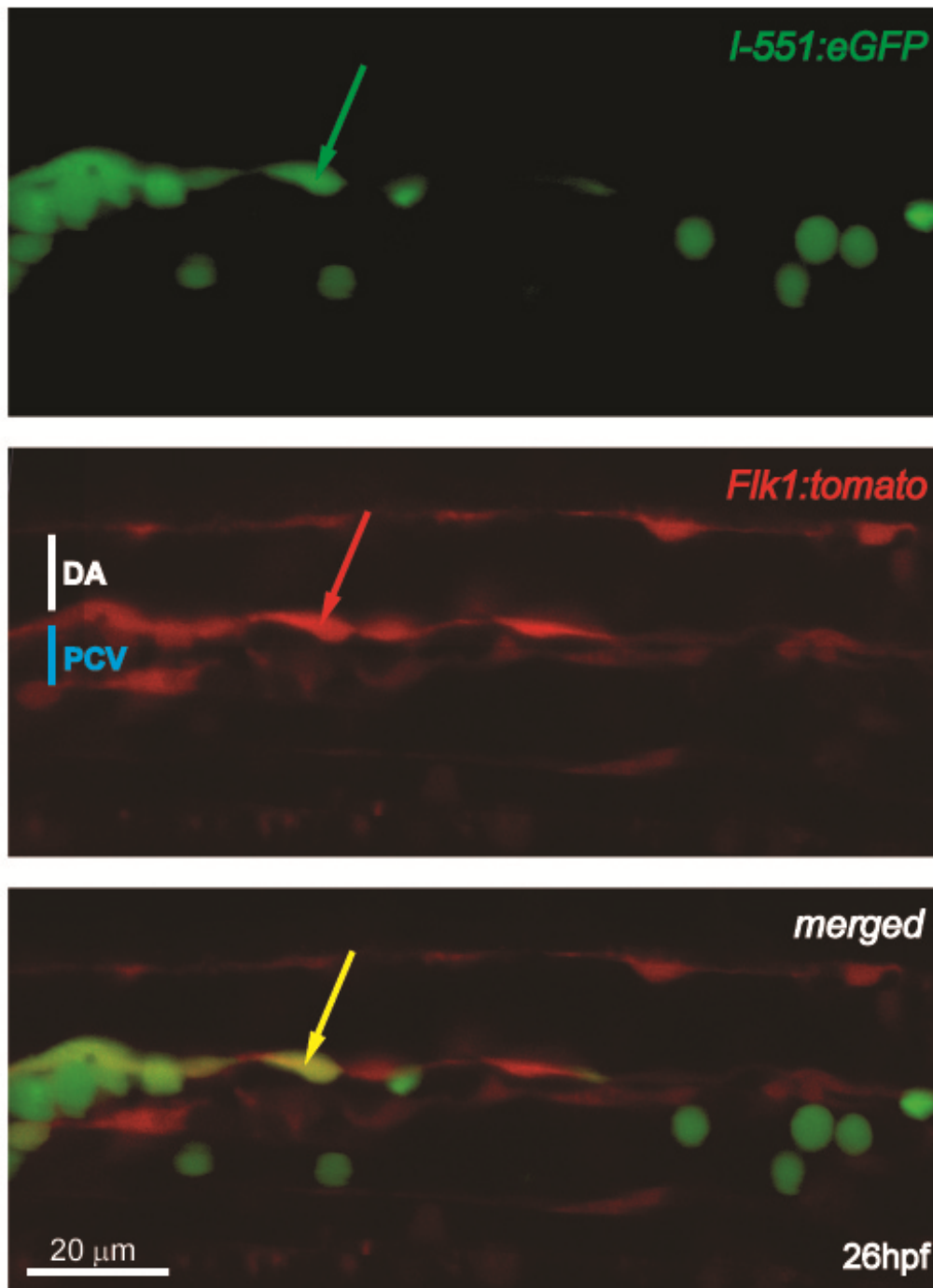


Figure 3.11: *I-551:eGFP* and *Flk1:tomato* are co-expressed in the ventral wall of the dorsal aorta Double transgenic *Tg(I-551:eGFP;Flk1:tomato)* embryos were immunostained for eGFP and dsRED and imaged using a confocal microscope. A 4 μ m section through the trunk of the embryo is shown in this image. Double positive endothelial cells can only be detected in the position of the ventral wall of the DA (yellow arrow). The circulating round cells are only positive for eGFP and do not express Tomato (green arrow). The anterior region of the embryo is to the left. DA: dorsal aorta, PCV: posterior cardinal vein.

3.4.5.2 *EfnB2a:tomato* and *I-551:eGFP* are co-expressed in the ventral wall of the artery at 27 hpf

In order to further verify the arterial nature of the eGFP positive cells, we made a *EfnB2a:tomato* transgenic line where the red fluorescent protein Tomato is expressed in arterial endothelial cells is under the control of the *efnB2a* promoter. Because *efnB2a* is also known to be expressed in the somites and in the presumptive hindbrain (Durbin et al, 1998), Tomato expression is also observed outside the endothelium. In addition, we detected ectopic expression in the hatching gland of the embryo at 27 hpf (see supplemental Figure 1 B).

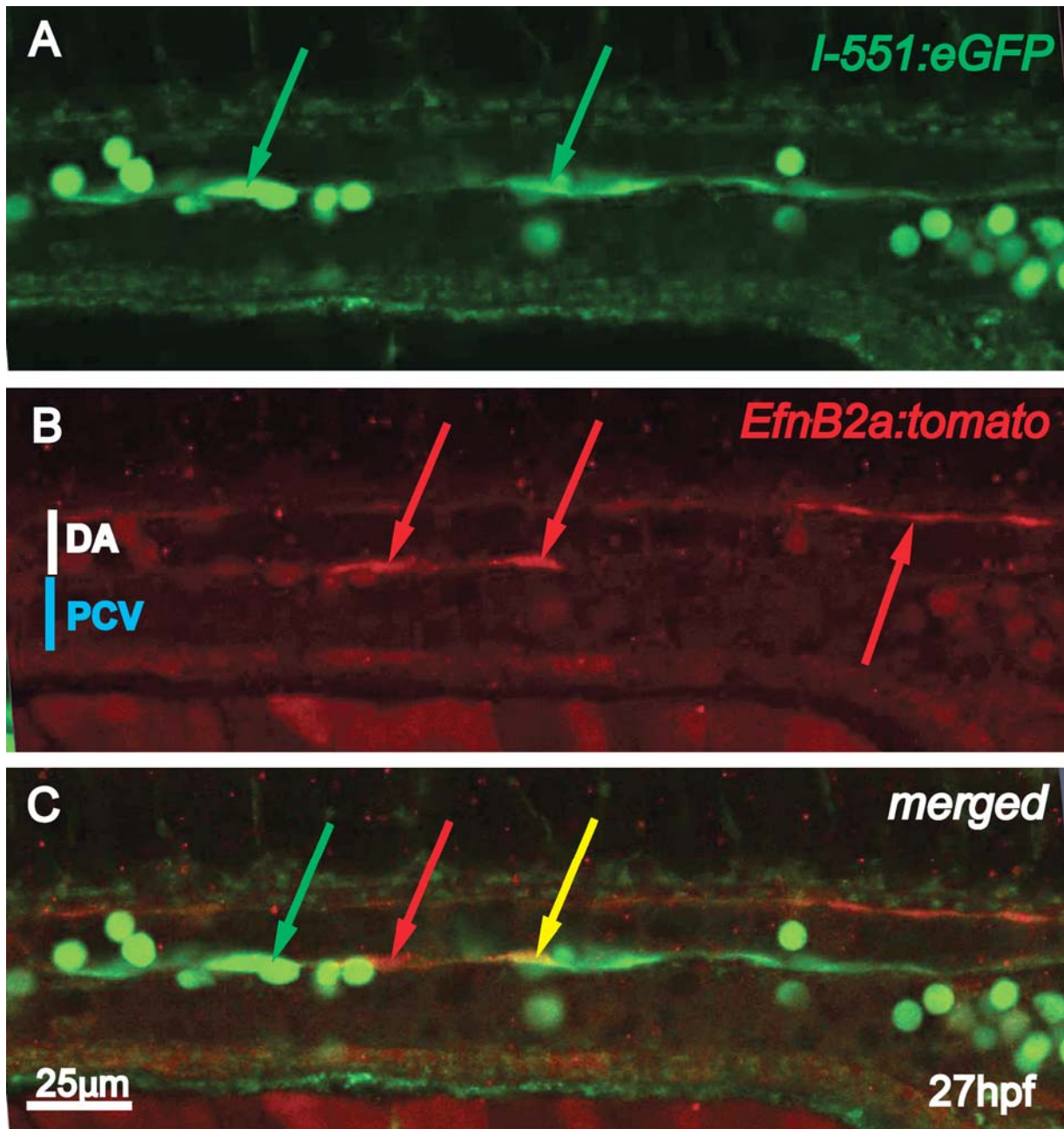


Figure 3.12: EGFP and Tomato are co-expressed in the ventral wall of the DA in Tg (*I-551:eGFP;EfnB2a:tomato*) embryos. Tg (*I-551:eGFP;EfnB2a:tomato*) were immuno-stained for eGFP and dsRED. The image shows a 4 μm sagittal section through the trunk of a 27 hpf old embryo. The green arrows point at the green fluorescent endothelial cells and the red arrows marks the EfnB2a positive arterial cells in the double transgenics. The yellow cell in the ventral wall of the artery in the bottom panel (yellow arrow) is expressing both fluorophores. The anterior region of the embryo is to the left. DA: dorsal aorta, PCV: posterior cardinal vein.

I-551:eGFP and *EfnB2a:tomato* double transgenic embryos have cells in the ventral wall of the DA which express both reporter genes (Figure 3.12, yellow arrow). We could therefore conclude that the endothelial cells in *I-551:eGFP* were restricted to the ventral wall of the DA at 26- 27 hpf.

3.4.5.3 *12xCLS:cerulean* and *I-551:eGFP* are co-expressed in the ventral wall of the artery at 28hpf

The arterial nature of the *I-551:eGFP* positive endothelial cells were further examined by investigating whether *I-551* positive endothelial cells experience active Notch signalling. For this purpose a *12xCLS:cerulean* transgenic line based on the *12xCLS:venus* transgenic line was generated (A Haase, K McMahon, unpublished data). Both transgenic lines reflect the *notch* activity in the embryo, since the promoter consists of 12 *CLS* (*CBF1/RBPjk*, *Su(H)*, and *Lag-1*) repeats. These repeats are binding sites for the Notch co-factors CLS. Consequently, the transgene is active in tissues, where *notch* is active. Analysis of the *12xCLS:venus* line has provided evidence that the expression of the transgene reflects Notch activity in the embryo (A Haase, K McMahon, unpublished data). Transgene expression was also observed in the DA from 18 hpf (A Haase, K McMahon, unpublished data).

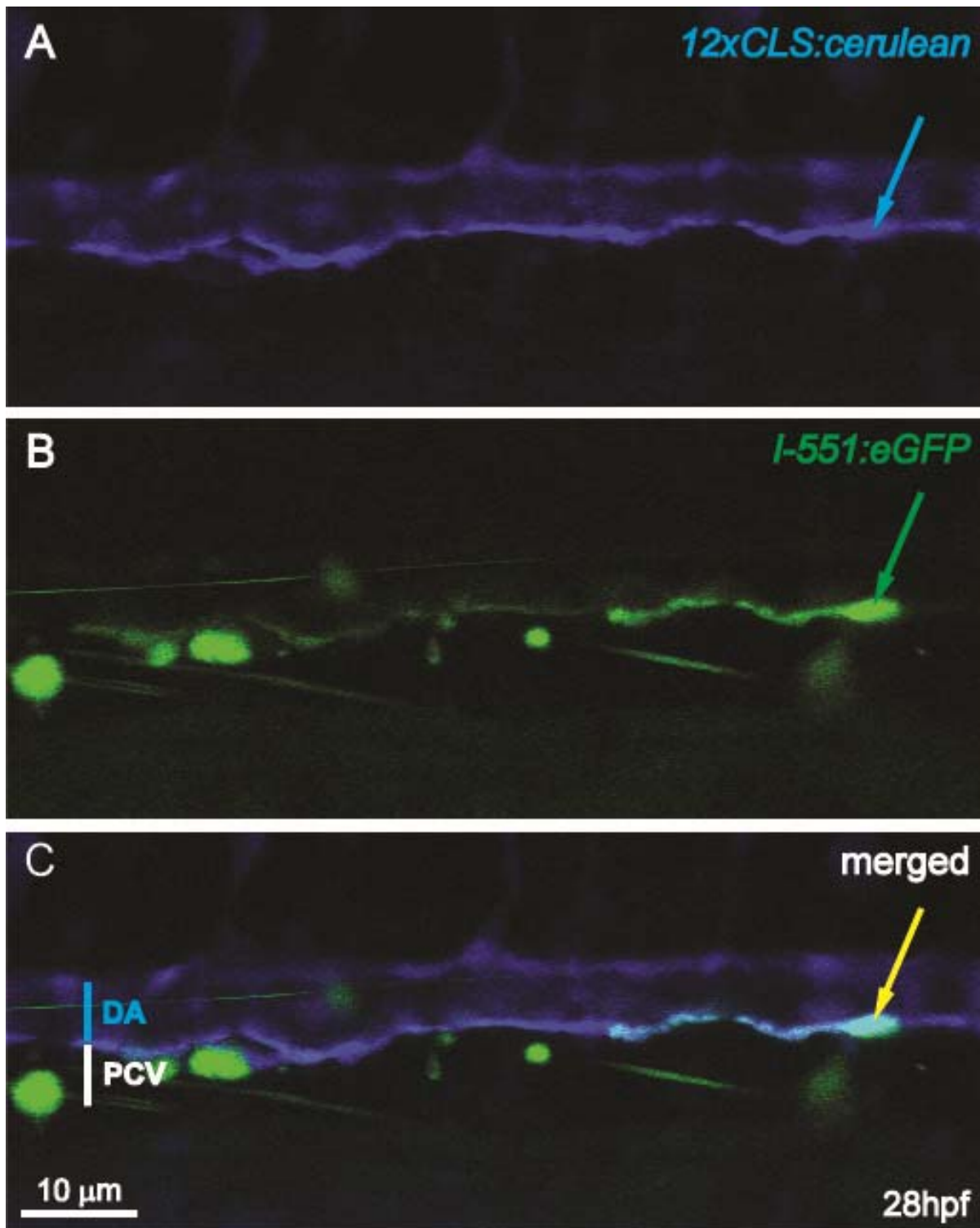


Figure 3.13: *notch* signalling is active in *I-551* positive cells of *Tg (I-551:eGFP;12xCLS:cerulean)* Double transgenic embryos were imaged live at 27 hpf using a confocal laser scanning microscope. A 4 μ m optical section is depicted in this image. *Cerulean* is expressed throughout the artery of the embryo (A, blue arrow). *I-551* expression is restricted to the ventral wall of the artery and to primitive red blood cells (B, green arrow). Picture C shows a merged view of A and B. Cells in the ventral wall are co-expressing both transgenes (C, turquoise arrow), while the primitive red blood cells

express only eGFP (C, green arrow). The dorsal arterial cells and the ISVs only express cerulean (C, blue arrow). DA: dorsal aorta, PCV: posterior cardinal vein.

Figure 3.13A shows the expression of the *12xCLS:cerulean* transgene in the embryo. The *notch* activity in the trunk is restricted to the artery and to the forming ISVs (Figure 3.13A, blue arrow). *I-551* endothelial expression is detected in the ventral wall of the DA and in primitive red blood cells as described before (Figure 3.13,B, green arrow). In the double transgenic embryos, both transgenes are co-expressed in the cells of the ventral wall of the dorsal aorta (Figure 3.13 C). This result verifies that *I-551* positive cells are amongst cells in the DA and that *notch* is active in these cells.

Summary of chapter 3.4:

- The circulating eGFP positive cells in *I-551:eGFP* are confirmed as primitive red blood cells by crossing the line with *Gata1:dsRED*
- a sagittal section through the posterior blood island of double transgenic embryos reveals distinct population of cells with unique expression of the transgenes
- Flow cytometrical analysis of *I-551:eGFP* and *Gata1:dsRED* double transgenic embryos at 26 hpf and 30 hpf shows a decline in fluorescence in the double positive primitive red blood cell population at 30 hpf
- the endothelial expression in *I-551:eGFP* is localised to the ventral wall of the dorsal aorta by crossing the line to the *Flk1:tomato*, *EfnB2a:tomato* and *12xCLS:cerulean* transgenic lines

3.5 The trapped gene in the transgenic line *I-551:eGFP* is identified as *gfi1.1*

3.5.1 Southern blot analysis of *Tg(I-551:eGFP)* reveals 7 genomic integrations of the gene trap vector *ptol2rst*

The reporter gene expression of the transgenic line *I-551:eGFP* in the ventral wall of the dorsal aorta and other haematopoietic tissues prompted us to map the insertion in the genome. To find out the location of the gene trap in the genome, inverse PCR was intended. But first we wanted to determine the number of insertions in the transgenic line. This would indicate the number of inverse PCR products we should expect. In the first instance, 7 insertions were detected in the southern blot analysis of *I-551:eGFP* transgenic animals when the gDNA was digested with two different restriction enzymes (Figure 3.14, lane 1 and 2). Because of the high number of insertions, we decided to out-cross the fish carrying the *I-551:eGFP* phenotype to wild type fish of the opposite sex over 2-3 generations, in order to reduce the number of insertions.

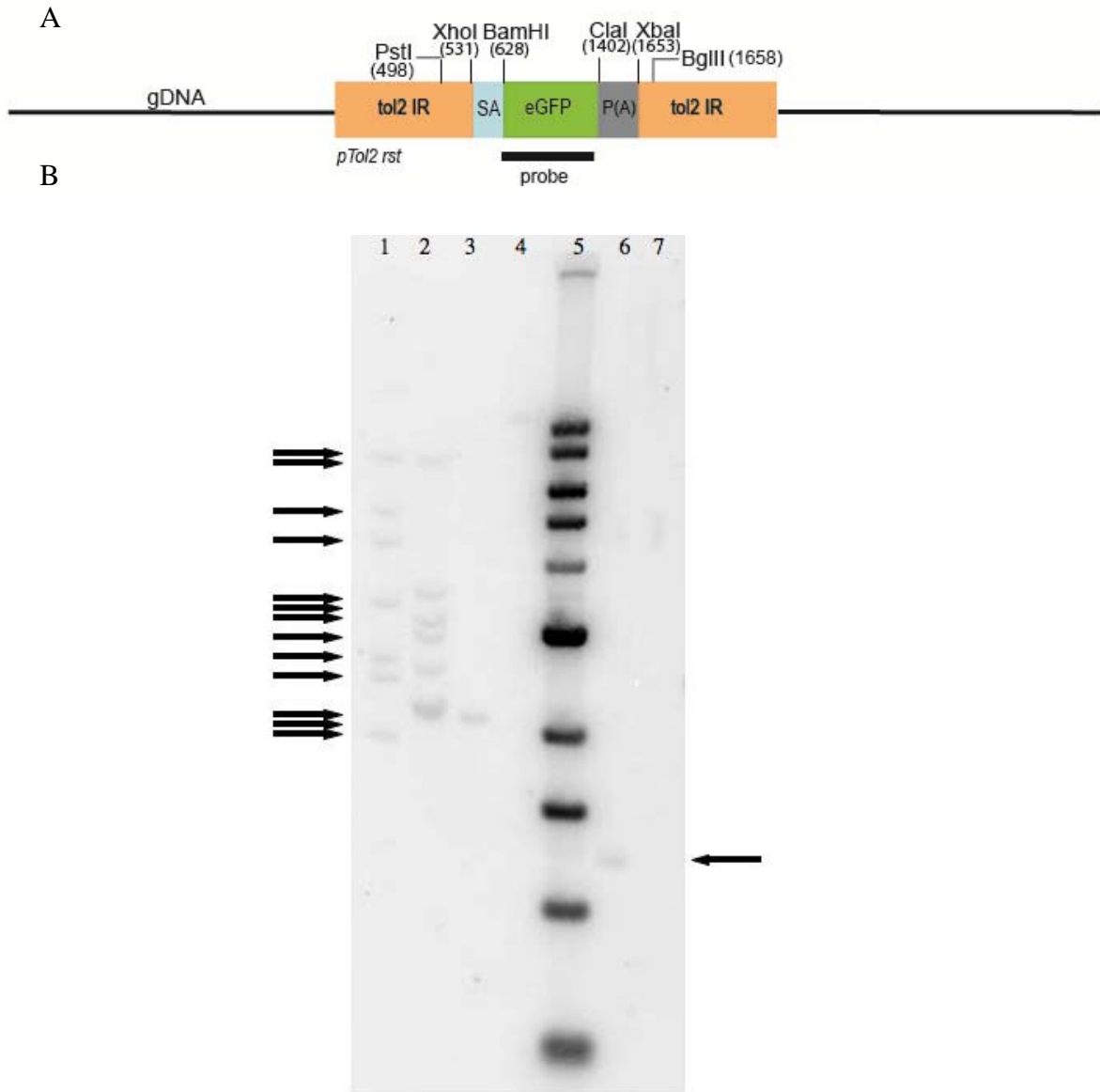


Figure 3.14: Southern blot analysis of *Tg(I-551:eGFP)* and *Tg(173-11:eGFP)* A) Schematic diagram depicting the restriction sites in the *ptol2rst* gene trap vector insertion in the genome. The region targeted by the southern blot probe is shown as a black line. B) The gDNA of *Tg(I-551:eGFP)* and *Tg(173-11:eGFP)* were both digested with the restriction enzymes *PstI* and *BglIII*. As a positive control, gDNA derived from *I-551:eGFP* was also digested with *XhoI* and *XbaI*. The combination of these two restriction enzymes results in an 1122bp long fragment which includes the eGFP coding region (A). The blot was probed with a 744 bp *BamHI-ClaI* fragment consisting of the coding sequence for the eGFP protein (A). 5 μ g of each gDNA sample was loaded. B: Lane 1: *I-551* gDNA/*BglIII*, Lane 2: *I-551* gDNA/*PstI*, Lane 3: *173-11* gDNA/*BglIII*, Lane 4: *173-11* gDNA/*PstI*, Lane 5: 1 kb ladder, Lane 6: *I-551* gDNA/*XhoI* and *XbaI*, Lane 7: wild type gDNA/*BglIII*

3.5.2 The *ptol2rst* insertion is mapped to the first intron of *gfi1.1*

We then continued to perform inverse PCR on the gDNA of this out-crossed *I-551:eGFP* transgenic fish (Figure 3.15).

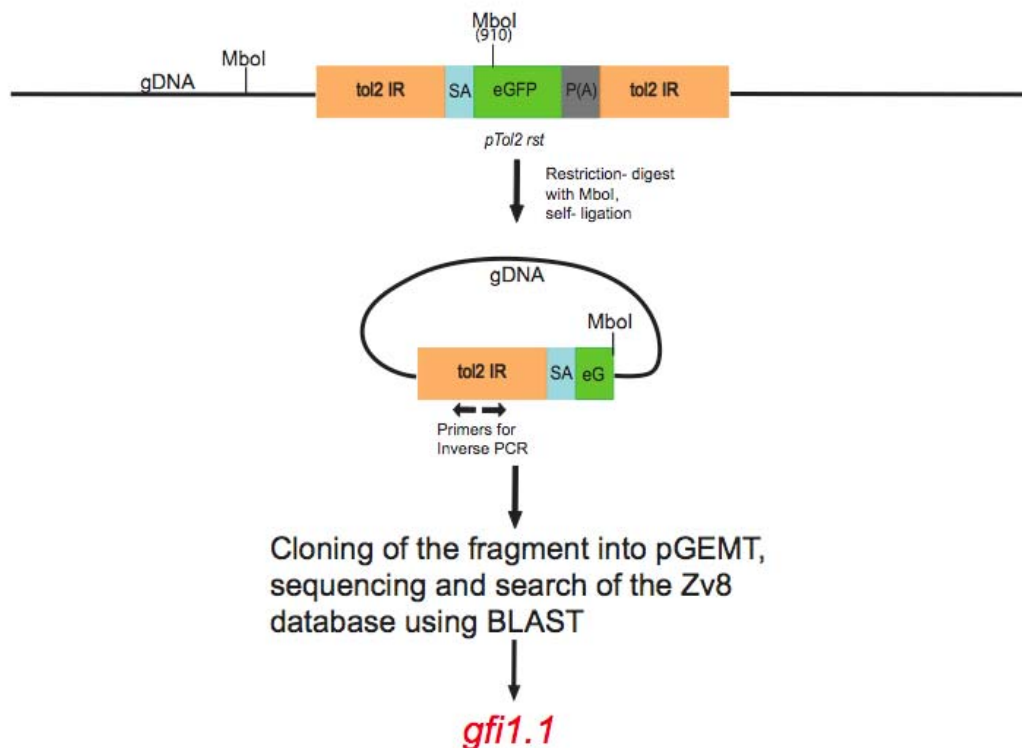


Figure 3.15: The insertion responsible for the reporter gene expression in the line *I-551:eGFP* can be localized to the gene *gfi1.1* The diagram illustrates the strategy used to map the insertion in *I-551:eGFP*. The restriction enzyme *Mbol* with a restriction site in the insert was used to digest the gDNA. The gDNA fragments underwent a self-ligation and inverse PCR with primers in the insert and pointing towards each other were used to amplify the adjacent gDNA to the insertion. The PCR product was cloned into *pGEMT* vector and sequenced using the *T7* promoter. A blast search was performed against the zebrafish genome (*Zv8*).

The method allows to clone unknown sequences adjacent to known sequences. First, the genomic DNA was cut with a restriction enzyme with a restriction site in the

known sequence. We used the enzyme *HaeIII* and *MboI* which have a recognition site in the *ptol2rst* vector. The restriction in the unknown genomic DNA region will occur every 1024 bp since both enzymes recognize and cut a 4 bp long sequence. Next, the genomic DNA fragments are self-ligated at low concentrations and form a circular molecule (Figure 3.15). The sequence of interest is now surrounded by the known transposon sequence. Primers that bind either side of the sequence of interest are used to amplify across the sequence. We used different sets of genomic DNA for this purpose. We separated the progeny of an *I-551:eGFP* transgenic animal into eGFP positive and eGFP negative embryos. We treated the genomic DNA derived from these embryos separately. This will allow us to distinguish between insertions which are common between eGFP positive and negative embryos and therefore not derived from the *I-551:eGFP* phenotype and between insertions which are specific to the eGFP expression seen in *I-551*. We also tried to determine the insertion in another transgenic line derived from the gene trap screen, *SN 413* which expresses eGFP in the heart. We obtained nested PCR fragments for each of the genomic DNA used. For *I-551 eGFP* positive embryos, an 800 bp long fragment was obtained, using the genomic DNA that was cut with *MboI* (Figure 3.16, lane 2). The fragments obtained with *HaeIII* restriction are similar for eGFP positive and negative embryos (Figure 3.16, lane 1 and 3) and therefore could be either unspecific fragments or insertion sites which are common to both eGFP positive and negative embryos. For *SN413*, a 1.1kb fragment was isolated (Figure 3.16, lane 6). The PCR products (Figure 3.16) were cloned into *pGEMT* and sequenced. The 800 bp sequence that was cloned from *I-551/MboI* included a 134 bp sequence of gDNA adjacent to the insertion.

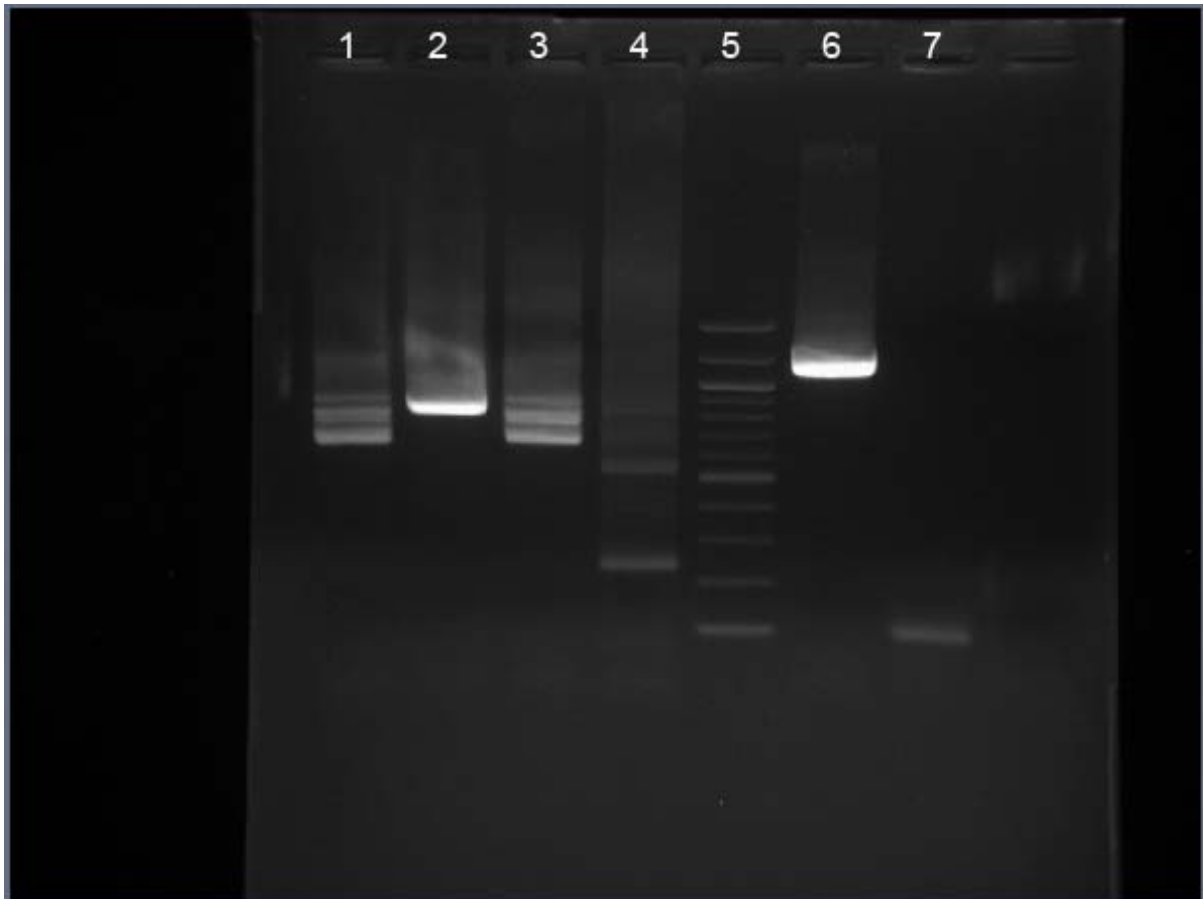
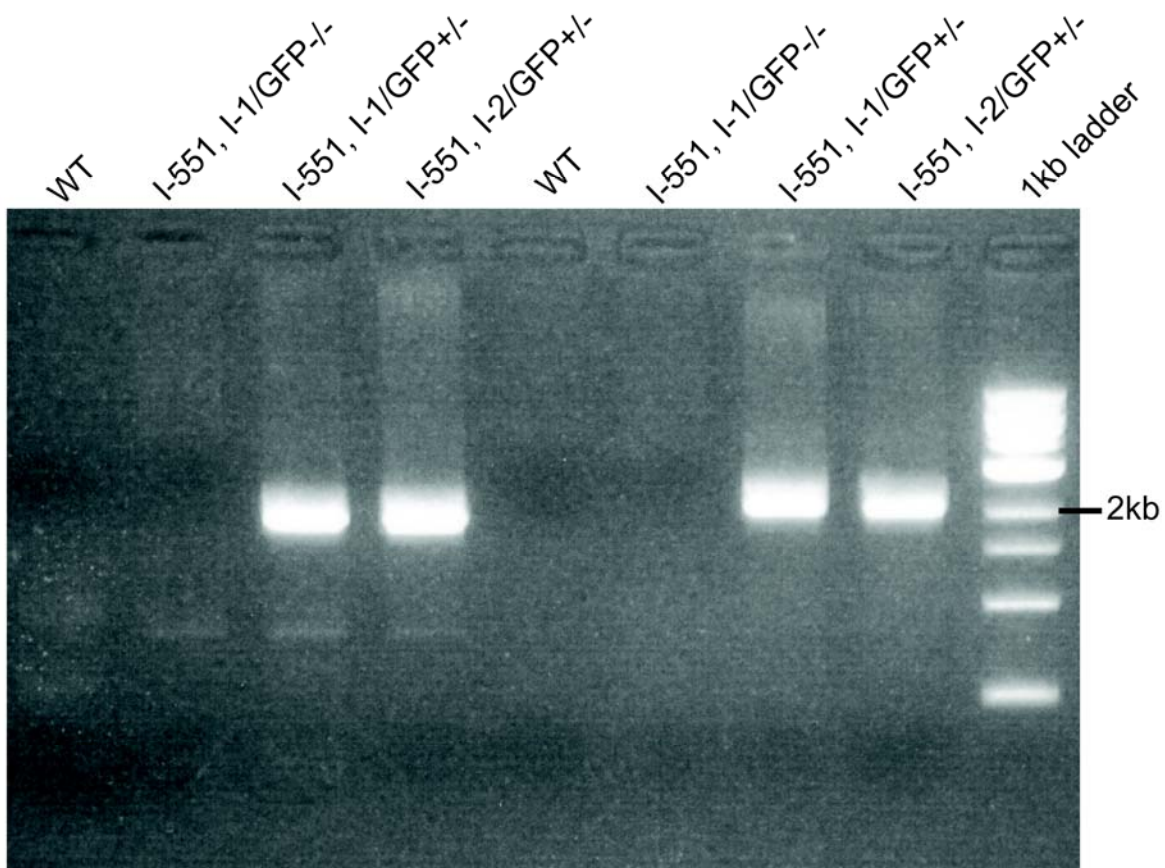


Figure 3.16: nested Inverse PCR with gDNA from *I-551:eGFP* and *SN:413:eGFP*. Lane1: gDNA from *I-551*, GFP positive/*HaeIII*, lane2: gDNA from *I-551*, eGFP positive/*MboI*, lane3: gDNA from *I-551*, GFP negative/*HaeIII*, lane4: gDNA from *I-551*, GFP negative/*MboI*, lane 5: 100bp ladder, lane6: gDNA from *SN413/HaeIII*, lane7: gDNA from *SN413/MboI*. The PCR products were run on a 1.5% agarose-gel.

3.5.3 Two sets of PCRs confirm the insertion in *I-551:eGFP* as *gfi1.1*

A blast search was performed to identify the corresponding sequence of interest in the genome. Surprisingly, five potential loci in the zebrafish genome displayed 100% identity in the ZV8 (August 2010) database from ensemble. Three hits were located close to unidentified/novel protein and one hit was in the 3'UTR of a gene. But one of the hits corresponded to a sequence in the first intron of *gfi1.1*, a homolog of the characterised *gfi1* in the mouse. To confirm that the gene trap responsible for the

observed eGFP expression pattern was located in intron 1 of *gfi1.1* in the zebrafish genome, two sets of PCR experiments were performed on genomic DNA isolated from eGFP positive and eGFP negative siblings derived from two *I-551:eGFP* outcrosses. The same PCR was also performed on genomic DNA isolated from wild type embryos. We used primers that hybridise to the sequence in *gfi1.1* intron1 and combine it with primers that bind to the sequence inside the eGFP locus in the insert. If the insertion was located in the first intron of *gfi1.1*, we would expect to amplify two DNA fragments with sizes of 2.2 kb and 1,8 kb, respectively (Figure 3.17).



Primers used in lanes 1-4: C and D; lanes 5-8: A and B

Figure 3.17: PCR on genomic DNA confirms the trapped gene in the transgenic line *I-551:eGFP* as *gfi1.1* Two sets of primers were used to confirm the insertion sites in *I-551:eGFP* line. In lanes 1-4 the primers A and B were used. The oligonucleotide A is located on the sense strand in the first intron of *gfi1.1*, the primer B maps to the reverse strand in the *egfp* coding region. A PCR product of 1.8 kb is expected. The second primer pair C and D will result in a 2.2 kb fragment if the insertion is located in *gfi1.1*. The forward Primer is in the

egfp sequence and the reverse primer is located downstream of the proposed insertion site. Four different sets of gDNA were used for this experiment. As a negative control wild type gDNA (lanes 1 and 5) was used as a template. The second control consists of gDNA derived from the *I-551:eGFP* eGFP-negative siblings (lanes 2 and 6). The following two sets of gDNA were from *I-551:eGFP* transgenics from two different crosses *I-1* (lanes 3 and 7) and *I-2* (lanes 4 and 8).

The PCR was done on four different genomic DNAs. The wild type negative control did not give any fragments as expected (Figure 3.17, lanes 1 and 4). *I-551:eGFP* embryos from both crosses were separated based on fluorescence. The occurrence of the transgenic animals followed a Mendelian ratio of 0.5. Embryos with no eGFP expression in erythroid and endothelial cells were pooled together as *I-551,I-1/GFP^{-/-}*. The PCR on this genomic DNA did not amplify a fragment (Figure 3.17, lanes 2 and 6). The PCR with genomic DNA from the remaining 50% of embryos with eGFP expression resulted in the expected two fragments (Figure 3.17, lanes 3, 4,7 and 8). In conclusion, we were able to confirm our candidate gene from the inverse PCR and the blast hit. These PCR experiments identified *gfi1.1* as the gene trapped in *I-551:eGFP* transgenic animals.

Summary of chapter 3.5:

- Southern blot analysis revealed 7 insertions of *ptol2rst* in the transgenic line *I-551:eGFP* and 1 insertion in *SN173-11*
- Using inverse PCR, a fragment containing a 134bp long sequence in the first intron of *gfi1.1* gene was cloned
- the integration of the *ptol2rst* in the first intron of the *gfi1.1* gene which is responsible for the *I-551:eGFP* expression was further confirmed by PCR.

3.6 *Gfi1.1* is expressed in the haemogenic endothelium

3.6.1 Endothelial eGFP expression in *gfi1.1:eGFP* is downstream of VEGF signalling

Gfi1.1:eGFP positive embryos were treated with 5 μ M of VegFR inhibitor with the intention to investigate if the endothelial eGFP expression would be affected negatively. VEGF signalling is known to be essential for arterial specification. If the eGFP positive endothelial cells were absent in this experiment, we would firstly, be able to locate the *gfi1.1* endothelial expression downstream of VEGF signalling and secondly confirm the arterial nature of the endothelial cells.

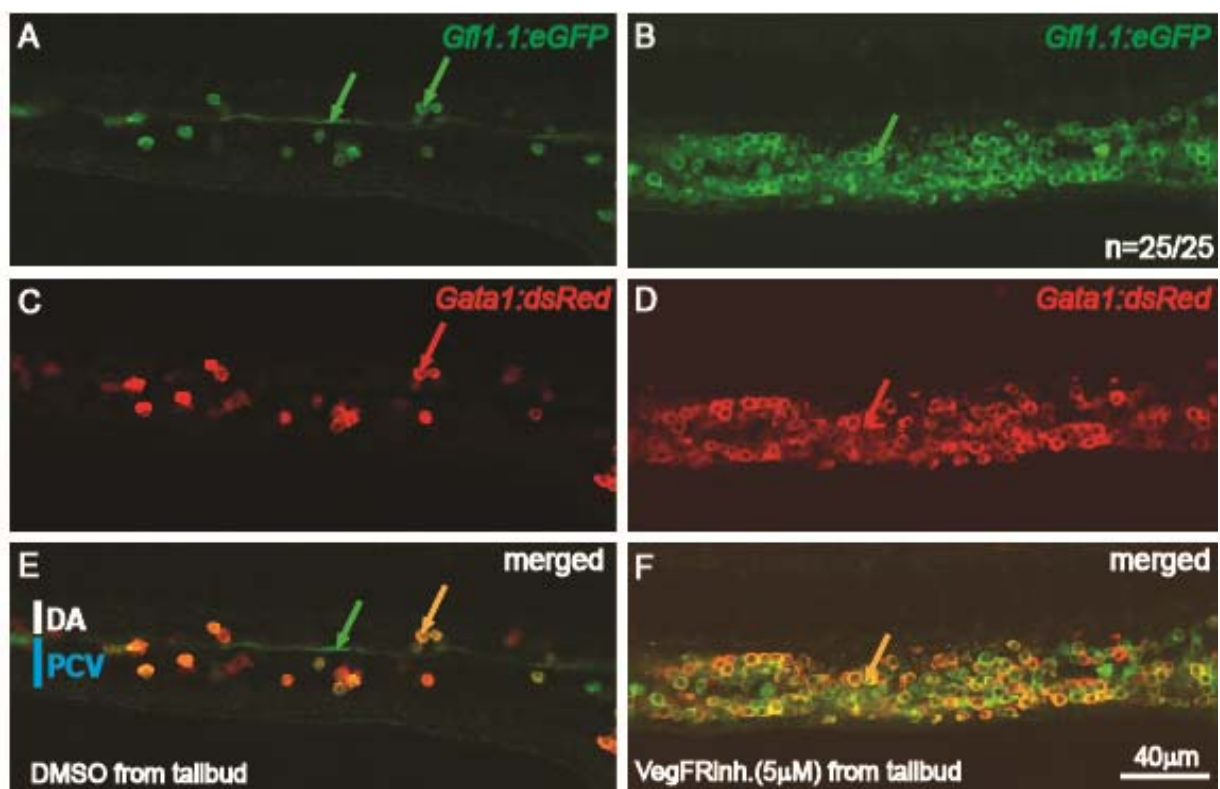


Figure 3.18: Endothelial *Gfi1.1:eGFP* expression is lost in embryos treated with 5 μ M VegfR inhibitor 25 *Gfi1.1:eGFP/Gata1:deRED* double transgenic embryos were treated with either 5 μ M VegfR inhibitor (B,D and F) or with 5 μ l of DMSO as a negative control (A,C and E) from tail bud. The embryos were immuno-stained for eGFP and dsRED and analyzed at 28hpf by taking 4 μ m optical sections with a confocal laser-scanning microscope through the

trunk of the embryo. In the control embryos, blood circulation occur and the *Gfi1.1:eGFP* positive endothelial cells are clearly visible in the ventral wall of the DA (A and E, green arrow). The primitive red blood cells can be detected as double positive cells (C and E, yellow arrow). The right panel shows embryos treated with the inhibitor. All of the 25 embryos lack circulation and there are only double positive round erythroid cells visible, but no elongated eGFP positive endothelial cells (B,D and F). The lateral view is shown and the anterior of the embryo is to the left. DA: dorsal aorta, PCV: posterior cardinal vein.

We treated 25 *Tg(Gfi1.1:eGFP;gata1:dsRED)* double transgenic embryos with 5 μ M of VegFR inhibitor as previously described (Gering et al, 2005). Since the double transgenic embryos co-express the fluorescent protein in primitive red blood cells, the use of the double transgenic embryos will allow us to easily distinguish between the spindle-shaped green endothelial cells and mostly red and green primitive red blood cells. The embryos were incubated in the Inhibitor from tail bud stage until 28 hpf, were fixed and then underwent immuno-histochemistry for *eGFP* and *dsRED*. They were then analyzed using a laser scanning microscope. We choose to take 4 μ m thick optical sections through the trunk of the embryos. Control embryos treated with the solvent DMSO develop normal axial vessels and blood circulation (Figure 3.18, A,C and E). The primitive red blood cells appear spherical and express mostly both transgenes (Figure 3.18, E, yellow arrow) while the endothelial cells display *eGFP* expression (Figure 3.18, A and E, green arrow). In contrast, the VegfR-inhibitor treated embryos lack blood circulation even at the age of 28 hpf. In these embryos, we were unable to detect any *eGFP* positive, spindle shaped endothelial cells (Figure 3.18, B, D and F). All the cells in the trunk of the embryos are round and appear to express both fluorescent markers, which indicate that they are primitive erythroid cells. These cells are unaffected by the inhibitor.

These findings suggest that the *eGFP* expression in the *gfi1.1* positive endothelial cells is downstream of *veg*f signalling and the primitive red blood cells are

independent of this process. The endothelial cells in *Gfi1.1:eGFP* are of arterial nature.

3.6.2 Notch signalling is required for the formation of eGFP positive endothelial cells in *Gfi1.1:eGFP* transgenic embryos

The co-expression of *Gfi1.1:eGFP* with *Flk1:tomato* and *EfnB2a:tomato* suggested that expression is located in the DA. The endothelial expression of the eGFP in *Gfi1.1:eGFP* was further shown to be *vegf*-dependent and therefore arterial. Since previous experiments had demonstrated that *12xCLS:cerulean* was co-expressed in eGFP positive *gfi1.1* endothelial cells, we decided to study the endothelial eGFP expression in the absence of *notch* signalling. We employed three different strategies to abrogate *notch* in *Gfi1.1:eGFP* positive embryos. First, we examined the knock-down of Notch activity in *Gfi1.1:eGFP* by injecting an *rpbja/b* antisense morpholino and by treating the embryos with the chemical inhibitor DAPM (Rowlinson et al, 2010, Echeverri et al, 2007; Sieger et al, 2004). We then also crossed the *Gfi1.1:eGFP* transgenic line into the *mindbomb* mutant background. The results of these three experiments would further support the evidence that *notch* is active in *gfi1.1* positive cells.

3.6.2.1 Endothelial expression of eGFP in the *Gfi1.1:eGFP* transgenics can be blocked by DAPM treatment

We treated 25 embryos with either 100 μ M of DAPM (γ -secretase inhibitor) or with DMSO as a control from tail bud stage. With ongoing somitogenesis these embryos started to develop a curly tail, a phenotype very common to mutants of the *notch* pathway (Van Eeden et al, 1996). The embryos were grown to 32 hpf and

subsequently fixed and immuno-stained for eGFP and dsRED. The embryos were then analyzed with confocal microscopy.

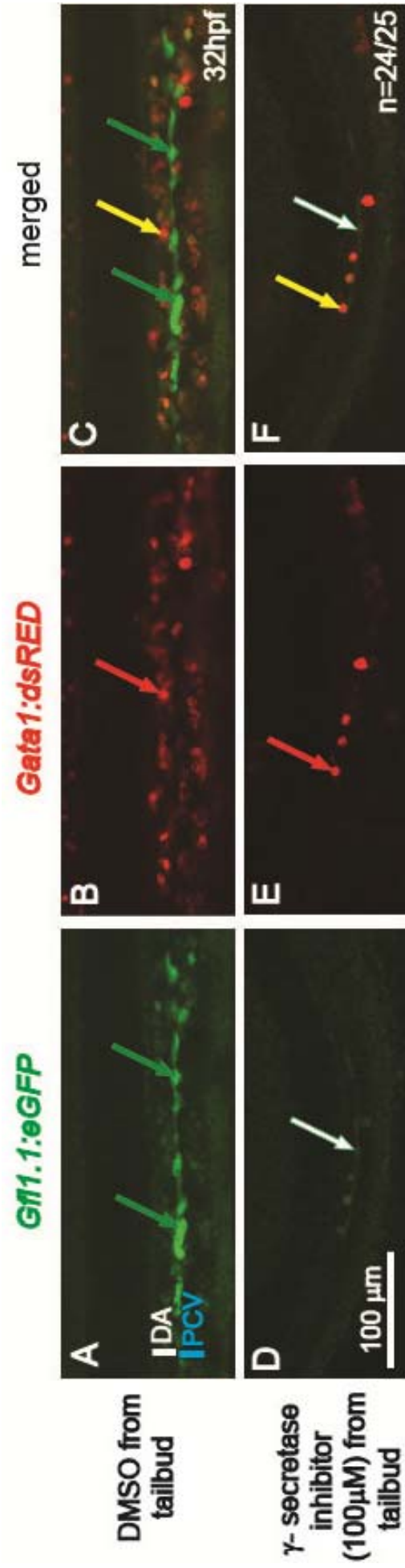


Figure 3.19: Endothelial expression of *Gf11.1:eGFP* is lost in DAPM treated embryos 25 Tg(*Gf11.1:eGFP*; *Gata1:dsRED*) double transgenic embryos were treated with 100 μM γ -secretase inhibitor DAPM from tail bud stage. As a negative control 25 double transgenic embryos were treated with the solvent DMSO. Both groups of embryos were incubated at 28.5°C until they reached the age of 32hpf and immuno-stained for eGFP and dsRED. 7 μm optical sections were taken using a confocal laser scanning microscope and are shown in these images. In the embryos treated with DMSO, *Gf11.1:eGFP* expression is unaffected and is clearly visible in the endothelial cells of the ventral wall in the dorsal aorta (green arrow, A and C). *Gata1* expression is detected in circulating red blood cells (red arrow, B and E). In 24/25 embryos treated with the γ -secretase inhibitor DAPM, the endothelial expression of eGFP is lost while the expression in the primitive red blood cells remains (D, white arrow). *Gata1* expression is unaffected by the inhibitor treatment (E, red arrow) and in the merged view only double positive red blood cells are present (F, yellow arrow). The anterior of the embryo is to the left. DA: dorsal aorta, PCV: posterior cardinal vein.

The expression of eGFP was lost in 24/25 *Gfi1.1:eGFP* and *Gata1:dsRED* double transgenic embryos treated with 100 μ M of DAPM (Figure 3.19 D and F, white arrows). The double positive primitive red blood cells stayed unaffected by the treatment (Figure 3.19, B and C, E and F). In order to show that the *gfi1.1* positive cells behave exactly as *runx1* positive cells, a further control experiment was performed. *Gfi1.1:eGFP* transgenic embryos were treated with DAPM as described before and underwent *in situ* hybridisation for *runx1*. As expected, the decrease in *runx1* positive cells correlates with the decrease in *gfi1.1* positive endothelial cells (see supplemental Figure 3). Altogether, these findings fit with our expectations and earlier hypothesis that *notch* is active in *gfi1.1* positive endothelial cells. Furthermore, treatment with the *y-secretase* inhibitor leads to a block of the *notch* activity. Consequently, arterial specification is impaired and results in the absence of eGFP positive cells in the ventral wall of the dorsal aorta.

3.6.2.2 Blocking the *notch* pathway by injecting the *rpja/b* morpholino abrogates endothelial expression of *Gfi1.1:eGFP*

Next, the *rpja/b* antisense morpholino (Rowlinson et al, 2010, Echeverri et al, 2007) was injected into one to four cell stage embryos. The ATG antisense morpholino will target the primary transcript by blocking the translation and thereby prevent the production of the RPBJA/B protein.

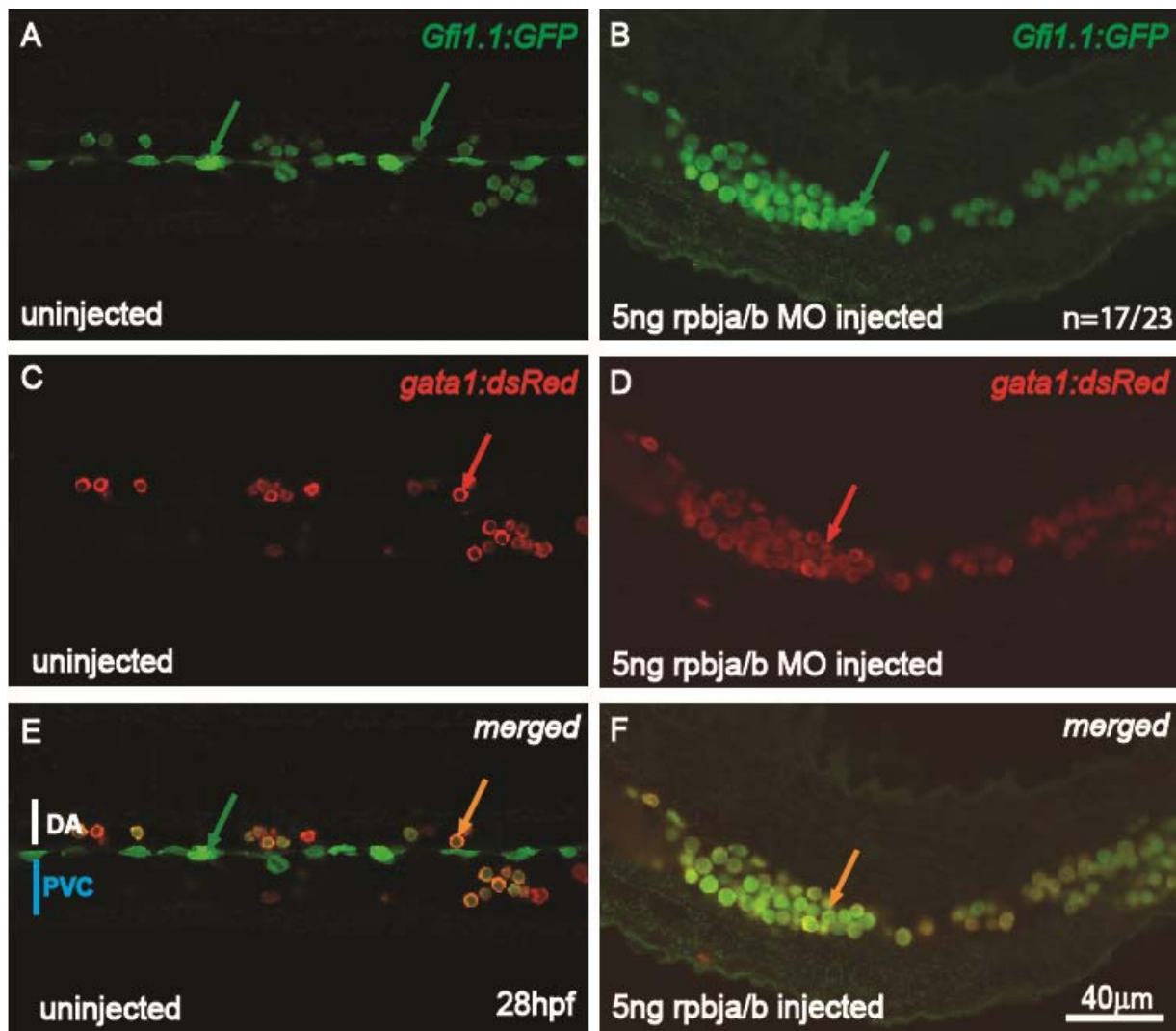


Figure 3.20: *Rpbja/b* MO-injected *Gfi1.1:eGFP* embryos lose eGFP expression in the ventral wall of the DA *Gfi1.1:eGFP* and *Gata1:dsRED* double transgenic embryos were injected with 5 ng of *rpbja/b* morpholino between one and four cell stage. In 17/23 injected embryos the eGFP expression in the spindle shaped, endothelial cells was lost at 28 hpf (B and F) compared to wild type embryos (A and E, green arrow). The remaining fluorescent cells have a round shape and are positive for both transgenes (F, yellow arrow). They therefore represent primitive red blood cells. The embryos were immuno-stained for eGFP and dsRED and 2µm sections through the trunk of the embryo are depicted. The anterior of the embryo is to the left. DA: dorsal aorta, PCV: posterior cardinal vein.

23 double transgenic *Gfi1.1:eGFP* and *Gata1:dsRED* embryos were injected with 5ng of *rpbja/b* morpholino and grown up to 28 hpf. In 17/23 embryos we observed kinked tails, a common phenotype seen in *notch* mutants (van Eeden et al, 1996). In the uninjected control group, no such observation was made. The control embryos had

vigorous blood circulation (Figure 3.16, A,C and E) and we could clearly distinguish between eGFP only endothelial cells (Figure 3.20, A and E, green arrow) and double positive primitive red blood cells (B and E, red and yellow arrows). In contrast, *rpbja/b* MO injected embryos showed a delay in their development (data not shown) and a poor blood circulation, which is caused by slightly malformed blood vessels (Burns et al, 2005). But the onset of pigmentation in the embryo was used to determine their developmental stage. Furthermore, the endothelial eGFP expression was lost in these embryos (Figure 3.20, B and F) and only double positive primitive red blood cells were identified (D and F, red and yellow arrows). We therefore conclude that the injections of the MO leads to the same phenotype as observed in DAPM treated embryos. *Gfi1.1:eGFP* positive endothelial cells are lost in *rpja/b* morpholino treated embryos.

3.6.2.3 *Gfi1.1:eGFP/mib^{-/-}* mutant embryos lack reporter gene expression in endothelial cells

We then crossed the *Gfi1.1:eGFP* transgenic line into the *mind bomb* mutant background. This experiment will validate earlier findings. We expected to see a loss of the endothelial EGFP cells in the mutants while the erythroid eGFP expression persists.

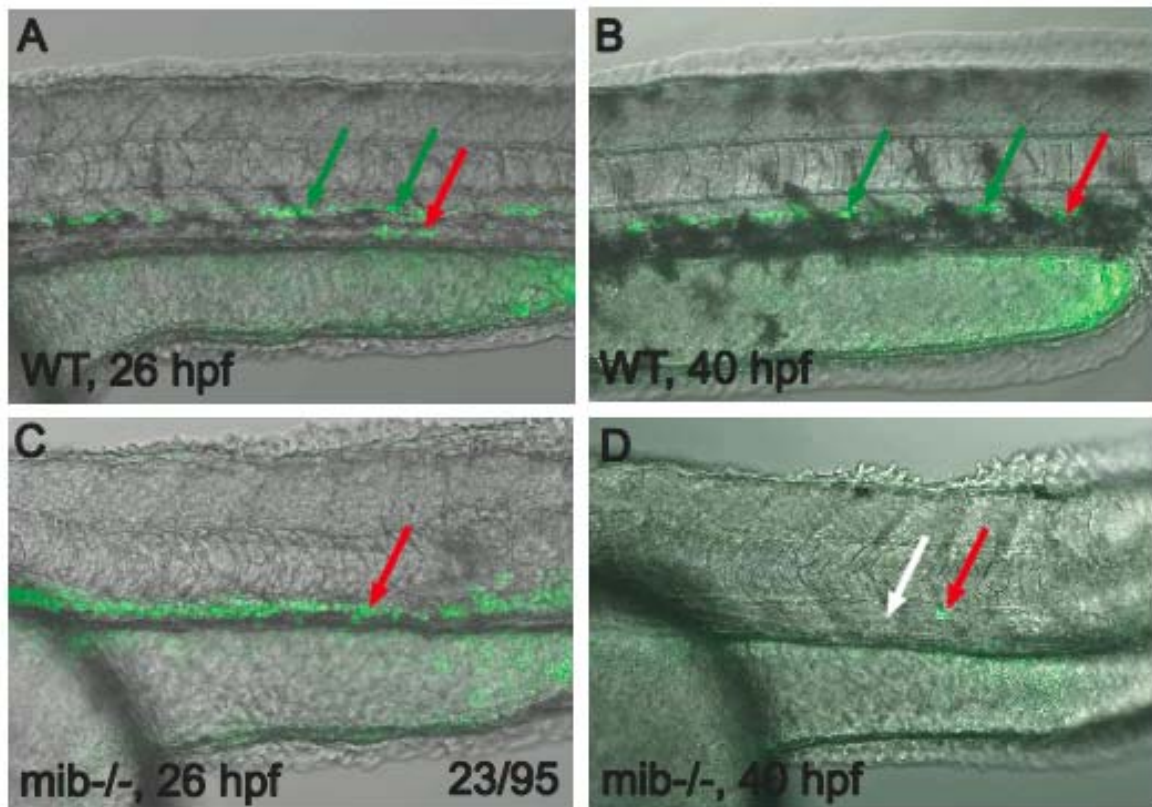


Figure 3.21: Endothelial expression of *Gfi1.1:eGFP* is lost in *mib*^{-/-} embryos
 Heterozygous *mib* carriers were crossed with each other and embryos were collected. In this clutch, 23/95 embryos showed *mib* mutant phenotype. Their tail was kinked and the onset of pigmentation was delayed and absent in the tail of *mib*^{-/-} embryos at 40 hpf (D) compared to wild type embryos (B). At 26 hpf, wild type embryos gained blood circulation and eGFP positive cells were visible in the endothelium (A, green arrow) and in primitive red blood cells (red arrow). In contrast, in *mib*^{-/-} the circulation was poor and all the cells in the blood vessels appeared round (C, red arrow). At 40 hpf, the eGFP expression in the primitive red blood cells had decreased and only endothelial eGFP expression remained in wild type embryos (B, red and green arrow, respectively). In *mib*^{-/-} embryos we were not able to see any endothelial eGFP positive cells (D, white arrow). Only a single still eGFP positive red blood cell is still expressing the transgene (D, red arrow). Embryos were imaged live with the anterior to the left.

Gfi1.1:eGFP transgenics were crossed with heterozygous carriers of the *mind bomb* mutation. GFP positive progeny were grown to adulthood and adult siblings were crossed with each other. If both fish used for the crosses were heterozygous for the mutation, then we expected to see homozygous mutant in the Mendelian ratio of 1:4.

In the clutch of embryos used for images in Figure 3.21, 23/93 of embryos were identified as homozygous *mind bomb* mutants, which correlates with the expected number. These embryos had a larger notochord (data not shown), a kinked tail and pigmentation defects at 40 hpf (Figure 3.21, D) compared to wild type embryos (Figure 3.21, B). Furthermore, they showed a delay in establishing blood circulation. All these attributes confirmed that they were homozygous *mib* mutants. We analyzed these embryos using the fluorescent microscope to examine the eGFP expression in *gfi1.1* positive cells. At 26 hpf, the phenotypic ally wild type embryos had eGFP expression in circulating red blood cells (Figure 3.21, A, red arrow) and endothelial cells lining the ventral wall of the artery (Figure 3.21, green arrow). In contrast, *Gfi1.1:eGFP/mib^{-/-}* embryos did not seem to have the endothelial expression of eGFP (Figure 3.21, C red arrow). The expression in the primitive red blood cells was unaffected which is consistent with red blood cells development being independent of *notch* signalling (Gering et al, 2005; Burns et al, 2005). We also examined the embryos at a later time point. At 40 hpf, when the expression in the primitive red blood cells is lost, we observed only *gfi1.1* endothelial cells in the wild type control embryos (Figure 3.21, B, green arrow). But in the mutants, there is almost no eGFP expressing cells left. With the decrease of fluorescence in erythroid cells, the trunk is devoid of eGFP positive cells (Figure 3.21, D red arrow). There are no endothelial cells expressing the transgene, although endothelial cells are present in these embryos.

We confirm our initial observations made in the DAPM treated embryos and in *rpbja/b* MO injected embryos. *Gfi1.1* expression in endothelial cells in the ventral wall of the aorta is dependent on *notch* signalling and is lost if the *notch* pathway is interrupted.

3.6.3 *Gfi1.1* positive cells in the wall of the dorsal aorta also express the haematopoietic marker genes *runx1* and *c-myb*

The previous experiments have shown that the endothelial cells in the transgenic line *Gfi1.1:eGFP* behave like putative haemogenic cells in zebrafish. Upon *vegfa* and *notch* inhibition the endothelial eGFP expression decreases. Here, we performed *in situ* hybridisation for the two established HSC markers *runx1* and *c-myb* followed by an immuno-histochemistry for eGFP on *Gfi1.1:eGFP* embryos. Co-expression of these markers in *gfi1.1* positive cells would ultimately prove that *Gfi1.1:eGFP* cells are haemogenic.

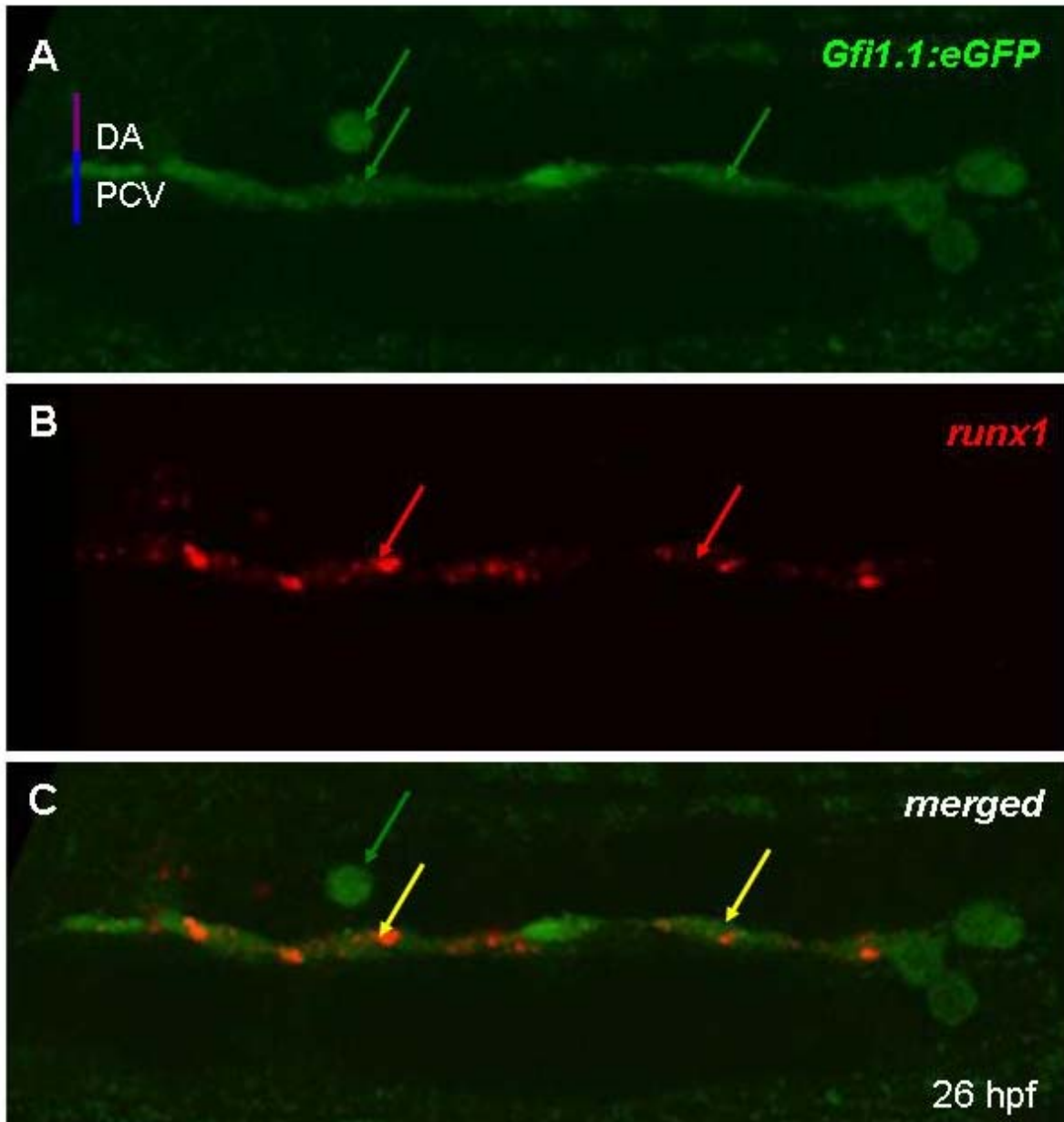


Figure 3.22: *Gfi1.1* and *runx1* are co-expressed in the ventral wall of the dorsal aorta at 26 hpf *Gfi1.1:eGFP* embryos were stained for *runx1* expression first and then underwent an immuno-histochemistry for eGFP. *Gfi1.1:eGFP* expression is confined to the primitive erythroid cells and endothelial cells in the DA (A, green arrows). *Runx1* expression is visible in the ventral endothelium of the DA (B, red arrows). *Runx1* and *gfi1.1* are co-expressed in the endothelial cells only (C, yellow arrow) at 26 hpf. The image represents a 2 μm section through trunk of the embryo using a confocal microscope. DA: dorsal aorta, PCV: posterior cardinal vein.

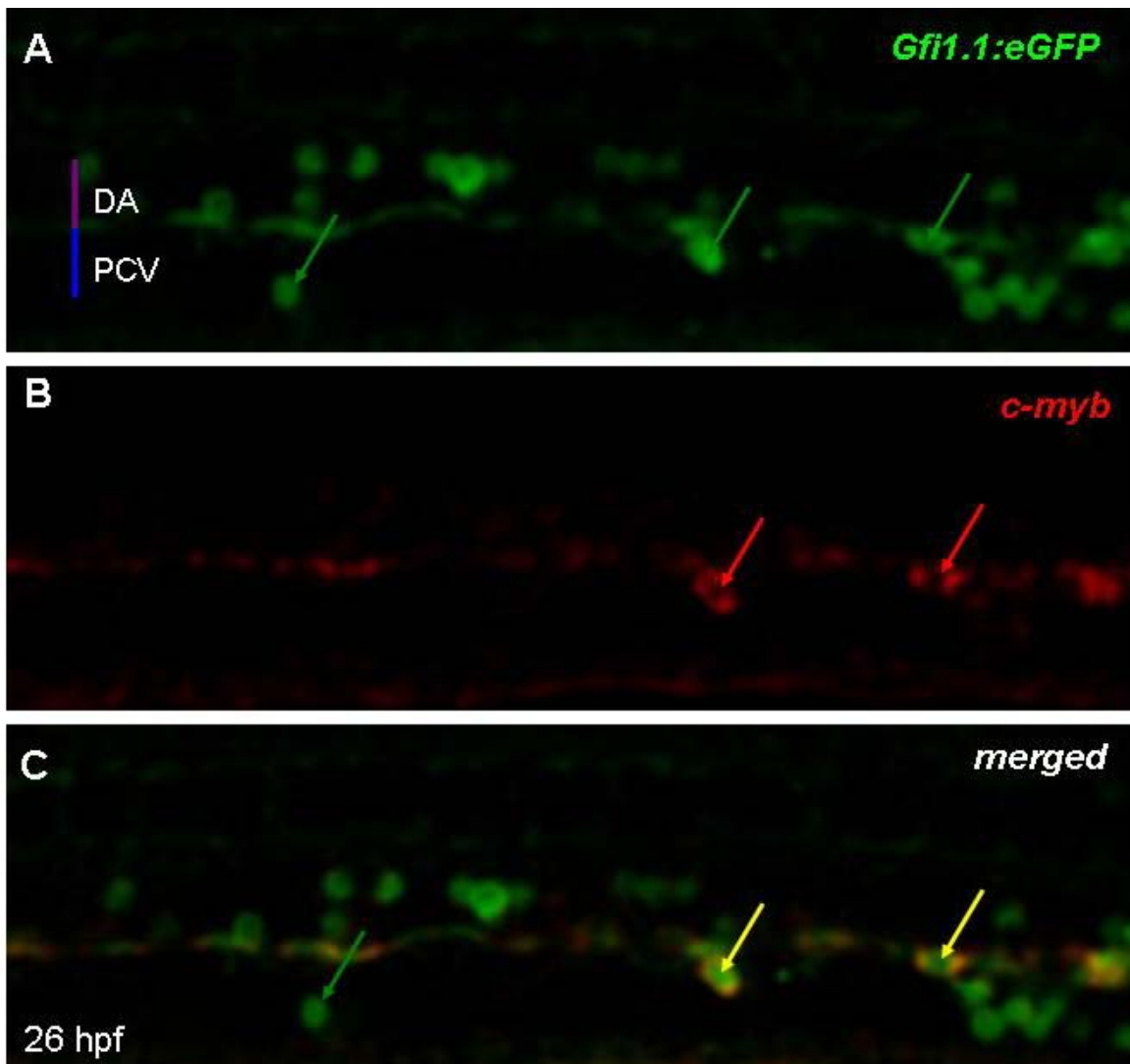


Figure 3.23: *Gfi1.1* and *c-myb* are co-expressed in the ventral wall of the DA *Gfi1.1* expression can be detected in the primitive red blood cells and in endothelial cells of the DA at 26 hpf (A, green arrow). *C-myb* expressing cells are located in the ventral wall of the DA (B, red arrows). Co-expressing cells can be seen in the ventral wall of the DA (C, yellow arrows). A 2 μ m section through the trunk of the embryo is shown. The image was taken on a confocal microscope. DA: dorsal aorta, PCV: posterior cardinal vein.

The double staining experiments for the HSC markers *runx1* or *c-myb* combined with an immuno-histochemistry for eGFP revealed that both marker genes are co-expressed with *gfi1.1* in the ventral wall of the dorsal aorta. The eGFP protein is distributed equally throughout the cells (Figure 3.22 A, green arrows, Figure 3.23 A green arrow). Fluorescent *runx1* expression is detected throughout the endothelium

as dotted spots (Figure 3.22, B and C, red and yellow arrows, respectively). The localisation of the mRNAs in the cytoplasm has been described before for tryamide based signal amplification in fluorescent *in situ* (Paratore et al 1999). *C-myb* mRNA is present in the cytoplasm of the cell, since the red dye is distributed outside the nucleus (Figure 3.23, B and C, red and yellow arrow, respectively). The expression is more restricted. *C-myb* is not expressed throughout the endothelium, but only in a subset of cells which appear to bud off from the ventral wall of the dorsal aorta.

The *in situ* experiments for *runx1* and *c-myb* combined with immuno-histochemistry for eGFP have provided the missing evidence that the transgenic line *Gfi1.1:eGFP* is labelling haemogenic endothelial cells and nascent haematopoietic stem cells. *Gfi1.1:eGFP* therefore enables us to visualize the emergence of these cells from the endothelium in the ventral wall of the DA and is a powerful tool to further study aspects of HSC formation, self-renewal and maintenance *in vivo*.

Summary of chapter 3.6:

- *Gfi1.1* expression in the ventral wall of the dorsal aorta is dependent on *vegf* and *notch* signalling
- all three approaches of *notch* inhibition result in a loss of *gfi1.1* expression specifically in the ventral wall of the dorsal aorta
- *gfi1.1* is co-expressed with *runx1* and *c-myb* in haemogenic endothelial cells

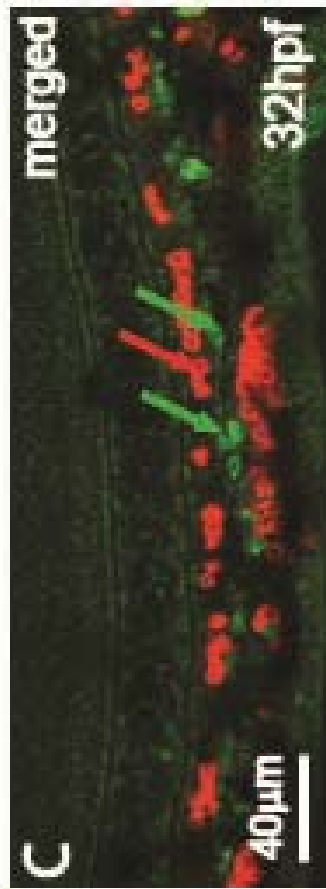
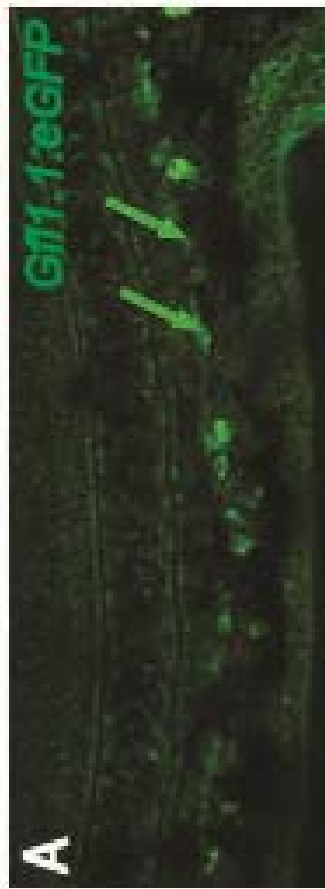
3.7 The dose and timing of *notch* signalling impacts the expression of *gfi1.1* in endothelial cells

3.7.1 Over-expression of *NICD* in *Gfi1.1:eGFP* transgenics leads to an expansion of *gfi1.1* positive endothelial cell population

Since we had confirmed that the eGFP expression in *gfi1.1* positive endothelial cells is downstream of *notch* activity, we wanted to determine if an over-expression of *notch* would lead to an expansion of these eGFP positive cells as described before (Burns et al, 2005). These induced cells have been demonstrated to express the HSC markers *runx1* and *c-myb*. But the haematopoietic potential of these induced cells still remains undetermined. We wanted to investigate if these cells also expressed *gfi1.1*, which would provide a further prove for their haematopoietic potential.

Carriers with the transgenes (*Hsp70:Gal4; UAS:NICD*) (Scheer et al, 1999) were crossed with *Gfi1.1:eGFP* transgenic fish. The embryos derived from this cross are triple transgenics and a heat shock treatment at 16 somites stage for 20 min at 38°C activates the *hsp70* promoter and leads to the synthesis of GAL4 protein. This activator will subsequently bind to the *UAS* sequence upstream of the *nicd* gene and lead to its induction. Consequently, *notch1a-NICD* will be over-expressed in the embryo and activate *notch* target genes. Figure 3.31 shows the outcome of these *notch* over-expression studies. We decided to perform *insitu* for β -EIGlobin and immunohistochemistry for eGFP on them. This will help us to confirm the expanded *gfi1.1* population is not erythroid in character.

Gfi1.1:eGFP



Gfi1.1/GAL4/NICD induced at 16s

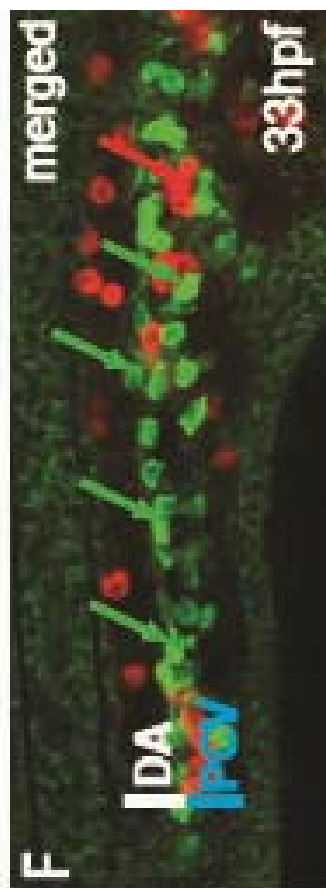


Figure 3.24: Over expression of NICD leads to an expansion of endothelial Gfi1.1 positive cells into the vein Embryos *Tg(Gfi1.1:eGFP/GAL4/NICD)* and *Tg(Gfi1.1:eGFP)* were heat-shocked at 16 somites for 20 minutes to induce NICD expression and were grown up to 32 hpf since the onset of blood circulation is delayed at earlier time-points. Subsequently, *in situ* and immunohistochemistry were performed. The embryos were analyzed using a confocal laser scanning microscope and 7 μ m optical sections through the trunk are shown in this figure. Wild type *gfi1.1* transgenic embryos show eGFP expression in endothelial cells in the artery and faint expression in primitive red blood cells (A and C, green arrow). β E1-Globin expression is restricted to red blood cells (B and C, red arrow). In NICD induced embryos, the endothelial eGFP expression is increased (D and F, green arrow), whereas the β -E1Globin expression remains stable (E and F, red arrow). The anterior of the embryo is to the left. DA: dorsal aorta, PCV: posterior cardinal vein.

We collected triple transgenic embryos and *Gfi1.1:eGFP* positive embryos for this experiment. Both groups of embryos were heat-shocked for 20 minutes at 38°C. Notch-induced embryos were selected based on their shortened body axis and stumpy appearance (not shown). 26 of these *notch*-induced embryos subsequently underwent immuno-histochemistry for eGFP and *in situ* hybridisation for *betaE1-globin*.

The experiment confirms that like *runx1* and *c-myb*, the number of *gfi1.1* positive cells is increased in heat shock treated embryos (Figure 3.24, D and F, green arrows). The eGFP positive cells do not express *β -E1globin*. Thus one can exclude that they are erythroid cells. The expanded population of *gfi1.1* expressing cells seem to reach into the dorsal wall of the vein as reported before (Burns et al, 2005). We can conclude, that the increased aortic cells, which have been described to express *runx-1* and *c-myb* also express *gfi1.1*. Notch is able to modify the number of nascent HSCs in the embryo at 16 somite stage.

3.7.2 Notch signalling is needed before 18 somite cell stage for endothelial *gfi1.1* expression in the ventral artery

The results from the VegFR inhibitor and *notch knock down* and gain of function experiments has lead to the hypothesis that *gfi1.1* positive endothelial cells are putative HSCs. Endothelial cells are programmed to contribute towards the vein or the artery from a very early time point. DAPM treatment of *Gfi1.1:eGFP* and *gata1:dsRED* double transgenics starting at different developmental stages were performed in order to investigate this question. DAPM treatment was undertaken from tail bud-, 10 somite-, 14 somite- and 18 somite stages. We then looked at the number of eGFP expressing cells in the artery of *Gfi1.1:eGFP* and *gata1:dsRED* double transgenic embryos and compared the numbers to those present in wild type embryos.

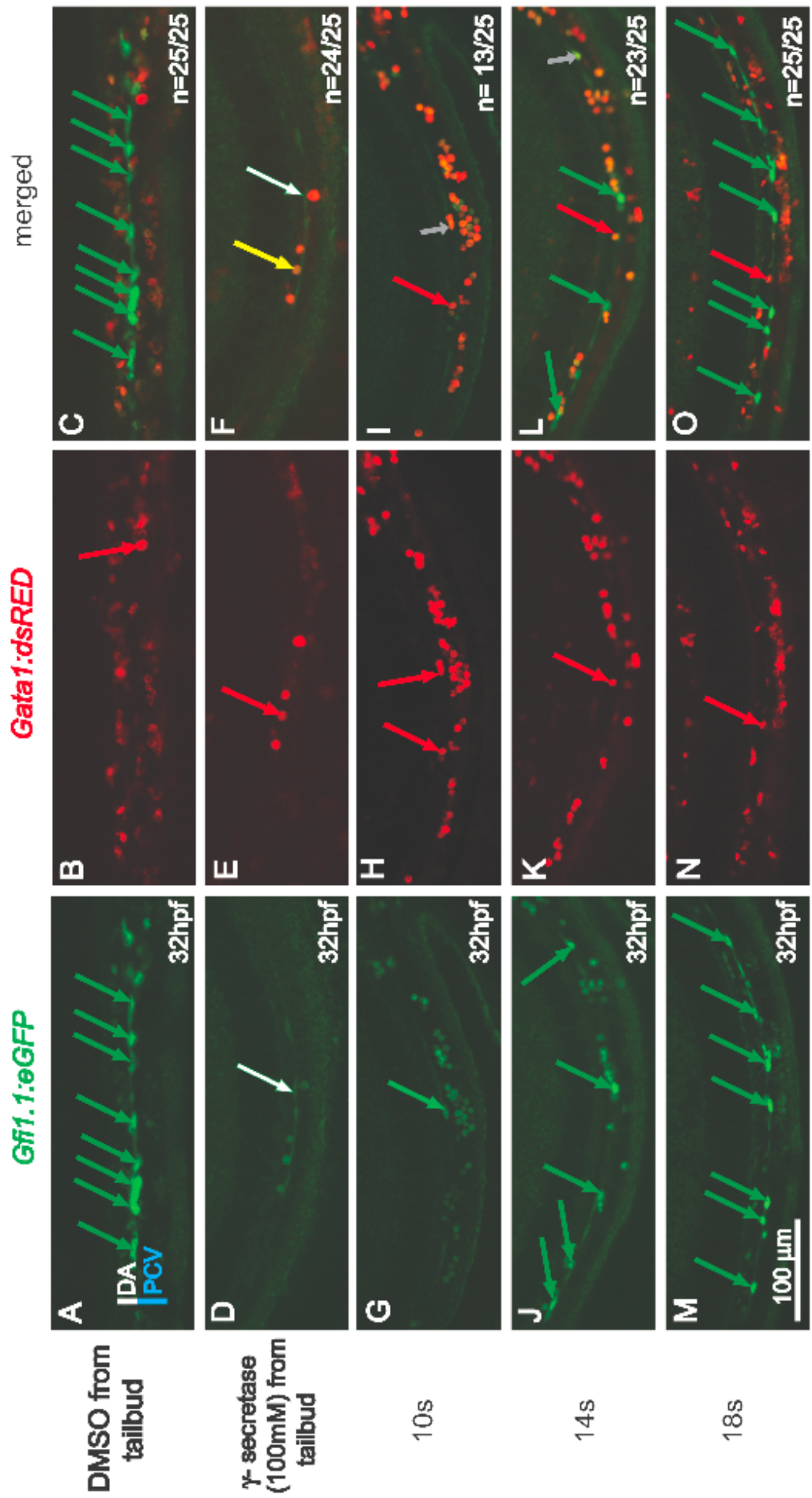


Figure 3.25: DAPM treatment reveals the need for *notch* signalling in HSC formation up until 18 somite stage DAPM treatments was started at tail bud, 10 somite, 14 somite and 18 somite stage, respectively. Embryos were grown to 32 hpf and underwent a double immuno-histochemistry for eGFP and dsRED before being analyzed by confocal microscopy. 7µm optical sections were imaged through the trunk of each embryo. In DMSO treated control embryos, endothelial eGFP expression is clearly visible (A and C, green arrow). DAPM treatment seems to affect the embryos in a time-dependent manner. Embryos treated from tail bud stage, have no endothelial expression of eGFP (D and F, white arrow), whereas the red blood cell expression remains normal (E and F, red and yellow arrow). If the DAPM treatment was started from 10 somites on, then a few endothelial eGFP expressing cell can be observed in 13/25 embryos. The number of endothelial cells expressing eGFP once the DAPM is added at 14 somite stage near to normal in 23/25 embryos (J and I, green arrows). Normal numbers of arterial eGFP expressing cells are present in embryos treated with DAPM from 18 somite stage (M and O, green arrow). DA: dorsal aorta, PCV: posterior cardinal vein.

At 32 hpf, Tg (*Gfi1.1:eGFP;Gata1:dsRED*) double transgenic embryos show high levels of eGFP expression in the ventral wall of the DA. The endothelial cells in the DA are not flat and elongated as observed at 26 hpf, but start to round up as if they were to bud off from the endothelium and reach into the mesenchyme (Figure 3.25, A and C, green arrow). In contrast, embryos treated with DAPM from tail bud stage, lack *gfi1.1* expression in the endothelium (Figure 3.32, D and F, white arrows) in 24/25 embryos. Only double positive erythroid cells are still visible (Figure 3.25 F, yellow arrow). We conclude that *notch* signalling is needed at this developmental stage to generate putative HSCs. We next started the DAPM treatment from 10 somite stage and analyzed the embryos for the presence of Gfi1.1 positive cells in the ventral artery. We could only detect the odd eGFP positive cell in 13/25 embryos (Figure 3.25 G and I, green arrow). This result indicated the need for Notch at 10 somite stage in HSC formation. But if the treatment was induced at 14 somite stage, a considerable number of eGFP positive cells in 23/25 embryos were detected,

although the number seemed less than in untreated embryos (Figure 3.25 J and L, green arrows). The embryos were treated with DAPM starting from the 18 somites stage. Here, the number of eGFP positive endothelial cells was comparable to DMSO treated embryos (Figure 3.25 M and O, green arrows). Endothelial expression is dependent on *notch* signalling until 18 somites. Thus, our data suggest that Notch is needed up to the developmental stage of 14 somites or even 18 somites in order to give rise to HSCs in the ventral wall of the DA.

Summary of chapter 3.7:

- over-expression of *notch* at 16 hpf leads to a expansion of *gfi1.1* positive cells in the ventral wall of the dorsal aorta and into the dorsal vein
- the induced *gfi1.1* positive cells do not express *beta-globin* and are therefore not primitive red blood cells
- the nature of the induced *gfi1.1* positive cells remains unclear
- blocking the *notch* pathway at different time points determines the need for *notch* before the 18 somite stage for *gfi1.1* expression

3.8 *Runx1* and blood circulation are essential for the seeding of the CHT by *gfi1.1* positive cells

3.8.1 In *silent heart* morphant embryos *Gfi1.1:eGFP* positive red blood cells do not switch off the eGFP expression after 30 hpf and the endothelial cells remain flat

The emergence of *runx1*- and *c-myb* positive cells in the DA have been shown to be dependent on blood flow (North et al, 2009). The *silent heart* (*sih*) mutation leads to

the formation of a non-contractile heart and encodes the gene *cardiac troponin T2* (*tnnt2*) (Sehnert et al, 2002, Haftfer et al, 1996). *Si*h mutant embryos never establish blood circulation. In these embryos the formation of HSCs is impaired, but blood flow stimulating small molecules have been shown to rescue the HSC phenotype (North et al, 2009). Here, we aimed to look at the endothelial expression of *gfi1.1* in *si*h morphant embryos in order to see if the endothelial cell expression is negatively affected by the missing blood flow. Thus, we injected 4 ng of the *tnnt2* antisense morpholino (Sehnert et al, 2002) into *Gfi1.1:eGFP* and *gata1:dsRED* double transgenic embryos to address this question.

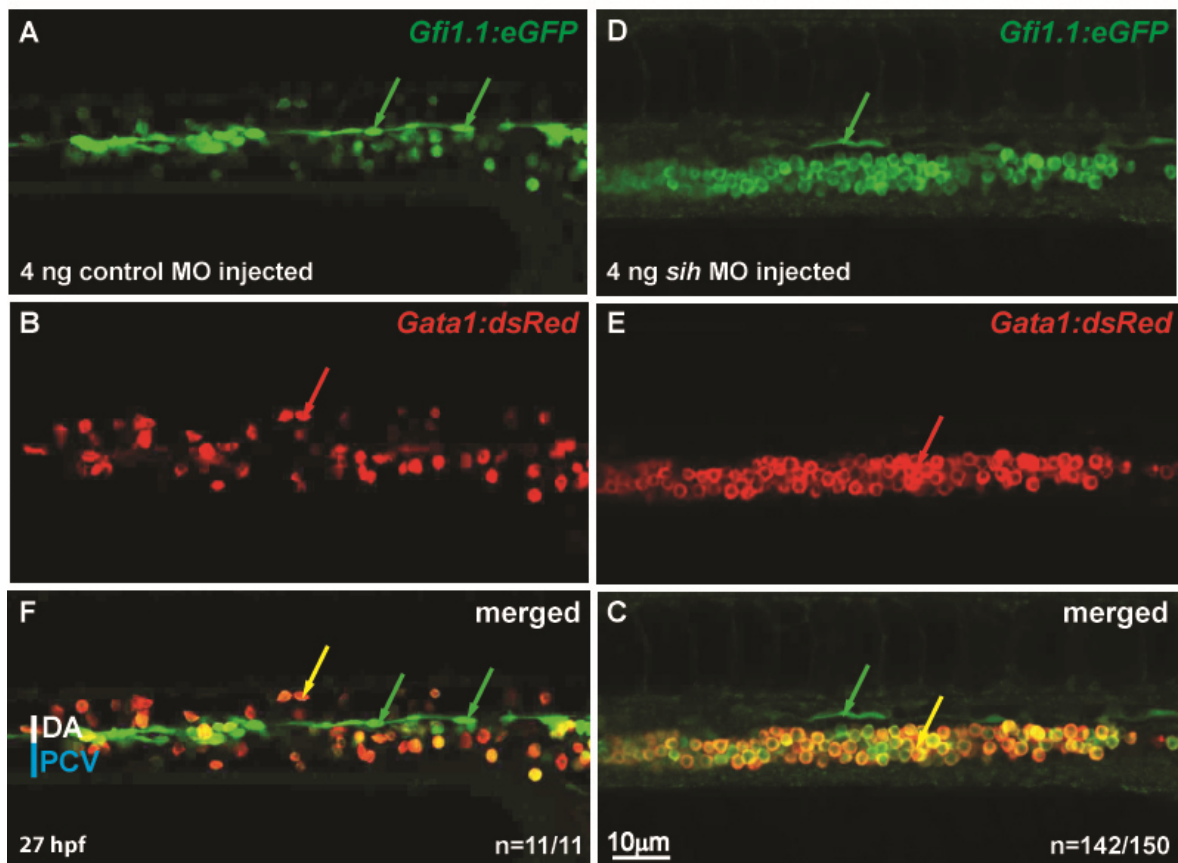


Figure 3.26: The endothelial cells in *Gfi1.1:eGFP* embryos injected with *si*h antisense morpholino remain flat Double transgenic *Gfi1.1:eGFP* and *gata1:dsRED* embryos were injected with 4 ng of *si*h antisense morpholino at one- to four cell stage. The embryos were immuno-stained for eGFP and dsRED at 27 hpf and analyzed using a confocal microscope. 2µm sections were taken through the trunk of the embryo. The control embryos show a

vigorous blood flow and the endothelial expression of *Gfi1.1* is very prominent. The endothelial cells are rounded up (E and F, green arrows). In contrast, *sih* morphants do not establish blood circulation. The red blood cells do not differentiate and *Gfi1.1* expression in these cells remains (B and C, green and yellow, respectively), but the endothelial cells appear flat (A and C, green arrow). DA: dorsal aorta, PCV: posterior cardinal vein.

The analysis of the *sih* morphant *Gfi1.1:eGFP* and *gata1:dsRED* embryos at 27 hpf showed that endothelial *gfi1.1* expression is retained in *sih* morphants. The endothelial cells in *sih* morphants look flat compared to the control embryos (Figure 3.26 A and C, green arrows). This might be due to a need of shear stress through blood circulation, which is needed to induce the budding of HSCs from the haemogenic endothelium. We then analyzed embryos at 50hpf for the presence of *gfi1.1* positive cells in the CHT. We found that no eGFP positive cells had migrated to the CHT in *sih* morphant embryos (Figure 3.27 and supplemental movie 3, I-551/gata1sih50hpf).

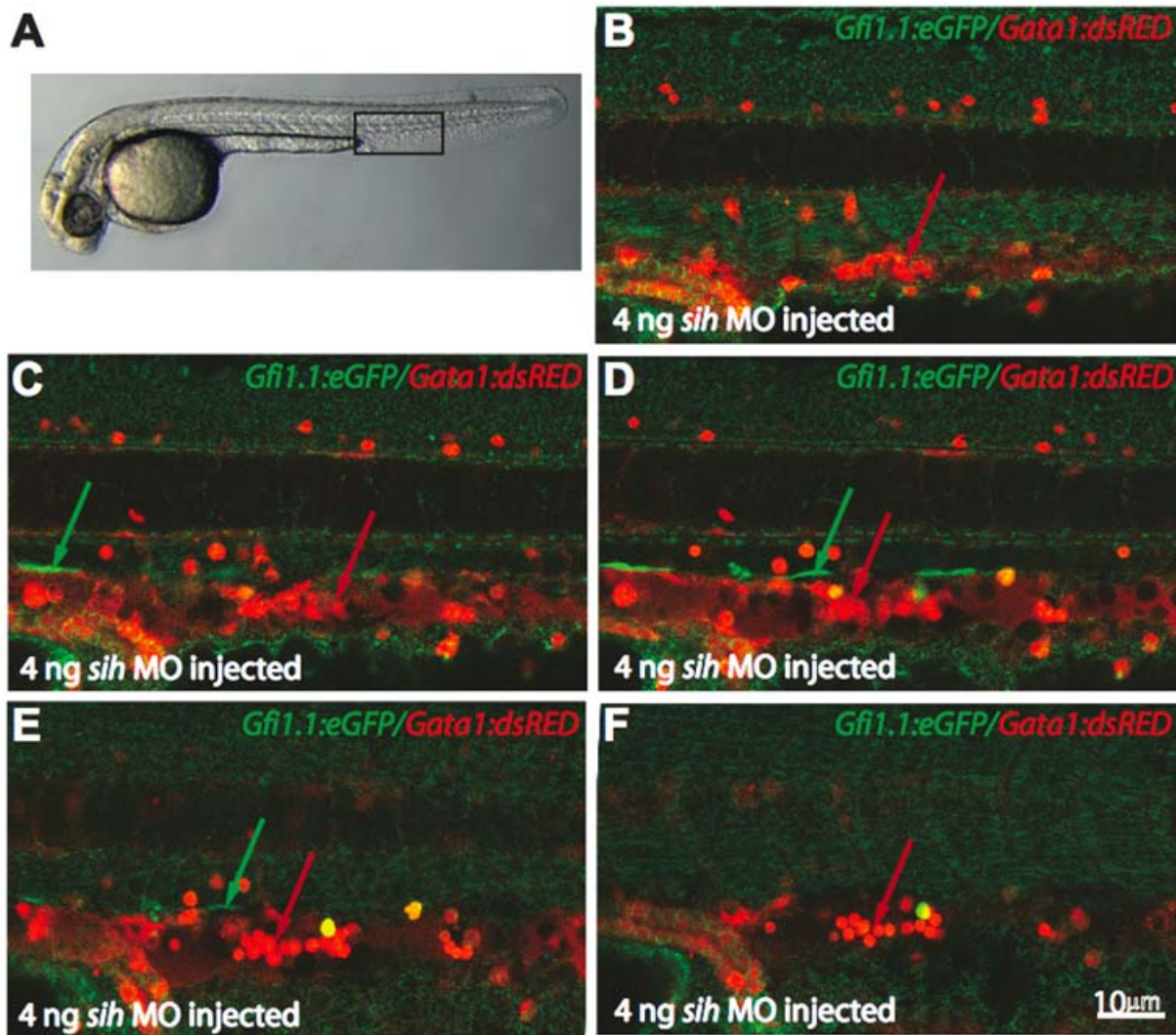


Figure 3.27: Z-stack images reveal the absence of *gfi1.1:eGFP* positive cells in the posterior blood island of *sih* depleted embryo A: whole mount images of a zebrafish embryo depicts the area (boxed region) of the confocal z-stacks. The *Tg(Gfi1.1:eGFP;Gata1:dsRED)* embryo (50 hpf) injected with 4 ng of *sih* MO shown in the images B-F was immuno-stained for eGFP and dsRED. The images show confocal z-stacks taken every 5µm, starting from 2µm in picture B. Fluorescent eGFP expression can be detected within elongated endothelial cells (green arrows), but in the posterior blood island only *Gata1:dsRED* positive cells are visible (red arrows). DA: dorsal aorta, PCV: posterior cardinal vein.

We can conclude that the endothelial expression of *gfi1.1* is dependent on blood flow and retained in *sih* morphant embryos unlike the reduction seen for *runx1* and *c-myb* in *sih* morphant embryos (North et al, 2009), but the cells remain flat and do not move to the CHT.

3.8.2 *Runx1* morphants have no *Gfi1.1* eGFP positive cells in the caudal haematopoietic tissue at 50 hpf

Runx1 is essential for the formation of HSCs. It is believed that *runx1* is responsible for the transition of endothelial cells into HSC progenitors, which then bud off from the ventral artery. In *runx1*-deficient embryos, primitive haematopoiesis occurs normally, but *c-myb* positive cells are absent at 36-40 hpf (Burns et al, 2005) and *rag1* expressing cells are absent at 6dpf (Gering et al, 2005). We investigated the behaviour of *gfi1.1* positive cells in *runx1* morphants. One to four cell stage embryos were injected with 8 ng of *runx1* morpholino and the effects of the knock down on *gfi1.1* eGFP expression in the CHT at 50 hpf was estimated. We hoped to see a decline in the number of *gfi1.1* positive cells in the CHT, which would further prove that these cells are putative HSCs. We therefore utilized *Gfi1.1:eGFP* and *gata1:dsRED* double transgenic embryos for the experiments, which would allow to distinguish between double positive primitive red blood cells and eGFP only endothelial cells and their progeny. Embryos were analysed at 50 hpf after performing immuno-histochemistry for dsRED and eGFP. Series of 2.4 µm optical sections through the whole of CHT of the embryo were taken on a confocal microscope. Using the imaris software, the z-series was then assembled to a 3D image that allowed counting the cells. The number of labelled cells in 4 morphant CHTs was assessed and compared to the numbers found in 4 wild type CHTs.

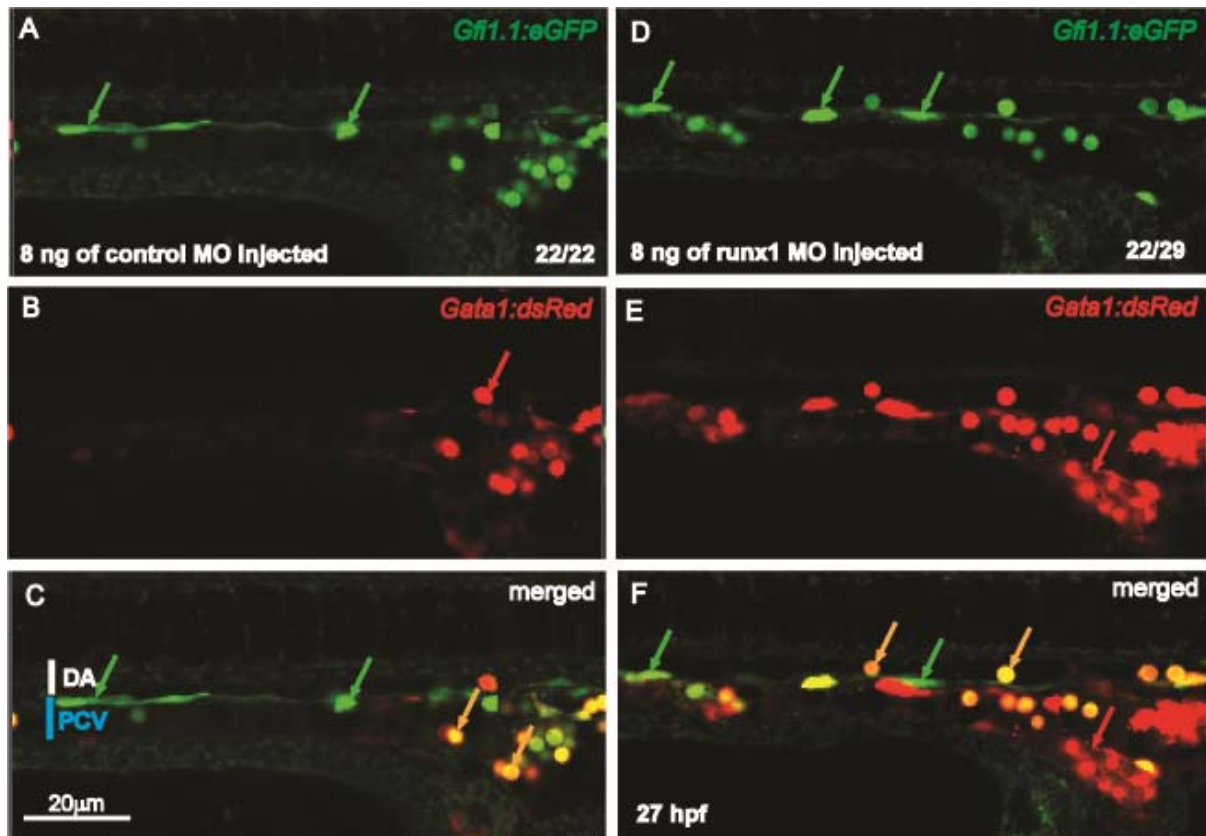


Figure 3.28: *Runx1* MO injection does not abrogate *gfi1.1* expression at 27 hpf. Double transgenic *Tg(gata1:dsRED;Gfi1.1:eGFP)* embryos were injected with 8 ng of *runx1* antisense morpholino at one to four cell stage. In *runx1* deficient embryos *gata1:dsRED* expression remains normal (E and F, red arrows) as in control MO injected embryos (B, red arrow). *Gfi1.1* positive endothelial cells are present in *runx1* MO injected embryos (D and F, green arrows) compared to control MO injected embryos (C, green arrows). Embryos were immuno-stained for eGFP and dsRed and 2.4µm sections were taken through the trunk of the embryo. DA: dorsal aorta, PCV: posterior cardinal vein.

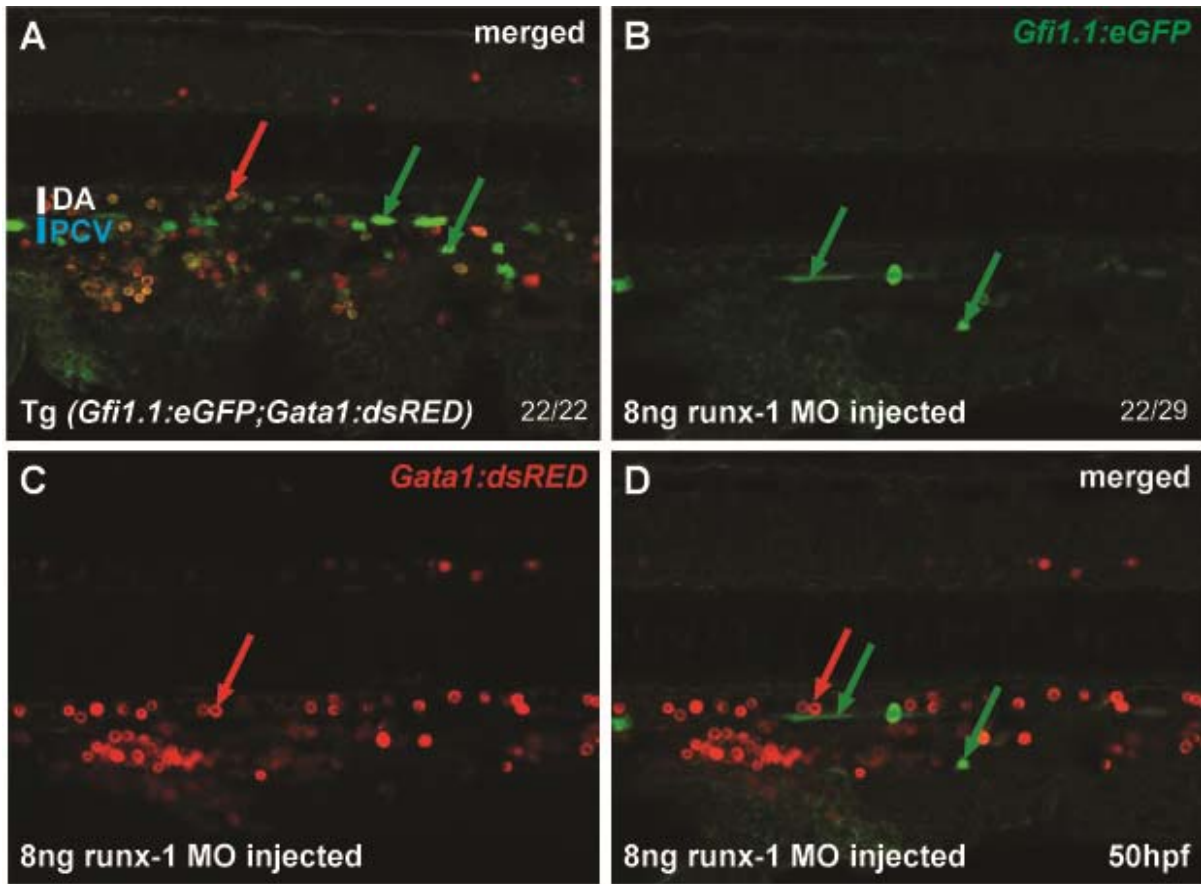
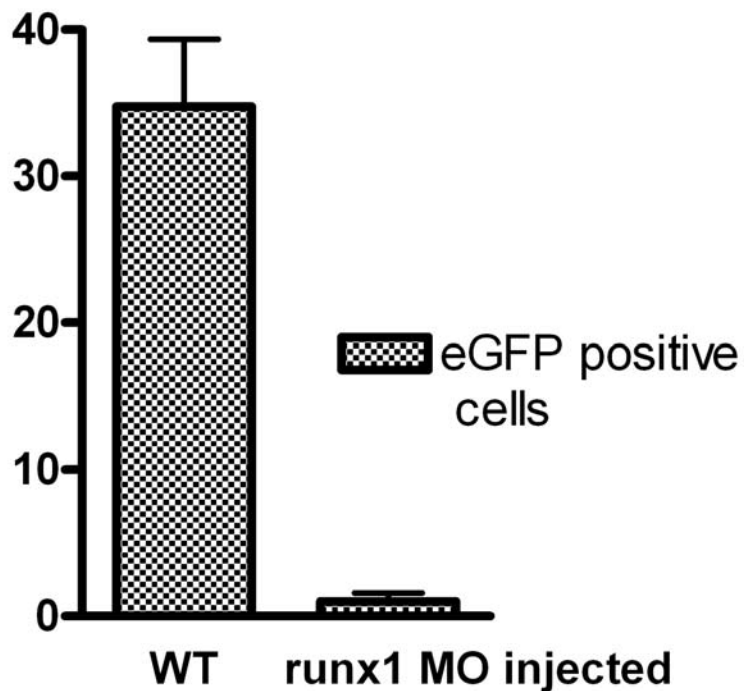


Figure 3.29: The number of *gfi1.1* eGFP positive cells were reduced in the CHT of *runx1* morphants at 50 hpf Double transgenic *gata1:dsRED* and *Gfi1.1:eGFP* embryos were injected with 8 ng of *runx1* antisense morpholino at the one to four cell stage. In *runx1* deficient embryos *gata1:dsRED* expression in the CHT remains normal (A and C, red arrows) in comparison to wild type CHT (D, red arrow). In contrast, *Gfi1.1:eGFP* positive endothelial cells are rare in *runx1* MO injected embryos (B and C, green arrows) compared to wild type (D, green arrows). Embryos were immuno-stained for eGFP and dsRed and 2.4 μ m sections were taken through the trunk of the embryo. DA: dorsal aorta, PCV: posterior cardinal vein.



Graph1: The number of eGFP positive cells in the CHT of *gfi1.1* embryos is significantly lower in *runx1* morphants than in wild type embryos Counting the number of eGFP cells in wild type and *runx1* morphants (n=4) shows a severe reduction in *runx1* morphants. In the wild type CHT, 35 eGFP positive cells were counted on average (left column) whereas in the *runx1* injected embryos, only 2 cells could be found on average (right column). The error bar depicts standard deviation of the mean.

The *runx1* antisense morpholino injected embryos were first examined for *c-myb* expression at 30 hpf (see Figure 4, supplemental data). The loss of the *c-myb* expression in the ventral wall of the DA (Figure 4 supplemental data, B white arrow), verified a specific knock down of the *runx1* transcript in the embryo by injecting 8 ng of the morpholino as reported before (Gering et al, 2005). Since it was difficult to assess the endothelial expression of eGFP in *runx1*-deficient embryos at 27 hpf due to delayed development and normal expression of *gfi1.1* in endothelial cells (Figure 3.28), we decided to look at the presence of *gfi1.1* positive cells in the CHT at 50 hpf when morphants had gained an almost normal blood circulation (Figure 3.29 A, red arrows). We restricted the analysis to *gfi1.1* positive eGFP cells since the number of

red blood cells are very variable in the embryos due to proliferation at this developmental stage. In un-injected embryos, we counted between 35 and 40 eGFP only cells at this time point (Figure 3.29, D, green arrow and Graph 1 left column). But in *runx1* deficient embryos the number of eGFP positive cells was dramatically decreased to only 2 or 3 per embryonic CHT (Figure 3.29, B and C, green arrow, graph 1, right column). We then analysed the data sets derived from the *runx1* morphants and un-injected *Gfi1.1:eGFP* embryos with a Student's T-Test. We obtained a p value of 0.00061965 assuming that the samples were derived from different populations. Therefore we are confident that the observed decrease in eGFP positive cells in *runx1* morphants in the 50hpf CHT is not by chance. We therefore conclude that *gfi1.1* expression in the CHT is dependent on *runx1* earlier on in the ventral wall of the dorsal aorta, just like *c-myb*. As we have evidence that eGFP positive *gfi1.1* cells derived from the ventral wall of the DA move into circulation (see 3.3.15), we can hypothesise that these cells from the artery seed the CHT. This process is known to be dependent on blood circulation (North et al, 2010). But in *runx1* morphants the *gfi1.1* do not appear in the CHT although the blood circulation is intact at 50 hpf. We therefore assume that *runx1* is needed for the budding of the *gfi1.1* positive cells from the endothelium, but the initial *gfi1.1* expression is independent of *runx1*.

Summary of chapter 3.8:

- *runx1* morphants express *gfi1.1* in the ventral wall of the dorsal aorta at 27 hpf
- at 50hpf, the *gfi1.1* positive cells are not present in the CHT of *runx1* deficient embryos

- similarly, in *sih* injected embryos where the blood circulation is impaired, *gfi1.1* positive cells are present in the ventral wall of the dorsal aorta, but do not move to the CHT

3.9 Phosphoinositide 3-kinase pathway is essential for *gfi1.1* positive cell development in the ventral DA

The PI3K and ERK/MAPK pathways have opposing roles in arterial versus venous specification (Hong et al, 2006). The ERK/MAPK signaling acts in arterial cells to promote their identity while PI3K inhibits ERK/MAPK in venous cells and thereby establishes a venous identity (Hong et al, 2006). Inhibition of *PI3K* with chemical inhibitors e.g. LY294002 leads to an activation of the ERK/MAPK in venous cells and expansion of arterial fate (Hong et al, 2006). Since HSC formation is tightly linked to blood vessel development, we intended to investigate if PI3K had a role in the emergence of HSC in the dorsal aorta. Previous work done by master students in the lab demonstrated that PI3K was need for the formation of *runx1* positive cells in zebrafish. Inhibitor treatment starting at different developmental stages revealed that PI3K was essential for *runx1* positive cell emergence from 10 somite (C Rode (2009) and Imran Khan (2008), unpublished data). We therefore aimed to look at *gfi1.1* positive, endothelial cells in LY294002 treated embryos. A loss of these cells would indicate that they are of haematopoietic nature like *runx1* positive cells.

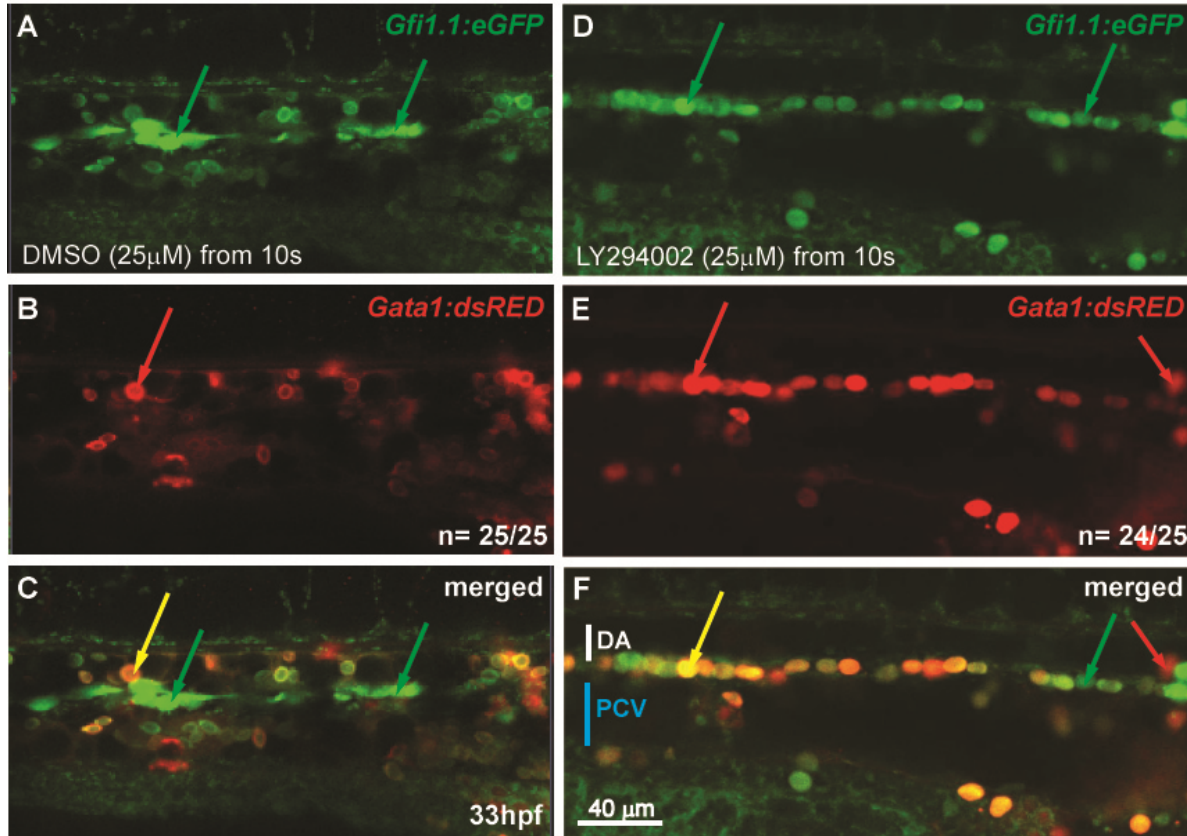


Figure 3.30: *Gfi1.1* positive endothelial cells are lost in LY294002 treated embryos
 Double transgenic *Gfi1.1:eGFP* and *Gata1:dsRED* embryos were treated with 25mM LY294002 inhibitor from 10 somite stage. At 33 hpf the embryos were immuno-stained for eGFP and dsRED and analyzed using confocal microscopy. The image shows is a 22 μm optical section through the trunk of the embryo. In DMSO treated embryos, *Gfi1.1:eGFP* expression is visible in primitive red blood cells and endothelial cells in the dorsal aorta (D and F green arrow, respectively). *Gata1* expression is restricted to erythroid cells (E, red arrows). Primitive red blood cells are positive for both transgenes and are visible as yellow cells (F, yellow arrow). *Gfi1.1* erythroid and *Gata1* positive cells are visible in the midline of the inhibitor treated embryos (A, B and C, yellow arrow). There are only a few cells, which express either *gata1* (B and C, red arrow) or *Gfi1.1* (A and C, green arrow). DA: dorsal aorta, PCV: posterior cardinal vein.

DMSO treated control *Gfi1.1:eGFP* and *Gata1:dsRED* double transgenic embryos showed vigorous blood flow through the blood vessels and detectable eGFP staining in the ventral wall of the DA at 33 hpf (Figure 3.30 D and E, green arrows). Since the primitive red blood cell expression of the *Gfi1.1:eGFP* reporter is reduced after 30

hpf, most erythroid cells appear as red *gata1* positive cells (Figure 3.30 E, red arrow).

In embryos treated with 25mM of LY294002 from 10 somite stage, the blood flow is reduced. Most of the labelled cells in the trunk of the double transgenics express both fluorescent markers (Figure 3.30 C, yellow arrow) and have a round shape. They therefore represent primitive red blood cells, although they appear to be located in the ventral wall of the DA (Figure 3.30 C yellow arrow). LY 294002 treatment on *Flk1:eGFP* and *gata1:dsRED* double transgenic embryos confirmed that the *gata1* positive cells are not *flk1* positive and are simply stuck between the blood vessels (Supplemental Figure 5, D and F, red and green arrows).

There are only a few cells in Tg (*Gfi1.1:eGFP;Gata1:dsRED*) embryos treated with Ly294002, which express either the green or the red fluorescent protein, respectively and none of them has a spindle shape, characteristic for endothelial cells (Figure 3.30 A, B and C, green and red arrows). We therefore concluded that the eGFP expression in the spindle shaped endothelial cells is lost due to the inhibitor treatment.

Summary of chapter 3.9:

- Ly 294002 treatment is known to inhibit the emergence of *runx1* and *c-myb* positive cells from the haemogenic endothelium
- Here, we show the *gfi1.1* expression is also lost specifically in the ventral wall of the dorsal aorta when treated with Ly294002

3.10 *Gfi1.1* positive cells detach from the haemogenic endothelium and join the blood circulation

In order to investigate if we can see the *gfi1.1* positive cells leaving the endothelium as described by Kissa et al, 2008; Lam et al, 2009 and Bertrand et al, 2010, we decided to take time-lapse images of *Gfi1.1:eGFP* and *gata1:dsred* double transgenic embryos (see also supplemental data, *I-551:eGFP; gata1:dsRed* 37 hpf time-lapse movie). At 37 hpf we observed a number of eGFP positive cells rounding up in the ventral wall of the dorsal aorta (Figure 3.31 a). After 15 minutes one of these cells seems to divide (Figure 3.31 b) and give rise to a daughter cell (Figure 3.31 c). The daughter cell is fully detached from the progenitor by 45 minutes (Figure 3.31 d) and starts to move dorso-laterally into the mesenchyme below the DA (Figure 3.31 e-g).

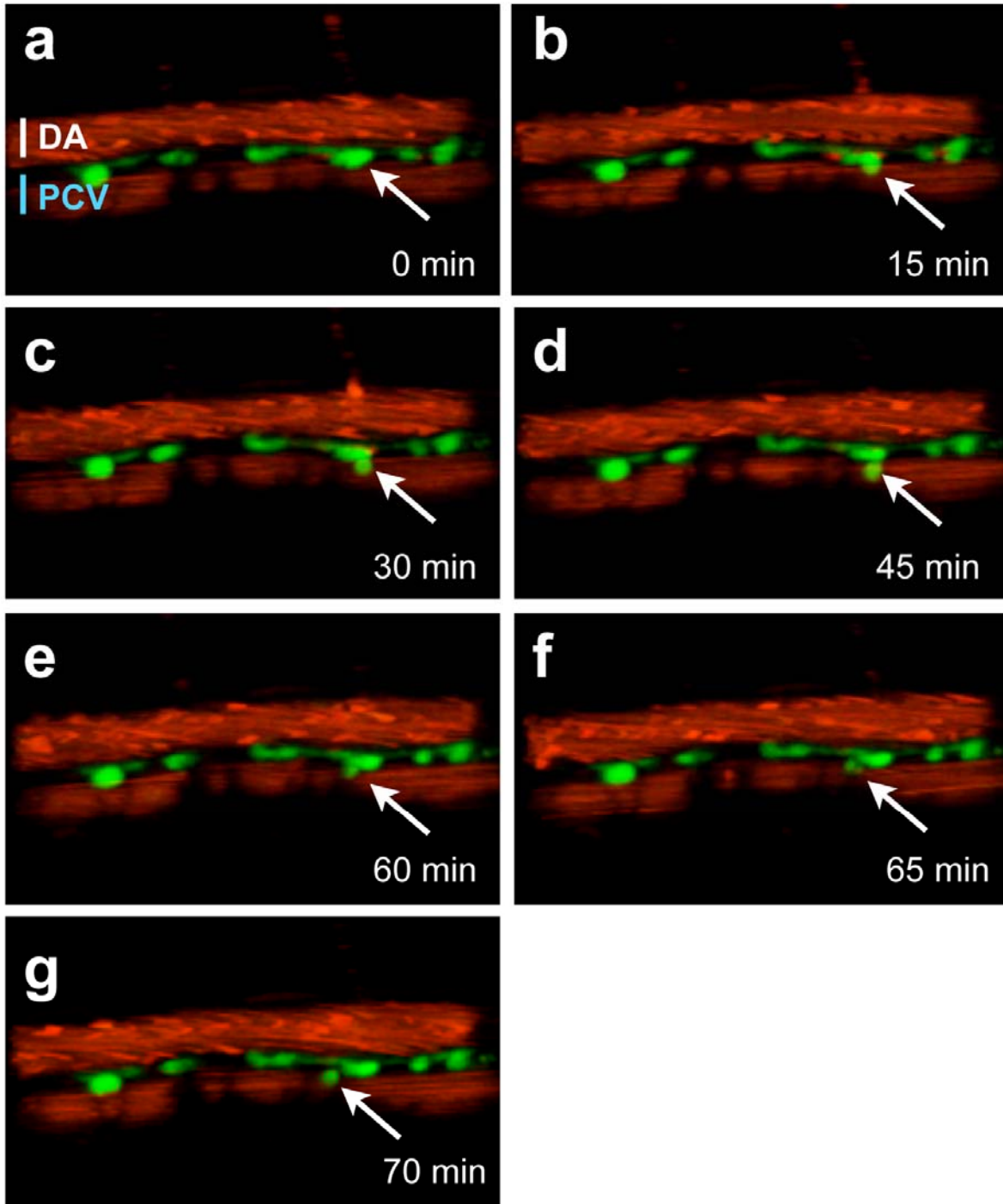


Figure 3.31: A *Gfi1.1:eGFP* positive cell leaves the haemogenic endothelium A double transgenic embryo for *Gfi1.1:eGFP* and *gata1:dsRED* is imaged over 75 minutes using a confocal laser scanning microscope in order to image the behaviour of *gfi1.1* positive cells over time. In the first image, the shape of the *gfi1.1* (white arrow) is still spherical, but rounding up already (a). In the following image, the endothelial cell seems to divide and give rise to a daughter cell (white arrow) (b). The round daughter cell is now detached from the mother cells (white arrow) (c). The daughter cell remains is still located close to the ventral

wall (white arrow) (e). The round cell now moves rostral and towards the vein of the embryo (f and g). (Images composed by M Gering). DA: dorsal aorta, PCV: posterior cardinal vein.

We made similar observations in Tg (*Gfi1.1:eGFP; Flk1:tomato*) embryos at 33 hpf (see supplemental data, *Flk1:tomato;Gfi1.1:eGFP* 33 hpf time-lapse). We documented how a *gfi1.1* positive cell, which is located in the ventral wall of the dorsal aorta, gives rise to another cell. This newly born cell buds into the lumen of the DA before it finds an exit place through the endothelium of the ventral DA in order to join the blood circulation. We therefore conclude that our *gfi1.1* positive cells behave like the *runx1* and *c-myb* positive cells. In addition, we have found a new behaviour of these cells. The observations we made with the Tg (*Gfi1.1:eGFP;Flk1:tomato*) whereby the eGFP positive cell first buds into the lumen of the DA has not been described before in zebrafish. It will be interesting to investigate if this behaviour is common to nascent HSC in zebrafish.

Summary of chapter 3.10:

- *Gfi1.1* positive cells are imaged while detaching from ventral wall of the dorsal aorta

3.11 *Gfi1.1* positive cells are found in the kidney of adult fish

The *Gfi1.1:eGFP* transgenic line and *in situ* hybridisations for *gfi1.1* have demonstrated that *gfi1.1* is expressed in the kidney of the 5 day old larvae. In order to investigate if *gfi1.1* positive cells are present in the adult fish kidney, flow cytometry was performed. The presence of *gfi1.1* positive cells in the kidney would indicate that

gfi1.1 expression is retained in adult haematopoietic cells. We isolated whole kidney marrow from adult Tg (*Gfi1.1:eGFP*;*Gata1:dsRED*) fish and analyzed the disassociated cells by flow cytometry.

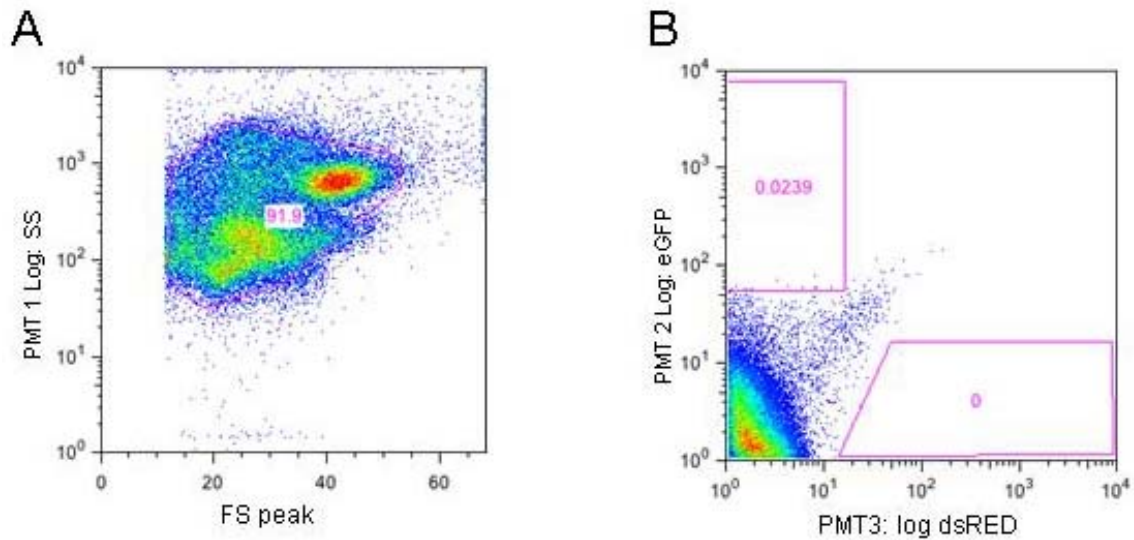


Figure 3.32a: Light scatter view of Tg(*Gfi1.1:eGFP*;*Gata1:dsRED*) WKM and fluorescent view of wild-type WKM The left plot depicts the WKM in a light scatter view. The right plot depicts the WKM of a wild type non-fluorescent fish used for gating.

Whole kidney marrow extracts from *Gfi1.1:eGFP/Gata1:dsRED* animals

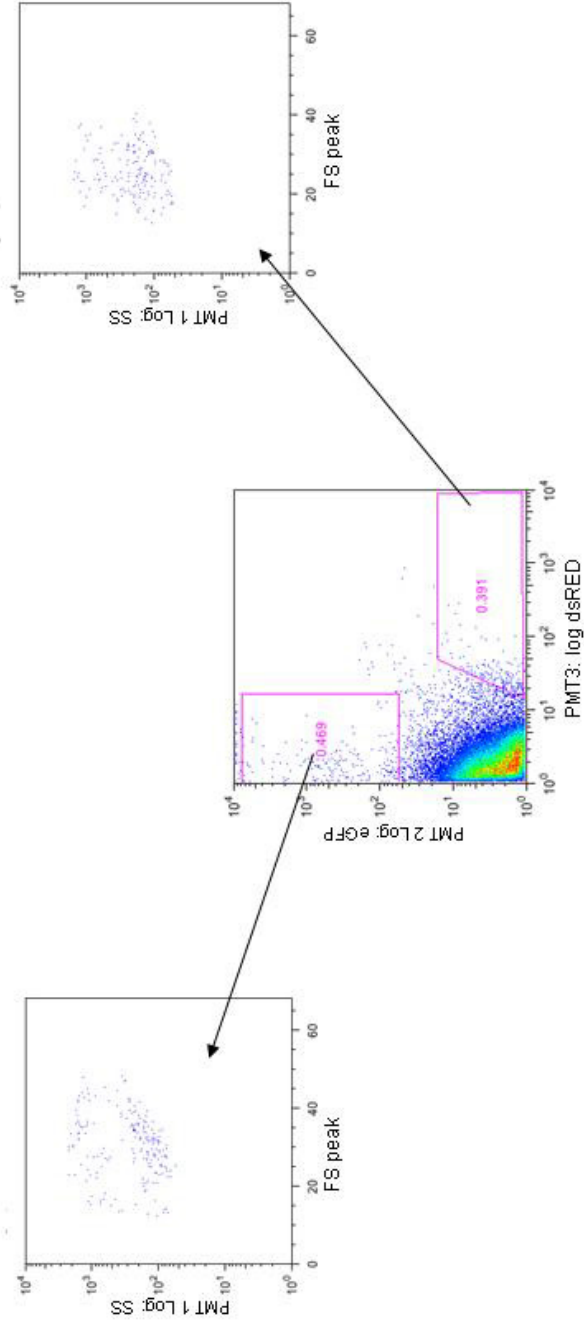


Figure 3.32b: *Gfi1.1:eGFP* positive cells are present in the WKM of adult *Tg(Gfi1.1:eGFP;Gata1:dsRED)* fish We analysed the WKM cells of *Tg (Gfi1.1:eGFP;Gata1:dsRED)* in adult fish. The FACS plot on the left shows the presence of an eGFP-only cell population and a dsRED-only cell population in the WKM. The analysis of these cells in the FS/SS profile shows that the eGFP positive cells have a diverse cell size and granularity whereas the dsRED cells are more clustered together. The gates used for this analysis are depicted in Figure 3.32a.

Genotype of whole kidney marrow extract	Percentage of cells	Cell count
Wilde type • live cells • <i>gata1</i> positive • <i>Gfi1.1</i>	- 91.1 0 0.0239	50000 45939 0 11
<i>Gfi1.1:eGFP/Gata1:dsRED</i> • live cells • <i>gata1</i> positive • <i>Gfi1.1</i>	- 84.9 0.391 0.469	50000 42450 166 199

Table 3.3: Cell count of whole kidney marrow extracts The table summarizes the percentage and number of cells of each cell population found in wild type and *Tg(Gfi1.1:eGFP;Gata1:dsRED)* whole kidney marrow.

Preliminary data suggest that eGFP expressing cells are present in the WKM (Figure 3.32b, table 3.3). These cells show a diverse FS/SS profile (Figure 3.32b). We can only assume that they include HSCs and haematopoietic progenitors based on their presence in the kidney. We also detected a dsRED only population in the kidney (Figure 3.32b, table 3.3). These cells are most likely to represent erythroid progenitors.

Summary of chapter 3.11:

- Flow cytometrical analysis of adult kidney marrow from *Gfi1.1:eGFP* and *Gata1:dsRED* double transgenic embryos suggest the presence of *gfi1.1* positive cells in the kidney of adult fish
- This result suggests that *gfi1.1* is also expressed in adult haematopoietic stem cells

3.12 Zebrafish *gfi1.1* is a homolog of the mouse *Gfi1*

There are two homologs of *Gfi1* in the mouse, *Gfi1* and *Gfi1b*. Both genes are expressed in haematopoietic cells. *Gfi1* is expressed in granulocytes and activated macrophages (Hock et al, 2003). In contrast, *Gfi1b* is enriched in erythroid precursors and megakaryocytes (Saleque et al, 2002). *Gfi1* is also expressed in thymic T-cells (Yucel et al, 2003).

Both genes are reported to be active in HSCs. In *Gfi1*^{-/-} mice, HSCs undergo excessive proliferation and in turn lose their self-renewal properties (Hock et al, 2004; Zheng et al, 2004). Subsequently, their long-term engraftment potential in the bone marrow is affected. *Gfi1b* is needed intrinsically to regulate dormancy and the release of the HSCs into the peripheral blood (Khandanpour et al, 2010). It is thought that the elevated number of HSCs seen in the blood is due to reduced expression of cell adhesion proteins (Khandanpour et al, 2010). There are no reports for *Gfi1b* outside the haematopoietic system. *Gfi1* on the contrary, is expressed in a variety of tissues. These tissues include the intestinal epithelium (Shroyer et al, 2005), the pulmonary neuroendocrine cells in the lung (Ito et al, 1999), the ganglion cells in the retina (Yang et al, 2003) and the inner ear hair cells (Wallis et al, 2003).

Little is known about the *gfi* genes in zebrafish. The first publication about *gfi1* (*gfi1.2*) in zebrafish describes its expression in the otic placode, in the ganglion cells of the retina, the neuromasts of the lateral line organ and in the parapineal organ (Dufourcq et al, 2004). Dufourcq et al describe *gfi1* expression in some cells in the DA at 2 dpf, but they are unsure about the nature of these cells. A further homolog of the zebrafish *gfi1* was published recently. An enhancer trap screen resulted in a transgenic line with eGFP expression in primitive red blood cells. The enhancer trap was found to have inserted near the *gfi1.1* gene (Wei et al, 2008). Their insertion was

mapped to 20 kb upstream of the transcription start site. Morpholino experiments suggest a role for *gfi1.1* in erythroid differentiation and suppression of the myeloid lineage (Wei et al, 2008). Their transgenic embryos only express eGFP in primitive red blood cells. The gene has not been reported to be expressed in definitive haematopoietic cells in zebrafish.

3.12.1 Identification of the novel gene *gfi1b-like* in zebrafish

It was unclear if the *gfi1.1* was an ortholog of the mouse *Gfi1* or *Gfi1b* since the erythroid expression is restricted to the mouse *Gfi1b* and not *Gfi1* (Saleque et al, 2002). We intended to examine the relationship of *gfi1.1* to the other *Gfi1* genes. We first looked for further *gfi1* homologs in the zebrafish genome. A amino acid blast search of the zebrafish genome (Zv8, August 2010) with the mouse GFI1B protein sequence revealed the existence of a third *gfi1* homolog. The newly identified transcript showed a 44% similarity at the C-terminus to the mouse GFI1B (Figure 3.33a). This is the region where the zinc-finger repeats are located. A closer look at the genomic region revealed the existence of two predicted transcripts, si:ch211-231o62 and LOC100151531 (Figure 3.33b). The transcripts are verified in cDNA and EST libraries (Figure 3.33b). The latter transcript is predicted to include one more exon than si:211-231o62 (Figure 3.33b). Since the additional exon in LOC100151531 is also present in the *gfi1b* transcript, we chose to analyze the longer LOC100151531 closer (Figure 3.33b). The transcript was named *gfi1b-like*.

```

Query location      : unnamed                      97 to      355 (+)
Database location  : ENSDARP00000012222          560 to      806 (+)
Genomic location   : 4                          37390045 to 37402155 (+)

Alignment score    : 538
E-value           : 1.8e-43
Alignment length   : 260
Percentage identity: 33.85

Query: 97  EPPPEYKPSFSMDTLASSYSHSYTQTP-STMQSAFLERSVRLYGSPLVPSTESPLDFRLR 155
          E PP YK S  D  +  +  TQ  T  +  +  S  G  L  +++S L  LR
Sbjct: 560 EKPP-YKCSHC-SKRFNQLTDLKTQKRINTGEEKPY---SCTQCGKSL--ASKSKLKIHLA 612

Query: 156 YSPGMDTYHCVKCKNKVFPSTPHGLEVHVRRSHSGTRPFACDVCGKTFPGHAVSLEQHTHVHS 215
          G  + C +C K F S  L  H+  H+G RPF C  CGK+F  +  S  QH  +H+
Sbjct: 613 IHTGEEKPFTCTQCGKSFSHSEANLNQHMII-IHTGERPFMCTPCGKSFSQLSSFNQHMRIHT 671

Query: 216 QGVPAQSSPTPTLAVXXXXXXXXXXXXXXXXXRFLRQERSFECRMCGKAFKXXXXXXXXXXXXX 275
          G  P  R  E+ F C  CGK+F
Sbjct: 672 -----GEEKPFSCTQCGKSFSQSSNLNLHMRIHTGEEKPFTCTQCGKSFSHSSNLNQHMMI 726

Query: 276 XDTRPYPCQFCGKRFRHQKSEMKKHTYIHTGEXPHKQVCGKAFPSQSSNLITHSRKHTGFK 335
          +P+ C  CGK F Q S  + +H  IHTGEEKP  C  CGK+FS+SS+L  H  +  HTG  K
Sbjct: 727 TGEKPFPTCTQCGKSFSQSSSLNQHMMIHTGEXPFPTCTQCGKSFSKSSSLYRHMXIHTGKX 786

Query: 336 PFSCELCYNGFQRKVDLRMH 355
          PF+C  C K F  L  RH
Sbjct: 787 PFTCPQCGKSFSLSLSSLYRH 806

```

Figure 3.33a: A zebrafish locus on Chromosome 21 has a high similarity with the mouse GFI1B The mouse GFI1B protein sequence was compared to the zebrafish genome (Zv8, August 2010). The alignment shows a high correlation between C-termini of the mouse GFI1B and a protein encoded by the novel transcript found in zebrafish.

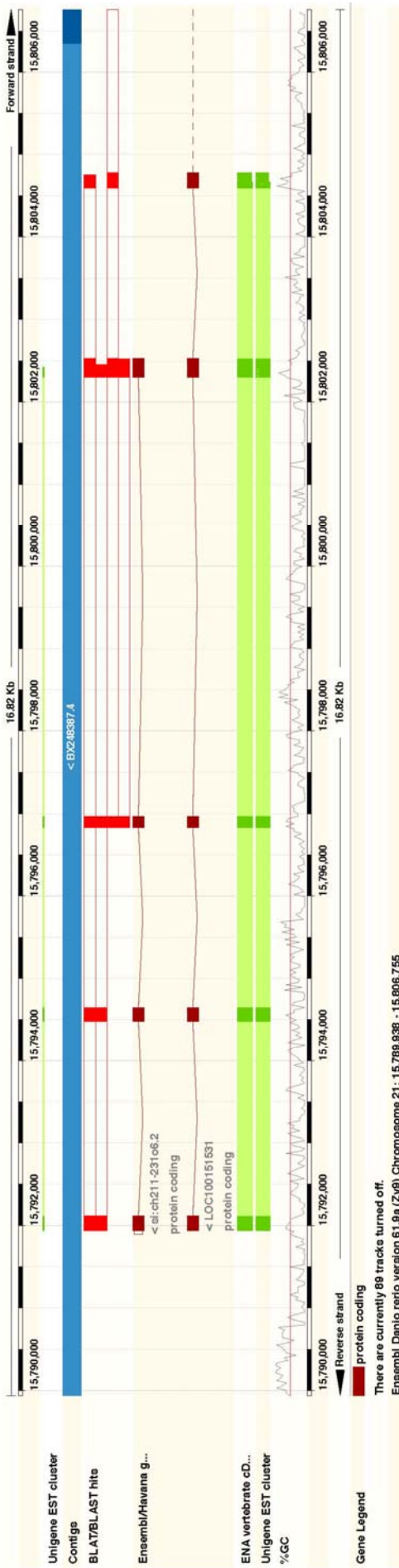


Figure 3.33 b: LOC100151531 encodes a uncharacterised protein in zebrafish The diagram depicts the region on chromosome 21 in the zebrafish genome hit by the blast search with the mouse GF1B (red boxes). The locus is in contig BX248387.4 and there are two predicted transcripts by ensemble and Havana (brown shaded boxes) in that region. Furthermore, the existence of these transcripts is supported by cDNA and EST libraries (bottom panel, green boxes). Of these two transcripts, LOC100151531 is the longer one, with one more exon than si:ch211-23106.2 (brown boxes).

3.12.2 The novel transcript *gfi1b-like* is an ortholog of the murine *Gfi1b* gene

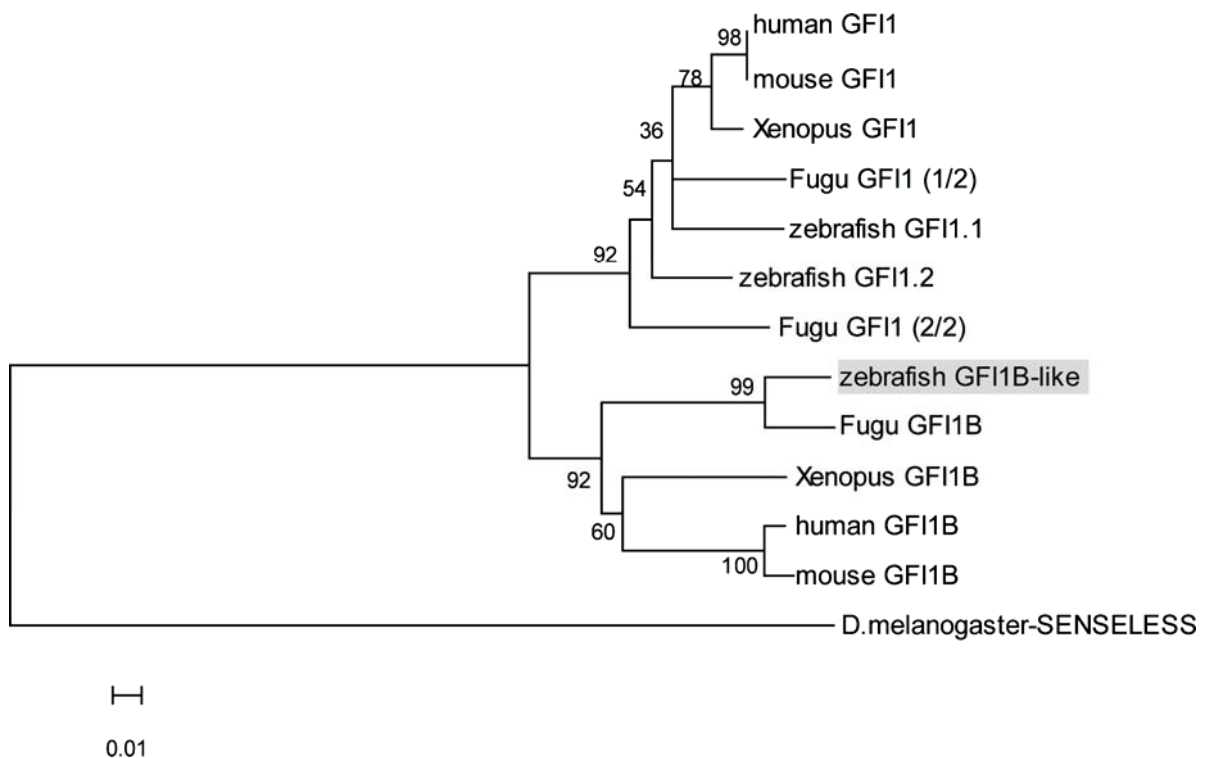


Figure 3.34: Evolutionary relationships of the zebrafish GF11.1, GF11.2 and GF1B-like (LOC100151531) The phylogenetic tree shows the relationship between the GFIs in *D. melanogaster*, *xenopus*, *Fugu*, zebrafish, mouse and human. The SENSELESS protein is the out-group for this analysis. The analysis was conducted using MEGA4.

The phylogenetic tree in Figure 3.25 shows the relationship of the GFIs. The evolutionary history was inferred using the Neighbour-Joining method (Saitou et al, 1987). The bootstrap consensus tree inferred from 1000 replicates is taken to represent the evolutionary history of the taxa analyzed. Branches corresponding to partitions reproduced in less than 50% bootstrap replicates are collapsed. The percentage of replicate trees in which the associated taxa clustered together in the bootstrap test (1000 replicates) are shown next to the branches. The tree is drawn to scale, with branch lengths in the same units as those of the evolutionary distances used to infer the phylogenetic tree. The evolutionary distances were computed using the Poisson

correction method and are in the units of the number of amino acid substitutions per site. All positions containing gaps and missing data were eliminated from the dataset (Complete deletion option). There were a total of 176 positions in the final dataset. We choose to build the tree with an invertebrate as the out-group and to include xenopus, fugu, mouse and human in the analysis (see supplemental figure 2 for the original sequence files). The Drosophila homolog SENSELESS was used as an out-group (Figure 3.15). The tree splits up into two major groups with 92% confidence. There is the group of GFI1, where the zebrafish GFI1.1 and GFI1.2 fall into (with 36% and 54% confidence, respectively) (Figure 3.34). This indicates that these are true homolog of the mouse and human GFI1 (fidelity of 98%). The newly found GFI1B-LIKE (LOC100151531) is related to the mouse and human GFI1B with 92% fidelity (Figure 3.34). These results mean that we have found a yet uncharacterized homolog of GFI1B in fish and very recently, the transcript LOC100151531 has been annotated in the ensemble database (Zv9, Nov 2010) as *gfi1b*. Both of the Gfis, GFI1.1 and GFI1.2 are more similar to the mouse GFI 1 than to GFI1B.

Summary of chapter 3.12:

- *Gfi1.1* was verified as a homolog of the mouse *Gfi1*
- A novel *gfi1b-like* was identified in the zebrafish genome

3.13 The expression patterns of GFIs during zebrafish development

Since the zebrafish GFI1.1 is also expressed in erythroid cells unlike its mouse homolog, we wanted to investigate, if there are differences in the expression patterns between mouse and zebrafish.

In order to investigate the expression pattern for these genes, whole mount *in situ* hybridisations were performed for each of these genes.

3.13.1 The mRNA expression pattern of *gfi1.1* is similar to the expression of eGFP in *gfi1.1:eGFP* transgenics

Figure 3.26 shows the expression pattern of the *gfi1.1* mRNA transcript. The expression starts at 3-4 somites in the posterior lateral mesoderm (Figure 3.126, A red arrow) as described before (Thisse et al, 2004). As the posterior lateral plate mesoderm coalesces to form the ICM, the expression in the cells remains (Figure 3.35, B red arrow). A sense probe against the *gfi1.1* transcript was used as a negative control. In these embryos, no expression was detected (Figure 3.35, C, dotted red arrow). This observation proves the specificity of the anti-sense probe. With the onset of vasculogenesis the *gfi1.1* expression levels decrease in the trunk (Figure 3.36, A red arrow). Only a few cells are positive for *gfi1.1* at 21 hpf, which is consistent with earlier findings by Wei et al (Wei et al, 2004).

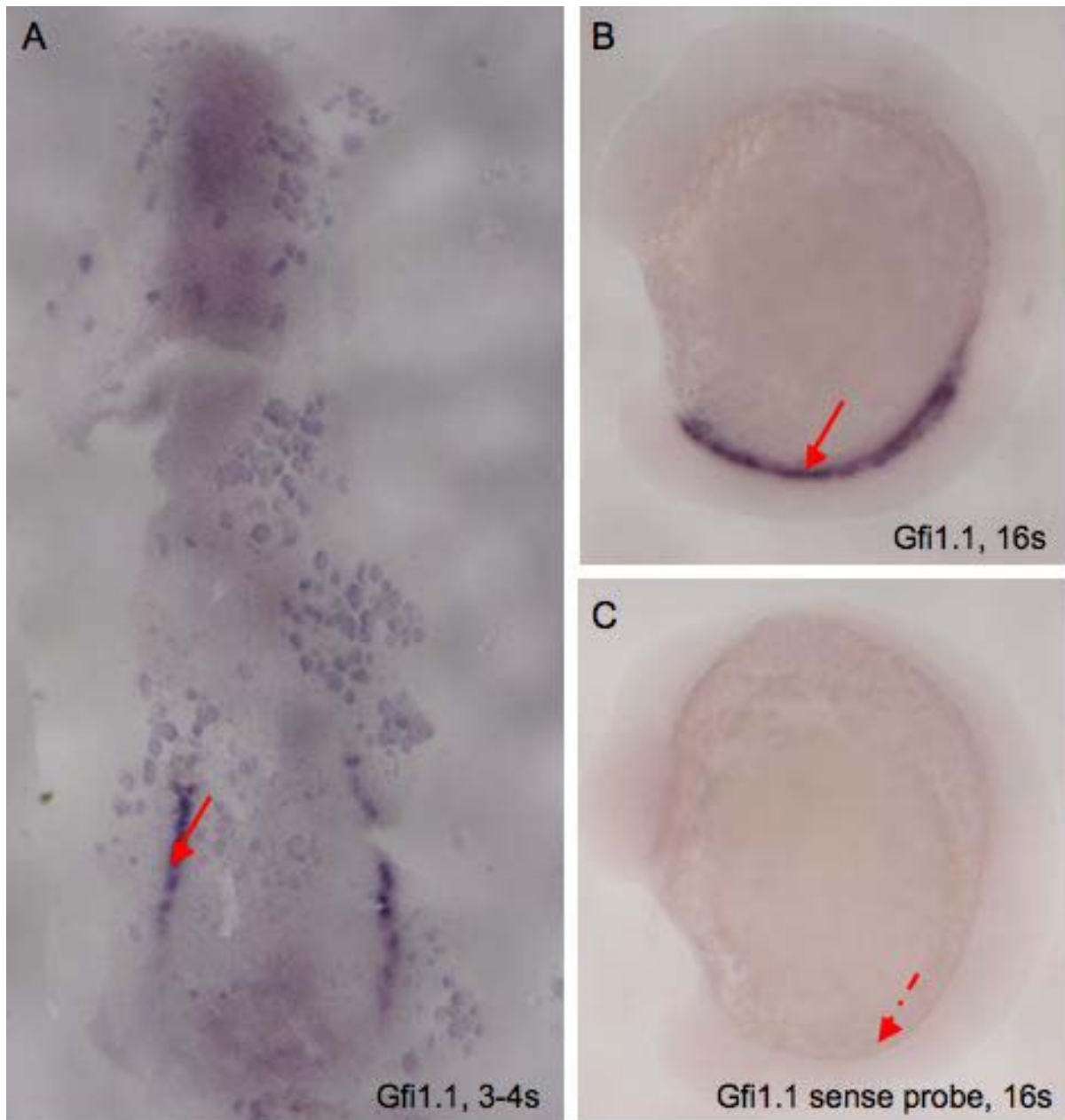


Figure 3.35: Early expression pattern of *gfi1.1* in the zebrafish embryo First expression of *gfi1.1* can be detected by *in situ* hybridisation in the posterior lateral mesoderm at 3-4 somite stage (A, red arrow); *gfi1.1* positive cells are visible in the forming ICM at 16 somite stage (B, red arrow); C shows the sense probe for *gfi1.1* for the experiment.

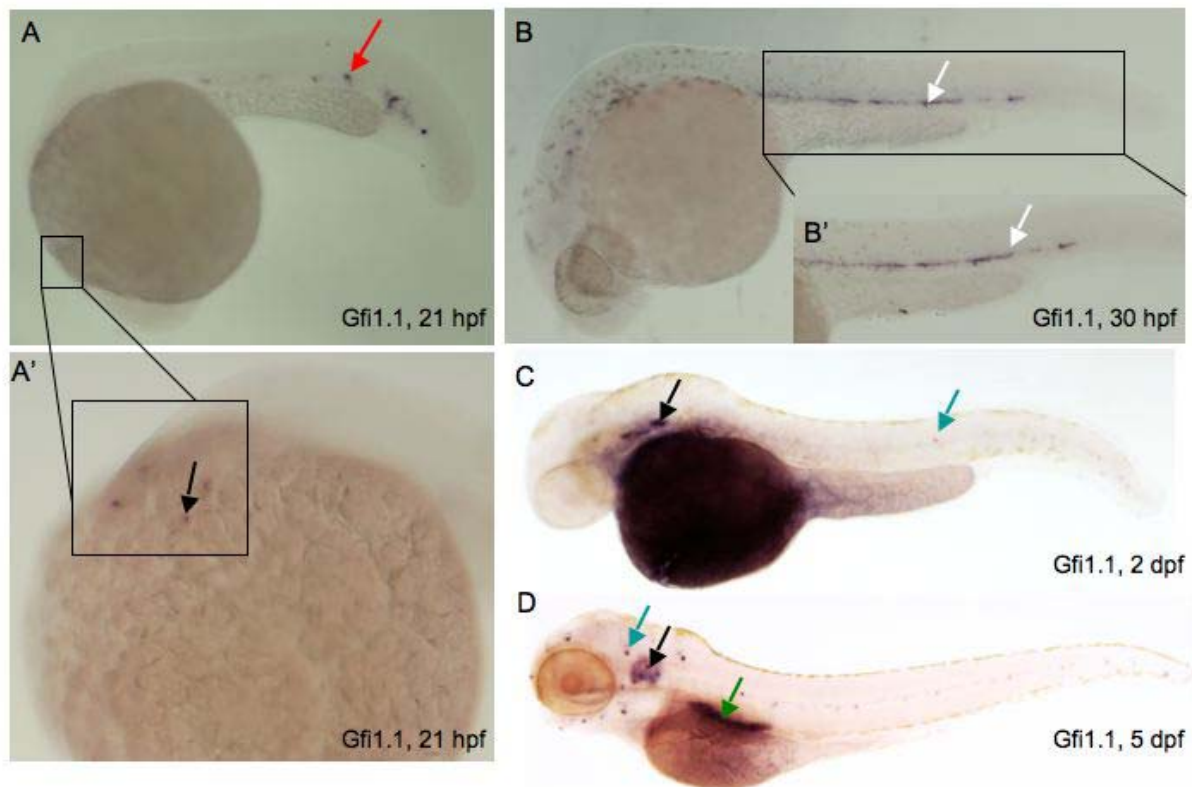


Figure 3.36: *Gfi1.1* is expressed in the artery at 30 hpf At 21 hpf, *gfi1.1* expression is scattered along trunk (A, red arrow) and is also present in the otic vesicle (A', black arrow). The expression in the artery can be observed at 30 hpf (B and B', white arrow). At day 2, the embryos show staining in the otic vesicle (C, black arrow) and the neuromast of the lateral line organ (C, blue arrow). The expression level in the lateral line organ is more prominent at day 5 (D, blue arrow) whereas the otic staining is stable (D, black arrow).

But the expression in the midline soon starts to be confined to the artery (Figure 3.36, B and B', red arrow) as reported before (Thisse et al, 2004). There is no staining in the primitive red blood cells at 30 hpf as seen in the *Gfi1.1:eGFP* transgenic embryos. The *gfi1.1* mRNA transcript can be detected in the otic vesicle starting from 21 hpf (Figure 3.36, A' black arrow) and is visible at 2 and 5 dpf (Figure 3.36 C and D, black arrow). We have not been able to locate eGFP expression in the otic vesicle in the *Gfi1.1:eGFP* transgenics at 21 hpf. We interpret the staining in the lateral head region as staining in thymic cells (Figure 3.36). At 2 dpf, the neuromasts of the lateral line organ begin to produce *gfi1.1* mRNA (Figure 3.27, C and D, blue arrow), which is

consistent with earlier findings (Thisse et al, 2004). The expression in the lateral line is stronger at 5 dpf (Figure 3.36, D blue arrow). The additional expression in the spleen and intestinal cells observed in *Gfi1.1:eGFP* embryos could not be confirmed by *in situ* experiments for *gfi1.1* in wild type embryos.

3.13.2 The mRNA expression profile of *gfi1.2* throughout development reveals expression in the ventral wall of the dorsal aorta at 2 dpf

Next, the expression pattern of *gfi1.2* was examined by *in situ* hybridisation. *Gfi1.2* is known to be expressed in the developing inner hair cells, the lateral line organ and in the parapineal organ (Duforcq et al, 2004). We detected the first expression in the inner ear hair cells at 18 hpf (Figure 3.37, A, black arrow) and at 30 hpf we could not detect any other expression than in the otic vesicle (Figure 3.37, B). However, the expression pattern expands on the second day to the parapineal organ (Figure 3.37 C, green arrow), the lateral line organ (Figure 3.37 C and C', blue arrow) and to cells in the ventral wall of the DA (Figure 3.37 C and C', red arrow). *Gfi1.2* expression in the DA has been described by Duforcq et al, but they did not further explore the nature of these cells (Duforcq et al, 2004). In contrast, a recent PhD thesis was able to locate the *gfi1.2* expression in the DA to the ventral wall (R. Wilkinson, 2008). The staining in the artery is lost by day 5 (Figure 3.37, D) while the expression in the parapineal organ (Figure 3.37, D green arrow), the otic vesicle (Figure 3.28, black arrow) and in the lateral line organ (Figure 3.37, D blue arrow) persists.

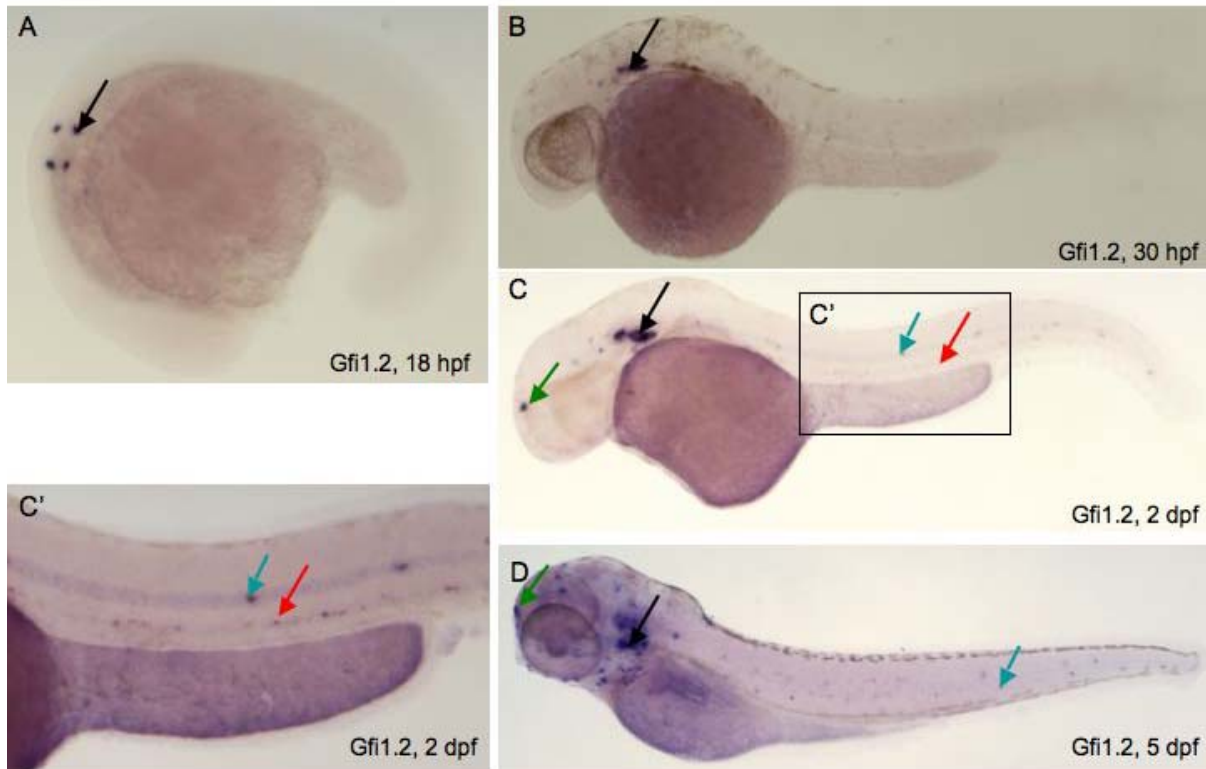


Figure 3.37: *Gfi1.2* is expressed in the ventral wall of the DA at 2 dpf The *in situ* staining emerges at 18 hpf in the otic vesicle of the embryo (A, black arrow). At 30 *hpf* *gfi1.2* transcript is detected in the otic vesicle (B, black arrow). At 2 dpf, the staining can now be detected in the parapineal organ (C, green arrow), the otic vesicle (C, black arrow), in the lateral line organ (C, blue arrow) and in the ventral wall of the DA (C, red arrow). C' is a close up of the boxed region in C. But the expression in the DA is lost at 5 dpf (D), while the expression in the other tissues remains.

3.13.3 The novel transcript *gfi1b-like* is exclusively expressed in erythroid cells

In situ hybridisation for the novel *gfi1b* showed that this gene is exclusively expressed in the erythroid lineage. We started to detect the transcript at 10 somite stage in the posterior lateral mesoderm (Figure 3.38, A red arrow). The expression is observed in the area where primitive red blood cells originate. These cells move medially to form the ICM (Figure 3.38, B red arrow) and go into circulation at 26 hpf (Figure 3.38, C red arrow). There is no expression in any other tissue.

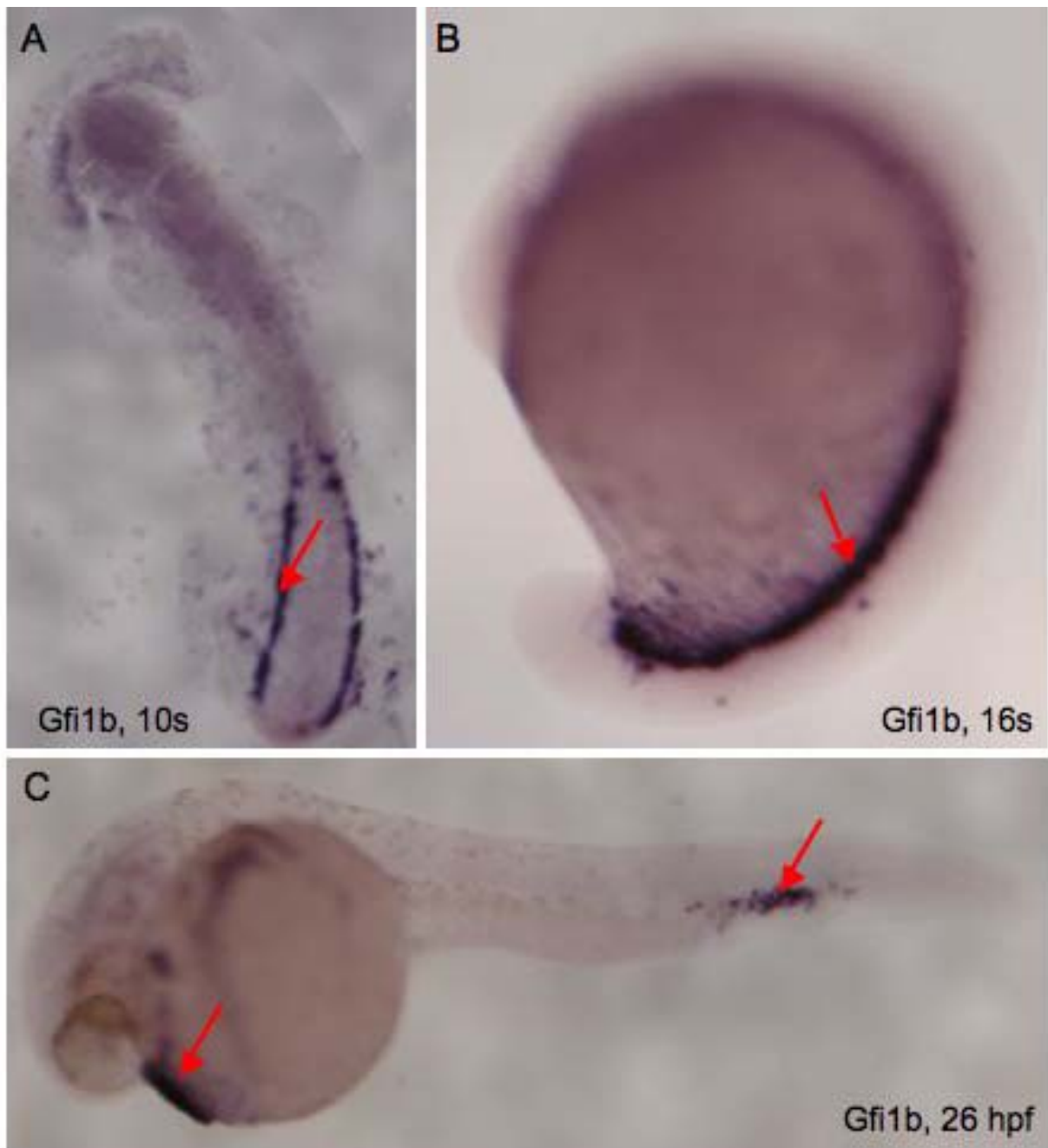


Figure 3.38: *Gfi1b* expression marks the development of primitive red blood cells *Gfi1b* transcripts are first detected in the posterior lateral plate mesoderm at 10 somite stage (A, red arrow). The *Gfi1b* positive cells move into the midline and are found amongst cells forming the ICM (B, red arrow). At 26 hpf the cells are in circulation (C, red arrows).

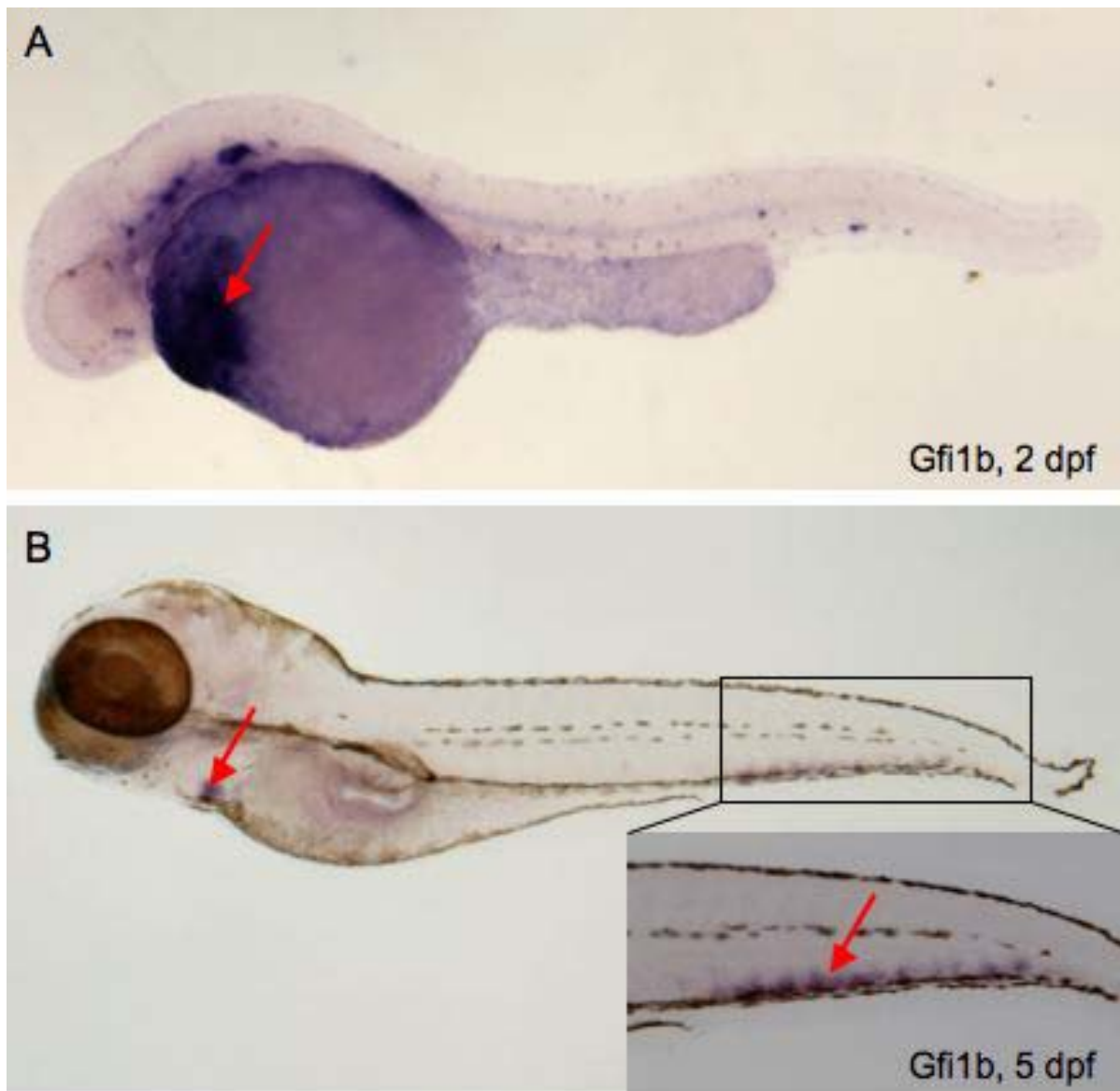


Figure 3.39: *Gfi1b* expression is restricted to the erythroid lineage Picture A shows the *Gfi1b* expression at 2 dpf. Most of the erythroid cells are gathered in the heart region (a, red arrow). At 5 dpf the expression is restricted to the mesenchyme in the tail (b, boxed region) and in the heart (B, red arrow).

Even at 2 dpf (Figure 3.39, A) only circulating red blood cells are expressing the gene. The expression is visible in the region of the heart where the red blood cells are accumulated (Figure 3.39, A and B, red arrows). By 5 dpf, the *gfi1b* expression is mainly restricted to the mesenchyme in the tail (Figure 3.39, B boxed region). This area has been implicated in the formation of definitive erythroid progenitors in the fish

(Monteiro et al, 2010). We conclude that the *gfi1b* is expressed in primitive as well as definitive red blood cell progenitors like its mouse homolog *gfi1b*.

The *in situ* experiments enable us to analyze the distribution of the *gfi 1b-like* mRNAs in the embryo. We were able to show that *gfi1b-like* is restricted to the erythroid lineage. *Gfi1b-like* is a conserved ortholog of mouse *gfi1b*.

Summary of chapter 3.13:

- *In situ* hybridisation for *gfi1.1*, *gfi1.2* and *gfi1b* were performed at different developmental stages starting from early somite stages up to 5 dpf
- *Gfi1.1* mRNA is expressed in a similar pattern to the eGFP expression in *Gfi1.1:eGFP* transgenic line
- *Gfi1.1* mRNA was detected in the otic vesicle of 21hpf old embryos, but not in the *Gfi1.1:eGFP* transgenic line
- In the *Gfi1.1:eGFP* transgenic line, eGFP expression is also present in intestinal cells at 5dpf, but we did not detect any mRNA for *gfi1.1* by *insitu* hybridisation
- *Gfi1.2* is expressed in the ventral wall of the dorsal aorta at 2 dpf, the mRNA is also expressed in non-haematopoietic tissues
- *Gfi1b-like* expression is restricted to the erythroid lineage

Discussion

Since little is known about the cellular origin and molecular programming of HSCs, we conducted a *tol2* transposon based gene trap screen to target genes involved in haematopoiesis. The gene trap construct has an eGFP gene as a reporter which allows to label cells *in vivo*. The screen resulted in 174 transgenic lines, including 2 lines which expressed the reporter gene in haematopoietic cells. The first transgenic line, *SN173-11:eGFP*, showed eGFP expression in primitive red blood cells and cells of the hatching gland. The second transgenic line, *I-551:eGFP*, revealed marker gene expression in primitive red blood cells from 12 hpf to 30 hpf and in spindle shaped, endothelial-like cells in the ventral wall of the DA.

Immuno-histochemistry for eGFP was performed on 30 hpf old transgenic embryos to validate the eGFP expression profile. In transverse sections, taken through the trunk of the embryo, round cells were located within the vessels, whereas the spindle-shaped cells were confined to the floor of the top vessel, just ventral to the notochord. In order to confirm that these endothelial cells are located in the dorsal aorta, we examined the cells by crossing the *I-551:eGFP* line to *Flk1:tomato* line, which expresses Tomato in all endothelial cells and to the *EfnB2a:tomato* line, where Tomato is expressed exclusively in the DA within the vasculature. Co-expression of eGFP and Tomato in Tg (*I551:eGFP;Flk1:tomato*) and Tg(*I551:eGFP;EfnB2a:tomato*) demonstrated that the eGFP expression in the endothelial cells was located in the ventral wall of the DA. Furthermore, the *I-551:eGFP* transgenic line was also crossed to the *12xCLS:cerulean* line. Co-expression of eGFP and Cerulean was observed in the ventral wall of the DA, supporting the previous data that eGFP positive cells endothelial cells are arterial. In experiments where *vegf* and *notch* signalling were depleted in *I-551:eGFP* positive embryos, the *I-551* transgenic embryos specifically

lost the eGFP expression in endothelial cells, confirming the arterial nature of these cells. Furthermore, in order to investigate, if the eGFP positive endothelial cells are haemogenic endothelial cells, we conducted combined *in situ* hybridisation for c-Myb and Runx1 with immuno-histochemistry for eGFP. EGFP positive cells in the ventral wall of the DA expressed both haematopoietic transcription factors. In order to determine the trapped gene in *I-551:eGFP*, we performed inverse-PCR and located the insertion in the first intron of the *gfi1.1* gene, the homolog of the mouse *gfi1*. In the murine model, *gfi1* is known to be expressed in HSCs. Consistent with the idea that *gfi1.1* positive endothelial cells are haemogenic and give rise to nascent HSCs, we observed eGFP positive progeny emerging from *gfi1.1* positive, endothelial cells in the ventral wall of the DA in preliminary time-lapse experiments. The nascent HSCs seed the CHT at 2 dpf and eGFP expression is not only detected in the thymus, but also in the larval and adult kidney after 4 dpf. The migration of the eGFP positive cells to the CHT is dependent on blood flow. When blood circulation was abolished using the *silent heart* MO, a reduction in the number of *gfi1.1* positive cells in the CHT at 50 hpf was observed. The CHT seeding is also affected when the *runx1*-MO was used. *Gfi1.1* expression in the haemogenic endothelial cells remained intact at 27 hpf, but *gfi1.1* positive cells were absent from the 50 hpf CHT, arguing for a *runx1*-independent initiation of *gfi1.1* expression. We therefore conclude that *gfi1.1* is expressed in haemogenic endothelial cells at the time-point of HSC emergence and possibly continues to be expressed in the adult kidney. We extended our analysis to the other *gfi1s* in zebrafish by *in situ* hybridisation. The endogenous expression of *gfi1.1* is similar to the expression patterns observed in the transgenic line. We also examined the expression profile of *gfi1.2*, the paralog of *gfi1.1*, from early somite stages to 5 dpf, and found that both genes have an over-lapping expression in the ventral wall of the DA, albeit at different time-points, in the otic

vesicle and in the lateral line organ. We also identified a novel homolog of *gfi1* in zebrafish, *gfi1b-like*. Like its murine counterpart *gfi1b*, it is expressed in erythroid cells starting from 3-4 somites. *Gfi1* and *gfi1b* are known to have redundant roles in murine development, apart from the inner ear hair cell development, where *gfi1b* cannot substitute for *gfi1*'s function. Therefore we might need to target all three *gfi* genes in zebrafish in order to assess the function of these genes.

4.1 *Tol2* mediated gene trap approach in zebrafish is an effective tool to generate transgenic animals with tissue-specific gene expression

The microinjection of 2853 one-cell staged embryos with *Tol2KIXGnewSA+attP* and transposase delivery resulted in 2107 embryos (73%) expressing eGFP transiently the following day (Table 3.1). This result indicates that the microinjection experiments were successful. 30% of the embryos survived to adulthood. This survival rate is comparable to the survival rate of WT larvae in our aquarium at the time. Overall, 639 of the embryos were maintained to adulthood and 536 of these potential founder fish were mated to wild type fish of the opposite sex (Figure 3.1). From these 536 fish, 160 founders accounting for 174 different visually identifiable insertions were detected (Figure 3.1). The total number of insertions remains unidentified, since we did not perform southern blot analysis on all the transgenics. The germ line transmission frequency for visually identifiable gene trap events is therefore at around 30%, which is higher than the visually detectable transmission frequency of 23% published by Kawakami et al in 2004. In their experiments they found that the average number of insertions per founders was 5.6 (Kawakami et al, 2004). Southern

blots were performed on genomic DNA derived from 2 transgenic lines and showed that *I-551:eGFP* and *SN173-11* had 7 and 1 insertion, respectively (Figure 3.14).

Another observation we made is that we trapped more ubiquitously expressed genes than genes with tissue-specific expression patterns (Figure 3.1). This observation is comparable to the results of the *N*-ethyl-*N*-nitrosourea (ENU) mutagenesis screen (Driever et al, 1996; Haffter et al, 1996). 70% of their mutated genes showed non-specific or common developmental defects, which was interpreted as ubiquitous or cell essential genes (Amsterdam et al, 2004), whereas 60% of the trapped genes in our gene trap showed ubiquitous eGFP expression. In conclusion, our gene trap screen was successful and the obtained results are comparable to previously published screens.

4.2 The gene trap screen results in two transgenic lines with eGFP expression in haematopoietic cells

We used a gene trap screen to create various transgenic lines. Two transgenic lines with reporter gene expression in haematopoietic tissues were isolated. The first transgenic line from the screen is the *SN173-11:eGFP*. In this line, reporter gene expression was observed in primitive red blood cells and cells of the hatching gland (Figure 3.3). The eGFP expression level was very low and short-lived and lasted only from around 22hpf to 25 hpf. Because of the transient nature of its expression in primitive red blood cells, this line was not analysed further. The second transgenic line, *I-551:eGFP* shows eGFP expression in primitive red blood cells and in endothelial cells at 25 hpf (Figure 3.4a C).

4.3 The trapped gene in *I-551:eGFP* is identified as *gfi1.1*

Using inverse-PCR the *ptol2rst* insertion was mapped to the first intron of the *gfi1.1* gene (Figure 3.21) and thus, the *I-551:eGFP* transgenic line was termed *Gfi1.1:eGFP*. *Gfi1.1* is a homolog of the mouse *gfi1*. Growth factor independent 1 (*gfi1*) and its paralog *gfi1b* are expressed in multiple tissues in zebrafish and mouse (see Chapter 3.3.17 and for a review see van der Meer, 2010). Both proteins have a small conserved SNAG (Snail/GFI1) domain at the N-terminus (Grimes et al, 1996; Tong et al, 1998) and a six C₂H₂-zinc finger repeat at the C-terminus (Lee et al, 2010). Both regions are conserved 89% between the two paralogs in mice, whereas the intermediate region only shows 39% similarity (van der Meer, 2010). In zebrafish, we have identified two orthologs of the mouse *gfi1*, *gfi1.1* and *gfi1.2* and one ortholog of the *gfi1b* gene, the novel transcript *gfi1b-like* (Figure 3.34). We hypothesize, that there was a duplication of *gfi1* and *gfi1b* in teleost fish (Postlethwait et al, 2006), leading to the two identified *gfi1.1* and *gfi1.2*, but we only found one *gfi1b* homolog. The second copy must have got lost in zebrafish during evolution. Our newly identified *gfi1b-like* has a highly conserved sequence homology in the C-terminus of the amino acid sequence to the mouse GFI1B (Figure 3.33a), although the N-terminal SNAG domain is missing, like in the invertebrate homologs SENSELESS and PAG-3 (Nolo et al, 2000). However, with the evidence from the phylogenetic tree, which groups the Gfi1b-like protein in zebrafish within the GFI1Bs of human, mouse and xenopus and with the expression pattern gained from *in situ* hybridisation experiments, we can be confident, that the *gfi1b-like* is a true homolog of *gfi1b* in mice.

Both paralogs have been studied in detail in the murine model. Gfi1 knock-out mice suffer from neutropenia (loss of neutrophils), low cellularity of thymocytes which lead to developmental defects during T-cell differentiation (Yücel et al, 2004; Hock et al,

2003) and loss of inner hair cells in the ear due to increased apoptosis (Wallis et al, 2003). By knocking in the eGFP gene into Exon 3-5 of the *gfi1* coding region, it was possible to study the expression and function of *gfi1* *in vivo*. Here, it was established that *gfi1* is up-regulated during early thymocyte differentiation and down-regulated during B cell maturation in the bone marrow (Yücel et al, 2004). *Gfi1b* knock-out mice, in contrast, die by E15.5 due to lack of erythrocyte differentiation (Saleque et al, 2002, Vassen et al, 2007). In a similar approach as for the *gfi1* gene, the eGFP was knocked into the *gfi1b* coding region, which allowed to study the expression pattern during haematopoiesis. EGFP expression was detected specifically in early erythroblasts and megakaryocytes and in very early thymic cells for a very brief period of time (Vassen et al, 2007). Like in the murine model, *gfi1b-like* is expressed in developing erythrocytes, starting from 10 somite stage (Figure 3.38). The expression remains in definitive erythrocytes as observed in 5 day old embryos in the caudal tail region, a site of erythro-myeloid proliferation in fish (Monteiro et al, 2010). It would be interesting to elucidate if *gfi1b-like* is also expressed in thrombocytes, the fish counterpart of the mouse megakaryocytes.

Insertion of the coding region of *gfi1b* into the *gfi1* gene locus completely rescues the haematopoietic phenotypes observed in *gfi1* mutant mice, suggesting that both proteins can compensate for each other, but the loss of hearing in *gfi1* mutant mice was not rescued by inserting the *gfi1b* gene into the *gfi1* locus (Vassen et al, 2007). This is indicative for a tissue specific function for *gfi1* in inner ear hair cell development.

Loss of either *gfi1* or *gfi1b* results in very different, non-overlapping haematopoietic deficiencies (van der Meer, 2010). This is likely due to the differences in their expression patterns and a tight control of protein activity at many levels. *Gfi1* is known to be regulated by microRNAs (Dabrowska et al, 2009) at the transcript level

and is also regulated at the protein level through ubiquitin-proteasome-mediated degradation (Marteijn et al, 2007). Both proteins negatively regulate each other and themselves (Doan et al, 2004; Yucel et al, 2004; Anguita et al, 2009). Both proteins have important roles in lineage fate decision within haematopoietic cells. *Gfi1b* is essential for erythroid and megakaryocytic differentiation whereas *gfi1* is involved in the development of all other blood lineages (Yücel et al, 2004, Vassen et al, 2007; van der Meer et al, 2010). Both gene products bind DNA and suppress gene expression through recruiting histone deacetylases and (de)methylases or by recruiting co-repressors which in turn recruit histone modifying proteins (Duan et al, 2005; Vassen et al, 2006, van der Meer et al, 2010).

Within the HSCs, *gfi1* and *gfi1b* are highly expressed in the *LSK* compartment, which comprises LT-, ST-HSCs and MPPs (Hock et al, 2004, Zeng et al, 2004, Khandanpour et al, 2010 a and b). Next to a *gfi1* knock-out (*gfi1*^{-/-}) mouse model (Hock et al, 2004), the *Gfi1:eGFP* mouse transgenic line was used to assess the function of *gfi1* in HSCs (Zeng et al, 2004). In *in vivo* culturing experiments, *gfi1*^{eGFP/eGFP} HSCs form smaller CFU-S colonies after 12 days and the numbers of these colonies are lower than colonies derived from WT-cells. Furthermore, transplantation of *gfi1*^{-/-} HSCs revealed a poor reconstitution of recipients, since one third of the recipients died after 35 days (Zeng et al, 2004). In competitive repopulation assays with *gfi1*^{-/-} and *gfi1*^{eGFP/eGFP} bone marrow cells, it was shown that *gfi1* deficient cells had a reduced ability to contribute towards the myeloid or lymphoid lineages (Zeng et al, 2004; Hock et al, 2004). Since the numbers of LT-HSCs in the bone marrow are elevated in *gfi1* deficient mice (Hock et al, 2004), it was speculated that *gfi1* is involved in restricting proliferation in HSCs. In support of this hypothesis, secondary transplantation of *gfi1*^{-/-} cells into irradiated recipient lead to anaemia after 6-8 weeks (Hock et al, 2004). Increased proliferation was further confirmed with BrdU

labelling experiments. *Gfi1*^{-/-} HSCs enter the cell cycle more frequently compared to WT-cells (Hock et al, 2004; Zeng et al, 2004). Recent studies suggest that *gfi1* may protect HSCs against stress induced apoptosis (Khandanpour et al, 2010a). *Gfi1* is only expressed at low levels in HSCs, but highly expressed in MPP, whereas *gfi1b* is more abundant in HSCs than in MPPs (Khandanpour et al, 2010b). When *gfi1b* was conditionally knocked-out in adult mice, a significant increase in the number of HSCs was observed in the bone marrow, spleen and peripheral blood (Khandanpour et al, 2010b). Hoechst staining experiments confirmed the elevated cycling of HSCs. Therefore *gfi1b* is implicated in controlling HSC dormancy.

The existing experimental data will help to elucidate the function of *gfi1.1* in zebrafish. Both zebrafish *gfi1s*, *gfi1.1* and *gfi1.2* are expressed in the dorsal aorta at 30 hpf and 2 dpf, respectively (Figure 3.36B and Figure 3.37C') and both transcripts can be detected in the otic vesicle (Figure 3.36 A' and Figure 3.37 A) like in mice (Wallis et al, 2003). The expression of both homologs in the lateral line organ reflects the function of *gfi1* in the development of the sensory organs across phyla. The invertebrate homologs *senseless* and *pag-3* are both involved in neuronal development (Nolo et al, 2000; Jia et al, 1997). Even during mouse development, *gfi1* mRNA is detected in sensory cells of the peripheral nervous system (Wallis et al, 2003). We detected expression of *gfi1.1* mRNA also in the thymus (Figure 3.36, black arrow) in the pancreas at 5 dpf (Figure 3.36D, green arrow). Both expression patterns are also evident in the *Gfi1.1:eGFP* transgenic line (Figure 3.4b A and C, green and purple arrow). Mouse *gfi1* is also expressed in the thymus (Wallis et al, 2003) whereas the expression of the *gfi1* homolog in the pancreas has not been reported before. *Gfi1.1* expression, which is only present in the transgenic line are seen in the kidney (Figure 3.5 red arrow), spleen (Figure 3.4 C black arrow) and intestinal cells (Figure 3.4b B, blue arrow). Since *gfi1* in the murine model is expressed in the bone

marrow, and the zebrafish kidney represents the equivalent haematopoietic organ in fish, we assume that this expression reflects the endogenous *gfi1.1* expression in haematopoietic cells. The spleen and gut cells in mice also express *gfi1* (Wallis et al, 2003). Therefore it is possible that our *in situ* hybridisation experiments at 5 dpf are not sensitive enough to detect the mRNA in the kidney, spleen and intestinal cells, since the tissue penetration of the probe can be limited at this time point. Alternatively, the mRNA might be short-lived and therefore not detectable in these tissues with *in situ* hybridisation experiments, whereas in the transgenic line, the eGFP which is more stable, is detected easily in these tissues.

It is interesting that *gfi1.1* mRNA and *Gfi1.1:eGFP* are initially also expressed in primitive red blood cells (Figures 3.4a, 3.6, 3.7, 3.9, 3.36 A). The endogenous *gfi1.1* mRNA was detected in erythroblasts starting from 3-4 somites, but the expression was almost absent at 21 hpf, apart from in a few cells (Figure 3.26). In contrast, eGFP expression was observed in primitive circulating red blood cells up to 30 hpf in the *Gfi1.1:eGFP* transgenic line. This difference in the expression profile of *gfi1.1* might be due to the long half life of the eGFP protein (Corish et al, 1999) in the transgenic line. A functional role for *gfi1* in red blood cell development was described by Hock et al (Hock et al, 2004). In experiments, the contribution of haemoglobin production in blastocysts was examined, a loss of contribution to haemoglobin production from *gfi1*^{-/-} cells was revealed (Hock et al, 2004). This observation links *gfi1* to erythropoiesis, but further experiments are needed to elucidate the possible role of *gfi1* in red blood cell development.

Since all 3 *gfi1s* are expressed in haematopoietic tissues, it would be interesting to investigate which role(s) each of them have. Based on their expression pattern (Figure 3.36 B' and Figure 3.37 C'), *gfi1.1* and *gfi1.2* might have a redundant role in HSC formation, despite the fact that *gfi1.2* is only expressed in the DA at 2dpf and

apparently in fewer cells. Therefore, both transcripts might need to be knock-down using anti-sense morpholinos. We expect to see an increase in *runx1*, *c-myb* and *gfi1.1* positive cells, since the absence of *gfi1.1* should lead to an increase in HSC proliferation. But since *gfi1* and *gfi1b* in mice are redundant, all three transcripts in zebrafish might need to be targeted in order to see a phenotype. First attempts at MO-mediated knock-down of all of the *gfis* were performed during this thesis, but did not result in any obvious phenotype (data not shown). Wei Wei et al showed that they could knock-down the fluorescence intensity of *gata1* in *Gata1:eGFP* transgenic line by injecting a *gfi1.1* MO (Wei Wei et al, 2004), but we were unable to reproduce this result with the same morpholino in our experiments. Since *gfi1b-like* is also expressed in primitive red blood cells and therefore might have a redundant role in primitive erythropoiesis, we might need to target *gfi1.1* and *gfi1b-like* in order to see a down-regulation of *gata1*. Further MO injections, targeting multiple transcripts are required to assess the roles of *gfis* in zebrafish. Maybe we will not see an early, embryonic defect in HSCs formation at all, but need to expect a late HSC defect like described for the murine model (Zeng et al, 2004, Hock et al, 2004). Here, HSCs are exhausted due to an increased proliferation rate and the secondary recipients of transplanted cells die due to anaemia (Hock et al, 2004). Since MO-mediated knock-down of *gfis* will only affect the transcript for a couple of days, knock-outs using the zinc-finger nuclease mediated approach are needed. In the second step we would need to isolate kidney marrow from the mutant fish and transplant them serially into irradiated fish. Although transplantation and cell-culture assays are becoming more accessible in zebrafish (Bertrand et al, 2007; Ma et al, 2011), both experimental procedures need time to be established. However, it will be informative to perform these experiments in order to reveal the function(s) of *gfi*(s) in zebrafish.

4.4 The transgenic line *Gfi1.1:eGFP* expresses eGFP in multiple haematopoietic tissues

In the transgenic line *Gfi1.1:eGFP*, the first eGFP positive cells are visible starting from 12 hpf. Subsequently, the eGFP signal intensifies and becomes visible in primitive red blood cells (Figure 3.4a red arrow and Figure 3.7 red arrow). We verify that eGFP is expressed in primitive red blood cells, unlike in the murine model, by crossing the *Gfi1.1:eGFP* transgenic line to the *Gata1:dsRED* line and demonstrating co-expression of eGFP and dsRED in those cells (Figure 3.7 red arrow). The eGFP expression in primitive red blood cells decreases after 30 hpf (Figure 3.8 b).

Endothelial cells in the ventral wall of the DA are also labelled. The endothelial expression is confined to the DA by different approaches. First, we verified the eGFP expression in the 30 hpf embryo by immuno-histochemistry against eGFP with DAB. Transverse sections through the trunk of the 30 hpf embryo revealed DAB stained in round cells within the vessels and spindle-shaped cells in the top vessel, just beneath the notochord. The stained spindle shaped cell (Figure 3.6 C, green arrow) covers the floor of the endothelium and is elongated into the lateral part of the DA. This morphology suggests an endothelial nature of the cell. Analysis of the fluorescent double transgenic embryos by confocal imaging followed. Confocal imaging allows to determine if the fluorescent proteins are present in the same cell since the optical thickness of the section can be modified to allow single cell resolution. By taking 2 μm sections through endothelial cells, we showed co-expression of *Gfi1.1:eGFP* positive cells in the ventral wall with *tomato* expressing cells of the *Flk1:tomato* transgenic line (Figure 3.11, yellow arrow). We also showed co-expression of eGFP and *tomato* in the ventral wall of the DA in Tg (*Gfi1.1:eGFP;efnB2a:tomato*) (Figure

3.12, yellow arrow). Here, the *EfnB2a:tomato* expression is not present in all arterial cells, but is restricted to a few cells (Figure 3.12, red cells). We are unsure if this due to the weak *Tomato* expression in the transgene or if the expression reflects endogenous *efnB2a* expression in endothelial cells of the DA. The arterial character of the endothelial cells in the *Gfi1.1:eGFP* transgenic line is also evident in Tg (*Gfi1.1:eGFP;12xCLS:cerulean*) embryos. Here, co-expression of the eGFP and Cerulean was again restricted to the ventral wall of the dorsal aorta. Thus, we have evidence to believe that the arterial expression in *Gfi1.1:eGFP* positive cells are confined to the ventral wall and therefore represent in haemogenic endothelial cells.

The expression profile changes at 2 dpf. Here, we observed eGFP positive cells in the CHT of the embryo (Figure 3.4a D, white arrow). Previous publications have reported that *runx1*, *c-myb* and *CD41* positive cells seed this region from 32 hpf (Jin et al, 2007; Kissa et al, 2008; Murayama et al, 2006, Lam et al, 2010). We therefore conclude that our *Gfi1.1:eGFP* positive cells behave like putative HSCs. At 4 and 5 dpf, the expression profile extends to the thymus, spleen and the kidney (Figure 3.4a,b and Figure 3.5). Progenitors of T lymphocytes are known to be present in the thymus by 4 dpf (Jin et al, 2007; Bertrand et al, 2008; Burns et al, 2005; Gering et al, 2005; Lam et al, 2010). We confirmed the presence of *gfi1.1* positive cells in the thymus after 4 dpf (Figure 3.4b), but double staining for *rag1/2* and eGFP is needed to support the expression of *gfi1.1* in T cell progenitors.

The eGFP staining in the spleen of *Gfi1.1:eGFP* transgenic animals requires further investigation. Since the spleen is closely associated with erythroid cells in vertebrates, *gfi1.1* might also label adult erythroid precursors, but we hypothesise from the FACS analysis performed on Tg (*Gfi1.1:eGFP; Gata1:dsRED*) adult kidney marrow that there is no overlap between eGFP and dsRED positive cells (Figure 3.38b). Alternatively, the staining in the spleen could compromise primitive red blood

cells which have accumulated in the spleen in order to be degraded. But it might be useful to examine the mesenchymal tissue between the caudal DA and PVC to see if definitive erythroid cells are labelled in *Gfi1.1:eGFP* transgenic embryos.

The pancreas is associated with B cell development based on *rag1* expression starting from 4 dpf in zebrafish (Danilova et al, 2002), but their origin from HSCs from the ventral wall of the DA still remains to be determined. We detected *gfi1.1* expression in the pancreas by *in situ* experiments and in the transgenic *Gfi1.1:eGFP* line at 5 dpf (Figure 3.4 b and 3.5, 3.36D). It remains unclear if *gfi1.1* is labelling haematopoietic cells within the tissue.

We also identified *gfi1.1* positive cells in the 5 day old kidney of the larvae and maybe in adult fish (Figure 3.5, 3.32b). The nature of these cells are undetermined, but are most likely to include HSCs since the staining in the kidney of the larvae is consistent with the staining seen in *runx1*, *c-myb* and *CD41* transgenic lines (Murayama et al, 2006; Bertrand et al, 2008; Kissa et al, 2008; Lam et al, 2010). We therefore think that *Gfi1.1:eGFP* is labelling haematopoietic cells including putative HSCs. But since *gfi1* is also expressed in neutrophils in mice (Hock et al, 2003), the *Gfi1.1:eGFP* transgenic line might also label this haematopoietic compartment. In order to investigate if neutrophils are amongst the eGFP positive cells in the CHT and kidney, the *Gfi1.1:eGFP* line can be crossed to the neutrophil-specific transgenic *myeloperoxidase (mpx)* line. This will allow us to assess if *gfi1.1* is expressed in neutrophils in zebrafish.

4.5 The endothelial expression in *Gfi1.1:eGFP* is downstream of *vegf* and *notch* signalling

Treatment with the *vegfR*-inhibitor leads to a loss of *runx1* positive cells in the DA at 26 hpf (Gering et al, 2005) due to the absence of arterial differentiation as shown by the lack of *efnB2a* positive cells (Lawson et al, 2002). We treated *Gfi1.1:eGFP* and *Gata1:dsRED* double transgenic embryos with the *VegfR*-inhibitor, in order to further gain evidence that the endothelial cells are arterial and depend on *vegf* signalling. In embryos treated with 5µM of the inhibitor (Figure 3.18 E and F) elongated cells as seen in the DMSO-control treated embryos are not present, although primitive red blood cells are unaffected. This result is consistent with earlier findings for *runx1* and *efnB2a* (Gering et al, 2005; Lawson et al, 2002). Since the differentiation of the artery is impaired, HSCs do not form in these embryos.

Arterial specification and HSC formation are dependent on *Notch* signalling (for a review see Gering and Patient, 2010; Bigas et al, 2010). HSC activity is lost in *notch1* mice mutants (Kumano et al, 2003). Consistent with these findings in mouse, *notch* signalling was shown to be essential for arterial specification (Zhong et al, 2001, Lawson et al, 2002; Gering et al, 2005). We showed that *notch* signalling is active in *gfi1.1* positive, endothelial cells at 27 hpf using different approaches. First, we made a *12xCLS:cerulean* transgenic line, in which *cerulean* expression responds to *notch* activity. Here, we reveal *notch* activity in *gfi1.1* positive cells (Figure 3.13 C). We showed that by knocking down the *Su(H)* transcript or by depleting *notch* signalling with the γ -secretase inhibitor DAPM, endothelial expression of *gfi1.1* disappears (Figure 3.19, Figure 3.25). We further confirmed the absence of *gfi1.1* positive cells in *notch*-deficient embryos, by crossing the *Gfi1.1:eGFP* transgenic line into the *mib* mutant background (Figure 3.21). In all these experiments, we confirmed that the

endothelial expression is dependent on active *notch* signalling as described before (Burns et al, 2005; Gering et al, 2005). We also observed an expansion of *gfi1.1* positive cells into the vein region of the embryo when *notch-ICD* was mis-expressed in the whole embryo following heat-shock induction at 16 somite stage (Figure 3.24) (Burns et al, 2005). Burns et al described the expansion of *runx1* positive cells upon ectopic *notch* expression, but did not comment on the nature of these cells. To exclude the possibility that *runx1*, *c-myb* and *gfi1.1* were mis-expressed in primitive red blood cells, we chose to combine β -*E1globin* *in situ*-hybridisation with a immunohistochemistry for eGFP in order to differentiate between red blood cells and haematopoietic precursors. The expanded eGFP positive cell population did not express β -*E1globin*. Thus, it is much more likely that these cells are endothelial in nature. Ideally, it would be interesting to isolate these cells by FACS and to test their haematopoietic potential *in vivo* by transplantation assays or *in vitro* by cell culture assays.

DAPM treatment beginning at different developmental stages were performed to investigate when *notch* is needed for the generation of *gfi1.1* positive cells. Our result suggests a role for *notch* up to 18 somites stage (Figure 3.25). After that time-point, DAPM treatment does not affect the formation of *gfi1.1* positive cells, although the *notch* reporter *12xCLS:cerulean* is active in the DA only from 18 hpf (M Gering, unpublished data). This inconsistency might be due to the fact that *notch* signalling is required twice for HSC formation. The non-cell-autonomous requirement for *notch* signalling has been narrowed down to 15-17 hpf for the formation of *runx1* and *c-myb* positive cells (Clements et al, 2011). We assume that we are affecting this early requirement of *notch* signalling in our DAPM treated embryos. The second requirement is within the DA angioblast after 18 hpf. But our DAPM treatment might

not block this *notch* activity. This could be due to the fact that the inhibitor DAPM does not penetrate the embryonic tissue enough to reach the DA at this time point.

In conclusion, we have been able to gain evidence that *vegf* and *notch* signalling are needed for the formation of *gfi1.1* positive cells in the dorsal aorta. These findings support the idea that we are labelling haematogenic endothelial cells in the DA in our *Gfi1.1:eGFP* transgenic line.

4.6 *Gfi1.1* positive cells need blood flow to seed the CHT

The injection of the *silent heart* morpholino leads to the formation of a non-contractile heart and to the absence of blood flow (Sehnert et al, 2002; Hafter et al, 1996). We aimed to investigate the role of blood flow in the development of *gfi1.1* endothelial cells in *Gfi1.1:eGFP* and *Gata1:dsRED* double transgenic embryos. In embryos injected with 4 ng of control MO, blood circulation occurred normally and circulating double positive cells were observed (Figure 3.26 A-C). In contrast, in 147/150 of *sih* morphant embryos, blood circulation was not established (Figure 3.26 D-F) at 27 hpf. The red blood cells remained in the intermediate cell mass instead. *Gfi1.1* positive endothelial cells are present in MO-injected embryos, but they appear flat and they are rare (Figure 3.26 D and F, green arrow), whereas *gfi1.1* positive endothelial cells in control MO-injected embryos appear at a higher frequency and undergo an endothelial to haematopoietic transition (Figure 3.26, A-C). The analysis of 50 hpf CHT in *sih* morphants showed that the seeding of the CHT by *gfi1.1* positive cells was severely reduced (Supplemental movie 3, *I-551:eGFP/Gata1:dsRED* 50hpf). This fact supports the notion that either the budding of the HSCs from the endothelium, or their subsequent migration to the CHT is dependent on blood flow as shown by Murayama et al. The number of c-Myb and Runx1 positive cells is

decreased in *sih* morphant embryos (North et al, 2009). Here, we can conclude, that like *runx1* and *c-myb* gene expression, *gfi1.1* expression in the ventral wall of the DA needs blood circulation. Furthermore, the subsequent seeding of the CHT is dependent on blood flow.

4.7 *Gfi1.1* positive cells are putative HSCs in zebrafish

In this thesis, we were able to accumulate evidence that *gfi1.1* eGFP positive endothelial cells are located in the ventral wall of the dorsal aorta. The presence of these cells in the DA is dependent on *vegf* and *notch* signalling. Analysis of the *Gfi1.1:eGFP* transgenic embryos revealed that cells in the CHT region start to express *gfi1.1* at day 2 (Figure 3.4a D, white arrow) and are detected in the thymus and the kidney at day 4, 5 dpf and in the adult kidney marrow (Figure 3.4b A,C and Figure 3.32b). But it still remains to be demonstrated that cells derived from the endothelium of *Gfi1.1:eGFP* transgenics seed the CHT, thymus and kidney. In order to investigate this issue, time-lapse imaging on *Gfi1.1:eGFP* and *Gata1:dsRED* double transgenic embryos starting from 37 hpf were performed (Figure 3.31 and *I-551:eGFP/Gata1:dsRED* 37 hpf time-lapse movie). We documented how *gfi1.1* endothelial cells rounded up, divided and gave rise to a daughter cell. This daughter cell remained in the mesenchyme below the DA before joining the blood circulation (Figure 3.31, *I-551:eGFP/Gata1:dsRED*). These observations are consistent with findings described for *runx1*-, *c-myb*- and *CD41* positive cells (Kissa et al, 2008; Murayama et al, 2006; Lam et al, 2010; Bertrand et al, 2010). Therefore, we assume that the *I-551* positive cells are too leaving the endothelium in order to seed the CHT. This idea is consistent with our findings that in the CHT seeding in *sih* morphants is decreased. But cell-labelling experiments are needed to support this hypothesis. Since the photo-activatable caged DNMB fluorescent dye Fluorescein dye is not

commercially available anymore and the available DNBM-rhodamine dye is subject to a high background staining when used in immuno-histochemistry, we resort to trying a new technique to label specific cells. *Kindling* (Evrogen) is a photo-activatable protein, which is non-fluorescent in the non-excited state, but can be irreversibly activated by a green laser to produce a red fluorescent protein in cells of interest. Our attempts to activate the fluorescent protein in the cells of the DA were not successful. We were not able to activate the fluorescent dye irreversibly and consequently, the labelled cells lost the fluorescent dye soon afterwards. More time and optimisation of the procedure are needed to improve the technique. In the meantime, we can only assume that *gfi1.1* positive cells from the endothelium seed the CHT.

In order to show that the ventral endothelium is haemogenic, double staining experiments for *gfi1.1* eGFP in combination with *runx1* and *c-myb* genes were performed. We revealed that *gfi1.1* is co-expressed with *runx1* and *c-myb* at 26 hpf (Figure 3.22 C and Figure 3.23 C). Since only 2 μ m thick optical slices were taken from the confocal microscope, we are certain that we are looking at double-staining in single cells. The co-expression data further support the view, that *gfi1.1* positive cells label putative HSC throughout their development. The first expression is already visible at 25 hpf in the endothelium, with the onset of blood circulation, continues to be expressed in haemogenic endothelial cells which co-express *runx1* and *c-myb* and remains in nascent HSCs that seed the CHT and subsequently *gfi1.1* expression is found in the thymus and the kidney.

Two more experiments were conducted to underline the fact that *gfi1.1* positive cells are putative HSCs. Previous experiments had shown that *runx1* positive cells are lost in embryos treated with the *PI3K* pathway inhibitor Ly294002 (C Rhode, I Khan, unpublished data). Our results show a similar loss of endothelial *gfi1.1* expression in Ly-treated embryos (Figure 3.30 D-F). Whereas in DMSO-control embryos

elongated, endothelial cells are observed at 33hpf, in 24/25 of Ly-treated embryos, there is a loss of these cells. Since round double positive cells were observed in the position of the DA (Figure 3.30), a control experiment was performed in order to determine the nature of these cells. The double positive and some eGFP only positive cells might be *gfi1.1* positive cells derived from the haemogenic endothelium or primitive red blood cells that had failed to enter circulation. But the control experiment (Supplemental Figure 5) revealed that the inhibitor treatment affects the stability of the vasculature. The *Gata1:dsRED* positive erythroid cells were simply stuck between the blood vessels. We could therefore conclude that *gfi1.1* expression is lost in endothelial cells of the DA in Ly-treated embryos.

Next, we set out to examine the effect of *runx1* knock down on *gfi1.1* haemogenic endothelial cells. The quality of the *runx1* MO injections was first assessed by *in situ* hybridisation for *c-myb* (Figure 4, supplemental data *c-myb* in *runx1* morphants). In 23 out of 30 morphants, a loss of *c-myb* positive cells in the ventral wall of the dorsal aorta at 26 hpf was detected. We could therefore be confident that we had effectively knocked-down *runx1*. Since the endothelial expression of *gfi1.1* was persistent in *runx1* morphants at 27 hpf, even though at a lower level compared to control-MO injected embryos (Figure 3.28), the CHT of morphants was analyzed for *gfi1.1* expression at 50 hpf. In *runx1*-depleted embryos, a decrease in *gfi1.1* positive cells was observed (Figure 3.29). The 40-fold decrease in cell number within the CHT argues for a specific loss of *gfi1.1* positive cells in *runx1* morphants (Graph 1). We therefore exclude defects in blood circulation as a cause for this decline, since the morphants had established vigorous blood circulation by this time.

It will be interesting to investigate, if *gfi1.1* acts upstream or in parallel of *runx1*. It is not possible to draw any conclusion from this experiment, since the decline in *runx1* positive cells in the CHT can be due to the need of *runx1* for the transition from the

endothelial to haemogenic cell fate. Supporting evidence for this hypothesis comes from a recent publication on a tissue-specific knock-out of *runx1* in the mouse. Here, *runx1* was removed from endothelial cells using *VE-Cadherin* driven *Cre-recombinase*. In these mice, the formation of intra-aortic clusters was impaired and CFU-C formation did not occur *in vitro* (Chen et al, 2009). In contrast, if *runx1* was specifically deleted in *Vav1* positive cells, which includes all HSCs, CFU-C formation was apparent (Chen et al, 2009). Furthermore, *runx1*-deficient *Vav1* positive HSCs could efficiently engraft recipients. Therefore *runx1* is essential in the haemogenic endothelium to form intra-embryonic HSC clusters, but is not essential for the self-renewal or proliferation potential of the HSCs. In zebrafish, *runx1* deficient putative HSCs have been suggested to burst and undergo apoptosis (Kissa et al, 2010). We will need to perform time-lapse imaging on our *runx1* morphants to validate this data. Furthermore, it would be interesting to see if *gfi1.1* knock down has any effect on *runx1*. Ideally, we are hoping to position *gfi1.1* in the pathway leading to HSC formation. Since the gene trap construct has inserted into the first intron of the *gfi1.1* gene (3.3.6), *gfi1.1* might knock down or knock-out by breeding homozygous *Gfi1.1:eGFP* transgenic embryos. We proposed that the rabbit β -Globin splice acceptor in the gene trap vector published by Kawakami et al might be inefficient and therefore allow splicing of the wild type transcript. Therefore, the splice acceptor was exchanged for a consensus-matched splice acceptor from the human. Although homozygous embryos for *gfi1.1* were analyzed visually for developmental defects during this PhD, it might be interesting to see if full length *gfi1.1* transcripts are generated in these embryos. By conducting *in situ* hybridisation for transcripts beginning from the second exon or by analyzing the transcript level through quantitative PCR, we should be able to answer these questions. In this context, it will also be interesting to investigate, if the eGFP transcript is fused to the 5'UTR of the

gfi1.1 transcript. Here, we can perform PCR on cDNA derived from homozygous transgenics with primers placed in the 5'UTR and eGFP. If the eGFP transcript is fused to the *gfi1.1* 5'UTR, then we should be able to obtain a PCR fragment. These experiments will allow to determine if the gene trap vector has the ability to mutate the gene it has inserted into.

4.8 The *Gfi1.1:eGFP* transgenic line is a powerful tool to study zebrafish HSC formation

From the evidence provided in this thesis, we can conclude that the transgenic line *Gfi1.1:eGFP* labels haemogenic endothelial cells from as early as 25 hpf and continues to be expressed in the putative HSCs in the CHT. *Gfi1.1* expression is then found in the thymus, kidney and spleen. This line provides a good opportunity to study nascent HSCs in detail. Although primitive red blood cells are also labelled during 16 hpf to 30 hpf, we can differentiate between haemogenic endothelial cells and their progeny and primitive red blood cells by crossing the line with *Gata1:dsRED* transgenic animals. In this way we are able to observe just the haemogenic endothelial cells and its progeny expressing eGFP whereas the primitive red blood cells are positive for both fluorescent dyes.

Non-specific labelling is also an issue in transgenic lines, which are available in general. Even the well published *runx1:eGFP* and *c-myb:eGFP* transgenic lines show marker gene expression which is not restricted to the ventral wall of the DA. Thus, endothelial cells isolated from these lines by FACS will not consist only of haemogenic endothelial cells. But such experiments are important in order to gain more insight into HSC formation. Haemogenic endothelial cells isolated by FACS can be used to do cell culture assays and deep sequencing. The resulting datasets, can

be used to identify new regulators of HSC development. Furthermore, since *Gfi1.1:eGFP* is expressed in the haemogenic endothelial cells with the onset of blood circulation, way before these cells are detected in other transgenic lines (transgene expression is first seen at 30 hpf in *C-myb:eGFP* and 33hpf in *CD41:eGFP*), we are in the unique position to isolate haemogenic endothelial cells with the onset of *runx1* expression. Although the transgenic line *runx1:eGFP* has been shown to be expressed in the DA from 22 hpf, the eGFP expression is not restricted to the DA, but is also present in the spinal chord and reaches into the PCV at 48 hpf (Figure 4.1, Lam et al, 2009).

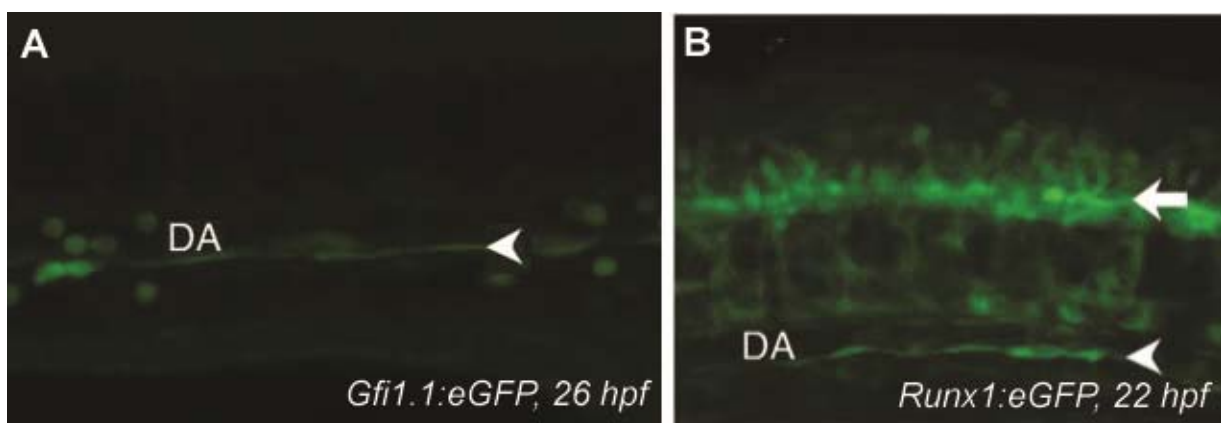


Figure 4.1: Tg (*Gfi1.1:eGFP*) is more restricted in its expression pattern than Tg (*Runx1:eGFP*) A: The eGFP expression in *Gfi1.1:eGFP* is restricted to the haemogenic endothelial cells and primitive red blood cells only at 26 hpf. B: The eGFP expression in *Runx1:eGFP* is present in the haemogenic endothelial cells, some cells of the notochord and in the spinal chord. Picture B is taken from Lam et al, 2009).

Thus the transgenic line *Gfi1.1:eGFP* will allow us to work with the earliest and most clearly labelled haemogenic endothelial cells possible from a very early time-point. It allows to compare haemogenic endothelial cells from different developmental stages and their gene expression profile with each other. During this PhD several transgenic

lines were established with the prospect of using them to isolate different sub-populations of endothelial cells. The *Flk1:tomato* line e.g. labels the whole of the vasculature and therefore is a good reference line to compare *Gfi1.1:eGFP* derived haemogenic endothelial cells to. As an alternative, the *EfnB2a:tomato*, line can be used. Although there are non-haematopoietic tissues labelled in the *EfnB2a:tomato* line, co-expressed with either *Flk1:eGFP* or *Gfi1.1:eGFP*, it can be used to identify arterial endothelial cells of the whole DA or the ventral wall, respectively. In this way we should be able to get insight into which genes are expressed during the arterial specification of a *flk1* positive cell into a *efnB2a* positive which then transforms into a haemogenic endothelial *gfi1.1* positive cell. We can also use the *Gfi1.1:eGFP* transgenic line to isolate HSCs at different developmental stages. It would be interesting to assess the potential of the different cell population present in the CHT (Figure 3.9). Although transplantation and reconstitution assays in irradiated fish using embryonic cells have not been established in any lab yet, it would be interesting to know if CHT-derived HSCs have the potential to repopulate the blood system or if they need to have been in a kidney micro-environment first. Since *gfi1.1* positive cells are also present in the kidney of larvae and adults (Figures 3.5 and 3.32b), we could try to perform reconstitution assays with kidney-derived cells first. This would allow to confirm that *gfi1.1* positive cells are HSCs. Another possibility is to cross the *gfi1.1* transgenic line with e.g. a *c-myb* transgenic line. The regulatory elements of the *c-myb* gene, which drive gene expression in the HSCs have been identified recently (JC Hsu, unpublished data). It would be interesting to see if the expression profiles in the HSCs overlap and if there are changes in the expression profile over time. Such information will help us to define HSCs in more detail. *Gfi1.1:eGFP* transgenic line can also be used to perform compound screening for HSC relevant drugs. The fluorescence intensity in the *Gfi1.1:eGFP* line can be used

as a read-out for HSC promoting or restricting drugs. All these possible approaches will help us ultimately to gain more insight into HSC development and homeostasis in zebrafish.

Summary

The main objective of this PhD was to create a transgenic line in which haematopoietic cells are labelled *in vivo*. We employed a gene trap based screen for this purpose. Using this approach, we were able to create 174 transgenic lines, including two lines with reporter gene expression in blood related tissues. The first transgenic line, *SN173-11:eGFP* expresses the reporter gene in primitive red blood cells or EMPs. The second transgenic line showed eGFP expression in primitive red blood cells and endothelial cells in the ventral wall of the DA. Although we were not able to trap a novel gene, we were able to identify the trapped gene as *gfi1.1*, the homolog of the mouse *Gfi1*. Additionally, we identified a novel *gfi1b-like* in zebrafish which is restricted to erythrocytes.

We employed crosses with the *Gfi1.1:eGFP* transgenic line to the *Flk1:tomato*, *Efnb2a:tomato* and *12xCLS:cerulean* transgenic lines to show that the eGFP expression in the endothelium is restricted to the ventral wall of the dorsal aorta. Within the dorsal aorta, the *gfi1.1* positive cells co express the haematopoietic marker genes *runx1* and *c-myb* at 26 hpf. The transgene expression in the endothelial cells is dependent on *vegf* and *notch* signalling. We also established that *notch* signalling is needed before the 18 somite stage for the emergence of *gfi1.1* positive cells. Depletion of Vegf or Notch leads to a specific loss of endothelial *gfi1.1* positive cells, while primitive red blood cell development is unaffected. Over expression of NICD leads to an expansion of the endothelial *gfi1.1* positive cell

population. Together, these results suggest that the *Gfi1.1:eGFP* transgenic line labels haemogenic endothelial cells. Preliminary time-lapse analysis show *gfi1.1* positive cells egressing from the haemogenic endothelium. We also provide evidence that this budding process is dependent on the transcription factor *runx1*. In *runx1* depleted embryos, the *gfi1.1* positive cells are present in the endothelium, but fail to seed the CHT at 50 hpf. We therefore propose that *gfi1.1* acts upstream or in parallel *runx1* within the gene regulatory network.

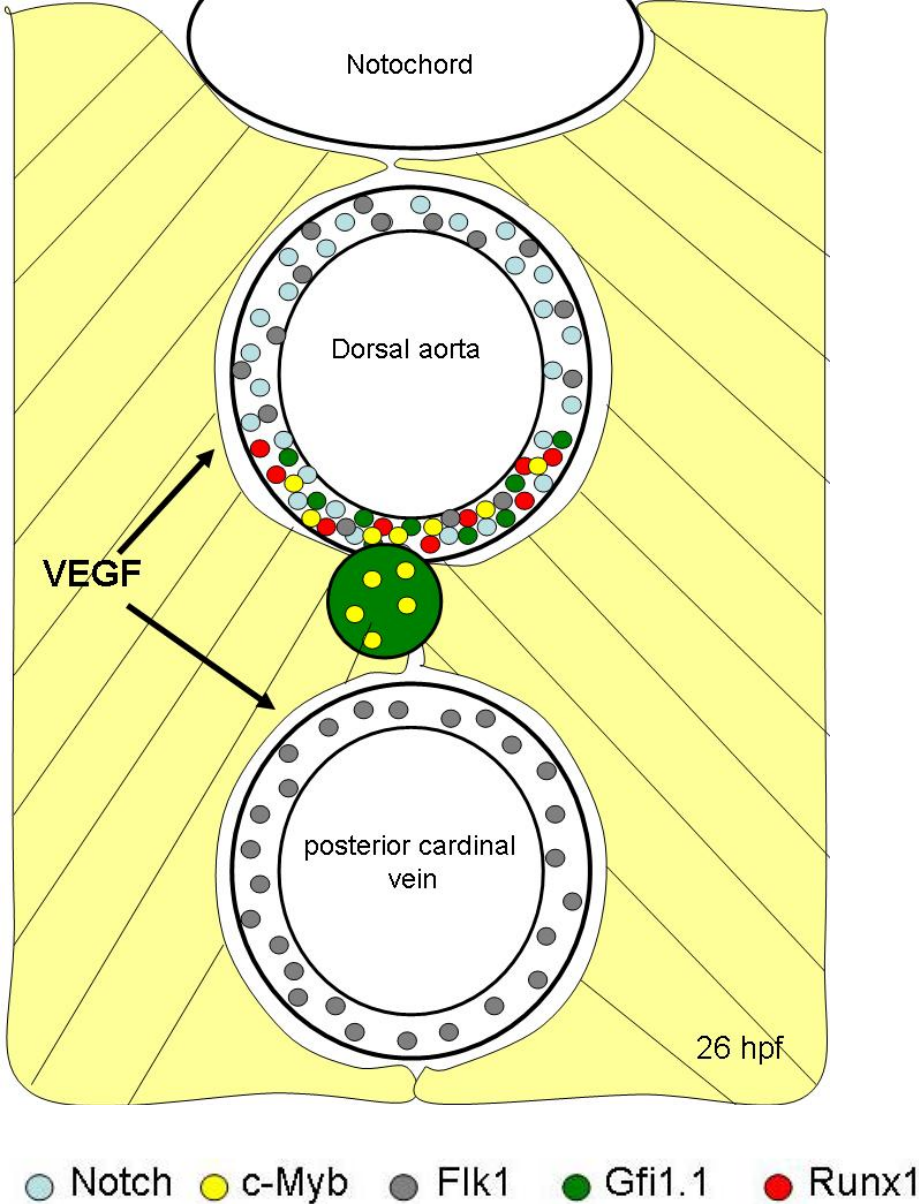
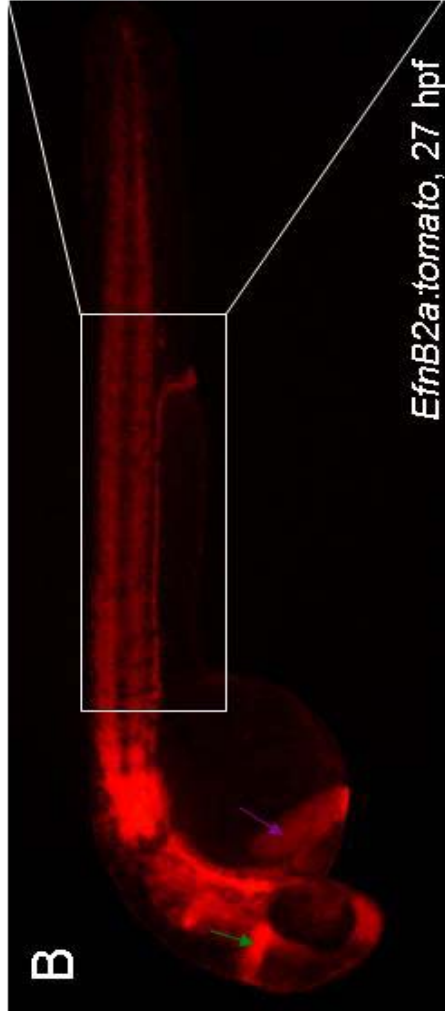
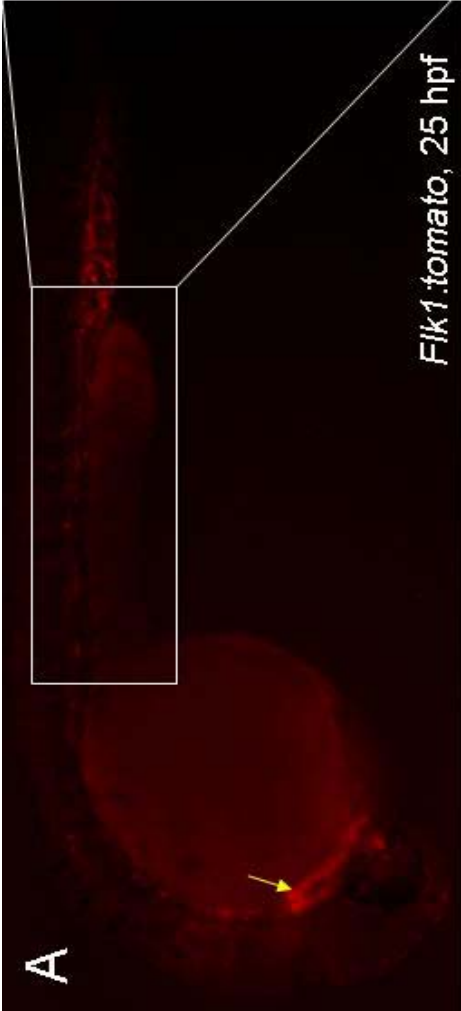
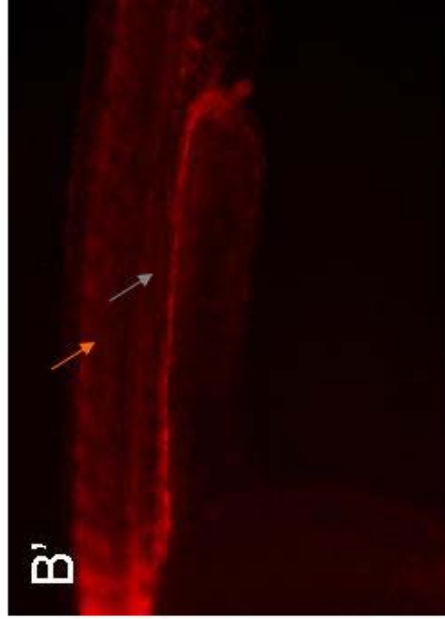
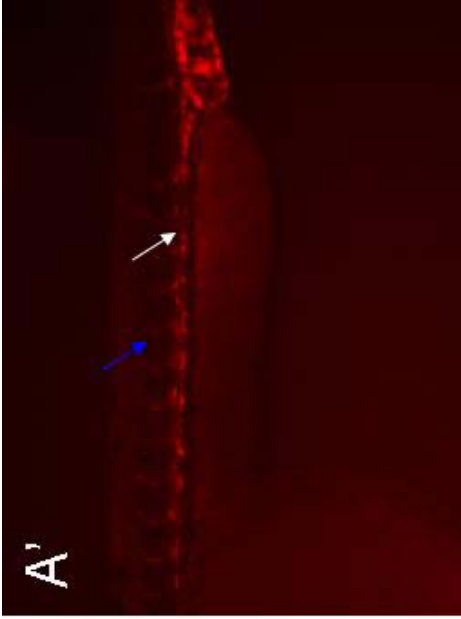


Figure 4.2: *Gfi1.1* is co expressed with *runx1* and *c-myb* in the ventral wall of the dorsal aorta and is dependent on *vegf* and *notch* signalling at 26 hpf VEGF signal from the somites (black arrow) induce Notch expression specifically in the aorta (blue). Flk1 (grey) is expressed throughout the vessels. Runx1 (red) and c-myb (yellow) and Gfi1.1 (green) are restricted to the ventral wall of the dorsal aorta. These three transcription factors might be responsible for the production of haematopoietic progenitors from the haemogenic endothelial cells. Within the haemogenic endothelium, it is unknown if Gfi1.1 act upstream or together with Runx1. Cells which bud from the haemogenic endothelium express Runx1 and Gfi1.1, but not Runx1.

Similarly, blood circulation is needed for this process. Embryos injected with the *sih* morpholino have intact vasculature, but lack blood circulation. Here, *gfi1.1* positive cells remain in the endothelium, even at 50 hpf. Subsequently, *gfi1.1* is detected in the kidney and thymus at 4 dpf. Therefore, this transgenic line faithfully recapitulates the developmental stages of HSCs in zebrafish. The transgene expression is similar to the endogenous *gfi1.1* mRNA expression although some differences exist.

Altogether, this thesis has accumulated evidence that *gfi1.1* is expressed in haemogenic endothelial cells. Preliminary FACS data support that pure haemogenic endothelial cells can be isolated at 26 hpf. In the future, these isolated cells can be used to perform microarrays and RNA sequencing in order to unravel novel transcription factors and genes involved in HSC.

Supplemental Figures



Supplemental Figure 1: An overview of the tomato expression in the Transgenics

***Flk1:tomato* and *EfnB2a:tomato* at 25 hpf and 27 hpf respectively.** A: *Flk1:tomato* is expressed in all endothelial cells at 25 hpf. The yellow arrow points at the endothelial cells in the heart. Tomato expression can also be detected in the trunk blood vessels (white arrow) and in the intersomitic blood vessels (blue arrow). B: The *EfnB2a:tomato* line expresses the fluorescent protein in the hindbrain (green arrow), hatching gland (purple arrow) and the somites (orange arrow). The artery specific expression within the endothelial cells is depicted by the grey arrow.

Supplemental Figure 2, Gfi sequences used for assembling the phylogenetic tree

>D.melanogaster-SENSELESS

MNHLSPPPSPHSQQPSPAGLGCHGAALDKQWMQRASAFNTVIASAAAQKLNGRD
LPFLYNPLLYSSALLWPQFLLSSATALGTPLTPMTPKSPASVVLGQRDRDFALTPEK
EHELQMNNNNENSKQDYQEDEDMPLNLSTKERITSDDSNRDQYHSSSNSSRS
SSSSEVEQLHPMTSLNVTTPPLSAVNLKSSSTPQQQRQRSQGNIIWSPASMCERSA
RREQYGLKMEEQGDEEEHQVDPIVRKFKYERRTASISSLQSPISSLSAPASNAVQDL
EFEVAQQQLYAHRSAFMAGLTGNNLELLTQHLKLGKSEQPQQQQQHQHRIKDEQQQD
NRSAAALMNLVAAAEFGYMRNQHQPPQQQQQQQLHHQQQPQQHQHQQQHPDS
TATDVARRSSSSSSSYQGENEEKRSGRNFQCKQCGKSFKRSSTLSTHLLIHS DTRPY
PCQYCGKRFHQKSDMKKHTYIHTGEKPHKCTVCLKAFSQSSNLITHMRKHTGYKPF
GCHLCDQSFQRKVDLRRHRESRHEEAPPVEDLKPLKMEVSSSSC

>zebrafish GF1B-like

MPRSFLVKSKSYNVHRPNGSSDQVLIFPALVPLEPKECKSPERPQVDPVTRPSHR
DPYDFIKCEREPDCPIPSLPELPTATRRPFYISEPQLAEFPPYYKSSFGWDHGPASY
QEFRHMGFSPSLLHHASSLYGAHLKQSAEPQPLDCSTHYSPSSNTYHCITCDKVFS
TPHGLEVHVRRSHSGTRPFECISCRKSFGHAVSLEQHMINVHSQERSFECKMCGKT

FKRSSTLSTHLLIHS DTRPYPCQYCGKRFHQKSDMKKHTYIHTGEKPHKCQVCGKA
FSQSSNLITHSRKHTGFKPFGCEICSKGFQRKVDLRRHHESQHSLK

>zebrafish GF11.1

MPRSFLVKSKRAHSYHQPRYLDDNCISIEKLLTCQESQTGQAPESPLDVGNQSPKA
SMVCTADQSSQQSPLSCEGSVCDRSSDYEDFWRPLSSGTSPDLKCPVPSPDDS
QPFDMFRPYVWSHSSSELRHLIQSCNRVSVDS DSSVGVYDAMDRRPSAHLIQP
TQSRRFYQDYGSLTPNLLDNRGFYTDFKMSTKVAETDSESDMTCTRLQLSGSYKCI
KCTKVFSTPHGLEVHVRRSHSGTRPFACEICGKTFGHAVSLEQHKAVHSQERVFSC
KICDKSFKRSSTLSTHLLIHS DTRPYPCQYCGKRFHQKSDMKKHTFIHTGEKPHKCQ
VCGKAFSQSSNLITHSRKHTGFKPFGCDLGGKGFQRKVDLRRHKETQHGLK

>zebrafish GF11.2

MPRSFLVKSKKAHSYHQPRSLEDDFNRLDNILAHICAESKTSDESECCADALTGDDT
GAGSPDHLDDQADLSSKSPLSCEESVCDRSSDYEDFWRPPSPSASPESEKSFSP
SVEETQPFVAVPFRPYAWSRYSGCEIRQLVQHTLNHHRSLDLERPTPTYNERVTEP
SIFTERGSGARIYNSYGSTASL FERATASGLFDDSSMLGKGTEMKSSSDVICSRLLL
NGAYKCIKCSKVFSTPHGLEVHVRRSHSGTRPFACDICGKTFGHAVSLEQHRAVHS
QERSFDCKICGKSFKRSSTLSTHLLIHS DTRPYPCQYCGKRFHQKSDMKKHTFIHTG
EKPHKCQVCGKAFSQSSNLITHSRKHTGFKPFGCDLGGKGFQRKVDLRRHKETQH
GLK

>Xenopus GF11

ESDLLCSRLLLNNGSYKCLKCSKVFSTPHGLEVHVRRSHSGTRPFACEMCGKTFG
HAVSLEQHKAVHSQERSFDCKICGKSFKRSSTLSTHLLIHS DTRPYPCQYCGKRFH
QKSDMKKHTFIHTGEKPHKCQVCGKAFSQSSNLITHSRKHTGFKPFGCDLGGKGF
QRKVDLRRHRETQHGLK

>Xenopus GF11B

MPRSFLVKSKKTHYHQHRYVEEQPVVGLDLLATSYAHCAEFPVEPPAFSTDRND
KVHTPENTTTEETDIDPGDSREKIPFISRSISPNFQGIALSSMRPSKPYDPSPLSAFY
AQNFSWETLHSTYGFKQIPSIHQHPSMLQNSINLYSCPPTLSDSDHPINYSMSYSPK
MDSYHCVKCSKVFSTSHGLEVHVRRSHSGTRPFVCNICGKSFGHAVSLEQHLNVH
SQERSFECKMCGKTFKRSSTLSTHLLIHS DTRPYPCQFCGKRFHQKSDMKKHTYIH
TGEKPHKCQVCGKAFSQSSNLITHSRKHTGFKPFSCDLCGKGFQRKVDLRRHREN
QHGLK

>Fugu GF11 (1/2)

DSSQFPQPLRSLSVTSEMPRSFMVKS KRAHSYHQHRTLEDDYSRLDTILAHICSEA
DRLPQDGEPPVDPFSLSPDLRDPAEFSPKSPLSCADSLCGRSSDYEDFWSPSPS
ASPVDSEKSMSPLVDETQPFTVPFRPYEWSSYPGVALRPPLLHQSLRPASGGPPA
VNFYVDRSRSSLYAERTVREDPYGDYGIHTAALIFPDRGLSAKAHSVRAQSELLCPS
LMLNTAYKCVKCTKVFSTPHGLEVHVRRSHSGTRPFACEICGKTFGHAVSLEQHKA
VHSQERSFDCKICGKSFKRSSTLSTHLLIHS DTRPYPCQYCGKRFHQKSDMKKHTFI
HTGEKPHKCQVCGKAFSQSSNLITHSRKHTGYKPFACDLCGKGFQRKVDLRRHKE
TQHGLK

>Fugu GF11 (2/2)

SGGFQTRSMPRSFLVKSKRAHSYHLP RYPDDDCSALDAILAHACAGGSVYERNYA
AKSADRLSPGSRLPSPCSLTSSSPLSCGGSVCDRSSDCDFWRPPSPSSSPDPEKC
STPAAQTGTNFNIPPLFPYPWNTHSSSELRRLVQRPFHPLQGHARGARLPVGVYSA

EDRAAEALYAQRAPVSGCYQDFSSTAHPICSRPPGDDFYVDVKQNTREPEIKPESD
FICSNLESSGSFKCVKCKVFSTPHGLEVHVRRSHSGTRPFECGVCCKTFGHAVSL
DQHRAVHSQERSFSCICKGKSFKRSSTLSTHLLIHS DTRPYPCQYCGKRFHQKSDM
KKHTFIHTGEKPHKCQVCGKAFSQSSNLITHSRKHTGFKPFGCDLGGKGFQRKVDL
RRHKETQHGLK

>Fugu GFI1B

MPRSFLVKNKRSSSYNLHRTYEDESKAAVTAVTYPILICCGFLEDRPEVESADSDRL
QSDEQSSPLDCRSFKKGDADPKSPRGVLDMSVPPSEPHMTGFHPYYKPTYAWEP
VSSSYDLHQLSFNPTVLQHASSLYSSHISCTTQPQQPLDCTTHYSPSSNTYHCITCD
KVFSTSHGLEVHVRRSHSGTRPFGCSVCRKTFGHAVSLEQHMMNVHSQEKSFECK
MCGKSFKRSSTLSTHLLIHS DTRPYPCQYCGKRFHQKSDMKKHTYIHTGEKPHKCQ
VCGKAFSQSSNLITHSRKHTGFKPFGCDICSKGFQRKVDLRRHHESQHGMK

>human GFI1B

MPRSFLVKSKKAHTYHQPRVQEDEPLWPPALTPVPRDQAPSNSPVLSTLFPNQCL
DWTNLKREPELEQDQNLARMAPAPEGPIVLSRPQDGDSP LSDSPPFYKPSFSWDT
LATTYGHSYRQAPSTMQSAFLEHSVSLYGSPLVPSTEPALDFSLRYS PGMDAYHCV
KCNKVFSTPHGLEVHVRRSHSGTRPFACDICGKTFGHAVSLEQHTHVHSQERSFE
CRMCGKAFKRSSTLSTHLLIHS DTRPYPCQFCGKRFHQKSDMKKHTYIHTGEKPHK
CQVCGKAFSQSSNLITHSRKHTGFKPFSCELCTKGFQRKVDLRRHRESQHNLK

>human GFI1

MPRSFLVKSKKAHSYHQPRSPGPDYSLRLENVPAPSRADSTSNAGGAKAEPRDRL
SPESQLTEAPDRASASPDSCEGSVCERSSEFEDFWRPPSPSASPASEKSMCPSLD
EAQPFPLPFKPYSWGLAGSDLRHLVQSYRPCGALERGAGLGLFCEPAPEPGHPA
ALYGPKRAAGGAGAGAPGSCSAGAGATAGPGLGLYGDFGSAAAGLYERPTAAAG

LLYPERGHGLHADKGAGVKVESELLCTRLLLGGGSYKCIKCSKVFSTPHGLEVHVR
RSHSGTRPFACEMCGKTFGHAVSLEQHKAVHSQERSFDCKICGKSFKRSSTLSTHL
LIHSDTRPYPCQYCGKRFHQKSDMKKHTFIHTGEKPHKCQVCGKAFSQQSSNLITHS
RKHTGFKPFGCDLCGKGFQRKVDLRRHRETQHGLK

>mouse GF11

MPRSFLVKSKKAHSYHQPRSPGPDYSLRLETVPAPGRAEGGAVSAGESKMEPRER
LSPDSQLTEAPDRASASPNSCEGSVCDPCSEFEDFWRPPSPSVSPASEKSLCRSL
DEAQPYTLPFKPYAWSGLAGSDLRHLVQSYRQCSALERSAGLSLFCERGSEPGRP
AARYGPEQAAGGAGAGQPGSCGVAGGATSAAGLGLYGDFAPAAAGLYERPSTAA
GRLYQDHGHELHADKSVGKVESELLCTRLLLGGGSYKCIKCSKVFSTPHGLEVHV
RRSHS GTRPFACEMCGKTFGHAVSL EQHKAVHSQERSFDCKICGK
SFKRSSTLSTHLLIHS DTRPYPCQYCGKRFHQKSDMKKHTFIHTGEKPHKCQVCGK
AFSQQSSNLITHSRKHTGFKPFGCDLCGKGFQRKVDLRRHRETQH

>mouse GF11B

MPRSFLVKSKKAHTYHQPRAQGDELWPPAVIPVAKEHSQSASPLLSTPLPSQTLTLD
WNTIKQEREMLLNQSLPKMASAPEGPLVTPQPQDGESPLSESPFYKPSFSWDTL
ASSYSHSYTQTPSTMQSAFLERSVRLYGSPVPSTESPLDFRLRYSPGMDTYHCVK
CNKVFSTPHGLEVHVRRSHSGTRPFACDVCGKTFGHAVSLEQHTHVHSQERSFEC
RMCGKAFKRSSTLSTHLLIHS DTRPYPCQFCGKRFHQKSDMKKHTYIHTGEKPHKC
QVCGKAFSQQSSNLITHSRKHTGFKPFSCLECTKGFQRKVDLRRHRESQHNLK

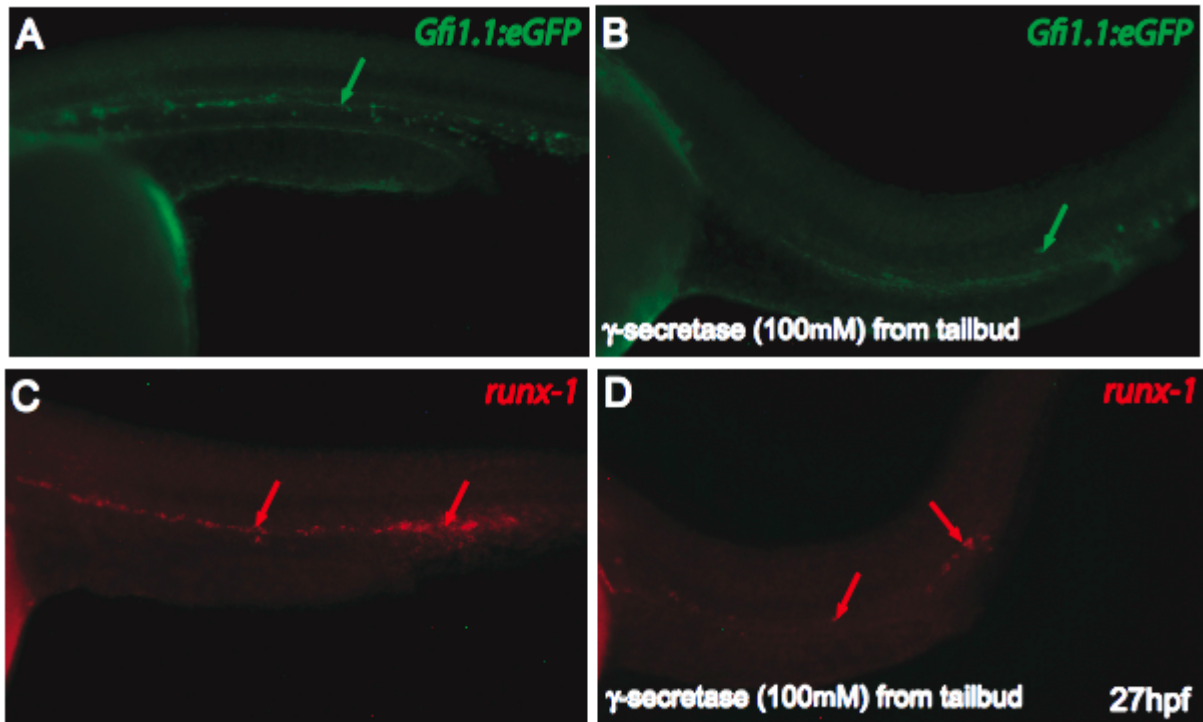


Figure 3, supplemental data: *runx1* and *I-551* expression in the ventral artery are lost in DAPM treated embryos In untreated embryos, *I-551* expression can be detected in the ventral wall of the DA (A, green arrow) similar to *runx1* (C, red arrows). In embryos treated with DAPM, endothelial *I-551:eGFP* expression is lost in 24/25 embryos(B, green arrow) and *runx1* is severely decreased in 23/25 (D, red arrow). Embryos were subject to either immunohistochemistry for eGFP or *runx1* in situ at 27 hpf.

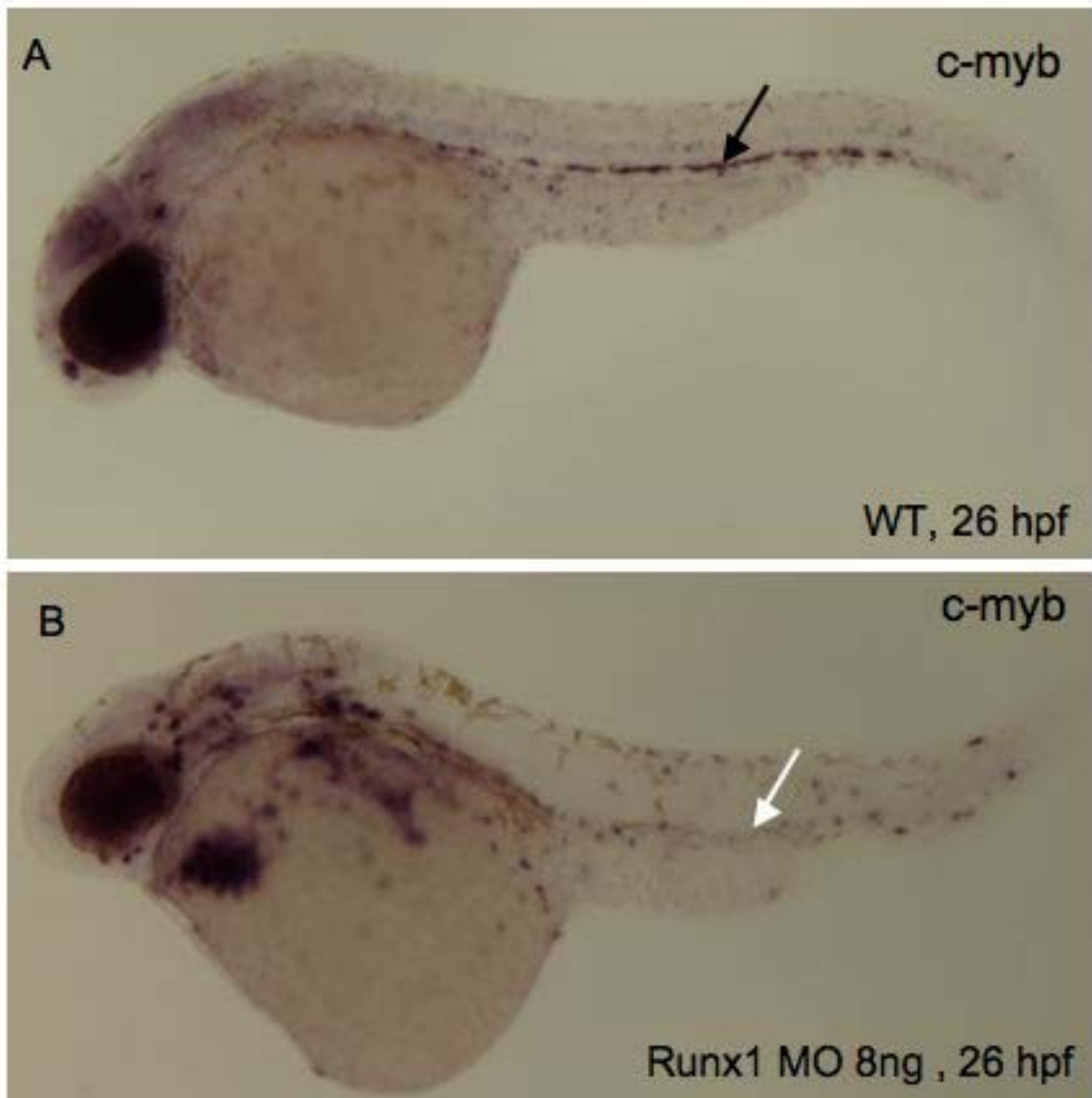
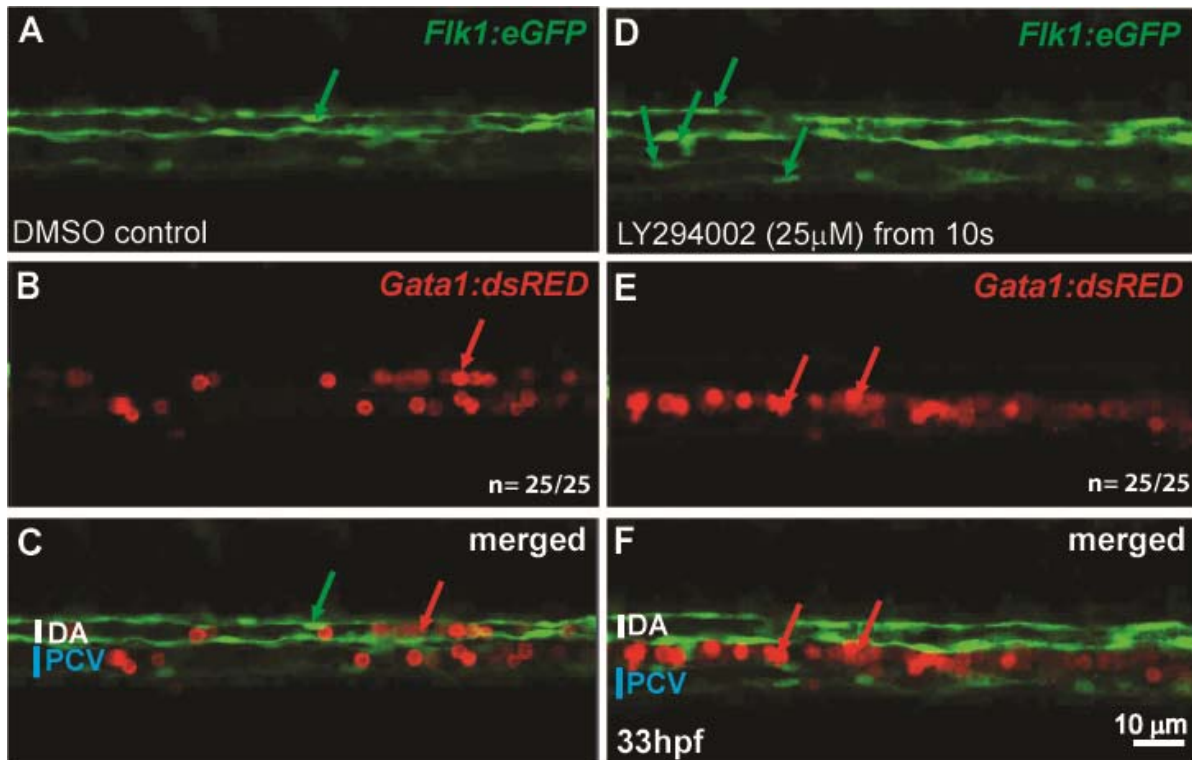


Figure 4, supplemental data: *c-myb* positive cells are decreased in *runx1* morphants In WT embryos *c-myb* is expressed in the ventral wall of the DA at 26 hpf (A, black arrow). This expression is lost in embryos (23/30) injected with 8 ng of *runx1* antisense morpholino (B, white line).



Supplemental Figure 5: Primitive red blood cells in Ly 294002- treated embryos are stuck between the blood vessels *Flik1:eGFP* and *Gata1:dsRED* double transgenic embryos were treated with 25 μM of *Ly294002* from 10 somite stage. Control embryos were treated with an equal amount of DMSO. In DMSO-treated embryos, blood circulation is established and *Gata1* positive cells are in circulation (B and C). In *Ly294002*- treated embryos, the blood circulation is poor and *gata1* positive cells seem to be stuck between the endothelium. The green arrows in D point at individual endothelial cells in the DA and PCV. In D it appears that there is a gap between the ventral wall of the DA and the dorsal wall of the PCV. Primitive red blood cells are located just in the gap (D and F).

References

- Alvarez-Silva, M., P. Belo-Diabangouaya, et al. (2003). "Mouse placenta is a major hematopoietic organ." *Development* 130(22): 5437-44.
- Amsterdam, A. (2003). "Insertional mutagenesis in zebrafish." *Dev Dyn* 228(3): 523-34.
- Amsterdam, A., S. Burgess, et al. (1999). "A large-scale insertional mutagenesis screen in zebrafish." *Genes Dev* 13(20): 2713-24.
- Amsterdam, A. and N. Hopkins (2006). "Mutagenesis strategies in zebrafish for identifying genes involved in development and disease." *Trends Genet* 22(9): 473-8.
- Amsterdam, A., S. Lin, et al. (1995). "The *Aequorea victoria* green fluorescent protein can be used as a reporter in live zebrafish embryos." *Dev Biol* 171(1): 123-9.
- Amsterdam, A., R. M. Nissen, et al. (2004). "Identification of 315 genes essential for early zebrafish development." *Proc Natl Acad Sci U S A* 101(35): 12792-7.
- Anguita, E., A. Villegas, et al. "GF11B controls its own expression binding to multiple sites." *Haematologica* 95(1): 36-46.
- Arslanova, D., T. Yang, et al. "Phenotypic analysis of images of zebrafish treated with Alzheimer's gamma-secretase inhibitors." *BMC Biotechnol* 10: 24.
- Balciunas, D., K. J. Wangensteen, et al. (2006). "Harnessing a high cargo-capacity transposon for genetic applications in vertebrates." *PLoS Genet* 2(11): e169.
- Becker, A. J., C. E. Mc, et al. (1963). "Cytological demonstration of the clonal nature of spleen colonies derived from transplanted mouse marrow cells." *Nature* 197: 452-4.
- Bertrand, J. Y., N. C. Chi, et al. "Haematopoietic stem cells derive directly from aortic endothelium during development." *Nature* 464(7285): 108-11.

Bertrand, J. Y., J. L. Cisson, et al. "Notch signaling distinguishes 2 waves of definitive hematopoiesis in the zebrafish embryo." *Blood* 115(14): 2777-83.

Bertrand, J. Y., S. Giroux, et al. (2005). "Characterization of purified intraembryonic hematopoietic stem cells as a tool to define their site of origin." *Proc Natl Acad Sci U S A* 102(1): 134-9.

Bertrand, J. Y., A. D. Kim, et al. (2008). "CD41+ cmyb+ precursors colonize the zebrafish pronephros by a novel migration route to initiate adult hematopoiesis." *Development* 135(10): 1853-62.

Bertrand, J. Y., A. D. Kim, et al. (2007). "Definitive hematopoiesis initiates through a committed erythromyeloid progenitor in the zebrafish embryo." *Development* 134(23): 4147-56.

Bigas, A., A. Robert-Moreno, et al. "The Notch pathway in the developing hematopoietic system." *Int J Dev Biol* 54(6-7): 1175-88.

Bolli, N., E. M. Payne, et al. "cpsf1 is required for definitive HSC survival in zebrafish." *Blood* 117(15): 3996-4007.

Borggreffe, T. and F. Oswald (2009). "The Notch signaling pathway: transcriptional regulation at Notch target genes." *Cell Mol Life Sci* 66(10): 1631-46.

Brown, L. A., A. R. Rodaway, et al. (2000). "Insights into early vasculogenesis revealed by expression of the ETS-domain transcription factor Fli-1 in wild-type and mutant zebrafish embryos." *Mech Dev* 90(2): 237-52.

Bryder, D., D. J. Rossi, et al. (2006). "Hematopoietic stem cells: the paradigmatic tissue-specific stem cell." *Am J Pathol* 169(2): 338-46.

Burns, C. E., T. DeBlasio, et al. (2002). "Isolation and characterization of runxa and runxb, zebrafish members of the runt family of transcriptional regulators." *Exp Hematol* 30(12): 1381-9.

Burns, C. E., D. Traver, et al. (2005). "Hematopoietic stem cell fate is established by the Notch-Runx pathway." *Genes Dev* 19(19): 2331-42.

Cai, Z., M. de Bruijn, et al. (2000). "Haploinsufficiency of AML1 affects the temporal and spatial generation of hematopoietic stem cells in the mouse embryo." *Immunity* 13(4): 423-31.

Chakrabarti, S., G. Streisinger, et al. (1983). "Frequency of gamma-Ray Induced Specific Locus and Recessive Lethal Mutations in Mature Germ Cells of the Zebrafish, BRACHYDANIO RERIO." *Genetics* 103(1): 109-23.

Challen, G. A., N. Boles, et al. (2009). "Mouse hematopoietic stem cell identification and analysis." *Cytometry A* 75(1): 14-24.

Chen, M. J., T. Yokomizo, et al. (2009). "Runx1 is required for the endothelial to haematopoietic cell transition but not thereafter." *Nature* 457(7231): 887-91.

Choi, K., M. Kennedy, et al. (1998). "A common precursor for hematopoietic and endothelial cells." *Development* 125(4): 725-32.

Ciau-Uitz, A., M. Walmsley, et al. (2000). "Distinct origins of adult and embryonic blood in *Xenopus*." *Cell* 102(6): 787-96.

Clarke, D., A. Vegiopoulos, et al. (2000). "In vitro differentiation of c-myb(-/-) ES cells reveals that the colony forming capacity of unilineage macrophage precursors and myeloid progenitor commitment are c-Myb independent." *Oncogene* 19(30): 3343-51.

Clements, W. K., A. D. Kim, et al. "A somitic Wnt16/Notch pathway specifies haematopoietic stem cells." *Nature* 474(7350): 220-4.

Corbel, C., J. Salaun, et al. (2007). "Hematopoietic potential of the pre-fusion allantois." *Dev Biol* 301(2): 478-88.

Corbel, M., N. Germain, et al. (2002). "The selective phosphodiesterase 4 inhibitor RP 73-401 reduced matrix metalloproteinase 9 activity and transforming growth factor-beta release during acute lung injury in mice: the role of the balance between

Tumor necrosis factor-alpha and interleukin-10." *J Pharmacol Exp Ther* 301(1): 258-65.

Corey, D. R. and J. M. Abrams (2001). "Morpholino antisense oligonucleotides: tools for investigating vertebrate development." *Genome Biol* 2(5): REVIEWS1015.

Culp, P., C. Nusslein-Volhard, et al. (1991). "High-frequency germ-line transmission of plasmid DNA sequences injected into fertilized zebrafish eggs." *Proc Natl Acad Sci U S A* 88(18): 7953-7.

Cumano, A., F. Dieterlen-Lievre, et al. (1996). "Lymphoid potential, probed before circulation in mouse, is restricted to caudal intraembryonic splanchnopleura." *Cell* 86(6): 907-16.

Cumano, A., F. Dieterlen-Lievre, et al. (1996). "Lymphoid potential, probed before circulation in mouse, is restricted to caudal intraembryonic splanchnopleura." *Cell* 86(6): 907-16.

Cumano, A., J. C. Ferraz, et al. (2001). "Intraembryonic, but not yolk sac hematopoietic precursors, isolated before circulation, provide long-term multilineage reconstitution." *Immunity* 15(3): 477-85.

Cumano, A., C. Furlonger, et al. (1993). "Differentiation and characterization of B-cell precursors detected in the yolk sac and embryo body of embryos beginning at the 10- to 12-somite stage." *Proc Natl Acad Sci U S A* 90(14): 6429-33.

Cumano, A. and I. Godin (2007). "Ontogeny of the hematopoietic system." *Annu Rev Immunol* 25: 745-85.

Dabrowska, M. J., K. Dybkaer, et al. (2009). "Loss of MicroRNA targets in the 3' untranslated region as a mechanism of retroviral insertional activation of growth factor independence 1." *J Virol* 83(16): 8051-61.

Danilova, N. and L. A. Steiner (2002). "B cells develop in the zebrafish pancreas." *Proc Natl Acad Sci U S A* 99(21): 13711-6.

Davidson, A. E., D. Balciunas, et al. (2003). "Efficient gene delivery and gene expression in zebrafish using the Sleeping Beauty transposon." *Dev Biol* 263(2): 191-202.

Davidson, A. J. and L. I. Zon (2004). "The 'definitive' (and 'primitive') guide to zebrafish hematopoiesis." *Oncogene* 23(43): 7233-46.

de Bruijn, M. F., X. Ma, et al. (2002). "Hematopoietic stem cells localize to the endothelial cell layer in the midgestation mouse aorta." *Immunity* 16(5): 673-83.

de Bruijn, M. F., N. A. Speck, et al. (2000). "Definitive hematopoietic stem cells first develop within the major arterial regions of the mouse embryo." *EMBO J* 19(11): 2465-74.

De Val, S. "Key transcriptional regulators of early vascular development." *Arterioscler Thromb Vasc Biol* 31(7): 1469-75.

Detrich, H. W., 3rd, M. W. Kieran, et al. (1995). "Intraembryonic hematopoietic cell migration during vertebrate development." *Proc Natl Acad Sci U S A* 92(23): 10713-7.

Dieterlen-Lievre, F. (1975). "On the origin of haemopoietic stem cells in the avian embryo: an experimental approach." *J Embryol Exp Morphol* 33(3): 607-19.

Dieterlen-Lievre, F. and C. Martin (1981). "Diffuse intraembryonic hemopoiesis in normal and chimeric avian development." *Dev Biol* 88(1): 180-91.

Doan, L. L., S. D. Porter, et al. (2004). "Targeted transcriptional repression of Gfi1 by GFI1 and GFI1B in lymphoid cells." *Nucleic Acids Res* 32(8): 2508-19.

Doyon, Y., J. M. McCammon, et al. (2008). "Heritable targeted gene disruption in zebrafish using designed zinc-finger nucleases." *Nat Biotechnol* 26(6): 702-8.

Driever, W., L. Solnica-Krezel, et al. (1996). "A genetic screen for mutations affecting embryogenesis in zebrafish." *Development* 123: 37-46.

Duan, Z., A. Zarebski, et al. (2005). "Gfi1 coordinates epigenetic repression of p21Cip/WAF1 by recruitment of histone lysine methyltransferase G9a and histone deacetylase 1." *Mol Cell Biol* 25(23): 10338-51.

Dufourcq, P., S. Rastegar, et al. (2004). "Parapineal specific expression of gfi1 in the zebrafish epithalamus." *Gene Expr Patterns* 4(1): 53-7.

Dzierzak, E. and N. A. Speck (2008). "Of lineage and legacy: the development of mammalian hematopoietic stem cells." *Nat Immunol* 9(2): 129-36.

Echeverri, K. and A. C. Oates (2007). "Coordination of symmetric cyclic gene expression during somitogenesis by Suppressor of Hairless involves regulation of retinoic acid catabolism." *Dev Biol* 301(2): 388-403.

Ellingsen, S., M. A. Laplante, et al. (2005). "Large-scale enhancer detection in the zebrafish genome." *Development* 132(17): 3799-811.

Emambokus, N. R. and J. Frampton (2003). "The glycoprotein IIb molecule is expressed on early murine hematopoietic progenitors and regulates their numbers in sites of hematopoiesis." *Immunity* 19(1): 33-45.

Emerson, S. G., B. O. Palsson, et al. (1991). "The construction of high efficiency human bone marrow tissue ex vivo." *J Cell Biochem* 45(3): 268-72.

Fehling, H. J., G. Lacaud, et al. (2003). "Tracking mesoderm induction and its specification to the hemangioblast during embryonic stem cell differentiation." *Development* 130(17): 4217-27.

Ferrara, N., K. Carver-Moore, et al. (1996). "Heterozygous embryonic lethality induced by targeted inactivation of the VEGF gene." *Nature* 380(6573): 439-42.

Foley, J. E., M. L. Maeder, et al. (2009). "Targeted mutagenesis in zebrafish using customized zinc-finger nucleases." *Nat Protoc* 4(12): 1855-67.

Fouquet, B., B. M. Weinstein, et al. (1997). "Vessel patterning in the embryo of the zebrafish: guidance by notochord." *Dev Biol* 183(1): 37-48.

Gaiano, N., A. Amsterdam, et al. (1996). "Insertional mutagenesis and rapid cloning of essential genes in zebrafish." *Nature* 383(6603): 829-32.

Gaiano, N. and N. Hopkins (1996). "Introducing genes into zebrafish." *Biochim Biophys Acta* 1288(1): O11-4.

Galloway, J. L., R. A. Wingert, et al. (2005). "Loss of *gata1* but not *gata2* converts erythropoiesis to myelopoiesis in zebrafish embryos." *Dev Cell* 8(1): 109-16.

Gekas, C., F. Dieterlen-Lievre, et al. (2005). "The placenta is a niche for hematopoietic stem cells." *Dev Cell* 8(3): 365-75.

Georgopoulos, K., S. Winandy, et al. (1997). "The role of the *Ikaros* gene in lymphocyte development and homeostasis." *Annu Rev Immunol* 15: 155-76.

Gering, M. and R. Patient "Notch signalling and haematopoietic stem cell formation during embryogenesis." *J Cell Physiol* 222(1): 11-6.

Gering, M. and R. Patient (2005). "Hedgehog signaling is required for adult blood stem cell formation in zebrafish embryos." *Dev Cell* 8(3): 389-400.

Gering, M., A. R. Rodaway, et al. (1998). "The *SCL* gene specifies haemangioblast development from early mesoderm." *EMBO J* 17(14): 4029-45.

Gering, M., Y. Yamada, et al. (2003). "*Lmo2* and *Scf/Tal1* convert non-axial mesoderm into haemangioblasts which differentiate into endothelial cells in the absence of *Gata1*." *Development* 130(25): 6187-99.

Gibbs, P. D., A. Gray, et al. (1994). "Inheritance of P element and reporter gene sequences in zebrafish." *Mol Mar Biol Biotechnol* 3(6): 317-26.

Gilks, C. B., S. E. Bear, et al. (1993). "Progression of interleukin-2 (IL-2)-dependent rat T cell lymphoma lines to IL-2-independent growth following activation of a gene (*Gfi-1*) encoding a novel zinc finger protein." *Mol Cell Biol* 13(3): 1759-68.

Godin, I., F. Dieterlen-Lievre, et al. (1995). "Emergence of multipotent hemopoietic cells in the yolk sac and paraaortic splanchnopleura in mouse embryos, beginning at 8.5 days postcoitus." *Proc Natl Acad Sci U S A* 92(3): 773-7.

Godin, I., J. A. Garcia-Porrero, et al. (1999). "Stem cell emergence and hemopoietic activity are incompatible in mouse intraembryonic sites." *J Exp Med* 190(1): 43-52.

Godin, I. E., J. A. Garcia-Porrero, et al. (1993). "Para-aortic splanchnopleura from early mouse embryos contains B1a cell progenitors." *Nature* 364(6432): 67-70.

Goessling, W., T. E. North, et al. (2009). "Genetic interaction of PGE2 and Wnt signaling regulates developmental specification of stem cells and regeneration." *Cell* 136(6): 1136-47.

Golling, G., A. Amsterdam, et al. (2002). "Insertional mutagenesis in zebrafish rapidly identifies genes essential for early vertebrate development." *Nat Genet* 31(2): 135-40.

Goodell, M. A., K. Brose, et al. (1996). "Isolation and functional properties of murine hematopoietic stem cells that are replicating in vivo." *J Exp Med* 183(4): 1797-806.

Greig, K. T., S. Carotta, et al. (2008). "Critical roles for c-Myb in hematopoietic progenitor cells." *Semin Immunol* 20(4): 247-56.

Grimes, H. L., T. O. Chan, et al. (1996). "The Gfi-1 proto-oncoprotein contains a novel transcriptional repressor domain, SNAG, and inhibits G1 arrest induced by interleukin-2 withdrawal." *Mol Cell Biol* 16(11): 6263-72.

Grunwald, D. J. and J. S. Eisen (2002). "Headwaters of the zebrafish -- emergence of a new model vertebrate." *Nat Rev Genet* 3(9): 717-24.

Grunwald, D. J. and G. Streisinger (1992). "Induction of mutations in the zebrafish with ultraviolet light." *Genet Res* 59(2): 93-101.

Haffter, P. and C. Nusslein-Volhard (1996). "Large scale genetics in a small vertebrate, the zebrafish." *Int J Dev Biol* 40(1): 221-7.

Harrison, D. E. (1980). "Competitive repopulation: a new assay for long-term stem cell functional capacity." *Blood* 55(1): 77-81.

Harrison, D. E. and C. M. Astle (1982). "Loss of stem cell repopulating ability upon transplantation. Effects of donor age, cell number, and transplantation procedure." *J Exp Med* 156(6): 1767-79.

Hart, D. O., M. K. Santra, et al. (2009). "Selective interaction between Trf3 and Taf3 required for early development and hematopoiesis." *Dev Dyn* 238(10): 2540-9.

He, S., D. Nakada, et al. (2009). "Mechanisms of stem cell self-renewal." *Annu Rev Cell Dev Biol* 25: 377-406.

Hirsh, D. and R. Vanderslice (1976). "Temperature-sensitive developmental mutants of *Caenorhabditis elegans*." *Dev Biol* 49(1): 220-35.

Hock, H., M. J. Hamblen, et al. (2004). "Gfi-1 restricts proliferation and preserves functional integrity of haematopoietic stem cells." *Nature* 431(7011): 1002-7.

Hock, H., M. J. Hamblen, et al. (2003). "Intrinsic requirement for zinc finger transcription factor Gfi-1 in neutrophil differentiation." *Immunity* 18(1): 109-20.

Hong, C. C., Q. P. Peterson, et al. (2006). "Artery/vein specification is governed by opposing phosphatidylinositol-3 kinase and MAP kinase/ERK signaling." *Curr Biol* 16(13): 1366-72.

Huber, T. L., V. Kouskoff, et al. (2004). "Haemangioblast commitment is initiated in the primitive streak of the mouse embryo." *Nature* 432(7017): 625-30.

Iida, A., K. Sakaguchi, et al. "Metalloprotease-dependent onset of blood circulation in zebrafish." *Curr Biol* 20(12): 1110-6.

Ito, T., N. Udaka, et al. (2000). "Basic helix-loop-helix transcription factors regulate the neuroendocrine differentiation of fetal mouse pulmonary epithelium." *Development* 127(18): 3913-21.

Ivics, Z., M. A. Li, et al. (2009). "Transposon-mediated genome manipulation in vertebrates." *Nat Methods* 6(6): 415-22.

Jaffredo, T., R. Gautier, et al. (2000). "Tracing the progeny of the aortic hemangioblast in the avian embryo." *Dev Biol* 224(2): 204-14.

Jaffredo, T., R. Gautier, et al. (1998). "Intraaortic hemopoietic cells are derived from endothelial cells during ontogeny." *Development* 125(22): 4575-83.

Jaffredo, T., W. Nottingham, et al. (2005). "From hemangioblast to hematopoietic stem cell: an endothelial connection?" *Exp Hematol* 33(9): 1029-40.

Jakobsson, L., K. Bentley, et al. (2009). "VEGFRs and Notch: a dynamic collaboration in vascular patterning." *Biochem Soc Trans* 37(Pt 6): 1233-6.

Jia, Y., G. Xie, et al. (1997). "The *C. elegans* gene *pag-3* is homologous to the zinc finger proto-oncogene *gfi-1*." *Development* 124(10): 2063-73.

Jin, H., R. Sood, et al. (2009). "Definitive hematopoietic stem/progenitor cells manifest distinct differentiation output in the zebrafish VDA and PBI." *Development* 136(4): 647-54.

Jin, H., J. Xu, et al. (2007). "Migratory path of definitive hematopoietic stem/progenitor cells during zebrafish development." *Blood* 109(12): 5208-14.

Kalev-Zylinska, M. L., J. A. Horsfield, et al. (2002). "Runx1 is required for zebrafish blood and vessel development and expression of a human RUNX1-CBF2T1 transgene advances a model for studies of leukemogenesis." *Development* 129(8): 2015-30.

Kawakami, K., K. Imanaka, et al. (2004). "Excision of the Tol2 transposable element of the medaka fish *Oryzias latipes* in *Xenopus laevis* and *Xenopus tropicalis*." *Gene* 338(1): 93-8.

Kawakami, K., A. Koga, et al. (1998). "Excision of the tol2 transposable element of the medaka fish, *Oryzias latipes*, in zebrafish, *Danio rerio*." *Gene* 225(1-2): 17-22.

Kawakami, K., A. Shima, et al. (2000). "Identification of a functional transposase of the Tol2 element, an Ac-like element from the Japanese medaka fish, and its transposition in the zebrafish germ lineage." *Proc Natl Acad Sci U S A* 97(21): 11403-8.

Kawakami, K., H. Takeda, et al. (2004). "A transposon-mediated gene trap approach identifies developmentally regulated genes in zebrafish." *Dev Cell* 7(1): 133-44.

Kazanjian, A., D. Wallis, et al. (2004). "Growth factor independence-1 is expressed in primary human neuroendocrine lung carcinomas and mediates the differentiation of murine pulmonary neuroendocrine cells." *Cancer Res* 64(19): 6874-82.

Kazazian, H. H., Jr. (2004). "Mobile elements: drivers of genome evolution." *Science* 303(5664): 1626-32.

Kennedy, M., M. Firpo, et al. (1997). "A common precursor for primitive erythropoiesis and definitive haematopoiesis." *Nature* 386(6624): 488-93.

Khandanpour, C., C. Kosan, et al. "Growth Factor Independence 1 (Gfi1) Protects Hematopoietic Stem Cells Against Apoptosis But Also Prevents the Development of a Myeloproliferative-Like Disease." *Stem Cells*.

Khandanpour, C., E. Sharif-Askari, et al. "Evidence that growth factor independence 1b regulates dormancy and peripheral blood mobilization of hematopoietic stem cells." *Blood* 116(24): 5149-61.

Kiel, M. J., O. H. Yilmaz, et al. (2005). "SLAM family receptors distinguish hematopoietic stem and progenitor cells and reveal endothelial niches for stem cells." *Cell* 121(7): 1109-21.

Kimmel, C. B., W. W. Ballard, et al. (1995). "Stages of embryonic development of the zebrafish." *Dev Dyn* 203(3): 253-310.

Kimmel, C. B., S. L. Powell, et al. (1982). "Brain neurons which project to the spinal cord in young larvae of the zebrafish." *J Comp Neurol* 205(2): 112-27.

Kingsley, P. D., J. Malik, et al. (2004). "Yolk sac-derived primitive erythroblasts enucleate during mammalian embryogenesis." *Blood* 104(1): 19-25.

Kissa, K. and P. Herbomel "Blood stem cells emerge from aortic endothelium by a novel type of cell transition." *Nature* 464(7285): 112-5.

Kissa, K., E. Murayama, et al. (2008). "Live imaging of emerging hematopoietic stem cells and early thymus colonization." *Blood* 111(3): 1147-56.

Kitaguchi, T., K. Kawakami, et al. (2009). "Transcriptional regulation of a myeloid-lineage specific gene lysozyme C during zebrafish myelopoiesis." *Mech Dev* 126(5-6): 314-23.

Knapik, E. W., A. Goodman, et al. (1996). "A reference cross DNA panel for zebrafish (*Danio rerio*) anchored with simple sequence length polymorphisms." *Development* 123: 451-60.

Knapik, E. W., A. Goodman, et al. (1998). "A microsatellite genetic linkage map for zebrafish (*Danio rerio*)." *Nat Genet* 18(4): 338-43.

Koga, A., A. Shimada, et al. (2007). "The Tol1 transposable element of the medaka fish moves in human and mouse cells." *J Hum Genet* 52(7): 628-35.

Koga, A., M. Suzuki, et al. (1996). "Transposable element in fish." *Nature* 383(6595): 30.

Kondo, M. "Lymphoid and myeloid lineage commitment in multipotent hematopoietic progenitors." *Immunol Rev* 238(1): 37-46.

Korzh, V. (2007). "Transposons as tools for enhancer trap screens in vertebrates." *Genome Biol* 8 Suppl 1: S8.

Kotani, T., S. Nagayoshi, et al. (2006). "Transposon-mediated gene trapping in zebrafish." *Methods* 39(3): 199-206.

Kumano, K., S. Chiba, et al. (2003). "Notch1 but not Notch2 is essential for generating hematopoietic stem cells from endothelial cells." *Immunity* 18(5): 699-711.

Lam, E. Y., J. Y. Chau, et al. (2009). "Zebrafish runx1 promoter-EGFP transgenics mark discrete sites of definitive blood progenitors." *Blood* 113(6): 1241-9.

Lam, E. Y., C. J. Hall, et al. "Live imaging of Runx1 expression in the dorsal aorta tracks the emergence of blood progenitors from endothelial cells." *Blood* 116(6): 909-14.

Lancrin, C., P. Sroczynska, et al. (2009). "The haemangioblast generates haematopoietic cells through a haemogenic endothelium stage." *Nature* 457(7231): 892-5.

Lawson, N. D., A. M. Vogel, et al. (2002). "sonic hedgehog and vascular endothelial growth factor act upstream of the Notch pathway during arterial endothelial differentiation." *Dev Cell* 3(1): 127-36.

Lawson, N. D. and B. M. Weinstein (2002). "In vivo imaging of embryonic vascular development using transgenic zebrafish." *Dev Biol* 248(2): 307-18.

Lee, S., K. Doddapaneni, et al. "Solution structure of Gfi-1 zinc domain bound to consensus DNA." *J Mol Biol* 397(4): 1055-66.

Lemischka, I. R., D. H. Raulet, et al. (1986). "Developmental potential and dynamic behavior of hematopoietic stem cells." *Cell* 45(6): 917-27.

Liang, D., J. R. Chang, et al. (2001). "The role of vascular endothelial growth factor (VEGF) in vasculogenesis, angiogenesis, and hematopoiesis in zebrafish development." *Mech Dev* 108(1-2): 29-43.

Liang, D., X. Xu, et al. (1998). "Cloning and characterization of vascular endothelial growth factor (VEGF) from zebrafish, *Danio rerio*." *Biochim Biophys Acta* 1397(1): 14-20.

Liao, E. C., B. H. Paw, et al. (1998). "SCL/Tal-1 transcription factor acts downstream of cloche to specify hematopoietic and vascular progenitors in zebrafish." *Genes Dev* 12(5): 621-6.

Liao, W., B. W. Bisgrove, et al. (1997). "The zebrafish gene *cloche* acts upstream of a *flk-1* homologue to regulate endothelial cell differentiation." *Development* 124(2): 381-9.

Liao, W., C. Y. Ho, et al. (2000). "Hhex and *scl* function in parallel to regulate early endothelial and blood differentiation in zebrafish." *Development* 127(20): 4303-13.

Lieschke, G. J., A. C. Oates, et al. (2002). "Zebrafish SPI-1 (PU.1) marks a site of myeloid development independent of primitive erythropoiesis: implications for axial patterning." *Dev Biol* 246(2): 274-95.

Lin, H. F., D. Traver, et al. (2005). "Analysis of thrombocyte development in CD41-GFP transgenic zebrafish." *Blood* 106(12): 3803-10.

Lin, S., N. Gaiano, et al. (1994). "Integration and germ-line transmission of a pseudotyped retroviral vector in zebrafish." *Science* 265(5172): 666-9.

Long, Q., A. Meng, et al. (1997). "GATA-1 expression pattern can be recapitulated in living transgenic zebrafish using GFP reporter gene." *Development* 124(20): 4105-11.

Lucitti, J. L., E. A. Jones, et al. (2007). "Vascular remodeling of the mouse yolk sac requires hemodynamic force." *Development* 134(18): 3317-26.

Lux, C. T., M. Yoshimoto, et al. (2008). "All primitive and definitive hematopoietic progenitor cells emerging before E10 in the mouse embryo are products of the yolk sac." *Blood* 111(7): 3435-8.

Ma, D., J. Zhang, et al. "The identification and characterization of zebrafish hematopoietic stem cells." *Blood* 118(2): 289-97.

Mansour, S. L., K. R. Thomas, et al. (1988). "Disruption of the proto-oncogene *int-2* in mouse embryo-derived stem cells: a general strategy for targeting mutations to non-selectable genes." *Nature* 336(6197): 348-52.

Marteijn, J. A., L. T. van der Meer, et al. (2007). "Diminished proteasomal degradation results in accumulation of Gfi1 protein in monocytes." *Blood* 109(1): 100-8.

Mates, L., Z. Izsvak, et al. (2007). "Technology transfer from worms and flies to vertebrates: transposition-based genome manipulations and their future perspectives." *Genome Biol* 8 Suppl 1: S1.

McCulloch, E. A. and J. E. Till (1960). "The radiation sensitivity of normal mouse bone marrow cells, determined by quantitative marrow transplantation into irradiated mice." *Radiat Res* 13: 115-25.

Medvinsky, A. and E. Dzierzak (1996). "Definitive hematopoiesis is autonomously initiated by the AGM region." *Cell* 86(6): 897-906.

Medvinsky, A. L., N. L. Samoylina, et al. (1993). "An early pre-liver intraembryonic source of CFU-S in the developing mouse." *Nature* 364(6432): 64-7.

Meng, X., M. B. Noyes, et al. (2008). "Targeted gene inactivation in zebrafish using engineered zinc-finger nucleases." *Nat Biotechnol* 26(6): 695-701.

Mikkola, H. K., Y. Fujiwara, et al. (2003). "Expression of CD41 marks the initiation of definitive hematopoiesis in the mouse embryo." *Blood* 101(2): 508-16.

Mikkola, H. K. and S. H. Orkin (2006). "The journey of developing hematopoietic stem cells." *Development* 133(19): 3733-44.

Miskey, C., Z. Izsvak, et al. (2005). "DNA transposons in vertebrate functional genomics." *Cell Mol Life Sci* 62(6): 629-41.

Miskey, C., Z. Izsvak, et al. (2003). "The Frog Prince: a reconstructed transposon from *Rana pipiens* with high transpositional activity in vertebrate cells." *Nucleic Acids Res* 31(23): 6873-81.

Moens, C. B., T. M. Donn, et al. (2008). "Reverse genetics in zebrafish by TILLING." *Brief Funct Genomic Proteomic* 7(6): 454-9.

Monteiro, R., C. Pouget, et al. "The gata1/pu.1 lineage fate paradigm varies between blood populations and is modulated by tif1gamma." *EMBO J* 30(6): 1093-103.

Moore, M. A. and D. Metcalf (1970). "Ontogeny of the haemopoietic system: yolk sac origin of in vivo and in vitro colony forming cells in the developing mouse embryo." *Br J Haematol* 18(3): 279-96.

Moore, M. A. and J. J. Owen (1965). "Chromosome marker studies on the development of the haemopoietic system in the chick embryo." *Nature* 208(5014): 956 passim.

Moore, M. A. and J. J. Owen (1967). "Chromosome marker studies in the irradiated chick embryo." *Nature* 215(5105): 1081-2.

Moore, M. A. and J. J. Owen (1967). "Experimental studies on the development of the thymus." *J Exp Med* 126(4): 715-26.

Morrison, S. J. and I. L. Weissman (1994). "The long-term repopulating subset of hematopoietic stem cells is deterministic and isolatable by phenotype." *Immunity* 1(8): 661-73.

Mucenski, M. L., K. McLain, et al. (1991). "A functional c-myb gene is required for normal murine fetal hepatic hematopoiesis." *Cell* 65(4): 677-89.

Mukoyama, Y., N. Chiba, et al. (1999). "Hematopoietic cells in cultures of the murine embryonic aorta-gonad-mesonephros region are induced by c-Myb." *Curr Biol* 9(15): 833-6.

Muller, A. M., A. Medvinsky, et al. (1994). "Development of hematopoietic stem cell activity in the mouse embryo." *Immunity* 1(4): 291-301.

Muller-Sieburg, C. E., C. A. Whitlock, et al. (1986). "Isolation of two early B lymphocyte progenitors from mouse marrow: a committed pre-pre-B cell and a clonogenic Thy-1-lo hematopoietic stem cell." *Cell* 44(4): 653-62.

Murayama, E., K. Kissa, et al. (2006). "Tracing hematopoietic precursor migration to successive hematopoietic organs during zebrafish development." *Immunity* 25(6): 963-75.

Nasevicius, A., J. Larson, et al. (2000). "Distinct requirements for zebrafish angiogenesis revealed by a VEGF-A morphant." *Yeast* 17(4): 294-301.

Nichogiannopoulou, A., M. Trevisan, et al. (1999). "Defects in hemopoietic stem cell activity in Ikaros mutant mice." *J Exp Med* 190(9): 1201-14.

Nishikawa, S. I., S. Nishikawa, et al. (1998). "In vitro generation of lymphohematopoietic cells from endothelial cells purified from murine embryos." *Immunity* 8(6): 761-9.

Nolo, R., L. A. Abbott, et al. (2000). "Senseless, a Zn finger transcription factor, is necessary and sufficient for sensory organ development in *Drosophila*." *Cell* 102(3): 349-62.

North, T., T. L. Gu, et al. (1999). "Cbfa2 is required for the formation of intra-aortic hematopoietic clusters." *Development* 126(11): 2563-75.

North, T. E., I. R. Babu, et al. "PGE2-regulated wnt signaling and N-acetylcysteine are synergistically hepatoprotective in zebrafish acetaminophen injury." *Proc Natl Acad Sci U S A* 107(40): 17315-20.

North, T. E., M. F. de Bruijn, et al. (2002). "Runx1 expression marks long-term repopulating hematopoietic stem cells in the midgestation mouse embryo." *Immunity* 16(5): 661-72.

North, T. E., W. Goessling, et al. (2009). "Hematopoietic stem cell development is dependent on blood flow." *Cell* 137(4): 736-48.

North, T. E., W. Goessling, et al. (2007). "Prostaglandin E2 regulates vertebrate haematopoietic stem cell homeostasis." *Nature* 447(7147): 1007-11.

Nusslein-Volhard, C. and E. Wieschaus (1980). "Mutations affecting segment number and polarity in *Drosophila*." *Nature* 287(5785): 795-801.

Ogawa, M., S. Nishikawa, et al. (1988). "B cell ontogeny in murine embryo studied by a culture system with the monolayer of a stromal cell clone, ST2: B cell progenitor develops first in the embryonal body rather than in the yolk sac." *EMBO J* 7(5): 1337-43.

Okada, S., H. Nakauchi, et al. (1992). "In vivo and in vitro stem cell function of c-kit- and Sca-1-positive murine hematopoietic cells." *Blood* 80(12): 3044-50.

Okuda, T., J. van Deursen, et al. (1996). "AML1, the target of multiple chromosomal translocations in human leukemia, is essential for normal fetal liver hematopoiesis." *Cell* 84(2): 321-30.

Oleykowski, C. A., C. R. Bronson Mullins, et al. (1998). "Mutation detection using a novel plant endonuclease." *Nucleic Acids Res* 26(20): 4597-602.

Osawa, M., K. Hanada, et al. (1996). "Long-term lymphohematopoietic reconstitution by a single CD34-low/negative hematopoietic stem cell." *Science* 273(5272): 242-5.

Ottersbach, K. and E. Dzierzak (2005). "The murine placenta contains hematopoietic stem cells within the vascular labyrinth region." *Dev Cell* 8(3): 377-87.

Paik, E. J. and L. I. Zon "Hematopoietic development in the zebrafish." *Int J Dev Biol* 54(6-7): 1127-37.

Palis, J. (2008). "Ontogeny of erythropoiesis." *Curr Opin Hematol* 15(3): 155-61.

Palis, J., S. Robertson, et al. (1999). "Development of erythroid and myeloid progenitors in the yolk sac and embryo proper of the mouse." *Development* 126(22): 5073-84.

Palis, J. and M. C. Yoder (2001). "Yolk-sac hematopoiesis: the first blood cells of mouse and man." *Exp Hematol* 29(8): 927-36.

Papathanasiou, P., J. L. Attema, et al. (2009). "Self-renewal of the long-term reconstituting subset of hematopoietic stem cells is regulated by Ikaros." *Stem Cells* 27(12): 3082-92.

Paratore, C., U. Suter, et al. (1999). "Embryonic gene expression resolved at the cellular level by fluorescence in situ hybridization." *Histochem Cell Biol* 111(6): 435-43.

Parinov, S., I. Kondrichin, et al. (2004). "Tol2 transposon-mediated enhancer trap to identify developmentally regulated zebrafish genes in vivo." *Dev Dyn* 231(2): 449-59.

Patterson, L. J., M. Gering, et al. (2007). "The transcription factors Scl and Lmo2 act together during development of the hemangioblast in zebrafish." *Blood* 109(6): 2389-98.

Patterson, L. J., M. Gering, et al. (2005). "Scl is required for dorsal aorta as well as blood formation in zebrafish embryos." *Blood* 105(9): 3502-11.

Persons, D. A. (2009). "Hematopoietic stem cell gene transfer for the treatment of hemoglobin disorders." *Hematology Am Soc Hematol Educ Program*: 690-7.

Pham, V. N., N. D. Lawson, et al. (2007). "Combinatorial function of ETS transcription factors in the developing vasculature." *Dev Biol* 303(2): 772-83.

Phng, L. K. and H. Gerhardt (2009). "Angiogenesis: a team effort coordinated by notch." *Dev Cell* 16(2): 196-208.

Porcher, C., W. Swat, et al. (1996). "The T cell leukemia oncoprotein SCL/tal-1 is essential for development of all hematopoietic lineages." *Cell* 86(1): 47-57.

Purton, L. E. and D. T. Scadden (2007). "Limiting factors in murine hematopoietic stem cell assays." *Cell Stem Cell* 1(3): 263-70.

Quinkertz, A. and J. A. Campos-Ortega (1999). "A new beta-globin gene from the zebrafish, betaE1, and its pattern of transcription during embryogenesis." *Dev Genes Evol* 209(2): 126-31.

Rampon, C. and P. Huber (2003). "Multilineage hematopoietic progenitor activity generated autonomously in the mouse yolk sac: analysis using angiogenesis-defective embryos." *Int J Dev Biol* 47(4): 273-80.

Ransom, D. G., P. Haffter, et al. (1996). "Characterization of zebrafish mutants with defects in embryonic hematopoiesis." *Development* 123: 311-9.

Reya, T., A. W. Duncan, et al. (2003). "A role for Wnt signalling in self-renewal of haematopoietic stem cells." *Nature* 423(6938): 409-14.

Rhodes, J., A. Hagen, et al. (2005). "Interplay of pu.1 and gata1 determines myeloid-erythroid progenitor cell fate in zebrafish." *Dev Cell* 8(1): 97-108.

Robb, L., I. Lyons, et al. (1995). "Absence of yolk sac hematopoiesis from mice with a targeted disruption of the scl gene." *Proc Natl Acad Sci U S A* 92(15): 7075-9.

Rossi, L., G. A. Challen, et al. "Hematopoietic stem cell characterization and isolation." *Methods Mol Biol* 750: 47-59.

Rothkamm, K. and M. Lobrich (2003). "Evidence for a lack of DNA double-strand break repair in human cells exposed to very low x-ray doses." *Proc Natl Acad Sci U S A* 100(9): 5057-62.

Rowlinson, J. M. and M. Gering "Hey2 acts upstream of Notch in hematopoietic stem cell specification in zebrafish embryos." *Blood* 116(12): 2046-56.

Rubin, G. M. and A. C. Spradling (1982). "Genetic transformation of *Drosophila* with transposable element vectors." *Science* 218(4570): 348-53.

Saleque, S., S. Cameron, et al. (2002). "The zinc-finger proto-oncogene Gfi-1b is essential for development of the erythroid and megakaryocytic lineages." *Genes Dev* 16(3): 301-6.

Samokhvalov, I. M., N. I. Samokhvalova, et al. (2007). "Cell tracing shows the contribution of the yolk sac to adult haematopoiesis." *Nature* 446(7139): 1056-61.

Scheer, N. and J. A. Campos-Ortega (1999). "Use of the Gal4-UAS technique for targeted gene expression in the zebrafish." *Mech Dev* 80(2): 153-8.

Schorpp, M., M. Bialecki, et al. (2006). "Conserved functions of Ikaros in vertebrate lymphocyte development: genetic evidence for distinct larval and adult phases of T cell development and two lineages of B cells in zebrafish." *J Immunol* 177(4): 2463-76.

Schy, W. E. and M. J. Plewa (1985). "Induction of forward mutation at the *yg2* locus in maize by ethylnitrosourea." *Environ Mutagen* 7(2): 155-62.

Sehnert, A. J., A. Huq, et al. (2002). "Cardiac troponin T is essential in sarcomere assembly and cardiac contractility." *Nat Genet* 31(1): 106-10.

Senapathy, P., M. B. Shapiro, et al. (1990). "Splice junctions, branch point sites, and exons: sequence statistics, identification, and applications to genome project." *Methods Enzymol* 183: 252-78.

Shalaby, F., J. Ho, et al. (1997). "A requirement for Flk1 in primitive and definitive hematopoiesis and vasculogenesis." *Cell* 89(6): 981-90.

Shalaby, F., J. Rossant, et al. (1995). "Failure of blood-island formation and vasculogenesis in Flk-1-deficient mice." *Nature* 376(6535): 62-6.

Shimoda, N., E. W. Knapik, et al. (1999). "Zebrafish genetic map with 2000 microsatellite markers." *Genomics* 58(3): 219-32.

Shivdasani, R. A., E. L. Mayer, et al. (1995). "Absence of blood formation in mice lacking the T-cell leukaemia oncoprotein tal-1/SCL." *Nature* 373(6513): 432-4.

Shroyer, N. F., D. Wallis, et al. (2005). "Gfi1 functions downstream of Math1 to control intestinal secretory cell subtype allocation and differentiation." *Genes Dev* 19(20): 2412-7.

Siekmann, A. F., L. Covassin, et al. (2008). "Modulation of VEGF signalling output by the Notch pathway." *Bioessays* 30(4): 303-13.

Siminovitch, L., E. A. McCulloch, et al. (1963). "The Distribution of Colony-Forming Cells among Spleen Colonies." *J Cell Physiol* 62: 327-36.

Sivasubbu, S., D. Balciunas, et al. (2006). "Gene-breaking transposon mutagenesis reveals an essential role for histone H2afza in zebrafish larval development." *Mech Dev* 123(7): 513-29.

Smith, L. G., I. L. Weissman, et al. (1991). "Clonal analysis of hematopoietic stem-cell differentiation in vivo." *Proc Natl Acad Sci U S A* 88(7): 2788-92.

Sood, R., M. A. English, et al. "Development of multilineage adult hematopoiesis in the zebrafish with a runx1 truncation mutation." *Blood* 115(14): 2806-9.

Soza-Ried, C., I. Hess, et al. "Essential role of c-myb in definitive hematopoiesis is evolutionarily conserved." *Proc Natl Acad Sci U S A* 107(40): 17304-8.

Staal, F. J. and T. C. Luis "Wnt signaling in hematopoiesis: crucial factors for self-renewal, proliferation, and cell fate decisions." *J Cell Biochem* 109(5): 844-9.

Stainier, D. Y., B. M. Weinstein, et al. (1995). "Cloche, an early acting zebrafish gene, is required by both the endothelial and hematopoietic lineages." *Development* 121(10): 3141-50.

Streisinger, G., C. Walker, et al. (1981). "Production of clones of homozygous diploid zebra fish (*Brachydanio rerio*)." *Nature* 291(5813): 293-6.

Stuart, G. W., J. V. McMurray, et al. (1988). "Replication, integration and stable germ-line transmission of foreign sequences injected into early zebrafish embryos." *Development* 103(2): 403-12.

Sugiyama, D., M. Ogawa, et al. (2003). "Erythropoiesis from acetyl LDL incorporating endothelial cells at the pre-liver stage." *Blood* 101(12): 4733-8.

Sumanas, S., T. Joraniak, et al. (2005). "Identification of novel vascular endothelial-specific genes by the microarray analysis of the zebrafish cloche mutants." *Blood* 106(2): 534-41.

Sumanas, S. and S. Lin (2006). "Ets1-related protein is a key regulator of vasculogenesis in zebrafish." *PLoS Biol* 4(1): e10.

Sumner, R., A. Crawford, et al. (2000). "Initiation of adult myelopoiesis can occur in the absence of c-Myb whereas subsequent development is strictly dependent on the transcription factor." *Oncogene* 19(30): 3335-42.

Sumoy, L., J. B. Keasey, et al. (1997). "A role for notochord in axial vascular development revealed by analysis of phenotype and the expression of VEGF-2 in zebrafish *flh* and *ntl* mutant embryos." *Mech Dev* 63(1): 15-27.

Swiers, G., M. de Bruijn, et al. "Hematopoietic stem cell emergence in the conceptus and the role of Runx1." *Int J Dev Biol* 54(6-7): 1151-63.

Szilvassy, S. J., R. K. Humphries, et al. (1990). "Quantitative assay for totipotent reconstituting hematopoietic stem cells by a competitive repopulation strategy." *Proc Natl Acad Sci U S A* 87(22): 8736-40.

Taoudi, S. and A. Medvinsky (2007). "Functional identification of the hematopoietic stem cell niche in the ventral domain of the embryonic dorsal aorta." *Proc Natl Acad Sci U S A* 104(22): 9399-403.

Taoudi, S., A. M. Morrison, et al. (2005). "Progressive divergence of definitive haematopoietic stem cells from the endothelial compartment does not depend on contact with the foetal liver." *Development* 132(18): 4179-91.

Tavian, M., L. Coulombel, et al. (1996). "Aorta-associated CD34+ hematopoietic cells in the early human embryo." *Blood* 87(1): 67-72.

Thisse, B., V. Heyer, et al. (2004). "Spatial and temporal expression of the zebrafish genome by large-scale in situ hybridization screening." *Methods Cell Biol* 77: 505-19.

Thompson, M. A., D. G. Ransom, et al. (1998). "The cloche and spadetail genes differentially affect hematopoiesis and vasculogenesis." *Dev Biol* 197(2): 248-69.

Till, J. E. and C. E. Mc (1961). "A direct measurement of the radiation sensitivity of normal mouse bone marrow cells." *Radiat Res* 14: 213-22.

Tong, B., H. L. Grimes, et al. (1998). "The Gfi-1B proto-oncoprotein represses p21WAF1 and inhibits myeloid cell differentiation." *Mol Cell Biol* 18(5): 2462-73.

Traver, D., B. H. Paw, et al. (2003). "Transplantation and in vivo imaging of multilineage engraftment in zebrafish bloodless mutants." *Nat Immunol* 4(12): 1238-46.

Ueno, H. and I. L. Weissman (2006). "Clonal analysis of mouse development reveals a polyclonal origin for yolk sac blood islands." *Dev Cell* 11(4): 519-33.

van der Meer, L. T., J. H. Jansen, et al. "Gfi1 and Gfi1b: key regulators of hematopoiesis." *Leukemia* 24(11): 1834-43.

Vanderslice, R. and D. Hirsh (1976). "Temperature-sensitive zygote defective mutants of *Caenorhabditis elegans*." *Dev Biol* 49(1): 236-49.

Vassen, L., K. Fiolka, et al. (2006). "Gfi1b alters histone methylation at target gene promoters and sites of gamma-satellite containing heterochromatin." *EMBO J* 25(11): 2409-19.

Vassen, L., T. Okayama, et al. (2007). "Gfi1b:green fluorescent protein knock-in mice reveal a dynamic expression pattern of Gfi1b during hematopoiesis that is largely complementary to Gfi1." *Blood* 109(6): 2356-64.

Visser, J. W., J. G. Bauman, et al. (1984). "Isolation of murine pluripotent hemopoietic stem cells." *J Exp Med* 159(6): 1576-90.

Visser, J. W. and S. J. Bol (1982). "A two-step procedure for obtaining 80-fold enriched suspensions of murine pluripotent hemopoietic stem cells." *Stem Cells* 1(4-5): 240-9.

Visvader, J. E., Y. Fujiwara, et al. (1998). "Unsuspected role for the T-cell leukemia protein SCL/tal-1 in vascular development." *Genes Dev* 12(4): 473-9.

Vogeli, K. M., S. W. Jin, et al. (2006). "A common progenitor for haematopoietic and endothelial lineages in the zebrafish gastrula." *Nature* 443(7109): 337-9.

Wadman, S. A., K. J. Clark, et al. (2005). "Fishing for answers with transposons." *Mar Biotechnol (NY)* 7(3): 135-41.

Wallis, D., M. Hamblen, et al. (2003). "The zinc finger transcription factor Gfi1, implicated in lymphomagenesis, is required for inner ear hair cell differentiation and survival." *Development* 130(1): 221-32.

Wang, D., L. E. Jao, et al. (2007). "Efficient genome-wide mutagenesis of zebrafish genes by retroviral insertions." *Proc Natl Acad Sci U S A* 104(30): 12428-33.

Wang, J. H., A. Nichogiannopoulou, et al. (1996). "Selective defects in the development of the fetal and adult lymphoid system in mice with an Ikaros null mutation." *Immunity* 5(6): 537-49.

Warga, R. M., D. A. Kane, et al. (2009). "Fate mapping embryonic blood in zebrafish: multi- and unipotential lineages are segregated at gastrulation." *Dev Cell* 16(5): 744-55.

Warga, R. M. and C. Nusslein-Volhard (1999). "Origin and development of the zebrafish endoderm." *Development* 126(4): 827-38.

Weber, G. J., S. E. Choe, et al. (2005). "Mutant-specific gene programs in the zebrafish." *Blood* 106(2): 521-30.

Wei, W., L. Wen, et al. (2008). "Gfi1.1 regulates hematopoietic lineage differentiation during zebrafish embryogenesis." *Cell Res* 18(6): 677-85.

Weissman, I. L., R. Warnke, et al. (1978). "The lymphoid system. Its normal architecture and the potential for understanding the system through the study of lymphoproliferative diseases." *Hum Pathol* 9(1): 25-45.

Wilkinson, R. N., C. Pouget, et al. (2009). "Hedgehog and Bmp polarize hematopoietic stem cell emergence in the zebrafish dorsal aorta." *Dev Cell* 16(6): 909-16.

Willett, C. E., H. Kawasaki, et al. (2001). "Ikaros expression as a marker for lymphoid progenitors during zebrafish development." *Dev Dyn* 222(4): 694-8.

Willett, C. E., A. G. Zapata, et al. (1997). "Expression of zebrafish rag genes during early development identifies the thymus." *Dev Biol* 182(2): 331-41.

Williams, C., S. H. Kim, et al. "Hedgehog signaling induces arterial endothelial cell formation by repressing venous cell fate." *Dev Biol* 341(1): 196-204.

Wood, H. B., G. May, et al. (1997). "CD34 expression patterns during early mouse development are related to modes of blood vessel formation and reveal additional sites of hematopoiesis." *Blood* 90(6): 2300-11.

Wu, A. M., J. E. Till, et al. (1968). "Cytological evidence for a relationship between normal hematopoietic colony-forming cells and cells of the lymphoid system." *J Exp Med* 127(3): 455-64.

Yang, L., D. Bryder, et al. (2005). "Identification of Lin(-)Sca1(+)kit(+)CD34(+)Flt3- short-term hematopoietic stem cells capable of rapidly reconstituting and rescuing myeloablated transplant recipients." *Blood* 105(7): 2717-23.

Yilmaz, O. H., M. J. Kiel, et al. (2006). "SLAM family markers are conserved among hematopoietic stem cells from old and reconstituted mice and markedly increase their purity." *Blood* 107(3): 924-30.

Yoder, M. C., K. Hiatt, et al. (1997). "Characterization of definitive lymphohematopoietic stem cells in the day 9 murine yolk sac." *Immunity* 7(3): 335-44.

Yokomizo, T., K. Hasegawa, et al. (2008). "Runx1 is involved in primitive erythropoiesis in the mouse." *Blood* 111(8): 4075-80.

Yucel, R., H. Karsunky, et al. (2003). "The transcriptional repressor Gfi1 affects development of early, uncommitted c-Kit⁺ T cell progenitors and CD4/CD8 lineage decision in the thymus." *J Exp Med* 197(7): 831-44.

Yucel, R., C. Kosan, et al. (2004). "Gfi1:green fluorescent protein knock-in mutant reveals differential expression and autoregulation of the growth factor independence 1 (Gfi1) gene during lymphocyte development." *J Biol Chem* 279(39): 40906-17.

Yue, R., Kang, J., Zhao, C., Hu, W., Tang, Y., Liu, X., and Pei, G. (2009). "Beta-arrestin1 regulates zebrafish hematopoiesis through binding to YY1 and relieving polycomb group repression." *Cell* 139(3): 535-546.

Zeigler, B. M., D. Sugiyama, et al. (2006). "The allantois and chorion, when isolated before circulation or chorio-allantoic fusion, have hematopoietic potential." *Development* 133(21): 4183-92.

Zeng, H., R. Yucel, et al. (2004). "Transcription factor Gfi1 regulates self-renewal and engraftment of hematopoietic stem cells." *EMBO J* 23(20): 4116-25.

Zhang, X. Y. and A. R. Rodaway (2007). "SCL-GFP transgenic zebrafish: in vivo imaging of blood and endothelial development and identification of the initial site of definitive hematopoiesis." *Dev Biol* 307(2): 179-94.

Zhong, T. P., S. Childs, et al. (2001). "Gridlock signalling pathway fashions the first embryonic artery." *Nature* 414(6860): 216-20.

Zovein, A. C., J. J. Hofmann, et al. (2008). "Fate tracing reveals the endothelial origin of hematopoietic stem cells." *Cell Stem Cell* 3(6): 625-36.
